

**BIOFILM CONTROL ON STAINLESS
STEEL SURFACE TO OPTIMISE
HYGIENE, PROCESS CONDITIONS AND
CORROSION RESISTANCE**

Tirivaviri Augustine Mamvura

A thesis submitted to the Faculty of Engineering and the Built Environment, University of Witwatersrand, in fulfilment of the requirements for the degree of Doctor of Philosophy

Johannesburg, 2014

DECLARATION

I declare that this thesis is my own unaided work. It is being submitted for the Degree of Doctor of Philosophy to the University of the Witwatersrand, Johannesburg. It has not been submitted before for any degree or examination to any other University.

.....

(Signature of Candidate)

.....day of.....year.....

day

month

year

ABSTRACT

The brewing industry is amongst industries that fall under health legislation. Progressively legislation has become more stringent in terms of bacterial load limits and process options. In addition water has become a scarce resource, now supplied from municipal, not private sources. The aim of the study was to consider methods that would assist clean-in-place (CIP) process in controlling and/or eliminating biofilms formed on pipes and process vessels in the brewing industry.

In the brewing industry CIP is the current method of choice to control biofilms, however, it both uses large quantities of water and does not seem to be fully meeting the required purpose. An increase in cases of material failures and product contamination caused by microbiologically influenced corrosion (MIC) and spoilage bacteria is evident in the sector. The current research addressed the possibility of the use of low-frequency ultrasound waves (power ultrasound) to assist the CIP process in “hot spot” contamination areas, so reducing the CIP need, saving water and improving performance using an environmentally-friendly process.

Pilot studies showed that sonication (cavitation in liquid) at 24 kHz reduced simulated *E. coli* biofilms grown onto 316L stainless steel coupons with different weld treatments with disinfection efficiencies of $\geq 80\%$. The second part of the study involved real biofilms formed on a small experimental rig. The rig was made

up from interconnected lengths of 60 mm OD, schedule 40 316L stainless steel pipes. These were subjected to different welding preparations and post welding treatments. Municipal water was circulated through the setup for two sets of five week experiments, each at different flow velocities to enable the growth of biofilm.

It was demonstrated that water supported biofilm growth and its treatment is of utmost importance. In addition, it was shown that ultrasound waves could pass through metal surfaces and clean the inside surfaces but the efficiency of the process ranged between 10 and 100% with regards to removal of biofilm because the thicknesses were high (3.91 mm for SS pipes and 3 mm for SS coupon plates), the clamping device used was heavy (1001 g) and also the device had to be under water for effective cooling during operation.

There was increased concentration of biofilm on and around weld areas include heat affected zones (HAZs) and it was difficult to control biofilms around such areas due to increased roughness. This was because welding introduces rough surfaces, geometrical difficulties (over-penetration and under-penetration), and gave wrought structures (formation of iron oxide or separation on grain boundaries). From the study it was observed that using 316L fillers resulted in better biofilm control than using 904L fillers (even though 904L welds had copper as a biocide) except when the welds were pickled and passivated. In this case 904L fillers resulted in lower intensities than 316L fillers. It was also observed that welding in the presence of argon gave better welds that resulted in reduced biofilm formation.

On top of that, flow direction and pipe position influenced biofilm formation, its control and the CIP process. This led to the conclusion that the CIP process to date was observed to be ineffective against biofilms and it became less effective with continuous use of pipes and process vessels. It was observed that the CIP process became less effective along pipe lengths and process vessels i.e. the further, the pipe or vessel from the CIP source, the less effective was the process.

The test for ultrasound was done by applying ultrasound waves indirectly to pipe walls in a water bath by clamping the sonication device to the pipe walls. This was so because in practice internal access results in non-sterile and impractical situation in a production environment.

The knowledge gained further enhanced the likely success of using ultrasound waves as one of the future methods for biofilm control in the food and beverage industry as it is easy to apply, and is an environmentally-friendly operation.

DEDICATION

To my love Leniency T. Matsekeza, my daughter Tatenda Ariela and my son
Tadanaishie Augustine

ACKNOWLEDGEMENTS

Firstly, I would like to thank God as I am still alive and all the wonderful things that happened and will happen in my life.

Secondly, I wish to express my greatest appreciation to my supervisors, Professor S. E. Iyuke and Dr A E Paterson for their guidance and invaluable support throughout the study.

Sincere thanks also to the Biology Electron Microscope Unit of the University of Witwatersrand for all their help during this study, Falcon Engineering for the WITS Microbrewery, South African Institute of Welding for undertaking all the welding requirements on coupons and pipes during the study and 3M for donating clean-trace swabs and the Clean-Trace™ NG bioluminometer used on the dynamic experiments.

My thanks also goes to Paul Burke for helping with analysis and facilitating donation of 3M equipment, Lucretia for *E. coli* used in the study from Biology and Mr John Cluett for all the help and guidance during the study.

To all my family members, I say thanks guys for your understanding all the time.

Lastly, I gratefully acknowledge the financial support from the Andrew W Mellon Foundation, Southern African Institute of Welding and WITS University.

TABLE OF CONTENTS

DECLARATION	ii
ABSTRACT	iii
DEFINITIONS	xxi
1. INTRODUCTION	2
1.1. Health legislation and safety in the brewing industry	5
1.2. Water scarcity and availability	7
1.2.1. Sources of water	7
1.2.2. Composition of brewing water	8
1.3. Standardisation of materials of construction	9
1.4. Stainless steel in the brewing industry	11
1.4.1. Application of Stainless Steels	13
1.5. Welding and its effects	15
1.5.1. Pickling and passivation	20
1.5.2. Effect of sulfur on welding	21
1.6. Motivation	23
1.7. Research gap	26
1.8. Research Problem	29
1.9. Research Aim and Objectives	29
1.10. Hypothesis	30

1.11.	Research Methodology	31
1.11.1.	Literature review	31
1.11.2.	Experimental design	31
1.11.3.	Data analysis	32
1.11.4.	Conclusions and recommendations	32
1.12.	Expected Research Outputs and Contributions	32
1.13.	Thesis layout	33
	References	35
2.	LITERATURE REVIEW	41
2.1.	Biofilms in various industries	42
2.1.1.	Biofilms	44
2.2.	Water analysis with emphasis on biofilm formation	63
2.2.1.	Water used in the brewing industry	64
2.3.	Clean-in-place systems used to control biofilms in food and beverage industry	66
2.3.1.	CIP systems	66
2.3.2.	Parameters influencing cleaning efficiency	72
2.3.3.	Types of CIP systems	77
2.4.	Controlling biofilms in the food and beverage industry	79
2.4.1.	Strategies employed to control biofilms	79
2.4.2.	Treatment and prevention of biofilms	80

2.4.3.	Water treatment methods in the brewing industry	90
2.5.	Surface functionality of stainless steel surface profiles in food and beverage industry	92
2.5.1.	Surface profile changes during treatment with ultrasound waves	94
	References	99
3.	EXPERIMENTAL PROCEDURE	116
3.1	Static experiments	116
3.1.1	Using ultrasound waves to control biofilms in brewing industry	116
3.1.2	Surface profile changes during use of ultrasound waves	121
3.1.3	Energy changes during treatment with ultrasound waves	123
3.1.4.	Button experiments	124
3.2	Dynamic experiments	126
3.2.1.	Welding filler characterisation	127
3.2.2.	Flow and velocity measurements	127
3.2.3.	CIP systems in combination with ultrasound waves	127
	References	146
4.	RESULTS AND DISCUSSION	151
4.1	Static experiments	151
4.1.1	Controlling biofilms using ultrasound waves	151
4.1.2	Surface profile changes during use of ultrasound waves	162
4.1.3	Energy changes during treatment with ultrasound waves	175

4.1.4	Button experiments	198
4.2	Dynamic experiments	202
4.2.1.	Welding filler characterisation	202
4.2.2.	Flow and velocity measurements	205
4.2.3.	CIP systems in combination with ultrasound waves	207
4.3	Summary of research results	246
4.3.1	Biofilms in the beverage industry	246
4.3.2	Water analysis with emphasis on biofilm formation	247
4.3.3	Controlling biofilms using ultrasound waves	247
4.3.4	Surface profile changes during use of ultrasound waves	248
4.3.5	Energy changes during treatment with ultrasound waves	250
4.3.6	CIP systems in combination with ultrasound waves	251
	References	253
5.	CONCLUSIONS AND RECOMMENDATIONS	263
5.1.	Conclusions	263
5.2.	Future work and recommendations	266
	APPENDICES	269

LIST OF FIGURES

Figure 1.1: Image showing biofilms	4
Figure 1.2: Effect of temperature over time on different carbon-grade SSs	17
Figure 1.3: Examples of good and bad welds	19
Figure 1.4: Effect of sulfur on weld penetration	21
Figure 2.1: Basic scheme representation of the brewing process	45
Figure 2.2: Conceptual drawing showing (front) attachment of planktonic cells and sequential stages of	57
Figure 2.3: Elements of an integrated antifouling strategy	81
Figure 2.4: Mechanism of ultrasound waves-induced cell damage	88
Figure 2.5: Surface erosion of SS subjected to ultrasound waves over time	99
Figure 3.1: One of three experimental coupons used in the study	118
Figure 3.2: Experimental setup and procedure using ultrasound waves to control biofilms from SS coupons	119
Figure 3.3: The energy transformation chain during ultrasonic treatment	123
Figure 3.4: Schematic of the test rig built to mimic biofilm formation in brewing operations	128
Figure 3.5: Test rig to investigate the effect of biofilm formation after CIP on brewing process systems	129
Figure 3.6: Sampling port located on each of the weld in the direction of flow	130
Figure 3.7: Stainless steel cylinder covered with biofilm after 7 days of growth	131

Figure 3.8: Clean-Trace™ NG bioluminometer	133
Figure 3.9: Schematic showing sampling numbering system for all pipes	139
Figure 3.10: Schematic showing sampling numbering system on each pipe	139
Figure 3.11: Arrangement during use of ultrasound waves for run 1	143
Figure 3.12: Arrangement during use of ultrasound waves for run 2	143
Figure 4.1: Effect of ultrasound intensity on the removal of	152
Figure 4.2: Effect of ultrasound intensity on the removal of	153
Figure 4.3: Effect of time of exposure on the removal of biofilms for surfaces facing ultrasound waves	155
Figure 4.4: Effect of time of exposure on the removal of biofilms for surfaces not facing ultrasound waves	156
Figure 4.5: A plot of $\log(N/N_0)$ against time for surfaces that were facing ultrasound waves	157
Figure 4.6: A plot of $\log(N/N_0)$ against time for surfaces that were not facing ultrasound waves	157
Figure 4.7: Effect of distance of probe from coupon surface on the removal of biofilms for surfaces facing ultrasound waves	158
Figure 4.8: Effect of distance of probe from coupon surface on the removal of biofilms for surfaces not facing ultrasound waves	159
Figure 4.9: Surface analysis for normal surface	164
Figure 4.10: Surface analysis for laser weld surface	165

Figure 4.11: Surface analysis for CMT weld surface	166
Figure 4.12: Surface analysis for MIG weld surface	167
Figure 4.13: Change in surface profile for normal surface in the presence of ultrasound waves	174
Figure 4.14: Plots showing displacement (x) and pressure (P) against time (t) for a typical wave	177
Figure 4.15: Electrical power density with change in amplitude due to treatment of distilled water with ultrasound waves	181
Figure 4.16: Rate of temperature change rise with change in amplitude due to treatment of distilled water with ultrasound waves	186
Figure 4.17: Acoustical energy change with amplitude due to treatment of distilled water with ultrasound waves	187
Figure 4.18: Cavitation energy change with amplitude due to treatment of distilled water with ultrasound waves	190
Figure 4.19: Efficiency of change in electrical energy to acoustical and cavitation energies with change in amplitude during treatment of distilled water with ultrasound waves	193
Figure 4.20: Effect of change in power density with distance from the probe	195
Figure 4.21: Effect of change in amplitude and distance from the probe on the attenuation coefficient	197
Figure 4.22: Effect of ultrasound intensity on the removal of biofilms for button and coupon surfaces facing ultrasound waves at a distance of 750 mm	200

Figure 4.23: Results of bacterial loading on aluminium surfaces with different treatments	201
Figure 4.24: Pump calibration chart showing flowrate and linear speed for runs 1 and 2	206
Figure 4.25: Examples of welds produced using 904L weld filler rods	211
Figure 4.26: Examples of welds produced using 316L weld filler rods	211
Figure 4.27: Photographs of weld caps of 50 mm ID, 3.91 mm wall thickness, 316L pipe apparatus conducted at SAIW using TIG welding and using 316L and 904L filler rods	212
Figure 4.28: Graph showing ambient temperature (ambient T) and experimental temperature (Experimental T) with change in time for run 1	214
Figure 4.29: Graph showing ambient temperature (ambient T) and experimental temperature (Experimental T) with change in time for run 2	215
Figure 4.30: Effect of water flow for run 1	225
Figure 4.31: Effect of water flow for run 2	226

LIST OF TABLES

Table 1.1: Important parameters to be determined during water analysis	8
Table 1.2: Special elements added to SSs to impart certain properties	12
Table 1.3: Characteristics of different types of SSs	14
Table 1.4: Change in sulfur concentration with time to mitigate its effects during welding	22
Table 1.5: Advantages and limitations of using ultrasound waves	24
Table 1.6: Some industrial uses of ultrasound waves	27
Table 2.1: Composition of biofilms obtained from fouled surfaces experiencing excessive frictional losses	53
Table 2.2: Typical CIP programmes used in the brewery, with programmes adapted to the part of the process to be cleaned, and some of the steps: alkali, acidic, or disinfection being left out	69
Table 2.3: Comparison of the three technologies of	89
Table 2.4: Relationship between surface function and quality	93
Table 2.5: Classification systems for form deviations according to DIN 4760	94
Table 3.1: Sampling ports numbering system	138
Table 3.2: Distance (measured in degrees) of sampling points for both weld types on experimental rig for run 1	140
Table 3.3: Distance (measured in degrees) of sampling points for both weld types on experimental rig for run 2	141

Table 3.4: Interpretation of data from Clean-Trace™ NG bioluminometer	141
Table 3.5: Summary of all conditions of the pilot rig for dynamic experiments	145
Table 4.1: E. coli bacterial loading concentration against surface type and maximum height	168
Table 4.2: Surface topography data (mean±SD) for the different surfaces used in the study	169
Table 4.3: Surface morphology data (mean±SD) for the different surfaces used in the study	172
Table 4.4: Error analysis between electrical power density	182
Table 4.5: Maximum displacement, maximum velocity and maximum acceleration experienced by water molecules during treatment with ultrasound waves	183
Table 4.6: Error analysis between cavitation power density values	191
Table 4.7: Bacterial loading before treatment with ultrasound waves on SS buttons and coupons	198
Table 4.8: Comparison of 316L and 904L welding rods composition	203
Table 4.9: Surface topography data (mean±SD) for SS 316 pipe surfaces used in the study	207
Table 4.10: Surface morphology data (mean±SD) for SS 316 pipe surfaces used in the study	209
Table 4.11: Blank swabs done at different points on dry pipe surfaces	213
Table 4.12: Results for water sampling using Aqua-Trace for run 1	217

Table 4.13: Sampling done at the entry and exit of the rig for runs 1 and 2	218
Table 4.14: Normalised data from Clean-Trace™ NG bioluminometer	221
Table 4.15: Summary of biofilm intensity for all pipes after CIP process and biofilm formation for run 1	222
Table 4.16: Summary of biofilm intensity for all pipes after CIP process and biofilm formation for run 2	223
Table 4.17: Effect of water flow along pipes for runs 1 and 2 after CIP and biofilm formation for 316L weld	229
Table 4.18: Effect of water flow along pipes for runs 1 and 2 after CIP and biofilm formation for 904L weld	230
Table 4.19: Effect of using 316L weld filler rods on CIP and biofilm formation for run 1	232
Table 4.20: Effect of using 904L weld filler rods on CIP and biofilm formation for run 1	233
Table 4.21: Effect of using 316L weld filler rods on CIP and biofilm formation for run 2	234
Table 4.22: Effect of using 904L weld filler rods on CIP and biofilm formation for run 2	235
Table 4.23: Effect of argon purging during welding for runs 1 and 2 after CIP and biofilm formation for 316L weld	237
Table 4.24: Effect of argon purging during welding for runs 1 and 2 after CIP and biofilm formation for 904L weld	238

Table 4.25: Effect of pickling and passivation after welding in the absence of argon for runs 1 and 2 after CIP and biofilm formation for 316L welds	240
Table 4.26: Effect of pickling and passivation after welding in the absence of argon for runs 1 and 2 after CIP and biofilm formation for 904L welds	241
Table 4.27: Effect of pickling and passivating after welding for runs 1 and 2 after CIP and biofilm formation for 316L weld	243
Table 4.28: Effect of pickling and passivating after welding for runs 1 and 2 after CIP and biofilm formation for HAZ welds	244
Table 4.29: Results showing combined effect of ultrasound waves and CIP process on biofilm intensity for runs 1 and 2	245

DEFINITIONS

Biofilm: a well-organised and cooperating community of microorganisms attached together with organic and inorganic substances to a surface by the help of extracellular polymeric substances, which are produced by the microorganisms to form a single layer or three-dimensional structure

Clean-in-place (CIP): a method of cleaning equipment without the need to disassemble them prior to cleaning. It is commonly used for interior cleaning of brewing equipment such as tanks, brewhouse vessels, heat exchangers, pipe-systems and hoses, and other production equipment like fillers. These days, in the brewing industry, almost any type of cleaning not directly involving hand scrubbing is commonly referred to as CIP

Microbiologically influenced corrosion (MIC): an accelerated deterioration of metals due to the presence of biofilms on their surfaces

Ultrasound waves: sound waves with a frequency higher than the upper limit of human hearing of 20 kHz.

Surface topography: the deviation of the actual surface profile from the flat surface, including roughness and waviness

Stainless steel (SS): a corrosion resistant alloy with iron being the major element to which small amounts of carbon, nickel and chromium (giving it a bright shiny gloss and make it highly resistant to tarnishing and corrosion) have been added

Cavitation: formation and subsequent dynamic life of bubbles in liquids subjected to a sufficiently low pressure

Disinfection efficiency (viability of biofilms): this is a measure of how much biofilm is removed by treatment with ultrasound waves. It is given by the formula:

$$\frac{\text{initial biofilm intensity} - \text{final biofilm intensity}}{\text{initial biofilm intensity}} \times 100\%$$

CHAPTER ONE

"IF A MAN DOES HIS BEST, WHAT ELSE IS THERE?"

- GENERAL GEORGE S. PATTON (1885-1945)

1. INTRODUCTION

Industrial plants which produce products subject to health legislation include food, dairy, pharmaceuticals, beverages and beer. Hygiene is a permanent concern for commercial producers of outputs that comply with legislation and the demands of consumers. Cost effective cleaning and disinfection are essential to ensure the microbiological safety of the product and avoid higher production costs (Detry *et al.*, 2010). International and local health legislation is increasingly demanding lower and lower bacterial (and spore) counts in the end product; however, many South African brewery plants were built starting from the mid 1960's (with a 30 year life expectancy). They were designed at a different time under different health legislation. Research has to find a way to bridge the gap at an economical cost as possible. To add to this, water quality has become less predictable and water has become more scarce, putting more pressure on these industries. This leads to the question: "How do we manage the fabrication of new plants and maintain the old plants to accommodate the changing legislation and operating conditions?"

Austenitic stainless steels (SS) have been used in various components and facilities of the food and beverage industries because of their excellent corrosion resistance, ductility and ease of cleanability (Folkmar Andersen *et al.*, 2006). Welding processes are generally used to permanently join standard components together. Process plants are typically made up of pipes linking treatment tanks, heat exchangers or distillation columns. Standard plates and pipes are formed, welded, screwed, bolted or flanged together into systems that meet prevailing or future perceived operating

environments. In South Africa, starting about 50 years ago and commonly used from about 30 years ago, austenitic SS established themselves as the material of choice for the construction of almost all pharmaceutical, food and beverage, dairy processing and storage equipment (Cluett et al., 2003). This was due to certain attributes which are:

- Corrosion resistance – SS remain uncorroded under normal atmospheric conditions (Guillamet *et al.*, 1993; Partington, 2006)
- General inertness – SS do not change colour or appearance or corrode making them ideal as food contact surfaces because the food or beverage will be untainted by metallic constituents or corrosion products i.e. the material will remain intact (Folkmar Andersen *et al.*, 2006; Partington, 2006)
- Ease of fabrication and welding – SS are easy to fabricate and manipulated as compared to other inert materials (Guillamet *et al.*, 1993; Partington, 2006)

Adhesion of bacteria to SS surfaces in aqueous media or humid environments is the initial step in the formation of biofilms (Figure 1.1). These films are known to cause problems such as microbiologically influenced corrosion (MIC) and they represent a chronic source of microbial contamination (Mamvura *et al.*, 2011; Medilanski *et al.*, 2002).



Figure 1.1: Image showing biofilms 1600x. Biofilms can be created by a single bacterial species but often contain many species of bacteria along with fungi, protozoa, algae, and organic or inorganic debris (Kunkel, 2009). Biofilm growth is enhanced by increased surface roughness, increased temperature and low flowrates

As the microorganisms grow on substratum surfaces, they produce various metabolic by-products, which might promote deterioration of the underlying substratum. These reactions refer to biocorrosion or MIC when the underlying substratum is a metal or metal alloy like SS (Sreekumari *et al.*, 2005). The magnitude of the problem of MIC necessitates a wider attention that should encompass collaboration between established research groups or laboratories with specialising researches on various aspects of metal microbe interactions viz. microbiology, metallurgy, chemical engineering, civil engineering, environmental engineering and biotechnology. Most of these disciplines were represented during the study and had significant contribution during the experiments undertaken.

1.1. Health legislation and safety in the brewing industry

Modern breweries use automated equipment for high volume manufacture. Process failures have an ever-increasing monetary impact such as costs of product spoilage, wasted production time and concerns for public health. In addition, a single report of contamination could put the reputation and future success of a manufacturer at risk (Piyasena *et al.*, 2003). Cleaning in the brewing industry is required for three reasons: (a) for the removal of any soiling which has the potential to introduce taints into products, (b) for the removal of soiling which has the potential to adversely affect the operation of parts of the plant like building up of scale on heat exchangers, and (c) for the disinfection to eliminate any risk of microbial spoilage as biofilms (Briggs *et al.*, 2004; Mamvura *et al.*, 2011; Praeckel, 2009).

Critical output variables in a brewery are as follows:

- Client – meeting capital asset performance objectives
- Customer – consistent product with desirable flavour, clarity, colour, and foam within specifications
- Health authorities – bacterial load in the final product
- OHS authorities – this encompasses correct design, fabrication, testing and operation
- Corporate risk management – risk analysis, safety of operational personnel, prevention of asset damage and consumer product safety

However, three broad challenges exist:

- (i) Water quality and scarcity
- (ii) Permissible bacterial intensity reduction by legislation (Cluett *et al.*, 2003), and
- (iii) Maintenance of existing plants (90%) and new build (10%) parameters

Recent health legislation has reduced acceptable bacterial levels in the final product. In terms of health legislation; sterilisation, disinfection, sanitisation, and cleaning represent decreasing ranks.

- (i) Sterilisation is intended to destroy all forms of life, especially microorganisms, either by chemical or physical means. Generally one uses an autoclave or heats an item for an extended period of time (Cluett *et al.*, 2003).
- (ii) Disinfection means to kill (as distinct from destroy) all the harmful microorganisms that can cause spoilage. A disinfectant is an anti-microbial agent intended for application on inanimate objects or surfaces to kill all pathogenic organisms (excluding spore-forming bacteria) within 10 minutes or less (Cluett *et al.*, 2003).
- (iii) Sanitisation means reducing contaminants to (currently) acceptable levels. When brewers talk about sterilising their brewing equipment they generally mean sanitising. No sanitising agents are capable of eliminating all bacterial spores and viruses (Cluett *et al.*, 2003).
- (iv) Cleaning is the process of removing all the dirt and grime from the surface in order to remove sites that can harbour or encourage biofilm microorganisms (Cluett *et al.*, 2003).

Note that CIP systems are used to clean without disassembly but they represent cleaning and sanitising only.

1.2. Water scarcity and availability

The continued availability of a supply of good-quality drinking water is of fundamental importance to the brewing industry because a carbonated soft drink or beer can contain about 87 to 92% water, while bottled water product may be pure (100%) natural spring water (Jyoti and Pandit, 2001; Olajire, 2012; Shachman, 2005; Taylor, 2006). As such, the quality of the water used in a beverage has a critical impact on the taste, health and appearance, as well as physical and microbiological stability on the shelves in the store (van der Bruggen and Braeken, 2006; Shachman, 2005).

In the brewing industry, water, apart from the main functions of brewing, sparging and dilution, is also used for cleaning the plant using manual or CIP systems, cooling, heating (either as hot water or steam), occupying lines before and after running beer through them, loading filter aids, washing yeast, slurring and conveying away wastes and washing beer containers. Water supplied to a brewery facility has a small quantity of dissolved gases, a dilute solution of various inorganic salts and also contains organic compounds (Taylor, 2006). Absolutely pure water (i.e. with no ions) has a flat taste such that some mineral content may be desirable and also it is very reactive leading to corrosion problems in the brewing industry (Taylor, 2006).

1.2.1. Sources of water

Water used in the manufacturing facilities comes from different sources: municipal water supply, privately owned wells, or springs. As springs are surface waters; however, these are avoided where possible (Elder and Budd, 2011; Shachman, 2005). Water is a base product used in all processes

and it was previously drawn from private sources but it is now drawn from municipal sources due to its scarcity. Municipality supplied water is of inconsistent quality over time.

1.2.2. Composition of brewing water

Water from municipal sources is typically of a high standard of purity and it is potable, however, it may not necessarily be fit for use in the brewing process due to its varying composition and temperature, and may not be necessarily sterile i.e. free of any microorganisms that can contaminate wort or beer, which must be the case for brewing liquors. Certain limits on elements (organic and inorganic) in brewing water need to be adhered to and they are summarised in Table 1.1.

Table 1.1: Important parameters to be determined during water analysis (Briggs *et al.*, 2004)

Smell	Residual alkalinity	Trihalomethanes	As ⁺	SO ₄ ²⁻ , Cl ⁻
Taste	Turbidity	Ca ²⁺	Fe ²⁺ , Fe ³⁺	HCO ₃ ⁻
Colour	Temperature	Mg ²⁺	Mn ²⁺	NO ₂ ⁻ , NO ₃ ⁻
KMnO ₄ consumption	Conductivity	NH ₄ ⁺	Na ⁺	SiO ₂

Before use municipal water need to be treated to adhere to brewing water standards but its purification costs are lower than natural water as it has undergone other purification stages from water purification stations.

Limits are set for dissolved solids and toxic ions in brewing water; however, yeast cells require trace amounts of many of them including Cu, Zn, Mn and Fe for growth which can be obtained from brewers' grist (Briggs *et al.*, 2004). Limits should be set for NH₃/NH₄⁺ and nitrogen levels as they often indicate contamination with decomposing organic matter. Nitrate levels which can vary widely are a cause of concern as water sources are increasingly contaminated with nitrates from leached agricultural fertilisers and the fear is that during the preparation of the beer or inside the consumer, the nitrates may be reduced to nitrites leading to carcinogens (Koparal and Ögütveren, 2002; Pintar, 2003).

Traces of pesticides widely used in different combinations at many stages of cultivation and during postharvest storage may remain in the beer produced from treated ingredients, but also the residues may also come from the soil itself (Navarro *et al.*, 2007). Lastly, there should be minimum levels for total hardness and alkalinity to limit corrosion in pipework; fluorine (added as a fluoride salt) is often added to drinking water but at the lower levels used it is harmless and without influence on fermentation or hardness (Elder and Budd, 2011).

1.3. Standardisation of materials of construction

There are obvious benefits to be derived from consensus standards which define the composition and mechanical properties of specific materials of construction. Some of the benefits include:

- (i) Standards allow designers and users of materials to work with confidence that the materials supplied will have the expected minimum properties (Siebert and Stoecker, 1997),
- (ii) Designers and users can also be confident that comparable materials can be purchased from several suppliers (Siebert and Stoecker, 1997), and
- (iii) Producers are confident that materials produced to an accepted standard will find a ready market and therefore can be produced efficiently in large factories (Siebert and Stoecker, 1997)

Some of the different standards used by different countries are ASTM in USA, BS in Great Britain, DIN in Germany, AFNOR in France and JIS in Japan. ISO are international standards agreed by all countries. Other countries adopt the national specifications of other countries e.g. South African industry has generally made use of BS alongside USA standards. More recently the EN standards developed to enable cross trade activity in Europe have become important. A list of some of the standards used is as follows:

1. American National Standards Institute (ANSI), formerly American Standards Association (ASA) – ANSI promulgates the piping codes used in the chemical process industries
2. American Society of Mechanical Engineers (ASME) – this society publishes Boiler and Pressure Vessel Codes
3. American Society for Testing and Materials (ASTM) – this society publishes specifications for most of the materials used in the ANSI Piping Codes and the ASME Boiler and Pressure Vessel Codes
4. International Organisation for Standardisation (ISO) – this organisation is engaged in generating standards for worldwide use. It has 80 member nations

5. South African Bureau of Standards (SABS) – standards developed in South Africa and used alongside international standards where appropriate

1.4. Stainless steel in the brewing industry

Stainless steel is an alloy of iron which by definition contains a minimum of 50% iron. It is a large family of alloys divided into four classes, austenitic, ferritic, martensitic and duplex. Precipitation hardening martensitic grades are often referred to as a fifth class. Each class represents hundreds of grades and sub-grades in the family (Tverberg, 2001). There are more than 70 standard types of SS and many special alloys produced in the wrought form and as cast alloy. Austenitic stainless steels are those commonly used in the beverage industry. They are heat and corrosion-resistant, non-contaminating, and easily fabricated into complex shapes (Siebert and Stoecker, 1997). The chromium content of SSs renders them passive due to the formation of a Cr rich oxide film (passive film) on its surface. This passive film is: (a) extremely thin (about $3-5 \times 10^{-6}$ mm thick), (b) uniform and continuous, (c) stable and tenacious, (d) smooth, and (e) self-repairing (Siebert and Stoecker, 1997). Other elements are added for special purpose as seen in Table 1.2.

Table 1.2: Special elements added to SSs to impart certain properties (Guillamet *et al.*, 1993; Partington, 2006; Siebert and Stoecker, 1997)

Element	Purpose	Element	Purpose
Chromium 12–30%	Oxidation resistance	Molybdenum	Increased resistance to chlorides and acids
Nickel 0–20%	Increased resistance to mineral acids and stabilises crystal structure by producing tightly adhering high temperature oxides	Manganese 0.75–1%	Similar to Ni; combines with sulfur and increases solubility of nitrogen; However, Mn is half as powerful as Ni so 2% is required to replace 1% Ni
Titanium	Stabilises carbides to prevent sensitisation	Niobium	Stabilises carbides to prevent sensitisation
Nitrogen	Improves resistance to chlorides	Aluminium	Deoxidiser; precipitation hardener
Carbon	0.035% maximum to prevent sensitisation	Tantalum	Stabilises carbides to prevent sensitisation

Sensitisation is a concern when joining by welding. It is the formation of grain boundary chromium carbide which precipitates adjacent to the welds where high temperatures between 500 °C and 800 °C are attained and held for a sufficient period. This a function of the C content. It favours inter-

granular corrosion or “weld decay”. To avoid precipitation, special SSs stabilised with titanium (Ti), niobium (Ni), or tantalum (Ta) have been developed or, alternatively low carbon SSs such as types 304L and 316L, with 0.03% maximum carbon can be used (Folkmar Andersen *et al.*, 2006). The effect is to increase the time window within which sensitisation occurs.

1.4.1. Application of Stainless Steels

The five families or classes of SS are named according to how their microstructure resembles a similar microstructure in steel. The properties of these classes differ, but are essentially similar within the same class. Table 1.3 lists the metallurgical characteristics of each class.

Austenitic SSs are preferred in food and beverage industries because of their good corrosion resistance, ductility, good hygiene, good cleanability, increased product purity, strong and excellent weldability properties (Guillamet *et al.*, 1993; Maller, 1998).

Duplex SSs can be used in areas where there is need for high resistance to chloride induced mechanisms of corrosion such as pitting corrosion and stress corrosion cracking (Tverberg, 2001).

Table 1.3: Characteristics of different types of SSs (Siebert and Stoecker, 1997; Tverberg, 2001)

SS group	Characteristics	Examples
Austenitic Cr:16–26%; Ni:6–22%	Non-magnetic; non-hardenable by heat treatment; single phase from 0 °K to melting point; face centred cubic crystallographic form; C <0.08% for non-L grades and <0.035% for L grades; easy to weld L grades	304, 304L,H,N,LN, 316, 316L,H,N,LN,Ti 317, 317L,LM, 321, 347, 904L
Ferritic Cr:15–30%; C<0.1%	Magnetic; non-hardenable by heat treatment; body centred cubic crystallographic form; low C grades easier to weld; good corrosion resistance but not against reducing acids like HCl	405, 409, 430, 430Ti, 439, 444
Duplex	Magnetic; non-hardenable by heat treatment; contains both austenite and ferrite; easy to weld	Alloy 2205; Alloy 2507
Martensitic Cr:12–20%; controlled C	Magnetic; heat treatable to high hardness levels; distorted tetragonal crystallographic form; hard to impossible to weld; corrosion resistance inferior to austenitic; used in mildly corrosive environments (atmospheric, fresh water, and organic exposures)	410, 420; 440A, 440B, 440C
Precipitation hardening	Magnetic; martensitic with micro-precipitates crystallographic form treated to high strength levels by heat; easy to weld	Custom types

Utility ferritic SSs cannot be used in components or equipment in direct contact with food and beverage being processed because they are not corrosion resistant against reducing acids like HCl. However, they can be used in peripheral applications where lower levels of maintenance are required like ducting, stairways and walkways, pipe racks and supports, cable trays, gullies and drains (Tverberg, 2001).

1.5.Welding and its effects

SS fabrication are normally joined by welding which provides high strength joints with minimum flow restrictions and prevents the major concern of crevice corrosion favoured by screw thread joints; however, elimination of crevices does not guarantee trouble free operation (Tverberg, 2001). Biofilm formation particularly in pipes and tubes, is a concern as interior walls are normally difficult to access. Smooth surfaces lead to less development of biofilms but welding processes introduce discontinuities which impact on surface smoothness. Weld regions are particularly attractive to microbes in food and beverage industries because the welding process alters the material surface characteristics. The combination of physical and compositional changes brought about by the welding process is believed to facilitate accumulation of organics onto the surface and subsequent colonisation by bacteria to form biofilms (Verran, 2005). The preference of weld as a site of colonisation by bacteria is evident and has been correlated to the surface roughness (Verran, 2005).

Welding is characterised by four effects and these include:

- (i) During welding, the heat from the process affects areas in the vicinity of the welding point. The affected areas are known as heat affected zones (HAZs). This is due to the formation of iron oxide when welding is done in the presence of oxygen and/or sensitisation when chromium reacts with carbon to form chromium carbides (usually occurs in the temperature range between 500 and 850 °C). HAZ might show a changed internal structure and composition and may in some circumstances act as a location where corrosion can be preferentially initiated due to biofilm formation. However, sensitisation may be overcome by using low carbon (L) grades like 304L or 316L, see Figure 1.2. (Folkmar Andersen *et al.*, 2006; Guillamet *et al.*, 1993)
- (ii) Geometry effects which include misalignment, crevices and root reinforcement (Sreekumari *et al.*, 2005)
- (iii) Filler composition used i.e. same as material composition or different because if the filler composition is different it may result in galvanic cells on the weld surface (Folkmar Andersen *et al.*, 2006), and
- (iv) Change from homogeneous wrought material to heterogeneous cast structure which favours formation of biofilms (Partington, 2006; Sreekumari *et al.*, 2005)

CIP processes are not completely effective because of these hidden areas or “hot spots”.

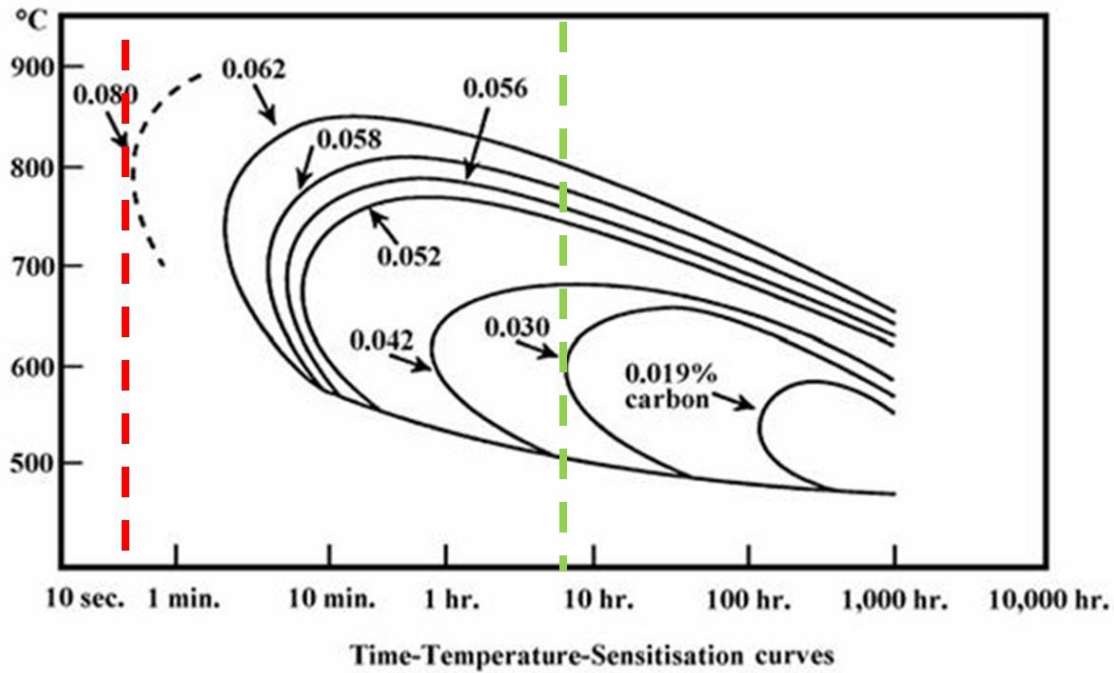


Figure 1.2: Effect of temperature over time on different carbon-grade SSs (Siebert and Stoecker, 1997)

Whilst welded areas normally constitute a very small part of the total area of the installation, incorrect welding and welding circumstances may lead to poor hygiene conditions in an otherwise hygienically well designed plant. Thus, a residual oxygen content of more than 1% in the baking gas (gas around weld after welding process) may lead to irregularities and burrs in the actual welding surface. Similarly, an initiating corrosion pocket may cause bacterial concentration pockets long before the actual corrosion is detected. Root defects in the welds must be avoided as they can lead to bacterial pockets (Verran, 2005).

The normal roughness of a well-performed weld is approximately 1.6–4 μm with maximum roughness accepted on product side being 6 μm (Verran, 2005). Corrosion supporting local bacterial biofilm concentration and potential collapse can significantly affect bacteria counts and impact on capital equipment life elsewhere, see Figure 1.3.

To avoid zones where biofilms can develop it is crucial that pipe selection, pre-welding and welding procedures be thorough to facilitate orbital welding. This can be achieved by:

- ✓ Choosing matching dimension pipes – commercial pipe (and bend) tolerances can introduce variations in material thickness (wall thickness), inside diameter, outside diameter, and ovality. For small diameter pipes it is difficult to control weld roots when they are mismatched (Partington, 2006)
- ✓ Matching chemical composition
- ✓ Parts that are to be welded must be square cut (not with a pipe cutter), sharp edged, deburred and thoroughly cleaned (Folkmar Andersen *et al.*, 2006)
- ✓ Welds should be carried out in an inert (argon) atmosphere to limit oxidation (Folkmar Andersen *et al.*, 2006)
- ✓ Use orbital welding as far as possible (Partington, 2006)

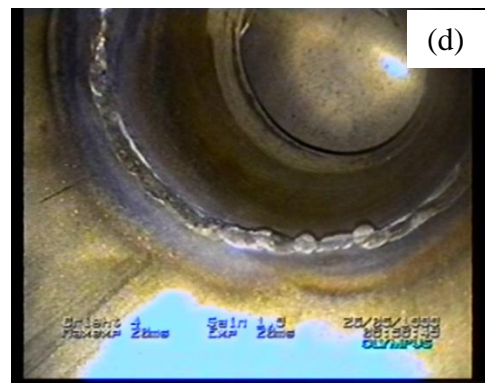
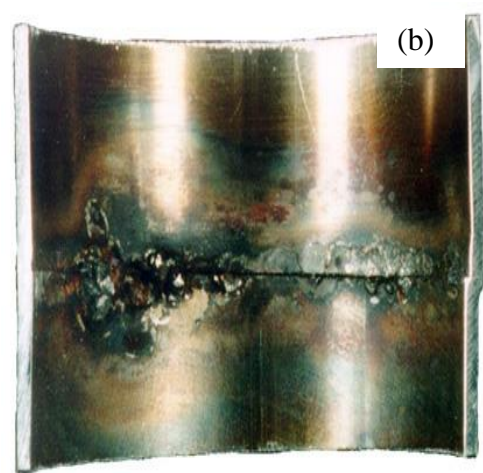
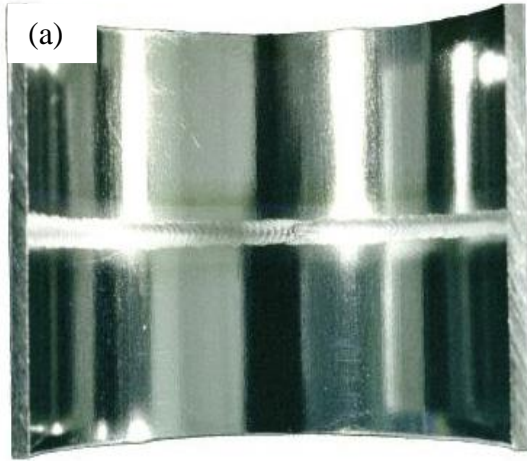


Figure 1.3: Examples of good and bad welds (Folkmar Andersen *et al.*, 2006). (a) is showing an ideal orbital weld on 316L electropolished SS showing full penetration with a uniform crevice-free inner weld bead with good alignment and internal diameter (ID) purged with argon (b) is showing manual weld showing defects which include lack-of-penetration, misalignment, huge crevice, and discoloration due to poor ID purge i.e. weld considered unacceptable by any sanitary standards (c) is showing good welds with gas protection, no discoloration and a flat uniform weld root, (d) is showing poor weld with insufficient gas protection

1.5.1. Pickling and passivation

Heat induced development of iron oxide resulting from inadequate oxygen purging is overcome by pickling followed by passivation to restore the original qualities of corrosion resistance and smooth surface pipes; however, the process may increase surface roughness (Cunat, 2007; Maller, 1998). Pickling is an aggressive chemical treatment typically comprising 90% nitric and 10% hydrofluoric acid at a suitable concentration for a specific time period (Maller, 1998; Partington, 2006). The intent is to remove existing oxidation, weld oxides scale and heavy contaminants. Passivation is a less aggressive treatment used to remove free iron and surface contaminants. The effects of the pickling process, composition and time of exposure are:

- Chemical polishing resulting from correct exposure of concentration with time (Cunat, 2007; Maller, 1998)
- Chemical etching resulting from over-exposure of concentration with time (Maller, 1998; Partington, 2006)
- Chemical milling resulting from extreme over-exposure with time (Cunat, 2007; Maller, 1998; Partington, 2006)

The latter two lead to undesirable surface roughness effects which favour biofilm formation (Cunat, 2007). Controlled passivation with nitric acid rebuilds the oxide surface. Pickling and passivation, if correctly applied and controlled, results in significant benefits to corrosion resistance; however, the process needs to be managed to avoid increasing surface roughness (Maller, 1998).

1.5.2. Effect of sulfur on welding

The element sulfur produces dramatic differences in the weld pool shape and penetration. These changes occur in the earlier specified concentration range specified for type 316 SS, see Figure 1.4 (Henon, 2008) and Table 1.4.

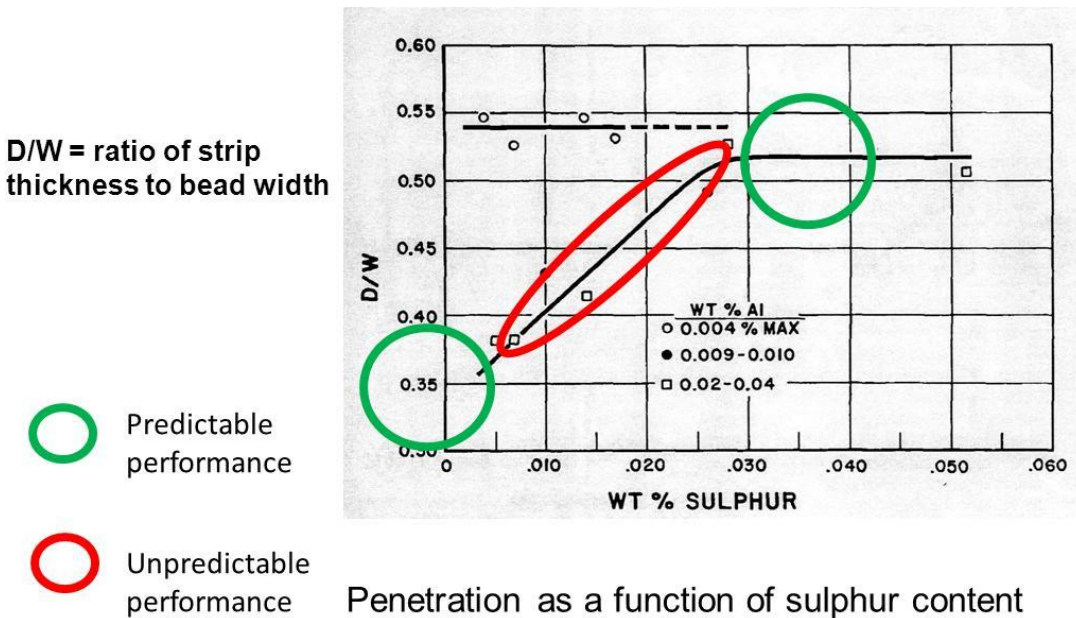


Figure 1.4: Effect of sulfur on weld penetration (Siebert and Stoecker, 1997)

If a SS tube with sulfur content range at the low end, i.e. below 0.005 wt%, is welded to a pipe/fitting at the upper end of the sulfur range (AISI specifies a maximum value of 0.030 wt%), the weld pool may shift towards the component with the lower sulfur concentration resulting in an unpenetrated weld (Henon, 2008).

Table 1.4: Change in sulfur concentration with time to mitigate its effects during welding (Siebert and Stoecker, 1997)

SAE designation	% Cr	% Ni	% C	% Mn	% Si	% P	% S	% N	Dates	Other
316L	16-18	10-14	0.03	2.0	0.03	0.04 5	<0.03	0.10	<1980	2.0-3.0Mo
316L	16-18	10-14	0.03	2.0	0.03	0.04 5	0.005- 0.017	0.10	2000	2.0-3.0Mo
316L	16-18	10-14	0.03	2.0	0.03	0.04 5		0.10	±2010	2.0-3.0Mo

Reducing the upper limit of sulfur has improved corrosion resistance and surface finish by limiting the number of manganese sulphide inclusions found in materials at the higher end of the AISI specification. However, electropolishing and corrosion resistance would be further improved by selection of materials with sulfur concentrations within the lower end of 0.005 wt%.

Manufacturers have responded by funding new research to decrease sulfur concentration and changing grade chemical specifications (see Table 1.4). Desulfurising of steels has led to a systematic reduction in sulfur effects over a 30 year period; however, capital equipment maintenance may need to accommodate these changing composition realities.

1.6.Motivation

Historically the term antifouling was associated only with biocidal compounds that had the potential to pollute the environment and required safety precautions to be undertaken whilst using them. But current antifouling strategies now focus on green, non-toxic technologies (Magin *et al.*, 2010). Whatever the material and mechanisms involved, one of the striking observations is the consistent incidence of MIC at and/or near welds and failures of SS occurring around or on welded areas (Sreekumari *et al.*, 2005).

Most species of bacteria produce colonies and spores which agglomerate in clusters. This provides resistance to conventional CIP chemicals or biocides such as chlorine. In other instances flocks of fine particles can entrap bacterial cells thereby protecting them from biocide attack (Hua and Thompson, 2000; Mamvura *et al.*, 2011). Ultrasound waves usually at low-frequency (high-power ultrasound) can inactivate bacteria cells and deagglomerate bacterial clusters through three processes (mechanical, physical and chemical effects) caused by acoustic cavitation in liquids (referred to as sonication). It is considered a 'green' technology that uses sound energy requiring no additional or reduced chemical quantity. The mechanism on microbial cells consists of cavitation phenomena and associated shear disruption (mechanical), localised heating (physical) and free radical (chemical) formation (Joyce and Mason, 2008). The advantages and limitations of using ultrasonic waves are described in Table 1.5.

Table 1.5: Advantages and limitations of using ultrasound waves (Fellows, 2000)

Advantages	Disadvantages
Effective against vegetative cells, spores and enzyme activity	Complex mode of action, not easily understood
Results in reduction of process times, chemical quantities and temperatures during CIP	Depth of penetration is affected by solids and air in the product (significant reduction in power delivered in solids or air)
Little adaptation required of existing processing plant	Unwanted modification to food structure and texture
There is increase in heat transfer	Possible damage of product by free radicals
There is a possibility of modification of food structure and texture	Needs to be used in combination with another process e.g. CIP or heating
Can be operated in time burst or continuously	It can have potential problems with scaling-up plant

The mechanical effects of high-power ultrasound in liquid have a dramatic effect on biological systems as micro-bubbles are formed. The imploding bubble produces high shear forces and liquid jets in the solvent that may have sufficient energy to physically damage the cell wall/membrane. Such collapse will also produce free radical species which are also capable of killing microorganisms.

On the other hand stable cavitation (bubbles that oscillate in a regular manner for many acoustic cycles) induce microstreaming in the surrounding liquid which can also induce stress in any microbiological species present resulting in cell death (Joyce *et al.*, 2010; Joyce and Mason, 2008; Nishikawa *et al.*, 2010; Oulahal *et al.*, 2004; Rajasekhar *et al.*, 2012). An important consequence of micro-convection induced by bubble collapse is a sharp increase in the mass transfer at liquid-solid interface and in the system, there are two zones where this ultrasonic enhancement of mass transfer will be important: (a) at the membrane and/or cell-wall and (b) in the cytosol i.e. the liquid present inside the cell (Joyce *et al.*, 2010; Joyce and Mason, 2008; Nishikawa *et al.*, 2010; Oulahal *et al.*, 2004; Rajasekhar *et al.*, 2012).

Due to these reasons, ultrasound waves were chosen for use in the study to access some hidden places during CIP cleaning especially near and on welds where there are geometrical discontinuities. The fact that there are three processes that occur almost at once increases the disinfection efficiency of the process. Ultrasound waves cannot replace CIP systems in food and beverage industry because the process is not 100% efficient but they can aid the process and at the same time reduce the chemical quantities and water required thereby making the whole process more environmentally-friendly. Elimination or efficient control of biofilms decreases the occurrence of MIC and equipment failure by dealing with the root cause of the problem at the source.

Concerns regarding biofilm control fall into two categories, existing process plants built under different anticipated operating circumstances (including overarching legislation) and new plants which take currently existing and foreseeable new operating circumstances into account. The work considered to date relates to management of existing plants. One aspect of new plants to be built was addressed, that of material selection, in particular tolerances specified for pipes.

1.7. Research gap

Ultrasound waves have been in use for a long time. Classical examples include their use in communication e.g. in bat navigation and dog whistles. Ultrasound waves are also used in medicine in foetal imaging, in underwater range finding (SONAR) for submarines and in non-destructive testing of metals for flaws. The basis for present-day generation of ultrasound waves was established as early as 1880 with the discoveries of piezoelectric effect by the Curries (Mason and Lorimer, 2002). Table 1.6 summarises some of the uses of ultrasound waves.

The destruction of microorganisms by power ultrasound has been of considerable interest in recent years. Early research in the field can be traced back to the work of Harvey and Loomis in 1929 who examined the reduction in light emission (related to bacterial kill) from a seawater suspension of rod shaped *Bacillus Fisheri* caused by sonication at 375 kHz at 19°C (Joyce and Mason, 2008).

Table 1.6: Some industrial uses of ultrasound waves (Mason and Lorimer, 2002)

Field	Application
Biology, Biochemistry	Used to rupture cell walls in order to release contents for further studies and in homogenisation
Engineering	Used to assist drilling, grinding, cutting; welding (both metals and plastics) and metal tube drawing. Useful for processing brittle materials like glass and ceramics
Dentistry	Cleaning and drilling of teeth, curing of glass ionomer fillings
Geography, Geology	Used in location of mineral and oil deposits and in depth gauges for seas and oceans by pulse/echo techniques. For echo ranging (SONAR)
Industrial	Dispersing pigments and solids in paint, inks and resins. Cleaning and degreasing engineering articles by immersion in ultrasonic baths. Acoustic filtration and metal casting
Medicine	Ultrasonic imaging is used in obstetrics, for observing foetus and guiding subcutaneous surgical implements. In physiotherapy, low frequency waves are used to treat muscle strains, dissolution of blood clots and cancer treatment
Agriculture	Used to improve germination of plant seeds i.e. increase germination and growth rates of seeds
Brewing industry	Used for clarification and stabilisation in beer production processes

Today it is applied in water and wastewater purification alone and in combination with other techniques, and surface decontamination (Joyce and Mason, 2008; Joyce *et al.*, 2010; Nishikawa *et al.*, 2010; Oulahal *et al.*, 2004; Rajasekhar *et al.*, 2012). Cavitation, the driving force in ultrasonic cleaning, has been experienced in different fields of study.

Pump cavitation or propeller cavitation are commonly encountered in process and marine industries respectively. Cavitation has been viewed as an unwanted phenomenon in these operations; however, it is now finding application in cleaning surfaces of equipment.

Ultrasonic cleaning has the advantage of reaching crevices and hidden surfaces without dismantling the instrument or component to be cleaned. Objects that can be cleaned range from large crates used for food packaging and transportation to delicate surgical implements such as endoscopes. Mason *et al.* (1996) suggested that ultrasound waves are more effective in cleaning surfaces than thermal processes as they lead to reduced processing times at the same temperatures. However, to date the process has not been successively applied in the food and beverage industry to help clean on and near welded surfaces (hot spots). Literature on use of ultrasound waves in cleaning surfaces (even SS surfaces) is available for experiments mostly done in laboratories but there has not been any focus found on cleaning welded or hidden areas or heat affected zones. This is the focus of this study.

1.8. Research Problem

Cleaning and sanitising chemicals are used to eliminate biofilms on equipment and processes in the food and beverage industry as part of automated (CIP) and manual systems. Formation of biofilms is prevalent especially on the inside surfaces of plant and equipment on and around welds or HAZ. In some cases these biofilms cause corrosion of the SS through MIC. Various questions that need to be answered arise and these include:

1. What constitutes the biofilms observed on surfaces; why and how do they form?
2. How can these biofilms be hygienically reduced or prevented, i.e. can other method(s) be used in conjunction with CIP systems to control or eliminate biofilm build-up? Ultrasound waves were chosen in this study due to reasons given in earlier sections
3. What are the safety, health and environmental implications during use of ultrasound waves to control biofilms?
4. What are the costs associated with the modifications to existing operational costs of using ultrasound waves generated from ultrasonic probes?

1.9. Research Aim and Objectives

The research project was established to solve the underlining problem of contamination through biofilm formation on SS surfaces in the food and beverage industry leading to corrosion as MIC. The main focus was in the brewing industry and on welds and weld affected areas. The challenges that had to be attained were set out as objectives which were summarised as follows:

1. To investigate the composition of water used in beer-brewing in relation to biofilm formation

2. To investigate the product composition (beer) in relation to biofilm formation
3. To determine the physical, chemical and biological composition of the biofilms observed on equipment surfaces in the brewing industry and understand the process of biofilm formation
4. To investigate the treatment on feed materials (mainly water) in relation to reducing biofilm formation and/or build up
5. To investigate the treatment methods applied to control biofilm formation and/or build up and increase corrosion resistance on the surfaces
6. To review the cleaning and sanitising chemicals and processes (CIP systems) currently used in brewing industry with a view for improvement

In this thesis:

- Objectives 1 and 4 were combined and presented in section 2.2
- Objectives 2 and 3 were combined and presented in section 2.1
- Objective 5 was presented in section 2.4, 2.5 and 4.1
- Objective 6 was presented in section 2.3 and 4.2.

1.10. Hypothesis

Biofilms attached to food-grade SS surfaces in food and beverage industries can be better controlled by using ultrasound waves at low frequency (high-power ultrasound) to supplement current CIP-systems.

1.11. Research Methodology

The research methodology for this study involved the following major tasks: review of the existing literature particular looking at formation, composition and methods on controlling biofilms; experimental design and materials selection for the two major experiments conducted; experimentation using coupons and pipe rig built; data analysis; a review of the costs associated with implementation of the process in industry; and conclusions and recommendations. These tasks were briefly discussed in the subsequent text.

1.11.1. Literature review

From the beginning of the chapter, introduction and subsequent discussions were focused on biofilms and their formation on food-grade surfaces, their composition, methods to control them and the implications on industry. The information from literature review served as the basis for formulating the experimental design for the two experiments conducted i.e. static and dynamic experiments.

1.11.2. Experimental design

SS 316L test coupons and pipes were used during the study for static and dynamic experiments respectively. Static experiments involved using coupons with three different welds where *E. coli* biofilms were grown under static conditions and ultrasound waves were used to remove these biofilms. The disinfection efficiency was measured for the normal surface against all welds to determine the effect of welding on biofilm formation and bacterial loading intensities. Results from those experiments were used to build a test rig which had pipes connected in series using 90°

elbows. There were a total of 12 welds all made using orbital welding (preferred in industry) with different pipe treatments during and after welding. All these treatments are used in industries, and the effect was to research their impact on biofilm formation process. Results from the studies were used to make conclusions about the CIP process, application of ultrasound waves to assist the process, and the costs associated with the modifications.

1.11.3. Data analysis

Laboratory tests and pilot scale test were conducted under different conditions and output data from these tests was used to determine the effectiveness of ultrasound waves in assisting CIP process.

1.11.4. Conclusions and recommendations

Conclusions were drawn from results determined during the study and the literature reviewed. Recommendations for future work was drawn up after questions were raised during experimentation and limits to experimental equipment observed.

1.12. Expected Research Outputs and Contributions

Listed below are some of the important research outcomes and contributions that were expected from this study:

- (i) Provision of the fundamental background information and concepts on the formation of biofilms in beverage plants

- (ii) Documentation of information on the formation of biofilms during beverage production and the effect of CIP process
- (iii) Documentation of information on the modified SS test coupons and real biofilms in pipes conducted to prevent biofilm build-up and increased corrosion resistance
- (iv) Documentation of the cost-effectiveness of the proposed integration of ultrasound waves to current CIP systems based on the data obtained in this study
- (v) Research data will be published in accredited ISI journals

1.13. Thesis layout

The thesis consisted of six chapters that seek to provide an answer to the aim and objectives set-out to be achieved at the beginning of the study.

Chapter one provided a basic introduction to the problem including problem statement, aim and objectives, hypothesis formulated and research outputs that would be gained from the study. Motivation behind the chosen method was given.

Chapter two provided an overview of literature review focussing on biofilm formation and its composition. This knowledge was vital so as to come up with the best solution to the problem that has continued to plague the beverage industry to date. The chapter also considered the main raw material (water) which had a significant impact on product quality as well as the treatment methods applied to it in relation to formation of biofilms in the brewing industry. Focus was given to the composition of the water at different stages and where the biofilms are most prevalent as a result

of contact with the liquid. Several methods to control biofilms formed on SS surfaces were reviewed and the best method was chosen for investigation.

Chapter three looked at the experimental review for the conducted studied using ultrasound waves and the test rig for final experiments. Justification for use of *E. coli* cells for static experiments and use of raw water for biofilm formation for the dynamic experiments were Biotrace ATP bioluminescence kit was used to test for bacteria (dead or alive) or product residues as biofilms. Ultrasound waves were able to deagglomerate and eliminate biofilms from SS surfaces.

Chapter four focussed on the results obtained whilst using the chosen method, major property which allowed biofilm formation (surface roughness); the effects of the chosen method on the surface profile of the SS and the way forward i.e. the pros and cons of the chosen method and the energy changes that occurred during treatment of SS surface with the chosen method i.e. efficiency of energy conversion during the process. Discussions of the obtained results were also undertaken to compare with literature. The chapter also looked at the combined use of the chosen method with CIP systems in existing plants and/or new plants.

Chapter five gave the conclusions from the study as well as the recommendations for future work thereby closing the thesis.

References were inserted at the end of each chapter, and Appendices were inserted at the end.

References

- Briggs, D.E., Boulton, C.A., Brookes, P.A. and Stevens, R. (2004) Microbiology. In: Brewing science and practice, D.E. Briggs., C.A. Boulton., P.A. Brookes and R. Stevens, Eds; Woodhead Publishing, Cambridge
- Cluett, J., Rowlands, D., Khanyile, D. and Hulse, G. (2003) Principles of hygiene in the beverage industry, The Institute of Brewing and Distilling (IBD)–Africa Section, Supreme Printers, Hout Bay, South Africa, ISBN: 0-620-31335-8, First Edition, pp. 1–12.
- Cunat, P-J. (2007) The welding of stainless steels: Materials and Applications Series. Euro Inox, Brussels, Belgium. Volume 3, 2nd Edition, ISBN 978-2-87997-180-3, pp. 2–36.
- Detry, J. G., Sindic, M. and Deroanne, C. (2010) Hygiene and cleanability: A focus on surfaces, *Critical Reviews in Food Science and Nutrition*, **50(7)**, 583–604.
- Elder, D., Budd, G. C. (2011) Overview of water treatment processes. In: Water quality and treatment – A handbook on drinking water. J. K. Edzwald (Ed), McGraw Hill, New York, 6th Edition.
- Fellows, P. J. (2000) Processing using electric fields, high hydrostatic pressure, light or ultrasound. In: Food Processing Technology – Principles and Practice (P. J. Fellows Ed), 2nd Edition, Woodhead Publishing Limited, Cambridge, England, pp. 210–227.
- Folkmar Andersen, J., Boye Busk Jensen, B., Boye-Møller, A. R., Dahl, M., Jepsen, E., Jensen, E-O., Nilsson, B., Olsen, B. and Thomsen, W. (2006) Design of piping systems for the food processing industry – with focus on hygiene, Danish Technological Institute, Kolding, Denmark, ISBN: 87-7756-750-1, pp. 1–29.

- Guillamet, R., Lopitiaux, J., Hannyer, B. and Lenglet, M. (1993) Oxidation of stainless steels (AISI 304 and 316) at high temperature. Influence on the metallic substratum, *Symposium C9, supplement to the Journal of Physics III*, **3**, 349–356.
- Henon, B. K. (2008) Considerations for orbital welding of corrosion resistant materials to the ASME bioprocessing equipment (BPE) standard, Stainless Steel American Conference, Unites States of America, 17 pages.
- Hua, I. and Thompson, J. E. (2000) Inactivation of *Escherichia coli* by sonication at discrete ultrasonic frequencies, *Water Research*, **34(15)**, 3888–3893.
- Joyce, E. M, and Mason, T. J. (2008) Sonication used as a biocide, A review: Ultrasound a greener alternative to chemical biocides, *Chemistry Today*, **26(6)**, 22–26.
- Joyce, E. M., Wu, X. and Mason, T. J. (2010) Effect of ultrasonic frequency and power on algae suspensions, *Journal of Environmental Science and Health Part A*, **45(7)**, 863–866.
- Jyoti, K. K. and Pandit, A. B. (2001) Water disinfection by acoustic and hydrodynamic cavitation, *Biochemical Engineering Journal*, **7(3)**, 201–212.
- Koparal, A. S. and Ögütveren, Ü. B. (2002) Removal of nitrate from water by electroreduction and electrocoagulation, *Journal of Hazardous Materials B*, **89(1)**, 83–94.
- Kunkel, D. (2009) Biofilm on a stainless steel surface, Dennis Kunkel Microscopy, Inc, http://www.ciriscience.org/ph_72-Biofilm_on_a_stainless_steel_surface_Copyright_Dennis_Kunkel_Microscopy, Accessed 18 Oct 2013.

- Magin, C. M., Cooper, S. P. and Brennan, A. B. (2010) Non-toxic antifouling strategies, *Materials Today*, **13(4)**, 36–44.
- Maller, R. R. (1998) Passivation of stainless steel, *Trends in Food Science and Technology*, **9(1)**, 28–32.
- Mamvura, T. A., Iyuke, S. E., Cluett, J. D. and Paterson, A. E. (2011) Soil films in the beverage industry: A review, *Journal of the Institute of Brewing*, **117(4)**, 608–616.
- Mason, T. J. and Lorimer, J. P. (2002) Introduction to applied ultrasonics. In: Applied sonochemistry: Uses of power ultrasound in chemistry and processing, T. J. Mason and J. P. Lorimer, Eds, Wiley-VCH Verlag GmbH & Co, Weinheim, Germany, pp.1–24.
- Mason, T. J., Paniwnyk, P. and Lorimer, J. P. (1996) The uses of ultrasound in food technology, *Ultrasonics Sonochemistry*, **3(3)**, S253 – S260.
- Medilanski, E., Kaufmann, K., Wick, L. Y., Wanner, O. and Harms, H. (2002) Influence of the surface topography of stainless steel on bacterial adhesion, *Biofouling*, **18(3)**, 193–203.
- Navarro, S., Pérez, G., Navarro, G and Vela, N. (2007) Decline of pesticide residues from barley to malt, *Food Additives and Contaminants*, **24(8)**, 851–859.
- Nishikawa, T., Yoshida, A., Khanal, A., Habu, M., Yoshioka, I., Toyoshima, K., Takehara, T., Nishihara, T., Tachibana, K. and Tominaga, K. (2010) A study of the efficacy of ultrasonic waves in removing biofilms, *Gerodontology*, **27(3)**, 199–206.

- Olajire, A. A. (2012) The brewing industry and environmental challenges, *Journal of Cleaner Production*, **In Press**, 1–21.
- Oulahal, N., Martial-Gros, A., Bonneau, M. and Blum, L. J. (2004) Combined effect of chelating agents and ultrasound on biofilm removal from stainless steel surfaces: Application to “*Escherichia coli* milk” and “*Staphylococcus aureus* milk” biofilms, *Biofilms*, **1(1)**, 65–73.
- Partington, E. (2006) Stainless steel in the food and beverage industry: Materials and Applications Series, Euro Inox, Brussels, Belgium, Volume 7, ISBN 2-87997-142-x, pp. 1–24.
- Pintar, A. (2003) Catalytic processes for the purification of drinking water and industrial effluents, *Catalysis Today*, **77(4)**, 451–465.
- Piyasena, P., Mohareb, E. and McKellar, R. C. (2003) Inactivation of microbes using ultrasound: a review, *International Journal of Food Microbiology*, **87(3)**, 207–216.
- Praeckel, U. (2009) Cleaning and disinfecting. In: Handbook of Brewing; Processes, technology, markets, H. M. Eßlinger, Ed, Wiley-VCH Verlag GmbH and Co, Weinheim, Germany, pp. 595–620.
- Rajasekhar, P., Fan, L., Nguyen, T. and Roddick, F.A. (2012) Impact of sonication at 20 kHz on *Microcystis aeruginosa*, *Anabaena circinalis* and *Chlorella* sp., *Water Research*, **46(5)**, 1473–1481.

- Shachman, M. (2005) Water treatment – The key process. In: The soft drinks companion, A technical handbook for the Beverage Industry, M. Shachman (Ed), CRC Press LLC, Florida.
- Siebert, O. W. and Stoecker, J. G. (1997) Materials of Construction. In: Perry's Chemical Engineers' Handbook, R.H. Perry, D.W. Green and J.O. Maloney (Eds), McGraw-Hill, USA. 7th edition, Chapter 28.
- Sreekumari, K., Sato, Y. and Kikuchi, Y. (2005) Antibacterial metals – A viable solution for bacterial attachment and microbiologically influenced corrosion, *Materials Transactions*, **46(7)**, 1636–1645.
- Taylor, D. G. (2006) Water. In: Handbook of brewing, F. G. Priest and G. G. Stewart (Eds), CRC Press, Boca Raton, pp. 91–135.
- Tverberg, J. C. (2001) Stainless steel in the brewery, *MBAA Technical Quarterly*, **38(2)**, 67–82.
- van der Bruggen, B. and Braeken, L. (2006) The challenge of zero discharge: from water balance to regeneration, *Desalination*, **188(1-3)**, 177–183.
- Verran, J. (2005) Testing surface cleanability in food processing. In: Handbook of hygiene control in the food industry (H. L. M. Lelieveld; M. A. Mostert and J. Holah, Eds), Woodhead Publishing Limited, Cambridge, England, pp. 556–572.

CHAPTER TWO

**"NOT EVERYTHING THAT CAN BE COUNTED COUNTS, AND NOT
EVERYTHING THAT COUNTS CAN BE COUNTED."**

- ALBERT EINSTEIN (1879-1955)

2. LITERATURE REVIEW

This chapter details the various processes used to prevent formation of biofilms or controlling already formed biofilms. The chapter starts with analysis of biofilms, their composition and how they form. This knowledge was vital so as to choose the best method that could be used to solve the current problem of biofilm formation under CIP process.

Water as it is the main ingredient in a beverage product (92 to 100% in beverages). This was vital knowledge as water can support biofilms which could contaminate product and product residues. Permissible treatment methods in line with food and beverage requirements were analysed and proposed. However, water treatment has been investigated thoroughly under food and beverage conditions and the best available method(s) have been proposed.

Methods to prevent and control biofilms on food-grade surfaces were analysed with a view to choose the best available method for implementation in plants already in operation. Methods applicable to new plants were also discussed. Comparison was done on the methods discussed to choose the best method for experimentation.

Finally thermodynamic analysis was conducted to try a model the chosen method (use of ultrasound waves to clean surfaces) to further understand how the process occur on the SS surface.

2.1. Biofilms in various industries

Part of this section was based on a paper published:

Mamvura, T.A., Iyuke, S.E., Cluett, J. D. and Paterson, A. E. (2011) Soil films in the beverage industry: A review, *Journal of the Institute of Brewing*, **117(4)**, 608–616.

In the food and beverage industry particularly in the brewing industry biofilms are a real, practical threat to hygiene and product quality, especially in the demanding world of draught beer (Quain and Storgårds, 2009). Residual matter derived from brewing materials, processes and the environment develop into biofilms on equipment surfaces and these become a threat throughout the brewing process (Cluett, 2001). It is estimated that biofilm formation costs approximately €250 million annually to the German brewing industry (Vaughan *et al.*, 2005). Biofilms are a well-organised and cooperating community of microorganisms attached together with organic and inorganic substances to a surface by the help of extracellular polymeric substances (EPS), which are produced by the microorganisms to form a single layer or three-dimensional structure (de Carvalho, 2007; Kokare *et al.*, 2009; Poulsen, 1999). Biofilms have been observed in different industries: they have been encountered in the medical industry (e.g. dental plaques on teeth, films on contact lenses, catheters, endotracheal tubes, prosthetic joints and mechanical cardiac valves), in the marine environment (e.g. fouling of ship hulls, ship and marine platforms, offshore rigs) and in the chemical process industry (fouling of membranes, heat exchangers, process vessels, pipes and product dispensing lines), resulting in poor hygiene and reduced product quality or sometimes

food contamination (Chambers *et al.*, 2006; Costerton, 2007; de Carvalho, 2007; Donlan, 2001; Flemming, 2002; Kumar and Anand, 1998; Poulsen, 1999; Zottola and Sasahara, 1994).

Materials often used in the food and beverage industry include plastics, rubber, glass, cement and SS with the capacity to support biofilm growth increasing from glass, SS, polypropylene, chlorinated PVC, unplasticised PVC, mild steel, polyethylene, ethylene-propylene to latex (van Houdt and Michiels, 2010). Stainless steels particularly austenitic grades 304 and 316 are the most commonly used food contact surfaces and grades 304L and 316L are often used due to less sensitisation after welding. L stands for low carbon. This is due to their chemical and mechanical or physical stability at various food processing temperatures, cleanability and high resistance to corrosion. Grade 316L has a higher resistance to corrosion by foods, detergents and disinfectants due to its anticorrosive properties from the added molybdenum as compared to 304L (van Houdt and Michiels, 2010).

Electron microscopy work has shown that biofilms can attach onto all types of surfaces e.g. plastic, soil particles, wood, medical implant materials, tissue, food products, SS, aluminium, glass, Buna-N and Teflon seals, and nylon materials; and that this attachment is facilitated by fimbriae, pilli, flagella with EPS acting to form a bridge between microorganisms and the conditioning film. Teflon, glass and nylon surfaces are smooth surfaces and the microorganisms appear to be attached, while SS surfaces have a rough appearance due to grain and grain boundaries, cracks and

crevices that can be sufficient to trap microorganisms responsible for biofilms (Kokare *et al.*, 2009; Kumar and Anand, 1998; Trachoo, 2003). Such a microstructure does not allow the escape of entrapped microorganisms due to shear forces of the bulk liquid and even the mechanical methods of cleaning may be inadequate to remove the trapped microorganisms (Kumar and Anand, 1998).

2.1.1. Biofilms

Biofilms in the brewing industry

All of the major raw materials used for brewing are potential sources of unwanted microorganisms, some of which could possibly be pathogenic. In addition, brewing aids such as finings, primings and filtration media, and containers (casks, bottles, etc.) can contribute contaminants (Hornsey, 1999). Figure 2.1 shows the brewing process and potential sources of microbial contamination.

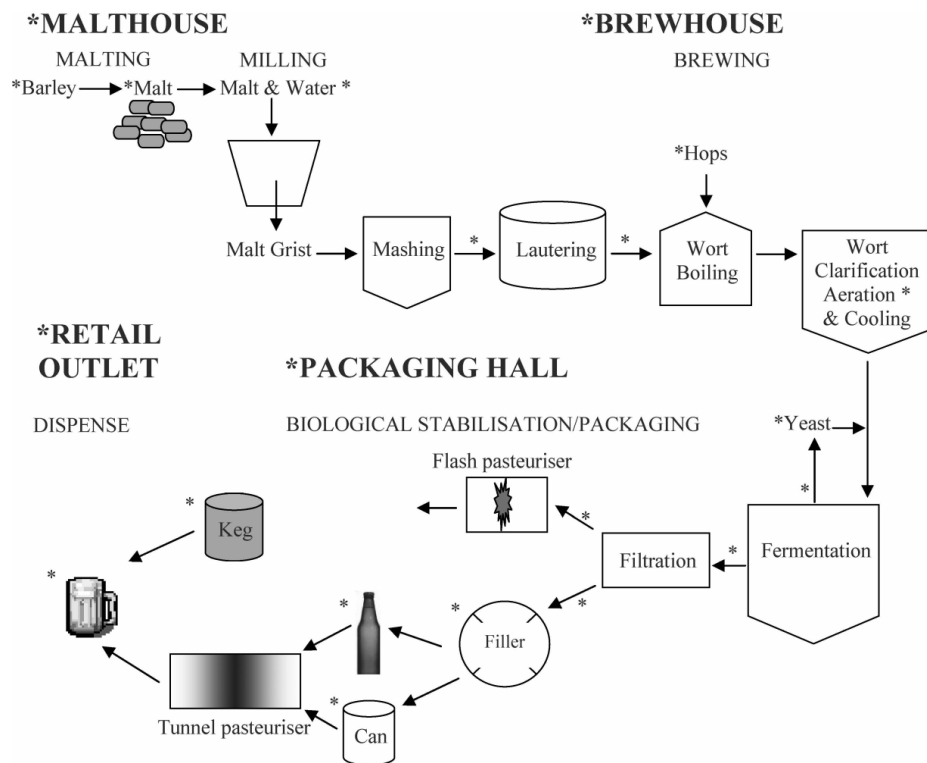


Figure 2.1: Basic scheme representation of the brewing process (Vaughan *et al.*, 2005). Potential sources of microbiological contamination are indicated by *

There are numerous operations involved in making beer, and each stage has a level of cleanliness that needs to be achieved from fouling encountered at that stage i.e. the cleaning challenges change throughout the brewing process:

- Malting – the biofilm is largely restricted to particulate materials and physical or visual cleaning requirements should be undertaken (Briggs *et al.*, 2004a)

- Wort production – the biofilm consists of proteins, dextrans, sugars, minerals, tannins and hop materials, therefore visual, chemical and microbiological cleaning requirements should be undertaken (Goode *et al.*, 2010)
- Wort boiling – scale is generated (beerstone or calcium oxalate) which become baked onto surfaces leading to visual and chemical cleaning requirements being implemented. There is no microbiological threat due to the high temperatures and so the plant is rendered microbiologically clean (Briggs *et al.*, 2004a)
- Wort cooling – the biofilm consists primarily of beer and yeast and as a result visual, chemical and microbiological cleaning requirements should be implemented (Goode *et al.*, 2010)
- Fermentation, conditioning, packaging and draught dispense – the biofilm is largely restricted to beer, yeast films and biofilms, and therefore chemical and microbiological cleaning requirements should be implemented at this stage (Briggs *et al.*, 2004a)

The initial phase of biofilm formation, attachment of microbes to a surface, is a fast process which takes only a few hours so it is hardly possible to disinfect frequently enough to avoid this initial step which may lead to the formation of biofilms especially in application fields like the brewing industry (Meyer, 2003).

Both wort and beer are prone to spoilage organisms, the former especially so since it provides a nutrient-rich, oxygenated environment required for microbial growth while beer has less nutrients, a low pH (3.8–4.7), contains alcohol from 3–7% by volume, which makes it less susceptible to

bacterial growth (Hornsey, 1999; Manzano *et al.*, 2011; Sakamoto and Konings, 2003; Suzuki, 2011).

Primary contaminants may originate from the environment, raw materials (e.g. malt, hops and adjuncts which can carry their own microbial contaminants), fermentation vessels and piping systems and brew house; and these may have a hand in biofilm formation, while secondary contaminants are introduced during bottling, canning or kegging (Vaughan *et al.*, 2005). Water as a brewing raw material is boiled during wort boiling, but later additions should be sterile to prevent contamination (Vaughan *et al.*, 2005). Microbes emanating from brewing liquor, malt and hops, and those found in wort will not survive the boiling stage, and together with the sterilisation of potable water to be used means that there are relatively few species of bacteria and fungi that cause spoilage problems; the list is restricted to a few wild yeasts and certain Gram-positive and Gram-negative bacteria (Hornsey, 1999).

Equipment used in the beer filling process is particularly prone to biofilm formation due to large volumes of water used for bottle rinsing, thereby creating an environment suitable for microbial attachment and accumulation on surfaces (Quain and Storgårds, 2009; Vaughan *et al.*, 2005).

Formation of biofilms

In order to have a thorough understanding of the dynamics and effects of biofilms, and to be able to design appropriate preventative or control measures, it is of significance to understand the natural processes of biofilm formation (Francolini and Donelli, 2010).

This formation can be grouped into four key stages: (i) initial attachment of organic and inorganic foulants, and charged ions resulting in a conditioned surface to neutralise surface charge that is likely to repel approaching microorganisms; (ii) attachment of microbial cells to the surface: this involves reversible attachment of microorganisms caused by weak interaction forces (van der Waals attraction, electrostatic, hydrophobic) between microbial cells and the surface followed by irreversible attachment of microorganisms caused by permanent bonding (dipole-dipole interaction, hydrophobic, ion-dipole, hydrogen, ionic bonding, covalent bonding and hydrophobic interaction) to the surface aided by the production of EPS; (iii) entrapment of inorganic and organic debris and nutrients in the system creating biofilms; and (iv) detachment of biofilms due to fluid shear stresses and aging of microbial cells (Chambers *et al.*, 2006; Characklis, 2009; Chmielewski and Frank, 2003; Francolini and Donelli, 2010; Kumar and Anand, 1998; Poulsen, 1999; van Loosdrecht *et al.*, 1990; Zottola and Sasahara, 1994). The irreversible attachment can take from 20 minutes to a maximum of 4 hours at 4–20°C (Chmielewski and Frank, 2003).

The conditioning process alters the physico-chemical properties of the surface including electrostatic charges, surface free energy and surface hydrophobicity (Francolini and Donelli, 2010; Kumar and Anand, 1998; Poulsen, 1999). Maximum attachment of biofilms depends upon high surface free energy and electrophoretic mobility or wettability of surfaces. Surfaces with high surface free energies such as SS and glass are more hydrophilic, generally showing greater bacterial attachment than hydrophobic surfaces such as teflon, Buna-N rubber and fluorinated hydrocarbon (Characklis, 2009; Chmielewski and Frank, 2003; Kokare *et al.*, 2009). The presence of multivalent cations (Mn^{2+} , Ca^{2+} , Mg^{2+} , Na^{+} and Fe^{3+}) has been shown to influence the attachment process, possibly by altering the surface characteristics or by bridging cellular anionic polyelectrolytes to anionic polyelectrolytes adsorbed on the wetted surface (Characklis, 2009; Donlan, 2002). Moreover, microorganisms tend to attach uniformly in a monolayer to hydrophilic surfaces (such as glass), while on hydrophobic surfaces (such as nylon and tin) they tend to adhere in clumps (Chmielewski and Frank, 2003).

Biofilms have also been examined under various hydrodynamic conditions such as laminar and turbulent flow. Films formed under laminar flow are found to be patchy with round cells, consisting of rough cell aggregates separated by interstitial voids, while those formed under turbulent flow are patchy, with elongated structures with streamers that oscillate in the bulk fluid (Chmielewski and Frank, 2003; Costerton and Wilson, 2004; Davey and O'Toole, 2000). Furthermore, biofilms formed in laminar flow have a low tensile strength and easily break, but

biofilms formed in turbulent flow are remarkably strong and resistant to mechanical breakage (Donlan and Costerton, 2002).

Another interesting point to note is that biofilms formed from single species *in vitro* and those produced in nature by mixed species consortia have been shown to exhibit similar overall structural features with some minor differences (Davey and O'Toole, 2000; Donlan and Costerton, 2002), with biofilms from mixed species being thicker, more compact and stable to environmental stress (Chmielewski and Frank, 2003; Donlan, 2002). This may be due to the production of a variety of EPS materials that result from the activity of different microorganisms (Kumar and Anand, 1998).

Composition of biofilms

Biofilms are composed primarily of microcolonies of different species of microbial cells (+15% v/v) and of matrix material (+85% v/v) (Costerton and Wilson, 2004; Donlan and Costerton, 2002; Kokare *et al.*, 2009). Researchers have been able to show that the EPS is mainly made up of polysaccharides (~24.5%) and proteins (~82.8%), polysaccharides existing in nature either as neutral or as polyanionic, as in the case for the EPS of Gram-negative bacteria (Characklis, 2009; Donlan, 2002; Flemming, 2002; Kokare *et al.*, 2009; Poulsen, 1999; Tian, 2008). The EPS also contains teichoic acid (secondary cell wall polymers), nucleic acids, phospholipids and other polymeric substances (Chaw *et al.*, 2005; Chmielewski and Frank, 2003). Intermolecular interactions between the various functional groups within the EPS macromolecules serve to

strengthen the overall mechanical stability of the EPS and, hence the survival of the enclosed microorganisms (Chaw *et al.*, 2005).

The composition of biofilms differ depending on the environment they are formed in, but the difference is usually small. The structure of biofilms, particularly the EPS, need to be understood as the mechanical stability of the EPS matrix has to be overcome in the cleaning process to eliminate and/or control biofilms (Flemming, 2002). The structure of the biofilm may be composed of the following:

- (i) Scaling or particle (inorganic) foulants: these may be deposits of inorganic precipitates of magnesium, calcium carbonate, iron oxides, silica, clay, mineral crystals, corrosion particles and other particles (Characklis, 2009; Donlan, 2002; Flemming, 2002; Kokare *et al.*, 2009; Kumar and Anand, 1998)
- (ii) Organic foulants: these may be deposits of organic substances e.g. oil, proteins, lipids, humic substances and EPS (Donlan, 2002; Flemming, 2002; Kokare *et al.*, 2009; Kumar and Anand, 1998; Xavier *et al.*, 2005)
- (iii) Biologically active foulants: these can be yeasts, moulds, viruses, fungi, spores, Gram-positive and Gram-negative bacteria that can adhere to surfaces and facilitate biofilm development (Baehni and Takeuchi, 2003; de Carvalho, 2007; Donlan, 2001; Flemming, 2002; Zottola and Sasahara, 1994). The microorganisms observed are almost in every physiological state known, from aerobic to anaerobic and from exponential to stationary phases of growth (Costerton and

Wilson, 2004) and they have a net negative surface charge usually behaving as hydrophobic particles (Chmielewski and Frank, 2003).

Inorganic and organic foulants usually originate from water and sometimes from other raw materials (e.g. proteins from the mashing process in the brewery industry; calcium and magnesium from brewing water) and fouling can be controlled by eliminating these foulants from the source. However, microorganisms are pseudo-particles, which can multiply, and pre-treatment to be done has to remove all the microorganisms, otherwise they will reattach, grow and actively multiply to form a colony of cells entrapping inorganic and organic debris, nutrients and other microorganisms, with their EPS resulting in biofilm formation again (Flemming, 2002; Kumar and Anand, 1998). The EPS has several functions. This includes facilitation of initial attachment of bacteria to a surface, formation and maintenance of microcolonies and biofilm structure, enhanced biofilm resistance to environmental stress and antimicrobial agents, and enabling the bacteria to capture nutrients (Poulsen, 1999). Most of the microorganisms in biofilms are aerobic, but anaerobic microorganisms are also present (Poulsen, 1999). Table 2.1 shows typical composition of biofilms observed on fouled surfaces.

Table 2.1: Composition of biofilms obtained from fouled surfaces experiencing excessive frictional losses (Characklis, 2009)

Component							%
Water							85.6
Volatile (organic) fraction							2.7
Fixed fraction							11.7
Total							100.0
Component (as % fixed fraction)	Si	Fe	Al	Ca	Mg	Mn	
%	7.0	18.5	7.5	1.0	2.5	59.5	

Table 2.1 showed that biofilms studied were mainly composed of water (85.6%), followed by inorganic foulants, mainly cations (11.7%) to stabilise the EPS and the film, and the rest was the organic fraction (2.7%). The composition of the inorganic fraction showed that Mn ions had the highest ratio (59.5%), followed by Fe ions (18.5%), and Al ions (7.5%).

Biologically active foulants

Biofilms consist of a complex consortium of microorganisms that provide niche environments for additional microbial communities (Vaughan *et al.*, 2005). Bacteria are the best-studied microorganisms with respect to colonisation of surfaces and subsequent biofilm formation, although fungi, yeasts, algae, protozoa and viruses have all been isolated from biofilms in industrial and medical settings (Lindsay and von Holy, 2006). The cell surfaces of most

microorganisms are anionic and this is normally due to the presence of negatively charged phosphate, carboxylate or sulphate groups in the cell wall or capsular or polysaccharide macromolecules (Škvarla, 1993). Most Gram-negative bacteria have long polysaccharide regions of their lipopolysaccharide and proteins exposed, resulting in a hydrophilic surface, while Gram-positive bacteria have the lipid portion of lipoteichoic acid extending outward from the cell, resulting in a hydrophobic surface (Trachoo, 2003). Gram-negative bacteria produce neutral or negatively charged biofilms, whereas Gram-positive organisms develop positively charged cationic matrices (Quain and Storgårds, 2009).

In vitro experiments have demonstrated that primary colonisers enable secondary bacteria to become part of the biofilms and in brewery biofilms, slime-producing *Acetobacteraceae* are considered as primary colonisers, providing favourable conditions for the aerotolerant, anaerobic and acidophilic *Lactobacillaceae* and the anoxic environment indispensable for *Pectinatus* and *Megasphaera* (Back, 1994).

As mentioned before, biofilms can be composed of moulds, viruses, fungi, spores, Gram positive, Gram negative bacteria and yeasts that can adhere to surfaces. However, it is common practice to differentiate brewery associated yeasts into *Saccharomyces* and non-*Saccharomyces* yeasts; and cultivation of independent analysis of brewery biofilms from bottling plants and adjacent areas has shown that yeasts are the dominating organisms of most biofilms (Timke *et al.*, 2008). Biofilms

formed by *Pseudomonas*, *Enterobacteriaceae*, *Lactobacillus*, *Acetobacter* and *Saccharomyces* have been frequently isolated and are well known in breweries (Zottola and Sasahara, 1994).

In another study conducted, most of the *Candida pelliculosa* strains showed biofilm formation on a microplate assay, but no *Saccharomyces cerevisiae* isolates were observed. Therefore, it was assumed that the *C. pelliculosa* species were involved in attachment and primary biofilm formation in beer bottling plants, while *S. cerevisiae* was a late coloniser of a preformed biofilm, and increased the beer spoiling potential of the biofilm (Timke *et al.*, 2008). Yeasts unable to multiply in beer can also cause problems, as they can attach to surfaces and become pioneer organisms for the development of biofilms. The species *Candida albicans* is well-studied biofilm-forming yeast (Timke *et al.*, 2005).

Also, other researchers have concluded that the primary colonisers could be non-beer spoiling Gram-negative bacteria (e.g. *Pseudomonas* species) and the secondary colonisers could be wild yeasts, particularly *Pichia anomala*, *Candida sake* and *Debaryomyces hansenii* (Quain and Storgårds, 2009; Timke *et al.*, 2008). Identity of wild yeasts recovered from biofilms, in and around the bottle filler of one brewery, showed that most were wild non-brewing strains of *S. cerevisiae* and *Pichia anomala*. In terms of attachment to surfaces, *P. anomala* can form biofilms, whereas the *S. cerevisiae* isolates are non-biofilm forming (Quain and Storgårds, 2009).

Alternatively, acetic acid bacteria and *Enterobacteria* accumulate in areas where process intermediate residues, beer or other products collect. These bacteria may not be harmful in the finished product by themselves but because they form slime (EPS), they protect accompanying microorganisms from dehydration and disinfectants (Vaughan *et al.*, 2005). If product residues are undisturbed for longer periods of time, yeasts begin to grow along with the acetic acid bacteria, producing metabolites that encourage LAB to grow (Vaughan *et al.*, 2005). The LAB produces lactic acid that can be metabolised to propionic acid by anaerobic species such as *Pectinatus* species and the cycle can result in a mixed species biofilm formation at the site (Back, 1994).

Outside of packaging, barley-associated biofilms have attracted attention as they have an important role in poor wort and in beer filtration after using contaminated grain (Quain and Storgårds, 2009). Beer that is commercially sterile on leaving a brewery and which is then dispensed at draught beer outlets can contain low levels ($\sim 10^3$ /mL) of planktonic or free cells (LAB and acetic acid bacteria and diverse yeasts) and this is a reflection of the biofilm within the dispense tubing, which slowly colonises lines from entry at the dispensing tap or the container end (Quain and Storgårds, 2009; Timke *et al.*, 2005).

Structure of biofilms

The presence of high levels of nutrients, macroscopic and microscopic deposits of food residues, and frequent stress from cleaning, sanitising or processing treatments in the beverage industry has

an influence on the biofilm structure (Chmielewski and Frank, 2003). In the past, biofilms were thought to be a compact structure, but recently studies have shown that they have a porous structure with capillary water channels to distribute water and nutrients and remove secreted waste (Costerton, 2007). The structure and architecture of the biofilm is dependent on the flow rate of the bulk fluid, the profile of the surface, the presence of poor and unhygienic welds and the number of different species involved (Poulsen, 1999), see Figure 2.2.

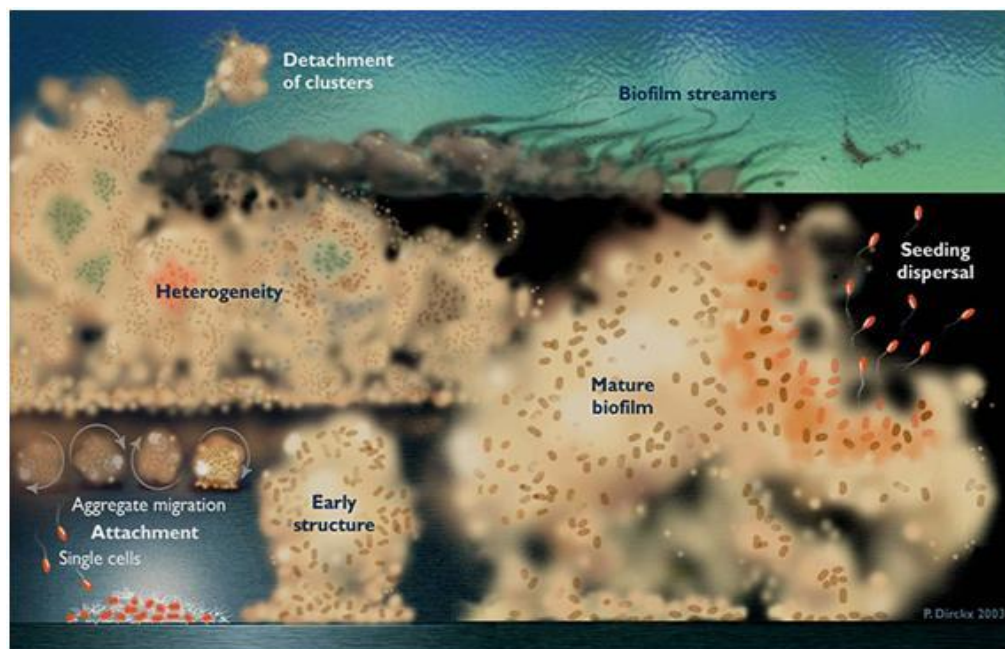


Figure 2.2: Conceptual drawing showing (front) attachment of planktonic cells and sequential stages of biofilm formation, including seeding and detachment (Costerton, 2007).

The figure shows the tendency to migrate (left) and to form mixed and integrated microcolonies (middle) for optimum metabolic cooperation and efficiency. The architecture of the biofilm is species-specific for single cultures and substrate-specific for multi-cultures. In heterogenic biofilms, the architecture is often irregular, probably due to the different growth and adherence patterns of the microorganisms (Poulsen, 1999). The thickness of biofilms is dependent on the flow rate, with maximum thickness obtained between laminar and turbulent flows (Poulsen, 1999). Furthermore, the thickness in the laminar zone is dependent on the substrate accessibility and on erosion in the turbulent zone (Poulsen, 1999).

Characterisation of biofilms

Biofilm development and structure can be analysed using various methods. This enumeration process helps to confirm the source and extent of contamination and the type(s) of microbial cells involved as contaminating agents (Kumar and Anand, 1998). The methods available can be divided into two broad categories, cultivation and microscopy.

Cultivation methods

These are conventional methods involving resuspending and redispersing biofilm cells, plating them onto a solid medium, incubating and counting (Kokare *et al.*, 2009; Wilson, 1996). The different methods used for sampling biofilms on external and internal surfaces are swabbing, rinsing, agar flooding, agar contact methods and sometimes scraping, vortexing or sonication (Donlan and Costerton, 2002; Kumar and Anand, 1998). These are quantitative methods that have been used frequently for years and they are generally inexpensive and easy to use, but they require appropriate media and culturing methods to be devised. Vortexing and sonication have the

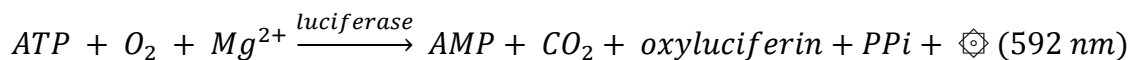
advantage of sampling internal and external biofilm cells, but the recovery efficiency is unknown (Donlan and Costerton, 2002). However, these techniques can be abrasive to attached cells and may result in injury, which could, in turn, result in viable but non-culturable cells (Lindsay and von Holy, 2006). Thus, most of these techniques normally incorporate a resuscitation step of several minutes to allow for cell recovery (Lindsay and von Holy, 2006).

Swab plating: In this method, moistened swabs or sponges are used to remove microbial cells from the surfaces. The sample liquid is then plated onto an agar plate or a selective medium, incubated, and then colonies are enumerated and identified if desired. The advantage of this method is that with selective media, specific bacteria, yeast, and moulds can be isolated and identified, but it is time consuming and also microorganisms may be selectively removed from the surface (Chmielewski and Frank, 2003).

Contact plating: Contact plating directly samples a surface by pressing a plate of solidified agar against the surface. This method is simpler than swabbing, but it is not possible to sample irregular or rough surfaces. The limitations of the method depend on how much pressure is applied to the agar, contact time, presence of soil, and if the agar picks up the contaminating microbial cells. In addition, microorganisms do not quantitatively adhere to the agar surface upon application, again resulting in selection for a specific microorganism or underestimating microbial numbers on the sampled surface (Chmielewski and Frank, 2003)

Adenosine triphosphate bioluminescence test: The universal presence of adenosine triphosphate (ATP) in living organisms and the reaction of this adenosine compound, with the substrate luciferin

and the enzyme luciferase, with the subsequent emission of visible light (562 nm) have provided a means of rapidly assessing the microbial status of an organism. Many foodstuffs, including beer, naturally contain adenosine triphosphate (ATP) as a biological residue and this has to be allowed for when interpreting results (Hornsey, 1999). The biochemical reaction is based on the enzyme that causes the tails of fireflies to glow, and requires the presence of oxygen and Mg^{2+} :



where AMP is adenosine monophosphate and PPi is inorganic pyrophosphate

This is a rapid biochemical method for estimating the total ATP collected by swabbing a surface, which is related to the amount of food residues and microorganisms collected by the swab, with a result obtained within seconds. However, the ATP bioluminescence test cannot detect low levels of microorganisms. More than 10^3 bacteria or 10^1 yeast cells must be collected by the swab to have positive results (Verran and Jones, 2000). The amount of light produced is measured using an illuminometer and is directly proportional to the amount of ATP (or microorganisms) present. ATP presence can also be due to dead organic material as well as viable organisms, and so the bioluminescence technique can also evaluate a general lack of hygiene (Hornsey, 1999). However, some researches have demonstrated that the bioluminometer measurements can be affected by chemical cleaning agents and commercial sanitisers (Costa *et al.*, 2006).

A number of instruments using ATP bioluminescence principles are commercially available; however, results from different instruments are not comparable (Carrick *et al.*, 2001). ATP reacts with the luciferin-luciferase enzymatic complex and the light emitted is measured by a bioluminometer and expressed in Relative Light Units or RLU (Costa *et al.*, 2006). The higher the amount of ATP on the surface or food samples, the higher the light output expressed in RLU (Costa *et al.*, 2006).

The somatic (food) cell ATP is destroyed by using detergents to lyse the cells and ATPase to destroy the ATP or to remove microbial cells from the sample by filtration prior to extracting their ATP (Caprita and Caprita, 2005). However, the most widespread application of ATP measurement is as a hygiene test to monitor the cleanliness of food production areas. For this, the surface is swabbed and the total ATP on the swab is extracted using chemicals and measured (Caprita and Caprita, 2005). In this application, it does not matter whether the ATP is derived from food residues or from microorganisms because both are indicative of an inadequately cleaned surface.

In food processing, there is often little value in trying to directly correlate microbial surface counts to ATP measurements since the ratio between microbial number and food debris is not constant and does not provide a strong mathematical correlation between both techniques. On internal surfaces of equipment in food and beverage industries, high ATP counts and low microbial counts are found; therefore, an increase in product residues can increase the bioluminescence

measurement but not the microbial number (Costa *et al.*, 2006). Similarly, ATP counts on raw food surfaces increase with higher increases in microbial numbers.

Microscopy methods

Microscopy methods involve using light, epifluorescence, differential interference contrast (DIC), transmission electron (TEM), scanning electron (SEM), atomic force (AFM) and confocal scanning laser microscopy (CSLM) (Chmielewski and Frank, 2003; Donlan, 2002; Kokare *et al.*, 2009; Kumar and Anand, 1998; Trachoo, 2003). The use of CSLM and epifluorescence microscopy requires the organisms in biofilms to be stained with fluorescent stains (Kokare *et al.*, 2009). Before the use of CSLM, electron microscopes were the preferred method of choice to examine microbial biofilms under high resolution. Unfortunately, sample preparation for electron microscopy resulted in dehydrated samples and as a result this provided a deceptively simplistic view of biofilm structure, since the biofilm collapsed when water was removed (Davey and O'Toole, 2000).

Epifluorescence microscope: The applications of this method include determination of viable cells, biofilm cell arrangement, microcolony formation, cell morphology, biofilm pH, and distribution of chemicals in biofilms (Trachoo, 2003).

CSLM: This is an improved version of an epifluorescence microscope, where viability can be determined by staining the transformed cells with a membrane impermeable fluorescent dye (Trachoo, 2003). CSLM needs digital imaging methods to create computer reconstructions of the chemical and physical conditions within the microenvironment of the bacterial communities

(Lindsay and von Holy, 2006). CSLM has been used to greater effect to characterise biofilms, as it allows direct observation of hydrated samples, producing three-dimensional structures.

AFM: This is a non-invasive microscopic technique capable of imaging surfaces at nanometre resolutions. Furthermore, as no stains or coatings are needed in this method, biofilms may be observed in situ (Lindsay and von Holy, 2006).

There is no practical method for quantitative determination of biofilm microorganisms in the beverage industry environment. This is because swabs and sponges do not quantitatively detach firmly adherent microorganisms. However, they provide useful information on the extent of microbial growth on a surface and on the extent to which cleaning has been effective (Chmielewski and Frank, 2003). The effectiveness of biofilm removal and control can be monitored using ATP-bioluminescence for rapid results or plate count procedures for sensitive results.

From the section, knowledge about formation, composition and characterisation of biofilms was gained and it was used to design experimental designs for the experiments done. The next section was to analyse the effect of water with respect to formation of biofilms.

2.2. Water analysis with emphasis on biofilm formation

Large amounts of water are used by breweries with actual amounts ranging from 4 to 11 hl water/hl beer (as measured from breweries in three African countries), but the accepted international best

practice benchmark is 6.5 hl/hl and the best technology level is 4 hl/hl (Braeken *et al.*, 2004; Feng *et al.*, 2009; Fillaudeau *et al.*, 2006; Olajire, 2012; Sturm *et al.*, 2012). The amount of water lost by evaporation and which comes out with by-products is relatively small which implies that large volumes of wastewater are produced (Olajire, 2012). However, brewery wastewater treatment is often minimal with the wastewater disposed-of and this affects receiving water bodies threatening water supplies of other users and neighbouring communities. Water scarcity has increased the focus on the use of wastewater as a resource by treating and recycling it back to production facilities or being used more efficiently by the next user e.g. agricultural or industrial.

2.2.1. Water used in the brewing industry

Brewery water functions

The main concern with groundwater is the presence of dissolved contaminants such as salts, organics, or gasses (Tansel, 2008). The salts may be dissolved from the previous strata through which it passes, meaning the water recovered from underground can be either soft or hard in contrast to surface water which will be comparatively soft. Historically, different regions became famous for particular types of beers and in part these beer types were defined by the water available for brewing. Water supplies may vary in their salt content imparting different tastes, and as such breweries have to adjust the composition of the water they use (Eumann, 2006).

Different grades of liquors are required at different stages of brewing. At some stages the ion content of water may need to be adjusted to be suitable for use whilst other stages require little or no bacterial count or oxygen. Different functions of water can be categorised as:

- Brewing liquor – water used as an ingredient to the beer; it is used in wort production and for standardisation to target alcohol content such as in high-gravity brewing (Eumann, 2006)
- Process water – water used for cleaning, rinsing and sterilisation of process vessels and pipework, pasteurisation and refrigeration. It should be of potable standard ideally softened and the Cl₂ level should not exceed 100 ppm to avoid corrosion of SS pipework (Taylor, 2006). All cleaners, detergents and sanitisers/disinfectants are diluted with water before being used. The salt composition of this water is important because Ca and Mg salts determine the hardness of the water while several heavy metals like Fe and Mn can react with complexing agents in the cleaners causing corrosion as they are important components of the water's redox system (Loeffler, 2006).
- General purpose water – water used for general washing down, site hygiene or office use and generally requires no further on-site treatment (Taylor, 2006)
- Service water – water used for boiler feed where it should not produce scaling i.e. it must be softened or fully demineralised with chloride content less than 50 ppm to avoid corrosion of SS (Eumann, 2006)

2.3.Clean-in-place systems used to control biofilms in food and beverage industry

Biocides and disinfectants have been the principal weapons used in combination with CIP systems to control unwanted biofilms and these agents work by destroying biofilm microorganisms, a strategy that is rendered ineffective by the reduced susceptibility of these microorganisms to antimicrobial challenges due to EPS (Chen and Stewart, 2000, Mamvura *et al.*, 2011). Oxidising agents like Cl₂ and peroxyacetic acid are normally used to try and penetrate the EPS.

2.3.1. CIP systems

In the brewing industry, any type of cleaning not directly involving hand scrubbing is referred to as CIP (Loeffler, 2006). In CIP systems, all functions for cleaning and disinfection are computer-controlled with chemical additions, cycle times and cleaning/rinsing cycles automatically programmed, monitored and recorded. The chemicals, equipment and procedures are designed and controlled so that the results are reproducible; and the cleaning solutions are recovered and reused as much as possible with discharge to the sewage system minimised and/or neutralised. The benefits of automated cleaning via CIP systems are: (a) consistent and repeatable cleaning results, (b) safe operation without much exposure to employees, and (c) an economical operation (Loeffler, 2006).

Theoretical aspects of cleaning

Biofilms are of significance to brewing for two reasons: (a) once formed they are difficult to remove, and they can act as permanent sources of contamination capable of seeding successive

batches of product and (b) analysis of suspended microbial counts may dramatically underestimate the true magnitude of contamination (Mamvura *et al.*, 2011). Usually assessment of contamination is based on measurement of free-living population but hygiene tests should be based on the swabbing of surfaces rather than analysis of rinse water (Briggs *et al.*, 2004a; Mamvura *et al.*, 2011). Cleaning regimes must be sufficiently vigorous to prevent biofilms forming i.e. turbulent cleaning regimes should be used during cleaning (Briggs *et al.*, 2004a).

Biofilms adhere to surfaces in very complex ways as they can be trapped mechanically in pores, cracks or other inclusions which have led to the use of hard-surface materials such as finished SS (Mamvura *et al.*, 2011). The sum of all binding forces combined can be expressed as the adhesion energy that has to be overcome during the cleaning process to remove biofilms attached to surfaces (Loeffler, 2006).

CIP basics

In industry, the operations of cleaning and disinfection are essential parts of the production process and the efficiency with which these operations are performed greatly affects the final product quality. Most cleaning regimes include removal of loose biofilms with cold or warm water followed by the application of chemical agents, rinsing and disinfection (Ferreira *et al.*, 2010).

Use of automatic scrubber or high pressure during cleaning is more effective in removing biofilms than gel cleaning or low pressure cleaning; however, high pressure cleaning may cause more

hygiene problems by spreading surviving microbes via aerosols (Meyer, 2003). Other ways of applying mechanical forces that do not generate aerosols are slowly running foam on vertical surfaces or turbulent flow in closed systems. Any kind of mechanical action will not only improve cleaning results, but will also result in increased microbial kill, when disinfectants are used (Meyer, 2003). The more mechanical energy is put into the removal of biofilms, the more efficiently the films are removed leading to an efficient cleaning process; however, there should be a limit as too much mechanical action may cause damage to the surface leading to increased bacterial loading (van Asselt and te Giffel, 2005).

Cleaning can vary depending on the amount and nature of the biofilms involved from aggressive (e.g., hot caustic solutions) to mild (e.g., occasional acid rinse), but the sequence of events is always a four step cycle of: pre-clean rinsing, clean, post-clean rinsing and sanitisation (Lewis and Bamforth, 2006). CIP procedures normally take about 35 minutes and are carried out in an auto-cycle (Davey *et al.*, 2013; Simões *et al.*, 2010). A typical CIP cycle is shown in the Table 2.2.

Table 2.2: Typical CIP programmes used in the brewery, with programmes adapted to the part of the process to be cleaned, and some of the steps: alkali, acidic, or disinfection being left out (Czechowski and Banner, 1992; Goode *et al.*, 2010; Mertens, 2009; Storgårds, 2000)

Action	Conditions	Purpose
Pre-rinsing	Cold or hot, 5–10 mins	Water is used to remove bulk soil by dissolution and/or shear force leaving surfaces less fouled
Alkali cleaning; NaOH	Cold or hot (60–85°C), 0.1–2wt% NaOH, 10–60 mins	Circulation of alkali-based chemicals to dissolve and remove remaining materials (usually any proteins deposited on surfaces) and kill microbes
Intermediate rinsing	Cold or hot, 10–30 mins	Circulation of water/chemicals to neutralise pH and remove traces of remaining alkali chemicals and materials
Acidic cleaning; H ₃ PO ₄ , HNO ₃ or H ₂ SO ₄ acid (1–2%)	Cold, 10–30 mins	Circulation of acids around the clean plant to kill remaining microbes and remove any encrusted salts
Intermediate rinsing	Cold or hot, 10–30 mins	Circulation of water/chemicals to neutralise pH and remove traces of remaining chemicals and materials
Disinfection	Cold, 10–30 mins	

-by disinfection solution	85–90°C, 45–60 mins	Circulation of solution around the clean plant to kill remaining microbes
-by hot water		Circulation of hot water around the clean plant to kill remaining microbes
Final rinsing if necessary	Cold, 5–10 mins	If necessary, disinfectant at low concentration or sterile water rinse to remove remaining traces of the chemical

The acid step also aids in the removal of traces of alkaline product from equipment surfaces, enhances draining and drying and provides bacteriostatic conditions that delay the growth of any remaining microorganisms (Bremer *et al.*, 2006). Many situations require the occasional use of acid cleaners to clean surfaces soiled with precipitated minerals or having high mineral content. Increasing the effectiveness of the caustic step may reduce the amount of acid required during acid cleaning and the need to use sanitisers. This is done by using caustic blends and caustic additives which contain surfactants, emulsifying agents, chelating compounds and complexing agents (Bremer *et al.*, 2006).

CIP mechanics

To ensure removal of gross soil and avoid its sedimentation, the minimum flow velocity through the CIP and transfer piping should be 1.5 m/s but a higher value of 2 m/s is recommended with the Reynolds number (Re) of the flow in the turbulent regime ranging from 10 000 to 30 000 to ensure good radial mixing, heat transfer (uniform heating), mass transfer (of cleaning chemicals and soils)

and momentum (scouring action of eddies) transfer (Chisti and Moo-Young, 1994; Czechowski and Banner, 1992; Lorenzen, 2005).

The CIP piping should be free of dead spaces as much as possible; if unavoidable, the depth of the dead zone must be less than two-pipe diameters to ensure adequate cleaning using CIP techniques (Chisti and Moo-Young, 1994).

Assuming the cleaning detergent in a process line has a velocity of 2 m/s, a T-section with a length equal to the diameter of the main pipe line will receive only 15% of this velocity, which is 0.3 m/s leading to a dead zone (Lorenzen, 2005).

Steps in biofilm removal process

According to Loeffler (2006), the process can be divided into four major steps:

1. Transport of the cleaning solution to the biofilm with complete wetting of the film
2. Chemical reactions and physical processes that occur during the cleaning process:
 - a. Reaction of the cleaning solution with hard water constituents and/or suspended biofilms
 - b. Convective and diffusive transport of the cleaning agents from the cleaning solution to the biofilm
 - c. Wetting or transport of the cleaning agents within the biofilm itself

- d. Reaction of cleaning solution with the biofilm, both chemically and physically
 - e. Diffusive transport of soil particles removed during the cleaning process
3. Removal of the biofilm from the surface and transfer into the cleaning solution via emulsification
 4. Preventing re-depositing of removed biofilms through stabilisation in the cleaning solution and transport of removed biofilms away from the surface

2.3.2. Parameters influencing cleaning efficiency

Three major groups of parameters which influence the cleaning efficiency are: (a) equipment parameters, (b) system parameters, and (c) operational parameters.

Equipment parameters

These are determined during the planning and construction phase of the brewery for optimal sanitation by avoiding parts or areas that cannot be in contact with cleaning solutions. Materials with high chemical compatibility, smooth surfaces and minimal electrostatic binding forces from relevant soil particles should be chosen for use in the brewing industry i.e. materials should be resistant to cleaning and sanitising chemicals (Briggs *et al.*, 2004b; Loeffler, 2006).

System parameters

These can be defined as factors that are determined through regular operation of the brewery such as chemical composition and quantity of biofilms as well as the quality of the process water used, particularly the water hardness.

Operational parameters

These are subdivided into four parameters that influence the overall cleaning efficiency:

Chemical properties

Chemical properties of cleaning agent: composition, concentration, pH, surface tension, activity and type of agent (cleaning agent should dissolve rapidly and completely in water) acting quickly on biofilm or deposits like proteins, fats, beer scale, hop resins, burnt yeast, trub, pulp (Ferreira *et al.*, 2010; Holah, 1992; Lelièvre *et al.*, 2002; van Asselt and te Giffel, 2005). The cleaning agent should also have a high soil-carrying capacity and be easy to flush off with water; not foam, and be compatible with other materials used in the plant (Lorenzen, 2005). Chemical agents like surface active agents or alkali compounds used as detergents work by suspending and dissolving contaminant residues, decreasing the surface tension of emulsifying fats and denaturing proteins, but they are currently used as a combination (Maukonen *et al.*, 2003).

Mechanical properties

Mechanical properties of the cleaning agent, such as flow velocity (range 1.5–4 m/s), Reynolds number, pressure (minimum 3–5 bars) and volume flow (Lelièvre *et al.*, 2002; Lorenzen, 2005; Praeckel, 2009; van Asselt and te Giffel, 2005). Mechanical action (water turbulence and scrubbing) are recognised as being highly effective in eliminating biofilms (Chmielewski and Frank, 2003; Maukonen *et al.*, 2003).

Temperature

Temperature of the cleaning agent, i.e. hot or cold cleaning should be considered. High temperatures can reduce the need for physical force and results in increased efficiency; however, pre-rinse steps above 40°C are not recommended since biofilms containing proteins or starch will undergo chemical changes at these temperatures and thus impede the subsequent washing steps i.e. at temperatures above 80°C proteins coagulate, resulting in an increase in fouling instead of a decrease (Carpentier and Cerf, 1993; Chmielewski and Frank, 2003; Lorenzen, 2005; van Asselt and te Giffel, 2005). In addition, cleaning at temperatures above 80°C results in higher energy consumption use without extra cleaning benefit and may lead to equipment damage due to corrosion (van Asselt and te Giffel, 2005).

Contact time

Contact time of the cleaning agent i.e. the longer the contact time, the greater the number of microorganisms inactivated resulting in greater the success and in most cases there is a direct link between contact time and concentration (Holah, 1992; Lelièvre *et al.*, 2002; Lorenzen, 2005; Praeckel, 2009; van Asselt and te Giffel, 2005). An optimal cleaning process may be obtained through carefully combining and/or interchanging selected parameters.

Cleaning procedures

An effective cleaning process must break up or dissolve the EPS associated with the biofilm so that disinfectants can gain access to the viable cells (Carpentier and Cerf, 1993; Gibson *et al.*, 1999; Mamvura *et al.*, 2011). The cleaning process can remove 90 % or more of microorganisms associated with the surface, but cannot be relied upon to kill them. However, bacteria can redeposit

at other locations and, given time, water and nutrients can form biofilms meaning disinfection must be implemented (Gibson *et al.*, 1999; Mamvura *et al.*, 2011; Srinivasan *et al.*, 1995). Disinfection is the use of antimicrobial chemicals to destroy microorganisms and its aim is to reduce the surface population of viable cells after cleaning and prevent microbial growth on surfaces before restart of production (Maukonen *et al.*, 2003). However, disinfectants do not penetrate the biofilm matrix left on a surface after an ineffective cleaning procedure, and thus do not destroy all living cells in biofilms (Holah, 1992; Carpentier and Cerf, 1993).

Organic matter such as food residues, milk stone, fat, carbohydrates, and protein based materials can interfere by reacting with the biocide, leaving a reduced concentration of antimicrobial agent for attack on microorganisms (van Asselt and te Giffel, 2005). Interfering organic substances, pH, temperature, water hardness, chemical inhibitors, concentration and contact time generally control the efficacy of disinfectants (Mosteller and Bishop, 1993; Cloete *et al.*, 1998). The disinfectants must be effective, safe and easy to use, and easily rinsed off from surfaces, leaving no toxic residues which affect the sensory values of the product or should not be harmful to the consumers' health.

CIP sanitisers

The most important components in CIP sanitisers and their properties are as follows:

- Alkalis (such as NaOH and/or KOH), soda ash, sodium hydrogen carbonate, sodium metasilicate and trisodium phosphate act as major components for removing the organic

component of biofilms like fats and proteins (Briggs *et al.*, 2004b; Chmielewski and Frank, 2003). They can be used in combination with sequestrant or chelators and anionic wetting agents which are compatible with acid or alkali cleaners (Chmielewski and Frank, 2003)

- Complexing or chelating agents react with Ca^{2+} and Mg^{2+} ions in the water preventing the precipitation of water hardness
- Surface active ingredients (surfactants, wetting agents) such as anionic, cationic, amphoteric and non-ionic surfactants, depending upon the electrical charge, are used for the removal of water-insoluble biofilms as well as to reduce the surface tension of water
- Acids such as phosphoric acid, nitric acid, amidosulfonic acid, urea nitrate, urea phosphate, and other organic acids are primarily used for removal of inorganic biofilm deposits like precipitated minerals or high food residue/mineral content such as milkstone (Chmielewski and Frank, 2003)
- Oxidisers such as sodium hypochlorite, hydrogen peroxide, sodium percarbonate or other oxygen donors are used to chemically modify deposits through oxidation
- Defoaming agents such as special alkalene oxide derivatives may be used to suppress foaming
- Corrosion inhibitors, often of a complex organic nature are used to protect materials from chemical attack
- Enzymes, such as proteases may be used for special cleaning applications such as membrane cleaning
- Sequestrants, such as sodium phosphate derivatives, are often required to chelate minerals depending on water hardness (Chmielewski and Frank, 2003)

- Non-ionic wetting agents are used in some formulations since they are good emulsifiers and control foaming

Most manufactures recommend that surfaces like glass, ceramic and SS be cleaned with alkali or non-ionic detergents, and that SS be cleaned with alkali or acid detergents (Chmielewski and Frank, 2003). For plastics, alkali cleaners and non-ionic detergents are recommended with detergent solutions being applied at temperatures between 40 and 90°C depending on soil type and the risk of re-deposition. Cleaning is best done with soft water (or with cleaners formulated to sequester calcium) as this avoids the deposition of “beer stone” on surfaces (Lewis and Bamforth, 2006).

2.3.3. Types of CIP systems

The four most commonly used CIP systems are:

Single-path CIP system

This system is commonly used in the pharmaceutical industry where a freshly made-up cleaning solution is supplied to the plant, and then drained with no residual circulation in the cleaning system. The single path system is used when there is a high degree of soiling or when it is critical to prevent cross-contamination (Lorenzen, 2005).

Single-use CIP system

This system is used when there is a high degree of soiling or when cross-contamination must be avoided with the volume of cleaning solution in the system low. A freshly made-up cleaning solution is supplied to the plant, circulated and then drained (Praeckel, 2009).

Recovery CIP system

This system allows for multiple uses of concentrated cleaning solutions encompassing several cleaning tasks to be carried out simultaneously. The cleaning plant is installed centrally and the cleaning solution is stored after circulation with large circulation volumes in the cleaning system (Lorenzen, 2005).

Satellite CIP system

This method combines recoverable and single-use cleaning systems where the cleaning solution can be used more than once, and several cleaning tasks can be carried out simultaneously and at different temperatures if necessary. The cleaning solution is supplied from a main CIP station to different single-use CIP systems in different sections of the plant, independently circulated in the different plant sections, and then drained or returned to the main CIP station. The circulation volumes in the cleaning system are low to average, and the main installation is centralised, with satellite systems set up where needed around the plant (Lorenzen, 2005; Praeckel, 2009).

In the food and beverage industries different CIP paths are used depending on the knowledge gathered during its construction. All these paths are in existence and this gives variations on the effectiveness of the CIP process. However, during dynamic experimentation, single use CIP system was used and it was combined with ultrasound waves.

2.4. Controlling biofilms in the food and beverage industry

Effective microbial destruction is imperative in food processing as a single report of contamination could put the reputation and future success of a manufacturer at risk (Piyasena *et al.*, 2003). Most species of bacteria produce colonies and spores which agglomerate in clusters offering resistance to conventional biocides such as chlorine; or in other instances flocks of fine particles can entrap bacterial cells thereby protecting them from biocide attack (Hua and Thompson, 2000; Mamvura *et al.*, 2011).

2.4.1. Strategies employed to control biofilms

Several strategies to control biofilms exist, namely: (i) mechanical cleaning of product residues, (ii) use of antimicrobial agents or biocides to control biofilms, (iii) removal of essential nutrients, (iv) inhibiting microbial attachment to a surface by modifying the SS surfaces, and (v) promoting biomass detachment (Francolini and Donelli, 2010; Xavier *et al.*, 2005). The primary objective of any treatment process is for the removal of product residues which indirectly leads to the removal, control and elimination of biofilms in the process (Mamvura *et al.*, 2011). Mechanical cleaning and antimicrobial agents are the most-used methods; however, mechanical cleaning can be costly, as it typically involves equipment down time or a significant labour expenditure (Xavier *et al.*, 2005). Also, it may not be applicable due to inaccessibility of the fouled surface.

Ultrasound waves which help in detaching biomass on the surfaces were chosen in this study because they inactivate and deagglomerate bacterial clusters through physical, mechanical and

chemical effects. Ultrasound waves are considered to be green technology as they do not result in environmental pollution (Joyce and Mason, 2008). There are several critical processing factors that have to be considered when using ultrasound waves: (a) the nature of the ultrasound waves i.e. amplitude and frequency, (b) the exposure time on the microorganisms, (c) the type of microorganisms, (d) the volume of food to be processed, (e) the composition of the food, and (f) the temperature and physical conditions of the medium (Butz and Tauscher, 2002; Piyasena *et al.*, 2003; Santos *et al.*, 2009). During the study some of these factors were investigated and others controlled.

2.4.2. Treatment and prevention of biofilms

The primary objective of a treatment process is the removal of product residues. Indirect removal of these residues is also a first critical point in the removal, killing and control of biofilms (van Houdt and Michiels, 2010). On the other hand, equipment design is important to control or eliminate biofilm formation on contact surfaces, but poor design can make the task difficult, especially when using mechanical treatments in cleaning, which have proved to be efficient in the removal of biofilms on good designs (Kumar and Anand, 1998). An overview of the situation and possible modules available for the design of specific and effective countermeasures is summarised in Figure 2.3.

Many countermeasures have been proposed in the literature, but the focus will be on four methods: (i) surface modification (biomimicry), (ii) use of silver ions and (iii) use of ultrasound waves.

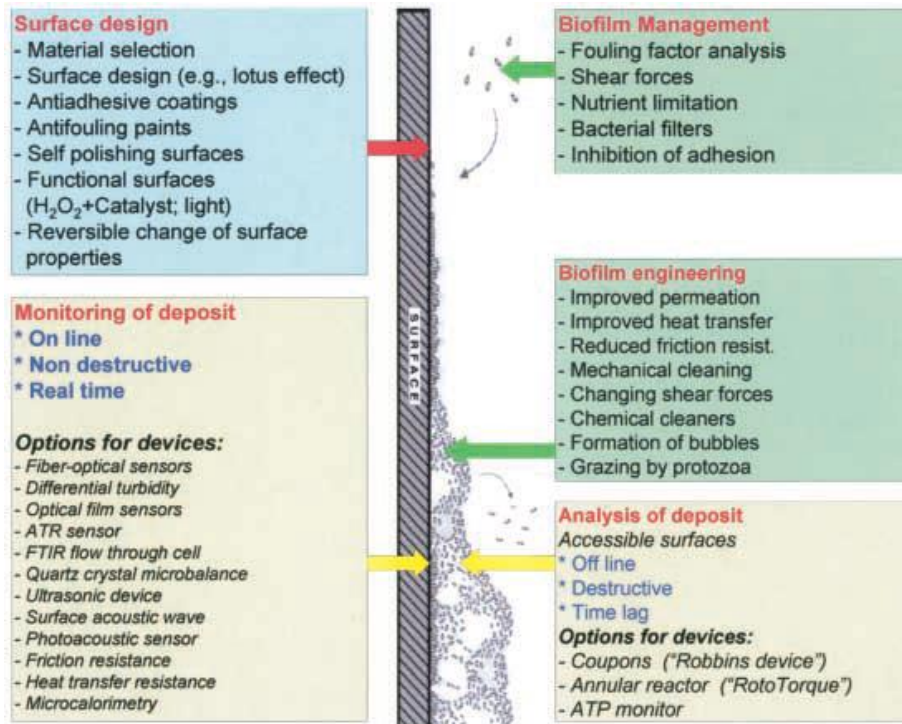


Figure 2.3: Elements of an integrated antifouling strategy (Flemming, 2002)

Surface modification (Biomimicry)

The term biomimicry deals with bio-inspired based designs, implying the use of the natural world as a model to base an engineering development or device for hierarchical structures (Chambers *et al.*, 2006). Innovations in materials science have led to a range of new products that can hinder microbial attachment to surfaces (Quain and Storgårds, 2009). Surface modification techniques have greatly improved in recent years with the ability to produce discrete, highly ordered surface

features on the micro- or nano-scale, to more accurately define this biological-surface interface, as this allows for the isolation of specific dimensions of feature geometry that may be dominant in inhibiting settlement of microorganisms (Schumacher *et al.*, 2007b). However, dimensional differences between target species makes combating microbial fouling a challenging task and necessitates the individual examination of each fouling organism for species-specific fouling control (Schumacher *et al.*, 2007b).

There are natural surfaces that are able to resist accumulation of biofilms using a combination of chemical and physical structures. Marine organisms such as sharks, mussels and crabs have natural antifouling defences, as does the endothelium of a healthy artery. However, these surfaces can lose their antifouling characteristics due to age, injury or disease (Magin *et al.*, 2010). Sharks have placoid scales, which have a vascular core of dentine surrounded by an acellular enamel layer similar to teeth (Magin *et al.*, 2010). A bio-inspired surface, Sharlet AF™, a design containing 2 µm wide rectangular-like ribs, periodic features (4, 8, 12 and 16 µm) in length and spaced at 2 µm, managed to reduce *Ulva* settlement by 86% as compared to a smooth surface (Carman *et al.*, 2006). This design was inspired by the nano- and microscopic patterns of a shark skin. These dimensions are smaller than the average diameter of the *Ulva* spore body (~5 µm), showing that the width and spacing of a topographical feature necessary to deter biofilm formation can be tailored to the size of the organism (Magin *et al.*, 2010). This means that antifouling strategies that exploit surface

topography can typically be based on a consideration of the length scale of the settling body of each targeted fouling organism (Schumacher *et al.*, 2007b).

It can be hypothesised that narrower channels and pillar spacing smaller than the dimensions of the microorganisms involved may be effective in reducing the settlement of the microorganisms (Schumacher *et al.*, 2007a). This indicates that an interaction exists between roughness measurements and feature spacing that must be considered when designing topographic surfaces (Schumacher *et al.*, 2007a). These engineered surface topographies have defined and ordered structural features that are tailored to the identified critical dimensions (i.e. feature width, spacing and height) of the fouling microorganisms of interest (Schumacher *et al.*, 2007b). The proposed criteria to identify topographical feature limits of a surface are: (i) the microorganisms must be forced to remain on top of the protruded topographical features and not be able to settle between features (feature spacing), (ii) the microorganisms must not be able to stabilise its entire mass on one single feature (feature size), and (iii) if the microorganism is bridged between two topographical features, it must not be able to contact the floor between features, i.e. the number of attachment points must be minimised (Scardino *et al.*, 2006).

On the other hand, surfaces can be designed to facilitate removal of a biofilm when it does occur. Surfaces may foul at the same rate, but the force required to remove fouling microorganisms can be markedly different (Scardino *et al.*, 2009). Research has shown that the only surface parameter

that strongly correlates with fouling removal is waviness; with the highest waviness profiles having the weakest fouling adherence (Scardino *et al.*, 2009). Researchers have also suggested that there is an inverse relationship that exists between the percentage of biofilm cells inactivated after exposure to antimicrobials and the width of crevices (i.e. roughness) on attachment surfaces (Lindsay and von Holy, 2006).

Use of silver ions

Several attempts have been made over the years to protect materials, instruments and equipment by plating, painting and application of enamel. Protection of surfaces include: addition of a non-adhesive or antimicrobial coating, release of a toxic agent at the surface, introduction of surface modifying additives and addition of biocidal substances (de Carvalho, 2007). Introduction of organic or inorganic compounds to superficial coatings or biocidal agents within the surface material to create antimicrobial surfaces may directly inactivate the microorganisms attached to the surface and/or prevent their adhesion. This entails that a suitable biocide should be selected to provide a broad activity against the microorganisms commonly found in the target application area and may be added to polymers during its manufacture (de Carvalho, 2007). Some natural materials such as silver are non-selective antimicrobials that are active against a broad range of aerobic, anaerobic, Gram-negative and Gram-positive bacteria, yeasts, filamentous fungi and viruses (Dong *et al.*, 2010).

One researcher reported that a titanium-silver alloy showed high antibacterial activity and good biocompatibility. However, although silver alloyed stainless steels showed less bacterial adhesion than their silver-free counterparts, the low solubility (<0.03%) of silver in SS can be an obstacle to bulk alloying. In addition, all these approaches produce a thin silver-containing layer (<0.2 μm) on soft substrates, which makes it difficult if not impossible to ensure high durability and antibacterial properties simultaneously (Dong *et al.*, 2010). With silver (0.042%), antimicrobial steels were shown to reduce the number of adhering bacteria by 99% compared to normal SS (Quain and Storgårds, 2009). Regrettably this effect declined with time and further work is required to explore this opportunity further (Quain and Storgårds, 2009).

The development in the synthesis of nanoparticles (NPs), and their numerous potential applications, has opened up new possibilities for engineering. Various nanometre sized metal and metal oxide particles can provide antibacterial properties, and silver NPs seem to be particularly attractive, due to excellent antimicrobial efficiency of silver itself that has known for a long time (Radetić *et al.*, 2008). The antimicrobial mechanism of the NPs is not known, but it can be assumed that it is similar to the ions, and this is due to their small size and high specific surface area, which makes them extremely reactive with the environment (Kaali *et al.*, 2011). Layers of silver produced by sputtering silver metal in a controlled atmosphere under different conditions to produce silver NPs species have been produced and studied and significantly higher bactericidal properties than simple Ag^+ solutions have resulted. This is due to the hypothesis that Ag^+ ions are responsible for the antimicrobial activity of silver, even as NPs (Fan and Bard, 2002).

Silver exerts its antimicrobial effect by progressive elution from the devices. Silver concentration of 100 µg/L, achieved by adding silver nitrate in solution is deemed safe for human consumption by the World Health Organization and the Environmental Protection Agency (Silvestry-Rodriguez *et al.*, 2008) and sub-millimolar concentrations of AgNO₃ are reported to be lethal to a range of bacterial species, both Gram-positive and Gram-negative. When silver ions bind to biological molecules containing thio, amino, carboxylate, imidazole, or phosphate groups, they inhibit activities that are vital to the microorganisms' regulatory processes and cause inactivation of microorganisms or they can displace other essential metal ions (Chaw *et al.*, 2005) such as Ca²⁺ and Zn²⁺. The exact mode of action is unknown, but Ag⁺-treated bacteria exhibit a characteristic initial stimulation in respiration before cell death occurs (Holt and Bard, 2005).

Use of ultrasound waves

In food processing industries a division is made between low-power and high-power ultrasound: (i) low-power ultrasound (high frequency between 2 and 10 MHz, intensity, $I < 1 \text{ W cm}^{-2}$) is concerned with the physical effect of the medium on the wave typically used for analytical purposes (ii) high-power ultrasound (low frequency between 20 and 100 kHz, $10 \leq I \leq 1000 \text{ W cm}^{-2}$) is used for cleaning, plastic welding and for sonochemistry by generating cavitation within liquid systems (Ince and Belen, 2001; Laborde *et al.*, 1998; Santos *et al.*, 2009). High-power ultrasound which has the ability to cause cavitation has uses in food processing to inactivate microbes (Ince and Belen, 2001). Cavitation, observed in the presence of ultrasound waves, is the formation and

subsequent dynamic life of bubbles in liquids subjected to a sufficiently low pressure (Li-xin *et al.*, 2008).

To achieve 100% disinfection with ultrasound waves only, it is necessary to use high ultrasonic intensities. This makes the technique relatively expensive to use for general large-scale decontamination; however, there is a drive towards the use of ultrasound alone or in combination with other inexpensive and relatively simple techniques to remove biofilms (Joyce and Mason, 2008). Ultrasound waves can be used associated with: (i) temperature – thermosonication, TS, (ii) pressure – manosonication, MS, or (iii) pressure and temperature together – manothermosonication, MTS (Piyasena *et al.*, 2003) leading to effective biofilm control on SS surfaces.

The mechanism of ultrasound interaction with microbial cells consists of cavitation phenomena and associated shear disruption with high-pressure spots of $P < 100$ MPa, short but intense localised heating $T < 5000$ °C and free radical formation through collapse of bubbles (Götz *et al.*, 2005; Joyce and Mason, 2008; Laurent *et al.*, 2009). Ultrasound waves generate heat by absorption of the ultrasonic energy in the propagation medium and ultrasonic bio-effects may be produced by this thermal mechanism (Miller, 1987). Brief exposure to ultrasound waves can cause thinning of cell walls which is attributed to the freeing of the cytoplasm membrane from the cell wall (Figure 2.4) and the apparatus used for this purpose is an acoustic horn (probe) system operating at low

frequency e.g. 24 kHz. The apparent chemical effects in liquid reaction media are either direct or indirect consequences of these extreme conditions experienced during cavitation (Hoffmann *et al.*, 1996).

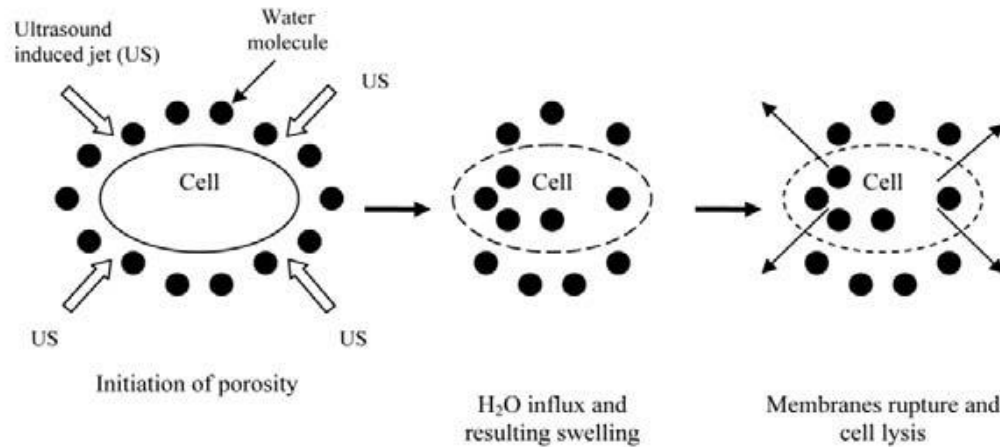


Figure 2.4: Mechanism of ultrasound waves-induced cell damage (Joyce and Mason, 2008)

Inactivation by ultrasound waves indicates that the action of ultrasound is dependent upon the frequency used but can be summarised in terms of mainly mechanical effects at low frequencies and mainly chemical effects at high frequencies, or a mixture of these at intermediate frequencies (Wu *et al.*, 2012).

The three control strategies mentioned above have their pros and cons and comparisons are made (Table 2.3).

Table 2.3: Comparison of the three technologies of biofilm control

Technique	Surface Modification	Use of Silver	Use of ultrasound waves
Objective	Inhibition and control	Control of biofilms	Control of biofilms
Mode of operation	Surface features inhibit settlement and adhesion of target microorganisms	Ag ⁺ ions target vital activities to cells resulting in inactivation of microorganisms	Mechanical, physical and chemical effects inactivate target microorganisms
Cost	Expensive to construct the mould with designed surface features	Cheap to produce Ag nanoparticles but expensive to plate, coat or alloy onto the surface	Cheap to use but expensive to mount probes along SS pipeworks and vessels
Area of application	Existing and new plants	Existing and new plants	Existing and new plants
Toxicity	Zero toxicity levels	Toxicity levels to be adhered to	Low toxicity due to radicals
Scale up	Difficulty in scale up	Relatively ease to scale up	Ease to scale up

2.4.3. Water treatment methods in the brewing industry

Most breweries find it necessary to treat incoming water to remove dissolved and suspended solids, and microorganisms that may be present in it as these may lead to formation of biofilms (Mamvura *et al.*, 2011). Microorganisms are a problem whether alive or dead because alive they can multiply at logarithmic rates and dead they are a source of pyrogens which contaminate beer (Madaeni, 1999; Mamvura *et al.*, 2011). In general water should be free of microbes, suspended matter, pesticides, other organic compounds, nitrates to help prevent nitrosamine formation or odorant chemicals which can cause flavour taints while certain ions should have a limit ($\text{Fe} < 0.5 \text{ mg/L}$ and $\text{Mn} < 0.3 \text{ mg/L}$).

The treatment processes applied can be grouped into various categories, namely: chemical, thermal or physical (mechanical) methods. Chemical methods involve adding various strong chemical oxidants to water to remove or reduce inorganic ions and microorganisms (basis of CIP systems); thermal methods involve applying heat energy to raise the temperature of water up to the required value to reduce inorganic ions, dissolved gases, organic matter and microorganisms; while physical processes involve manipulating physical properties like size or density to disinfect water by targeting mainly inorganic salts, organic matter and microorganisms (Al-Juboori *et al.*, 2010; Chaidez *et al.*, 2007; McDonnell and Russell, 1999; Momba *et al.*, 2000). In general, physical methods are preferred as they are very reliable and leave no residue behind; however, they cannot always be applied owing to restrictions such as temperature, safety of personnel and design of the equipment (van Asselt and te Giffel, 2005). In processing plants combination of two or more of

these processes is made use of to achieve optimum results and as a result most methods can be classified under two of the above three processes.

Water in breweries may be sterilised more than once at different stages and it can either be chemical or physical sterilisation (van der Kooij, 2003). Some of the chemical sterilants used are quaternary ammonium compounds (QACs), chlorine (Cl_2), chlorine dioxide (ClO_2), ozone (O_3), hydrogen peroxide (H_2O_2) and, less often, silver ions (Ag^+) while some of the physical sterilants used are exposure to ultraviolet light, sterilisation filtration and, rarely (except during the hop-boil), heat (Chaidez *et al.*, 2007; McDonnell and Russell, 1999; Momba *et al.*, 2000). All chemical sterilants used must be handled with care as they can be dangerous if exposed during use. Chemical treatment methods are applied either as stand-alone technologies or as an integral part of the treatment process with physical and/or thermal treatment methods (Cheremisinoff, 2002).

The treatment processes can also be categorised as primary, secondary or tertiary methods, whereby primary methods are undertaken at the beginning of the treatment followed by secondary methods and finally tertiary methods. Primary methods include screening, flocculation, sedimentation or filtration to remove colloidal and suspended solids, fats, oils and grease; secondary methods are applied to remove dissolved solids using ion exchange, reverse osmosis or membrane processes, deaeration and carbon adsorption; and tertiary methods are used for disinfection often achieved by chlorination, ozonation or ultraviolet radiation (Johns, 1995;

Momba *et al.*, 2000; Reid, 1998; Tansel, 2008). The distinction used varies from literature to literature but the results are normally almost the same.

Disinfectant efficiency depends on the type of microorganism, concentration, contact time, turbidity and temperature; and to minimise bacteriological risks, it is necessary to identify the optimal conditions in which a disinfectant can act at its maximum capacity (LeChevallier *et al.*, 1988; McDonnell and Russell, 1999).

2.5.Surface functionality of stainless steel surface profiles in food and beverage industry

Surfaces can be divided into two categories, functional and non-functional. A non-functional surface can either be mirror smooth or sandpaper rough without influencing the quality of the part e.g. the outside of a pipe where the surface has no specific function. A functional surface is required to perform a function that is related to the user's perception of the part's quality, see Table 2.4.

There are three broad categories of production processes that can influence surface topography: (i) material removing processes e.g. turning, grinding, honing, etching; (ii) material adding processes e.g. plating, painting, plasma coating; and (iii) forming processes e.g. rolling, shot peening, burnishing (Mummery, 1992).



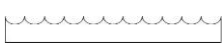
Table 2.4: Relationship between surface function and quality (Mummery, 1992)

Function	Criterion for Quality	Examples
Bearing	Low friction, wear	Crankshaft journal
Conduction	Large contact area	Electrical switch
Decoration	Consistent light reflection	Automotive body panel
Adhesion	Roughness, surface area	Sheet steel
Friction	Sharp peaks, low contact area	Driving roller
Sealing	Large contact area, low wear	Piston ring

Surface profile characteristics can be broken down into six categories as shown in Table 2.5. Form, waviness, and roughness are the main concerns in general manufacturing.

The problem with surface topography assessment is not with the measurement of the actual surface profile; rather it is the assignment of a numerical value to the surface that will give the user meaningful and universally acceptable information about it. However, certain parameters used to assign numerical values to surface deviations are presented in Appendix I.

Table 2.5: Classification systems for form deviations according to DIN 4760 (Mummery, 1992)

Form deviation	Examples	Examples of causes
Shape deviations 	Deviations from straightness, flatness, roundness, etc.	Faults in machine tool guide-ways, deflection of machine or workpiece, incorrect clamping of workpiece, hardening distortion, wear
Waviness 	Undulations	Eccentric clamping, deviations in the geometry or running of a cutter, vibration of the machine tool or tool chatter
Roughness 	Grooves	Form of tool cutting edge, feed or in-feed of tool

2.5.1. Surface profile changes during treatment with ultrasound waves

Austenitic SSs have been used in various components and facilities of the food and beverage industries because of their excellent corrosion resistance and ease of cleanability. Welding processes are used to join pipeworks together which are then used in the beverage industries. However, weld regions are particularly attractive to microbes as the welding process alters the material surface characteristics. Adhesion of bacteria to SS surfaces in aqueous media or humid environments is the initial step in the formation of biofilms which are known to cause problems such as MIC or they represent a chronic source of microbial contamination (Mamvura *et al.*, 2011;

Medilanski *et al.*, 2002). As the microorganisms grow on substratum surfaces, they produce various metabolic by-products, which can promote deterioration of the underlying substratum. These reactions are referred to as biocorrosion or MIC when the underlying substratum is a metal or metal alloy like SS. The magnitude of the problem of MIC necessitates a wider attention that might encompass collaboration between established research groups or laboratories specialising on researches on various aspects of metal microbe interactions viz. microbiology, metallurgy, civil and environmental engineering and biotechnology (Sreekumari *et al.*, 2005).

AFM has today become an essential tool to study surface structures down to atomic scale that can encourage biofilm formation on SS surfaces; and studies have led to the conclusion that rough SS surfaces are more prone to corrosion which can lead to the apparition of pitting and crevices, increasing the adhesion possibilities of the microorganisms and decreasing the cleanability of the surface (Detry *et al.*, 2010).

Frequency and thermal stress on SS surfaces

When a bubble collapses near the surface, it yields a micro-jet which impinges on the surface causing either erosion or fracture and when the cavity rebounds, it produces a shock wave which adds to this erosion. However, in both cases the elastic limit of the solid is crossed and erosion occurs in the plastic regime (Gandhi and Kumar, 1994). The impact of a micro-jet formed at the moment of a cavity collapse has a major role in causing erosion on neighbouring solid materials as this can lead to stress waves being generated on the SS when collapse impingement acts on its

surface resulting in material damage (Haosheng and Shihan, 2009). However, the magnitude of the shearing stress will decrease with distance from the impacting point i.e. if bubble implosion occurs at a distance from the surfaces (Haosheng and Shihan, 2009). The frequency stress generated has an effect on the internal structure of the SS and it facilitates formation of biofilms. Pitting and fracture can also activate the surface by physically dislodging any passivating layer leading to increase in corrosion rates at these sites (Gandhi and Kumar, 1994).

Thermal stresses are formed as a result of thermal processes, such as welding and they cause non-uniform temperature changes in materials (Uzun and Bilge, 2010). Associated local heating, expansion and contraction because of high heat and sometimes rapid cooling occur around the HAZ of the material but the expansion zone is only surrounded by the material that has not been heated and this part prevents material from expanding or contracting freely leading to residual stresses (Uzun and Bilge, 2010) that modify grains and grain boundaries thereby facilitating formation of biofilms. During welding, mixing of molten filler and the base metal results in a uniform chemical composition on the boundary and this becomes a weak spot (Ramlee *et al.*, 2010). Welding of 316L SS results in inter-dendritic structure being formed and this area is prone to corrosion attack and failure of SS particularly on weld zone is believed to be due to inter-dendritic attack of inter-dendritic structure (Ramlee *et al.*, 2010). For high carbon SS normally 304 or 316, sensitisation is often observed. Sensitisation results when carbon in steel diffuses to the grain boundaries in the sensitised regions and it is caused by segregation of impurities such as sulfur and phosphorus onto grain boundaries. The process occurs due to heat input during welding

process and it promotes acceleration of localised attack leading to premature structural failure due to inter-granular failure (Ramlee *et al.*, 2010).

There are different welding techniques which can be used and some of them are:

- Laser welding – laser beam welding (LBW) is a welding technique used to join multiple pieces of metal through the use of a laser. The beam provides a concentrated heat source, allowing for narrow, deep welds and high welding rates
- Cold Metal Transfer welding – the workpieces to be joined as well as the weld zones remain considerably "colder" in the cold metal transfer process (CMT) than they would with conventional gas metal arc welding. The cold metal transfer process is based on short circuiting transfer, or more accurately, on a deliberate, systematic discontinuing of the arc. Results are a sort of alternating "hot-cold-hot-cold" sequence. The "hot-cold" method significantly decreases the arc pressure. During a normal short circuiting transfer arc, the electrode is distorted while being dipped into the weld pool, and melts rapidly at high transfer arc current. A wide process window and the resulting high stability define the cold metal transfer process
- TIG Argon welding – gas tungsten arc welding (GTAW), also known as tungsten inert gas (TIG) welding, is an arc welding process that uses a non-consumable tungsten electrode to produce the weld. The weld area is protected from atmospheric contamination by a shielding gas (usually an inert gas such as argon), and a filler metal is normally used, though some welds, known as autogenous welds, do not require it. A constant-current welding power supply

produces energy which is conducted across the arc through a column of highly ionized gas and metal vapours known as a plasma

- MIG welding – gas metal arc welding (GMAW), sometimes referred to by its subtypes metal inert gas (MIG) welding or metal active gas (MAG) welding, is a semi-automatic or automatic arc welding process in which a continuous and consumable wire electrode and a shielding gas are fed through a welding gun. A constant voltage, direct current power source is most commonly used with GMAW, but constant current systems, as well as alternating current, can be used. There are four primary methods of metal transfer in GMAW, called globular, short-circuiting, spray, and pulsed-spray, each of which has distinct properties and corresponding advantages and limitations
- Orbital welding – orbital TIG/MIG most commonly used fusion process for welding in industries

Ultrasound waves

The oscillatory motion due to ultrasound waves causes molecular density and pressure anisotropies to form leading to cavitation thereby destroying biofilms (Catallo and Junk, 1995; Piyasena *et al.*, 2003). In the vicinity of weak spots in the molecular lattice (i.e. imperfections in the liquid continuum caused by gas pockets, micelles, particles, and crevices in container walls) this process can generate microcavities in the solution (Catallo and Junk, 1995; Kubo *et al.*, 2005) that leads to cavitation.

The undulations and craters that can be observed during use of ultrasound waves are as a result of plastic deformations which can increase the surface roughness, and they are considered as the main damage style at the incubation stage (Haosheng and Shihan, 2009). Total residual stress will increase around the weld zone; however, on weld start and end points, total residual stress is higher than at the centre of the weld (Uzun and Bilge, 2010). Figure 2.5 shows a schematic of surface erosion with change in time on a surface subjected to ultrasound waves.

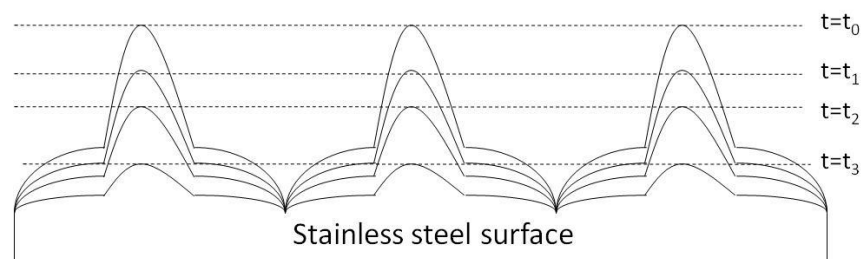


Figure 2.5: Surface erosion of SS subjected to ultrasound waves over time

It can be seen that ultrasound waves eroded the surface of the SS equally; however, cavitation which results in surface erosion is an uncontrolled process and sometimes it can erode the surface unevenly.

References

Al-Juboori, R., Aravinthan, V. and Yusaf, T. (2010) A review of common and alternative methods for disinfection of microorganisms in water, Southern Region Engineering Conference 11-12 November 2010, Toowoomba, Australia, 1–9.

- Back, W. (1994) Secondary contaminations in the filling area, *Brauwelt International*, **12**, 326–333.
- Baehni, P. C. and Takeuchi, Y. (2003) Anti-plaque agents in the prevention of biofilm-associated oral diseases, *Oral Diseases*, **9(1)**, 23–29.
- Braeken, L., van der Bruggen, B., Vandecasteele, C. (2004) Regeneration of brewery waste water using nanofiltration, *Water Research*, **38(13)**, 3075–3082.
- Bremer, P. J., Fillery, S. and McQuillan, A. J. (2006) Laboratory scale Clean-In-Place (CIP) studies on the effectiveness of different caustic and acid wash steps on the removal of dairy biofilms, *International Journal of Food Microbiology*, **106(3)**, 254–262.
- Briggs, D.E., Boulton, C.A., Brookes, P.A. and Stevens, R. (2004a) Microbiology. In: *Brewing science and practice*, D.E. Briggs., C.A. Boulton., P.A. Brookes and R. Stevens, Eds; Woodhead Publishing, Cambridge
- Briggs, D. E., Boulton, C. A., Brookes, P. A., Stevens, R. (2004b) Water, effluents and wastes. In: *Brewing science and practice*. D. E. Briggs., C. A. Boulton., P. A. Brookes., R. Stevens (Eds), Woodhead Publishing, Cambridge, England.
- Caprita, A. and Caprita, R. (2005) Applications of bioluminescence in quality assurance of food products, *Scientific Researches – Agroalimentary Processes and Technologies*, **11(1)**, 161–172.

- Carman, M. L., Estes, T. G., Feinberg, A. W., Schumacher, J. F., Wilkerson, W., Wilson, L. H., Callow, M. E., Callow, J. A. and Brennan, A. B. (2006) Engineered antifouling microtopographies: correlating wettability with cell attachment, *Biofouling*, **22(1)**, 11–21.
- Carrick, K., Barney, M., Navarro, A. and Ryder, D. (2001) The comparison of four bioluminometers and their swab kits for instant hygiene monitoring and detection of microorganisms in the brewery, *Journal of The Institute of Brewing*, **107(1)**, 31–37.
- Catallo, W. J. and Junk, T. (1995) Sonochemical dechlorination of hazardous wastes in aqueous systems, *Waste Management*, **15(4)**, 303–309.
- Chaidez, C., Lopez, J., Castro-del Campo, N. (2007) Quaternary ammonium compounds-An alternative disinfection method for fresh produce wash water, *Journal of Water and Health*, **5(2)**, 329–333.
- Chambers, L. D., Stokes, K. R., Walsh, F. C. and Wood, R. J. K. (2006) Modern approaches to marine antifouling coatings, *Surface and Coatings Technology*, **201(6)**, 3642–3652.
- Characklis, W. G. (2009) Fouling biofilm development: a process analysis, *Biotechnology and Bioengineering*, **102(2)**, 1923–1960.
- Chaw, K. C., Manimaran, M. and Tay, F. E. H. (2005) Role of silver ions in destabilization of intermolecular adhesion forces measured by atomic force microscopy in *Staphylococcus epidermidis* biofilms, *Antimicrobial Agents and Chemotherapy*, **49(12)**, 4853–4859.

- Chen, X. and Stewart, P.S. (2000) Biofilm removal caused by chemical treatments, *Water Research*, **34**(17), 4229–4233.
- Chisti, Y. and Moo-Young, M. (1994) Clean-in-place systems for industrial bioreactors: design, validation and operation, *Journal of Industrial Microbiology*, **13**(4), 201–207.
- Chen, Z., Zhu, C., Han, Z. (2011) Effects of aqueous chlorine dioxide treatment on nutritional components and shelf-life of mulberry fruit (*Morus alba* L.), *Journal of Bioscience and Bioengineering*, **111**(6), 675–681.
- Cheremisinoff, N. P. (2002) An overview of water and wastewater treatment. In: Handbook of water and wastewater treatment technologies. N. P. Cheremisinoff (Ed), Butterworth-Heinemann, Woburn, pp. 1–56.
- Chmielewski, R. A. N. and Frank, J. F. (2003) Biofilm formation and control in food processing facilities, *Comprehensive Reviews in Food Science and Food Safety*, **2**(1), 22–32.
- Cluett, J. D. (2001) Cleanability of certain stainless steel surface finishes in the brewing process, MPhil Dissertation, Rand Afrikaans University, Johannesburg, South Africa.
- Costa, P. D., Andrade, N. J., Brandão, S. C. C., Passos, F. J. V. and Soares, N. F. F. (2006) ATP bioluminescence assay as an alternative for hygiene-monitoring procedures of stainless steel milk contact surfaces, *Brazilian Journal of Microbiology*, **37**(3), 345–349.
- Costerton, J. W. (2007) The predominance of biofilms in natural and engineered ecosystems. In: The Biofilm Primer, J. W. Costerton (Ed), Springer-Verlag, Berlin, pp. 5–14.

- Costerton, J. W. and Wilson, M. (2004) Introducing biofilms, *Biofilms*, **1(1)**, 1–4.
- Czechowski, M. H. and Banner, M. (1992) Control of biofilms in breweries through cleaning and sanitizing, *MBAA Technical Quarterly*, **29(3)**, 86–88.
- Davey, K. R., Chandrakash, S. and O’Neill, B. K. (2013) A new risk analysis of clean-in-place milk processing, *Food Control*, **29(1)**, 248–253.
- Davey, M. E. and O’Toole, G. A. (2000) Microbial biofilms: from ecology to molecular genetics, *Microbiology and Molecular Biology Reviews*, **64(4)**, 847–867.
- Detry, J. G., Sindic, M. and Deroanne, C. (2010) Hygiene and cleanability: A focus on surfaces, *Critical Reviews in Food Science and Nutrition*, **50(7)**, 583–604.
- de Carvalho, C. C. C. R. (2007) Biofilms: recent developments on an old battle, *Recent Patents on Biotechnology*, **1(1)**, 49–57.
- Dong, Y., Li, X., Sammons, R. and Dong, H. (2010) The generation of wear-resistant antimicrobial stainless steel surfaces by active screen plasma alloying with N and nanocrystalline Ag, *Journal of Biomedical Materials Research Part B: Applied Biomaterials*, **93B**, 185–193.
- Donlan, R. M. (2001) Biofilms and device-associated infections, *Emerging Infectious Diseases*, **7(2)**, 277–281.

- Donlan, R. M. (2002) Biofilms: microbial life on surfaces, *Emerging Infectious Diseases*, **8(9)**, 881–890.
- Donlan, R. M. and Costerton, J. W. (2002) Biofilms: survival mechanisms of clinically relevant microorganisms, *Clinical Microbiology Reviews*, **15(2)**, 167–193.
- Elder, D., Budd, G. C. (2011) Overview of water treatment processes. In: Water quality and treatment – A handbook on drinking water. J. K. Edzwald (Ed), McGraw Hill, New York, 6th Edition.
- Eumann, M. (2006) Water in brewing. In: Brewing – New technologies. C. W. Bamforth (Ed), Woodhead, Cambridge, pp. 183–207.
- Fan, F. R. F. and Bard, A. J. (2002) Chemical, electrochemical, gravimetric, and microscopic studies on antimicrobial silver films, *The Journal of Physical Chemistry B*, **106(2)**, 279–287.
- Feng, X., Huang, L., Zhang, X., Liu, Y. (2009) Water system integration of a brewhouse, *Energy Conversion and Management*, **50(2)**, 354–359.
- Ferreira, C., Pereira, A.M., Melo, L.F. and Simões, M. (2010) Advances in industrial biofilm control with micro-nanotechnology. In: Current research, technology and education topics in applied microbiology and microbial technology, A. Méndez-Vilas (Ed), Formatex Research Center, Badajoz, Spain, number 2, vol. 2, pp. 845–854.

- Fillaudeau, L., Blanpain-Avet, P., Daufin, G. (2006) Water, wastewater and waste management in brewing industries, *Journal of Cleaner Production*, **14(5)**, 463–471.
- Flemming, H. C. (2002) Biofouling in water systems: cases, causes and countermeasures, *Applied Microbiology and Biotechnology*, **59(6)**, 629–640.
- Francolini, I. and Donelli, G. (2010) Prevention and control of biofilm based medical-device-related infections, *Immunology and Medical Microbiology*, **59(3)**, 227–238.
- Gandhi, K. S. and Kumar, R. (1994) Sonochemical reaction engineering, *Sadhana*, **19(6)**, 1055–1076.
- Goode, K. R., Asteriadou, K., Fryer, P. J., Picksley, M. and Robbins, P. T. (2010) Characterising the cleaning mechanisms of yeast and the implications for Cleaning In Place (CIP), *Food and Bioproducts Processing*, **88(4)**, 365–374.
- Götz, J., Rewesa, L., Walch, M. and Geissler, A. (2005) Influence of an ultrasonic treatment on the structure and flow behaviour of oxide ceramic masses, *Applied Rheology*, **15(4)**, S204–217.
- Haosheng, C. and Shihan, L. (2009) Inelastic damages by stress wave on steel surface at the incubation stage of vibration cavitation erosion, *Wear*, **266(1–2)**, 69–75.
- Hoffmann, M. R., Hua, I. and Höchemer, R. (1996) Application of ultrasonic irradiation for the degradation of chemical contaminants in water, *Ultrasonics Sonochemistry*, **3(3)**, S163–S172.

- Holah, J. T. (1992) Industrial monitoring: hygiene in food processing. In: Biofilms – Science and Technology, L.F. Melo., T.R. Bott., M. Fletcher, and B. Capdeville, (Eds), Kluwer Academic Publishers, Dordrecht, Netherlands, pp. 645–659.
- Holt, K. B. and Bard, A. J. (2005) Interaction of silver (I) ions with the respiratory chain of *Escherichia coli*: an electrochemical and scanning electrochemical microscopy study of the antimicrobial mechanism of micromolar Ag⁺, *Biochemistry*, **44(39)**, 13214–13223.
- Hornsey, I. S. (1999) Microbiology in the brewery. In: Brewing, I. S. Hornsey (Ed), The Royal Society of Chemistry, Cambridge, pp. 194–223.
- Hua, I. and Thompson, J. E. (2000) Inactivation of *Escherichia coli* by sonication at discrete ultrasonic frequencies, *Water Research*, **34(15)**, 3888–3893.
- Ince, N.H. and Belen, R. (2001) Aqueous phase disinfection with power ultrasound: Process kinetics and effect of solid catalysts, *Environmental Science and Technology*, **35(9)**, 1885–1888.
- Johns, M. R. (1995) Developments in wastewater treatment in the meat processing industry: A review, *Bioresource Technology*, **54(3)**, 203–216.
- Joyce, E. M., Wu, X. and Mason, T. J. (2010) Effect of ultrasonic frequency and power on algae suspensions, *Journal of Environmental Science and Health Part A*, **45(7)**, 863–866.
- Kaali, P., Strömberg, E. and Karlsson, S. (2011) Prevention of biofilm associated infections and degradation of polymeric materials used in biomedical applications. In: Biomedical

Engineering, Trends in Materials Science, A. N. Laskovski (Ed), InTech, Rijeka, Croatia, pp. 513–540.

Kokare, C. R., Chakraborty, S., Khopade, A. N. and Mahadik, K. R. (2009) Biofilms: importance and applications, *Indian Journal of Biotechnology*, **8(2)**, 159–168.

Kubo, M., Onodera, R., Shibasaki-Kitakawa, N., Tsumoto, K. and Yonemoto, T. (2005) Kinetics of ultrasonic disinfection of *Escherichia coli* in the presence of titanium dioxide particles, *Biotechnology Progress*, **21(3)**, 897–901.

Kumar, C. G. and Anand, S. K. (1998) Significance of microbial biofilms in food industry: a review, *International Journal of Food Microbiology*, **42(1-2)**, 9–27.

Laborde, J-L., Bouyer, C., Caltagirone, J.-P. and Gérard, A. (1998) Acoustic bubble cavitation at low frequencies, *Ultrasonics*, **36(1-5)**, 589–594.

Laurent, J., Casellas, M., Pons, M.N. and Dagot, C. (2009) Flocculation surface functionality assessment of sonicated activated sludge in relation with physico-chemical properties, *Ultrasonics Sonochemistry*, **16(4)**, 488–494.

LeChevallier, M. W., Cawthon, C. D. and Lee, R. G. (1988) Factors promoting survival of bacteria in chlorinated water supplies, *Applied and Environmental Microbiology*, **54(3)**, 649–654.

Lewis, M.J. and Bamforth, C.W. (2006) Sanitation and Quality. In: Essays in brewing science, Springer Science, New York, USA, pp. 161–171.

- Lelièvre, C., Antonini, G., Faille, C. and Bénézech, T. (2002) Modelling of cleaning kinetics of pipes soiled by *Bacillus* spores assuming a process combining removal and deposition, *Food and Bioproducts Processing*, **80(4)**, 305–311.
- Lindsay, D. and von Holy, A. (2006) Bacterial biofilms within the clinical setting: what healthcare professionals should know, *Journal of Hospital Infection*, **64(4)**, 313–325.
- Li-xin, B., Wei-lin, X., Zhong, T. and Nai-wen, L. (2008) A high speed photographic study of ultrasonic cavitation near rigid boundary, *Journal of Hydrodynamics*, **20(5)**, 637–644.
- Loeffler, D. (2006) Modern brewery sanitation. In: *Brewing; New technologies*, C.W. Bamforth, Ed, Woodhead Publishing Limited, Cambridge, England, pp. 308–334..
- Lorenzen, K. (2005) Improving cleaning-in-place (CIP). In: *Handbook of hygiene control in the food industry*, H. L. M. Lelieveld, M. A. Mostert and J. Holah (Eds), Woodhead Publishing Limited, Cambridge, England, pp 425–444.
- Madaeni, S. S. (1999) The application of membrane technology for water disinfection, *Water Research*, **33(2)**, 301–308.
- Magin, C. M., Cooper, S. P. and Brennan, A. B. (2010) Non-toxic antifouling strategies, *Materials Today*, **13(4)**, 36–44.
- Mamvura, T. A., Iyuke, S. E., Cluett, J. D. and Paterson, A. E. (2011) Soil films in the beverage industry: A review, *Journal of the Institute of Brewing*, **117(4)**, 608–616.
- Manzano, M., Iacumin, L., Vendrame, M., Cecchini, F., Comi, G. and Buiatti, S. (2011) Craft beer microflora identification before and after a cleaning process, *Journal of the Institute of Brewing*, **117(3)**, 343–351.

- McDonnell, G. and Russell, A. D. (1999) Antiseptics and disinfectants: Activity, action and resistance, *Clinical Microbiology Reviews*, **12(1)**, 147–179.
- Medilanski, E., Kaufmann, K., Wick, L. Y., Wanner, O. and Harms, H. (2002) Influence of the surface topography of stainless steel on bacterial adhesion, *Biofouling*, **18(3)**, 193–203.
- Mertens, R. (2009) Beer Dispensing. In: Handbook of Brewing; Processes, technology, markets, H. M. Eßlinger, Ed, Wiley-VCH Verlag GmbH and Co, Weinheim, Germany, pp. 339–357.
- Meyer, B. (2003) Approaches to prevention, removal and killing of biofilms, *International Biodeterioration and Biodegradation*, **51(4)**, 249–253.
- Miller, D. L. (1987) A review of the ultrasonic bioeffects of microsonation, gas-body activation, and related cavitation-like phenomena, *Ultrasound in Medicine and Biology*, **13(8)**, 443–470.
- Momba, M. N. B., Kfir, R., Venter, S. N. and Cloete, T. E. (2000) An overview of biofilm formation in distribution systems and its impact on the deterioration of water quality, *Water SA*, **26(1)**, 59–66.
- Olajire, A. A. (2012) The brewing industry and environmental challenges, *Journal of Cleaner Production*, **In Press**, 1–21.
- Piyasena, P., Mohareb, E. and McKellar, R.C. (2003) Inactivation of microbes using ultrasound: a review, *International Journal of Food Microbiology*, **87(3)**, 207–216.

- Poulsen, L. V. (1999) Microbial biofilm in food processing, *Lebensmittel-Wissenschaft und-Technologie*, **32(6)**, 321–326.
- Praeckel, U. (2009) Cleaning and disinfecting. In: Handbook of Brewing; Processes, technology, markets, H. M. Eßlinger, Ed, Wiley-VCH Verlag GmbH and Co, Weinheim, Germany, pp. 595–620.
- Quain, D. and Storgårds, E. (2009) The extraordinary world of biofilms, *Brewer and Distiller International*, **5(7)**, 31–33.
- Radetić, M., Ilić, V., Vodnik, V., Dimitrijević, S., Jovančić, P., Šaponjić, Z. and Nedeljković, J. M. (2008) Antibacterial effect of silver nanoparticles deposited on corona-treated polyester and polyamide fabrics, *Polymers for Advanced Technologies*, **19(12)**, 1816–1821.
- Ramlee, N., Harun, M. K., Amrin, A, and Ourjini, A. (2010) Effect of temperature and chloride concentrations on the corrosion behaviour of welded 316L stainless steel, *ICFMD*, 1–6.
- Reid, R (1998) Current and future roles of membranes in brewing, *Membrane Technology*, **101**, 5–8.
- Sakamoto, K. and Konings, W. N. (2003) Beer spoilage bacteria and hop resistance, *International Journal of Food Microbiology*, **89(2-3)**, 105–124.

- Santos, H.M., Lodeiro, C. and Capelo-Martinez, J-L. (2009) The power of ultrasound. In: *Ultrasound in chemistry-Analytical chemistry*, (J-L, Capelo-Martinez, Ed), Wiley-VCH, Weinheim, Germany, pp. 1–16.
- Scardino, A. J., Harvey, E. and de Nys, R. (2006) Testing attachment point theory: diatom attachment on microtextured polyimide biomimics, *Biofouling*, **22(1-2)**, 55–60.
- Scardino, A. J., Hudleston, D., Peng, Z., Paul, N. A. and de Nys, R. (2009) Biomimetic characterisation of key surface parameters for the development of fouling resistant materials, *Biofouling*, **25(1)**, 83–93.
- Schumacher, J. F., Carman, M. L., Estes, T. G., Feinberg, A. W., Wilson, L. H., Callow, M. E., Callow, J. A., Finlay, J. A. and Brennan, A. B. (2007a) Engineered antifouling microtopographies: effect of feature size, geometry, and roughness on settlement of zoospores of the green alga *Ulva*, *Biofouling*, **23(1)**, 55–62.
- Schumacher, J. F., Aldred, N., Callow, M. E., Finlay, J. A., Callow, J. A., Clare, A. S. and Brennan, A. B. (2007b) Species-specific engineered antifouling topographies: correlations between the settlement of algal zoospores and barnacle cyprids, *Biofouling*, **23(5)**, 307–317.
- Silvestry-Rodriguez, N., Bright, K. R., Slack, D. C., Uhlmann, D. R. and Gerba, C. P. (2008) Silver as a residual disinfectant to prevent biofilm formation in water distribution systems, *Applied and Environmental Microbiology*, **74(5)**, 1639–1641.

- Simões, M., Simões, L.C. and Vieira, M.J. (2010) A review of current and emergent biofilm control strategies, *LWT - Food Science and Technology*, **43(4)**, 573–583.
- Škvarla, J. (1993) A physico-chemical model of microbial adhesion, *Journal of the Chemical Society Faraday Transactions*, **89(15)**, 2913–2921.
- Sreekumari, K., Sato, Y. and Kikuchi, Y. (2005) Antibacterial metals – A viable solution for bacterial attachment and microbiologically influenced corrosion, *Materials Transactions*, **46(7)**, 1636–1645.
- Storgårds, E. (2000) Cleaning and disinfection. In: Process hygiene control in beer production and dispensing, Academic dissertation, Technical Research Centre of Finland, VTT Publication, pp. 37–45.
- Sturm, B., Hugenschmidt, S., Joyce, S., Hofacker, W., Roskilly, A. P. (2012) Opportunities and barriers for efficient energy use in a medium-sized brewery, *Applied Thermal Engineering*, **53(2)**, 1–8.
- Suzuki, K. (2011) 125th anniversary review: Microbiological instability of beer caused by spoilage bacteria, *Journal of the Institute of Brewing*, **117(2)**, 131–155.
- Tansel, B. (2008) New technologies for water and wastewater treatment: A survey of recent patents, *Recent Patents on Chemical Engineering*, **1(1)**, 17–26.
- Taylor, D. G. (2006) Water. In: Handbook of brewing, F. G. Priest and G. G. Stewart (Eds), CRC Press, Boca Raton, pp. 91–135.
- Tian, Y. (2008) Behaviour of bacterial extracellular polymeric substances from activated sludge: a review, *International Journal of Environment and Pollution*, **32(1)**, 78–89.

- Timke, M., Wang-Lieu, N.Q., Altendorf, K. and Lipski, A. (2005) Fatty acid analysis and spoilage potential of biofilms from two breweries, *Journal of Applied Microbiology*, **99(5)**, 1108–1122.
- Timke, M., Wang-Lieu, N. Q., Altendorf, K. and Lipski, A. (2008) Identity, beer spoiling and biofilm forming potential of yeasts from beer bottling plant associated biofilms, *Antonie van Leeuwenhoek*, **93(1-2)**, 151–161.
- Trachoo, N. (2003) Biofilms and the food industry, *Songklanakarin Journal of Science and Technology*, **25(6)**, 807–815.
- Uzun, F. and Bilge, A. N. (2010) Investigation of total welding residual stress by using ultrasonic wave velocity variations, *Gazi University Journal of Science*, **24(1)**, 43–49.
- Vaughan, A., O’Sullivan, T. and van Sinderen, D. (2005) Enhancing the microbiological stability of malt and beer: a review, *Journal of the Institute of Brewing*, **111(4)**, 355–371.
- van Asselt, A. J. and te Giffel, M. Z. (2005) Pathogen resistance to sanitizers. In: Handbook of hygiene control in the food industry, H. L. M. Lelieveld, M. A. Mostert and J. Holah (Eds), Woodhead Publishing Limited, Cambridge, England, pp. 69–88.
- van der Kooij, D. (2003) Managing re-growth in drinking water distribution systems. In: Heterotrophic plate counts and drinking-water safety – The significance of HPCs for water quality and human health, J. Bartram, J. Cotruvo, M. Exner, C. Fricker, and A. Glasmacher (Eds), IWA Publishing, London, UK, pp. 199–232.

- van Houdt, R. and Michiels, C. W. (2010) Biofilm formation and food industry, a focus on the bacterial outer surface, *Journal of Applied Microbiology*, **109(4)**, 1117–1131.
- van Loosdrecht, M. C. M., Lyklema, J., Norde, W. and Zehnder, A. J. B. (1990) Influence of interfaces on microbial activity, *Microbiological Reviews*, **54(1)**, 75–87.
- Verran, J. and Jones, M. (2000) Problems of biofilm in the food and beverage industry. In: *Industrial Biofouling*, J. Walker., S. Suramn. and J. Jass (Eds), John Wiley, New York, pp. 145–173.
- Wilson, M. (1996) Susceptibility of oral bacterial biofilms to antimicrobial agents, *Journal of Medical Microbiology*, **44(2)**, 79–87.
- Wu, X., Joyce, E. M. and Mason, T. J. (2012) Evaluation of the mechanisms of the effect of ultrasound on *Microcystis aeruginosa* at different ultrasonic frequencies, *Water Research*, **46(9)**, 2851–2858.
- Xavier, J. B., Picioreanu, C., Rani, S. A., van Loosdrecht, M. C. M. and Stewart, P. S. (2005) Biofilm-control strategies based on enzymic disruption of the extracellular polymeric substance matrix: a modelling study, *Microbiology*, **151(12)**, 3817–3832.
- Zottola, E. A. and Sasahara, K. C. (1994) Microbial biofilms in the food processing industry: should they be a concern, *International Journal of Food Microbiology*, **23(2)**, 125–148.

CHAPTER THREE

**"IN THE END, WE WILL REMEMBER NOT THE WORDS OF OUR
ENEMIES, BUT THE SILENCE OF OUR FRIENDS."**

- MARTIN LUTHER KING JR. (1929-1968)

3. EXPERIMENTAL PROCEDURE

3.1 Static experiments

3.1.1 Using ultrasound waves to control biofilms in brewing industry

The method used involved subjecting 24 kHz ultrasound waves to SS coupon surfaces with biofilms attached to determine disinfection efficiency, if any, by swabbing coupon surfaces to enumerate biofilm attached. The analysis was done before and after exposure to ultrasound waves. *Escherichia coli* (*E. coli*) cells were used in initial studies to confirm that ultrasound waves work on bacterial cells as the cells combine to form biofilm. In addition *E. coli* could be detected in system because it comes in water. However, *E. coli* must be eliminated before the brewing process and as such its use in initial studies under static experiments served that purpose. The biofilm was attached under static conditions hence static experiments i.e. the coupon surfaces were dipped in an *E. coli* solution with no shaking, pumping or circulating of the solution during the experiments. This meant that it took long for the biofilm to build on the coupon surfaces.

Preparation of stock culture

Pure cultures of *E. coli* obtained from the School of Molecular and Cell Biology, University of the Witwatersrand, Johannesburg, South Africa were grown in *Luria Bertani* (*LB*) media for 16–24 hours at 37 °C and 110 rpm in a shaking incubator (Ince and Belen, 2001). *LB* media was prepared by mixing 10g of Tryptone (Merck), 5g of yeast extract (Merck), and 10g of NaCl (Merck) in 1 L of distilled water; followed by sterilisation in an autoclave at 121 °C for 20 minutes. Bacterial concentration in the medium at the end of the incubation period was approximately 10⁹ cfu/ml on

average in accordance with a previously calibrated SQ-4802 Double Beam Scanning UV/Visible Spectrophotometer (Appendix II) at 660 nm (Wu *et al.*, 2012).

Stainless steel coupon preparation

To simulate SS surfaces that may be encountered in a food-processing environment, food-grade SS coupons (AISI 316L) were obtained from Falcon Engineering, Johannesburg, South Africa. Coupons were welded together using three different types of welds {Laser, cold metal transfer (CMT) and gas tungsten arc welding (GTAW) also known as tungsten inert gas (TIG) welding or gas metal arc welding (GMAW), also known as metal inert gas (MIG) welding or metal active gas (MAG) welding} at Southern African Institute of Welding (SAIW), Johannesburg, South Africa. After welding, all coupons were rectangular (surface area was on average 30×22 cm², thickness was 3 mm) and mechanically polished giving the same surface finish as for industrial purposes. Smooth surfaces are used in the food and beverage industry on the premise that surface polishing provides a more cleanable surface which decreases biofilm formation (Woodling and Moraru, 2005). Before biofilm adhesion and treatment, all coupons were cleaned with acetone to remove grease, etched with hydrochloric acid for a few minutes (to chemically etch all peaks to achieve uniform peak heights), individually rinsed in distilled water, allowed to air-dry under a laminar hood, and then autoclaved at 121 °C for 20 minutes (Vinnichenko *et al.*, 2002).

Disinfection experimental set-up

An air-sealed 45 L container in a closed fumehood to maintain a relatively constant temperature was used to build biofilm on three SS coupons with different welds (Laser, CMT and TIG/MIG)

over two weeks (Figure 3.1). *LB* media was replaced every 72–96 hours to favour growth of biofilms on SS coupon surfaces only.



Figure 3.1: One of three experimental coupons used in the study

During replacement of spent *E. coli* solution, coupons were rinsed with distilled water to remove any loose cells not attached to the surfaces and the container was cleaned of any microbial cells attached to the walls. After biofilms were attached on surfaces, a 24 kHz Hielscher UP200S transducer, Germany, (200W, 24 kHz) with transducer horn/probe (tip diameter of 14 mm, probe surface area of 1.54 cm² and maximum amplitude of 125 μm) was submerged (maximum 90 mm)

in distilled water containing coupons and subjected to ultrasound waves in vertical mode. 24 kHz frequency was chosen to maximise the potential for ultrasonic-induced cavitation and also because it was above the higher-frequency level of human hearing of 20 kHz. Figure 3.2 shows the experimental setup.



Figure 3.2: Experimental setup and procedure using ultrasound waves to control biofilms from SS coupons

Different conditions were assessed for optimum biofilm removal in the hope of implementing the recommendations in the food and beverage industry. Of the critical processing factors to be considered when using ultrasound waves (section 2.4.1), the following parameters were investigated:

- | | | |
|------------------------------------|---|---|
| (a) Frequency | – | Controlled parameter at 24 kHz |
| (b) Ultrasound intensity/amplitude | – | Investigated |
| (c) Time of exposure | – | Investigated |
| (d) Distance from probe | – | Investigated |
| (e) Physical conditions of medium | – | pH, temperature monitored over time |
| (f) Type of microorganisms | – | Controlled, <i>E. coli</i> cells used |
| (g) Volume to be processed | – | Controlled, constant SS coupon surface |
| (h) Composition of food | – | <i>E. coli</i> cells on SS surfaces and <i>LB</i> media |

Disinfection efficiency (viability of biofilms) was assayed using swab techniques and enumerated before and after treatment with ultrasound waves on front and back surfaces of normal and welded coupon surfaces; and results were reported as percentage of remaining bacterial cells against initially attached bacterial cells. Swabbing was done using sterilised cotton wool and enumerated using a previously calibrated SQ-4802 Double Beam Scanning UV/Visible Spectrophotometer (Appendix II) at 660 nm (Wu *et al.*, 2012). The disinfection efficiency was calculated as:

$$\text{Disinfection efficiency} = \frac{\text{initial biofilm intensity} - \text{final biofilm intensity}}{\text{initial biofilm intensity}} \times 100\%$$

As discussed under Definitions.

3.1.2 Surface profile changes during use of ultrasound waves

During treatment of coupon surfaces with ultrasound waves, various effects occurred on the coupon surfaces. These were caused by cavitation (implosion of microbubbles on coupon surfaces) and may have led to coupon surface erosion.

Determination of surface roughness of coupons

Stainless steel coupons used during the experiments were cleaned with 95% ethanol solution to remove any residues prior to roughness measurements (Boulangé-Petermann *et al.*, 1997). Measurements were quantified using topographic and morphological parameters: average roughness (R_a), root-mean-square profile height (R_q), maximum peak-to-valley height (R_{max}), surface skewness (R_{skw}) and surface kurtosis (R_{kur}) with parameters defined below and further elaborated in Appendix I.

- (a) Average roughness (R_a) – it is the average distance from the profile to the mean line over the length of assessment, measured in μ inch or μ m
- (b) Root-mean-square (RMS) profile height (R_q) – this is the square root of the average of the square of the deviation of the profile from the mean line
- (c) Maximum peak-to-valley height (R_{max}) – it is the maximum peak-to-valley height within one cut-off
- (d) Surface skewness (R_{skw}) – it is a measure of the direction of the asymmetry of the distribution of heights in the sample or a measure of the average of the first derivative of the surface i.e. the departure of the surface from symmetry

(e) Surface kurtosis (R_{kur}) – it is a measure of the peakedness of the distribution of heights in the sample by comparing it to the normal distribution

Three parameters R_a , R_q and R_{max} were utilised to evaluate the coupon's surface topography, while R_{skw} and R_{kur} were used to describe the surface morphology (Ivanova *et al.*, 2011). Analysis was done on normal surface and three welded surfaces available and comparison was done against the normal surface as the original surface available at the beginning of the study.

Atomic force microscopy

Dimension 3100 AFM using Nanoscope version 5.30 was used to view coupon surfaces before and after experiments. The images of SS surfaces were obtained in non-contact (tapping) mode using standard cantilevers. AFM (a scanning probe microscopy) allowed obtaining precise three-dimensional (3D) topography of the coupon surface and geometrical parameters of the elements with a subnanometer resolution for a scanning area of $25 \times 25 \mu\text{m}^2$. All measurements were done under ambient conditions with AFM images processed with Nanoscope v.5.30 software and Nanotec Windows Scanning X (Force, Tunneling, and Near Optical) Microscope (WSxM) v.5.1 software (Horcas *et al.*, 2007).

Optical microscopes

These were used initially to view the surfaces produced after welding and compared to the normal surface available initially. The microscopes used were Carl Zeiss SteREO Discovery microscope.V12 (Germany) and Leica DM6000M microscope (Japan).

3.1.3 Energy changes during treatment with ultrasound waves

Various energy changes occurred during use of ultrasonic probe and the energy changes had to be quantified.

Measurement of energy changes and determination of efficiency conversion

Energy conversion during irradiation with ultrasound waves was determined by measuring the energy changes along the process against a change in amplitude varied from 0 to 100% in steps of 20%. There are five types of energy changes (Figure 3.3) encountered during use of ultrasonic probes, but only three types of energy changes (electrical, acoustic and cavitation) were monitored and used in the analysis to have an estimate of the cost-effectiveness of the process.

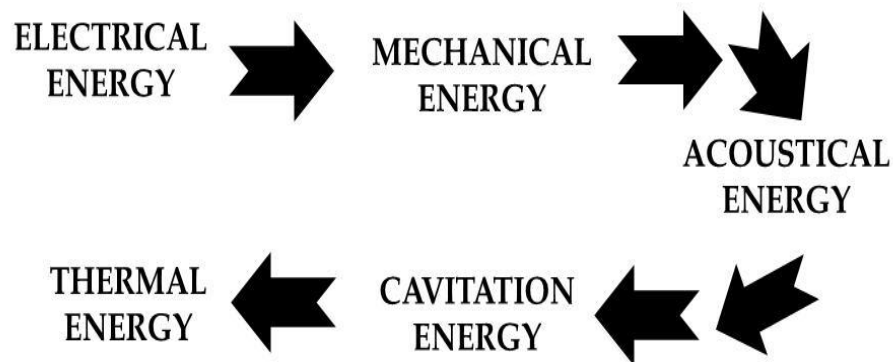


Figure 3.3: The energy transformation chain during ultrasonic treatment (Kobus and Kusińska, 2008)

- (i) Electrical power was obtained from two methods: power density values were obtained from measurements of voltage and current and calculating the power density as $Power =$

$Voltage(V) \times Current(I) / volume\ of\ distilled\ water\ (cm^3)$ and compared against values calculated after measurement of maximum pressure amplitude from the Nexus hydrophone (Miniature hydrophone – Type 8103; Brüel & Kjær, Ferndale, South Africa). The values obtained by using the hydrophone were verified by calculating the maximum displacement amplitude at 100% amplitude and compared against the set amplitude of 125 μm stipulated on the manual for the ultrasonic generator

- (ii) Acoustical power density was calculated by measuring the rate of temperature increase of distilled water during treatment with ultrasound waves and using equation 4.8 to determine power density by plotting a graph of temperature (T) against time (t) to determine its slope
- (iii) Cavitation power was obtained by determining the calorimetric energy in both cavitating and non-cavitating liquid and using equation 4.9. The values obtained were compared against values calculated using the maximum pressure amplitude obtained from the Nexus hydrophone, and using equation 4.6 and mathematical manipulation

The efficiency of conversion from electrical to acoustic and cavitation energies was determined by dividing the acoustic energy or cavitation energy by the electrical energy with change in amplitude.

3.1.4. Button experiments

Previous work on Aluminium (Sithole, 2007) had added silver to the extruded metal surface through deposition into micro-pores developed during the anodising process. The surface was unsealed to enable interaction of silver with microorganisms. The purpose of adding silver to the aluminium substrate was to ascertain whether the presence of silver acted as a biocide in health

industry applications where access to cleaning was not always possible and this proved successful in laboratory simulations. A similar idea was proposed for the current work in stainless steel. As welding is inherently rougher than the wrought pipe surface, it is inherently more prone to biofilm growth. The inclusion of a biocide in the welding filler (904L) alongside the pipe material matching filler (316L) was implemented. Copper was used instead of silver as it was commercially available.

Welding filler rods 316L and 904L were melted in an inert gas atmosphere (to exclude oxygen and hydrogen) at Mintek and developed into two buttons (unfortunately, the button forming process was flawed as the final specimens included oxygen. It appeared as if the base filler materials which have a natural affinity for oxygen were not adequately pre-cleaned of surface oxide before melting.) In addition, two square coupons of 904L and 316L respectively were provided to test the biocidal properties of 904L against 316L, parent material. The difference between the two rods was due to the presence of copper in 904L which acted as a biocide just like silver. There was one 316L button, one 904L button, two square 904L coupons and two square 316L coupons (from previous study). The filler rods were characterised initially and compared against the parent metal (AISI 316L from Euro Steel, South Africa). This characterisation was performed under section 3.2.1 and the results presented in section 4.2.1 as the rods were used to weld pipes under dynamic experiments.

The coupons and buttons were combined and inserted in *LB* media to investigate bacterial growth against material used and treatment with ultrasound waves at a distance of 750 mm from the probe. The same procedure as for preparation of stock culture and SS coupon preparation as in section 3.1.1 was followed to determine bacterial intensity on the two materials with the exception of subjecting the buttons to ultrasound waves.

3.2 Dynamic experiments

Experiments were developed to model real applications where product flows through 50 mm ID 316L pipes. These experiments were performed with municipal water circulated (hence dynamic) in the pilot rig under different conditions to favour formation of biofilms on pipe wall surfaces. The design included different during and post weld treatment and used both standard filler (316L) and a copper containing filler (904L) to ascertain whether the copper would act as a biocide. The rig used 4 mm thick wall to accommodate grub screws used to access opposite walls. Six pipes were interconnected by screwed elbows. The general layout was shown in Figure 3.4. Two sets of tests each of five weeks duration under different flow velocities were conducted. The purpose was to address the following questions:

- Is there an increased concentration of biofilm in welding areas?
- Does using 316L filler result in worse effects than 904L?
- Does the flow direction influence results (geometric impacts)?
- What is the influence of the heat affected zone (HAZ)?
- What benefits are achieved by using argon?

- What benefits are achieved by pickling and passivation?
- How effective is the CIP process?
- How does the CIP process degrade over the length of the pipe as the concentration decreases?

3.2.1. Welding filler characterisation

The composition of the two welding fillers used in the fabrication of the test rig was checked by melting the rods used in an inert argon gas atmosphere into buttons at Mintek, South Africa. The composition was checked at SAIW. Flat coupons in 316L and 904L were used to test the biocidal properties of 904L against 316L.

The 316L SS pipes were characterised by the mill and the specifications were reported and compared with filler rods.

3.2.2. Flow and velocity measurements

Flow and velocity measurements were conducted on the test apparatus to determine the operating conditions for both CIP and biofilm formation for the two runs conducted over five week periods each under different flow conditions.

3.2.3. CIP systems in combination with ultrasound waves

Determination of surface roughness of pipe

A piece of SS 316L pipe used during the experiments was cleaned with 95% ethanol solution to remove any residue prior to roughness measurements and quantified using topographic and

morphological parameters: R_a , R_q , R_{max} , R_{skw} and R_{kur} . Analysis was done on normal surface and comparison was done against the normal surface of the coupons used in static experiments. Analysis was done using Dimension 3100 AFM using Nanoscope version 5.30 in non-contact (tapping) mode using standard cantilevers. All measurements were done under ambient conditions with AFM images processed with Nanoscope v.5.30 software and Nanotec Windows Scanning X (Force, Tunneling, and Near Optical) Microscope (WSxM) v.5.1 software (Horcas *et al.*, 2007).

Pipe considerations

A test rig to mimic brewing process conditions in pipes was built using 6x1 m 316L SS pipes connected through 90° elbows as shown in Figures 3.4 (schematic) and 3.5 (actual rig).

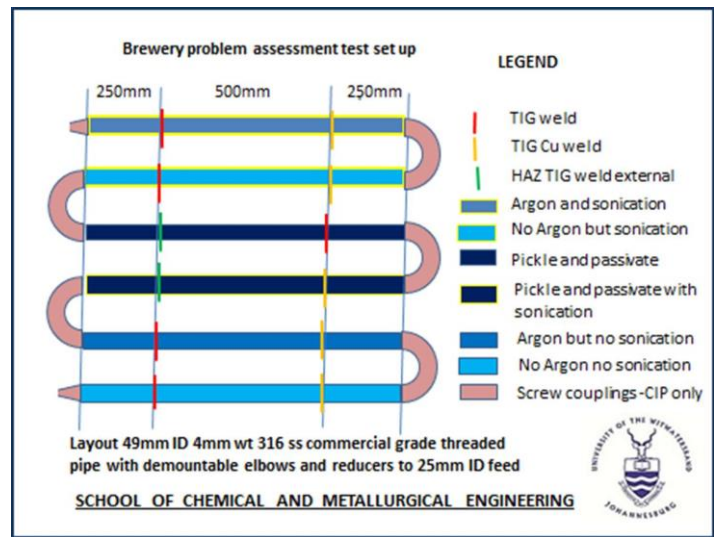


Figure 3.4: Schematic of the test rig built to mimic biofilm formation in brewing operations



Figure 3.5: Test rig to investigate the effect of biofilm formation after CIP on brewing process systems

The apparatus included 13 sampling stations, 10 stations represented different operating circumstances with either 316L or 904L filler welding rods used while 2 stations had HAZ weld i.e. they were welded outside to investigate the effect of heat on biofilm formation (and material roughness). Each station included three parallel rows of three grub screw access ports i.e. 3x3 sampling points and in each line, ports were separated by 120° positioned over the bead and 10 mm on either side staggered by 40° to limit overlap. This was done to get a proper representative of biofilm intensity on a particular point as more microorganisms would attach at the bottom, followed by the side walls and lastly on the top of the pipe inside. On each port position, the grub screw was individually identified and represented 45° transverse swab sweeps on the opposite pipe

wall (see Figure 3.6). This type of sampling was similar to that done by Carbone (2001) in Figure 4 of the author's patent.

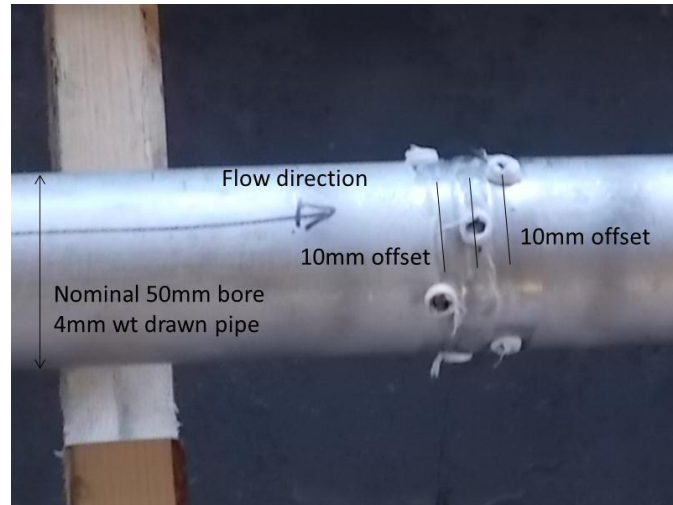


Figure 3.6: Sampling port located on each of the weld in the direction of flow

The 13th station on the final pipe (pipe F) in the flow sequence was intended to provide a control and it was divided into 4 substations, each including three access ports separated by 120°. The 904L was intended to check the effect of a bactericide; copper in this case (if copper was effective, silver could be tried as copper is not a favoured elemental additions to beer).

Analysis of biofilms on pipe surfaces has been done differently in literature by inserting small coupons inside pipe sections and withdrawing them for swabbing and computing intensity either by cell counts or using bioluminometer machines or they take a sample of water for analysis to

infer biofilm intensity (Boe-Hansen *et al.*, 2003; Deines *et al.*, 2010; Juhna *et al.*, 2007; Lee, 2013; Pachepsky *et al.*, 2011; Park and Kim, 2008; Szczotko and Krogulski, 2010; Yu *et al.*, 2010). The results were reported either as RLU/cm² and CFU/cm², the area being the swabbed sample area or as RLU/cm³ and CFU/cm³, the volume being the sampled water for analysis. However, the current study had biofilms swabbed directly on the pipe surface using sterile swabs and the method used by Simões (2005 page 52) was followed. Simões (2005) investigated biofilm formation on cylindrical SS pipes on the outside (see Figure 3.7) and determined intensity as mass/area i.e. mg/cm² where area was determined by πDL , D = inside diameter in the current study and L being the length before and after the weld i.e. 20 mm.



Figure 3.7: Stainless steel cylinder covered with biofilm after 7 days of growth (Simões, 2005 page 167)

Other authors followed similar setup and determined biofilm intensity per unit area (Flint, 1998 on page 28). The calculated surface area was:

$$\text{Surface area} = \pi D_{\text{inside}} L = \pi * 5.251\text{cm} * 2\text{cm} = 33.0\text{cm}^2$$

Whilst consideration was given to circulating wort, the final decision was to circulate municipal supply water. This recognised the importance of water both as the largest component of beer and to facilitate the process. Water also was seen as the main raw material that was in contact with food surfaces for a greater part, be it in transporting other raw materials, in washing before and after beer or in CIP. On top of that using water meant that the possibility of residue settling was eliminated. After assembly, the rig was fully degreased and cleaned using the same CIP process and chemicals as used in the brewing industry (see experimental procedure below for runs 1 and 2). Thereafter initial bacterial intensity readings were taken at each port using standard ATP swabs from 3M. Bacterial intensity readings were directly assessed using a Clean-Trace™ NG bioluminometer, see Figure 3.8.

After sufficient biofilm growth (about five weeks), all 120 ports were assessed for bacterial intensity using ATP swabs. The bacterial intensity readings were analysed to determine the effects of the process and filler variables involved. A control pipe with no welds or any HAZs was considered but it was not adopted both as it would have introduced a new variable because it was coming from a new batch of SS316L pipe and it was believed that a spread of 500 mm between welds was enough to even out flows.

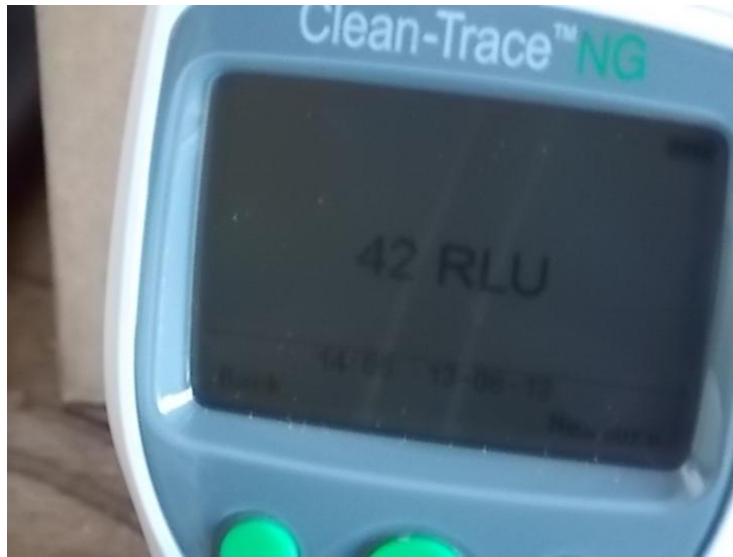


Figure 3.8: Clean-Trace™ NG bioluminometer

Note that station 12 on pipe F included 12 inspection grub screws spread over four substations and staggered at 30° between succeeding screws. This would enable one to assess many effects including acting as the control section and it provided a 360° flow of events around the pipe cross-sectional area during biofilm formation or CIP processes.

Experimental procedure for run 1

The steps which were followed during run 1 are as follows:

1. Complete work to experimental rig
2. Disassemble pipes C and D
3. Pickle and passivate pipes C and D using standard solutions from Duva Chemicals – procedure was undertaken at and by Duva Chemicals

4. Reassemble rig
5. Connect the experimental rig to the fermenter through one pump and connection hoses
6. Pump water through to verify maximum system flow velocity (volume or mass flow with change in time) – and make a calibration chart
7. Fill the 100L tank to half full (50L) and degrease the system using dish washer in solution (5% or 500 ml dish washer in 50L) for 10 minutes at room temperature
8. Rinse the system for 2 minutes with tap water until all the soap has been flushed out of the system at 40 Hz
9. Apply CIP procedure:
 - a. Rinse with Trisol 2000 (Ecolab) at 2% concentration at room temperature circulating for 15 minutes at 0.3L/s. This is a caustic based detergent
 - b. Rinse for 10 minutes at 0.3 L/sec
 - c. Sterilise with Vortexx (Ecolab) at 0.1% solution for 5 minutes at 0.3 L/sec at room temperature. Vortexx contains peroxyacetic and peroxyoctanoic acids, considered the most effective against biofilm formation. This product does not need rinsing after circulation. Make sure that the pipes are empty before starting to circulate the "culture medium" used to promote biofilm formation. Each end of the pipes should be "capped" to prevent recontamination
 - d. Rinse for 2 minutes at 0.3L/s to ensure nothing but water remains in the pipes as not all the water could be taken out
 - e. Total time = 32 minutes

10. Take swab samples on all 120 sites to check on initial biofilm bacterial intensity using bioluminometer
11. Take a sample of the water for analysis and store in the fridge
12. Add 50 – 100L water to 100L tank
13. Experiment start – circulate water slowly through the 6 pipe system at 0.13 m/s for about 5 weeks
14. Every 2 – 3 days after three weeks take a small sample of water from the fermenter to check for bacterial contamination (sample port on fermenter available) and, if possible, determine the concentration of bacteria
15. Once verified that there is significant bacteria based biofilm, take swab samples after 2 – 3 days on pipe F to confirm degree of biofilm intensity using bioluminometer. Avoid contact with grub screw threads. (Disinfect external area around grub screws with alcohol before swabbing)
16. Once adequate biofilm build-up has been confirmed, setup for analysis
17. On the day of analysis, stop circulating water through the system
18. Insert the whole rig into sterile static water for sonication experiments in a vertical position with sufficient volume to limit heat build-up effects from sonication (ultrasound)
19. Perform sonication in and against direction of flow for pipe C and in and against direction of flow for pipe D
20. Take swab samples on all 120 sites to check on biofilm intensity
21. CIP the whole system as in step 11

22. Take swab samples on all 120 sites to check CIP effectiveness
23. Once done, fill fermenter with 2% Trisol solution and run through the system for 10 – 20 minutes
24. Leave the solution in the system with the pump switched off
25. After 2 – 4 hours, discard all Trisol and rinse for next experiment

Experimental procedure for run 2

1. Assemble rig
2. Connect the experimental rig to the 100L heater tank, swimming pool pump and connection hoses
3. Pump water through to verify maximum system flow velocity (volume or mass flow with change in time) – See below for calibration chart
4. Apply CIP procedure:
 - a. Rinse with Trisol 2000 (Ecolab) at 2% (1 L Trisol in 50 L water) concentration at room temperature circulating for 15 minutes at 0.65L/s (50 Hz). This is a caustic based detergent
 - b. Rinse for 10 minutes at 0.65L/s (50 Hz)
 - c. Sterilise with Vortexx (Ecolab) at 0.1% (50 mL Vortexx in 50 L water) solution for 5 minutes at 0.65L/s at room temperature. Vortexx contains peroxyacetic and peroxyoctanoic acids, considered the most effective against biofilm formation. This product does not need rinsing after circulation. Make sure that the pipes are empty

before starting to circulate the "culture medium" used to promote biofilm formation.

Each end of the pipes should be "capped" to prevent recontamination.

- d. Empty all the Vortexx out of pipes and leave system for swabbing and experiments
 - e. Total time = 30 minutes
5. Take swab samples on all 120 sites to check on initial biofilm bacterial intensity using bioluminometer
 6. Take a sample of the water for analysis and store in the fridge
 7. Add 100 L water into tank
 8. Experiment start – Circulate water slowly through the 6 pipe system under laminar conditions (0.34 m/s for faster biofilm build-up) for 5 weeks
 9. After 5 weeks setup for analysis
 10. On the day of analysis, stop circulating water through the system
 11. Transfer the rig into a water bath and subject pipes A, B and D to ultrasound waves under static conditions while clamped on the pipes. Use 100% amplitude, continuous operation for 5 minutes on each pipe
 12. Take swab samples on all 120 sites to check on biofilm intensity
 13. CIP the whole system as in step 4
 14. Take swab samples on selected sampling sites to check CIP effectiveness

Interpretation of results

120 sampling points were grouped and identified according to the following numbering system shown in Table 3.1. Figures 3.9 and 3.10 helped to clarify the numbering used in Table 3.1.

Table 3.1: Sampling ports numbering system

Pipe	Number	Comments
A	1 and 2 for two weld stations	Three sets of sampling points for each station; one on weld bead, other two separated by 10 mm either side of weld bead. Each set included three points separated by 120°. Total nine sampling points per station separated by $120/3=40^\circ$. 18 stations on all pipes
B	3 and 4 for two weld stations	As above
C	5 and 6 for two weld stations	As above
D	7 and 8 for two weld stations	As above
E	9 and 10 for two weld stations	As above
F	11, 12 and 13 for two welds and central (control) sampling points	As above for 11 and 13. Station 12 is divided into four subsets of three sampling points separated by 90mm. On station 12 sampling points at each subset divided by 120°. Overall angular difference between succeed subsets staggered by 30°. This pipe length includes 30 sampling points, 9 for each station 11 and 13, and 12 for station 12

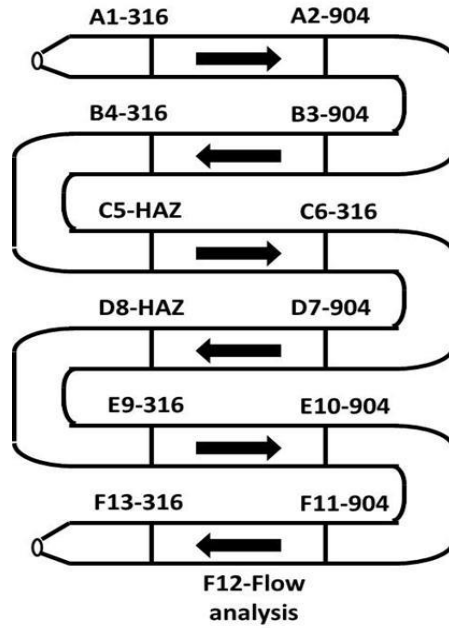


Figure 3.9: Schematic showing sampling numbering system for all pipes

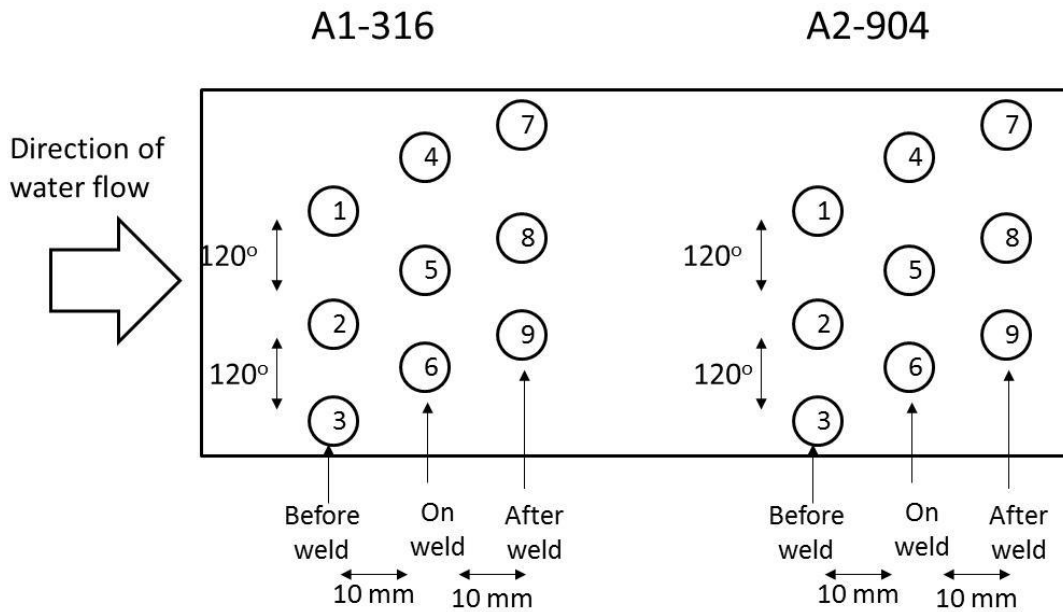


Figure 3.10: Schematic showing sampling numbering system on each pipe (pipe A in this case)

Tables 3.2 and 3.3 showed the position of the sampling points in clockwise direction in the direction of flow for all pipes for runs 1 and 2. There were minor differences in the orientation because physically it was difficult to align all the pipes in the same way. The numbering system showed 1, 2 and 3 as points before the weld; 4, 5 and 6 as points on the welds; and finally 7, 8 and 9 as points after the weld. Interpretation of data from bioluminometer based on industry standards was shown in Table 3.4.

Table 3.2: Distance (measured in degrees) of sampling points for both weld types on experimental rig for run 1

Pipe	Before weld			On weld			After weld		
	1	2	3	4	5	6	7	8	9
A	40	160	280	0	120	240	320	80	200
B	80	320	200	40	280	160	80	240	120
C	0	120	240	320	80	200	280	40	160
D	40	280	160	0	240	120	320	200	80
E	0	120	240	320	80	200	280	40	160
F	40	280	160	0	240	120	320	200	80

Table 3.3: Distance (measured in degrees) of sampling points for both weld types on experimental rig for run 2

Pipe	Before weld			On weld			After weld		
	1	2	3	4	5	6	7	8	9
A	0	120	240	320	80	200	280	40	160
B	40	280	160	0	240	120	320	200	80
C	80	200	320	40	160	280	0	120	240
D	80	320	200	40	280	160	0	240	120
E	80	200	320	40	160	280	0	120	240
F	80	320	200	40	280	160	0	240	120

Table 3.4: Interpretation of data from Clean-Trace™ NG bioluminometer

Intensity range	Explanation	Corrective action
0 – 150 RLU	Surface relatively clean	No CIP required
150 – 300 RLU	Caution area	Continuous monitoring
>300 RLU	Unacceptable – surfaces have biofilms	CIP required depending on intensity levels

The results obtained from the Clean-Trace™ NG bioluminometer could not be compared with other manufacturers' equipment as they gave different values for the same sampling position. As a result, the data and interpretations were based only on this bioluminometer.

The details for the equipment and the swabs used during the analysis were as follows:

- (a) Machine used was Clean-Trace™ NG serial number TMM118 and information for swabs used:
- (b) Before run: Clean-Trace surface ATP, batch number 891, expiry 28 Mar 2014
- (c) After run before & after CIP: Clean-Trace surface ATP, batch number 872 (expiry 22 Feb 2014) and 891 (expiry 28 Mar 2014)

In the first run, pipes C and D were externally sonicated after the run to check the effect of ultrasound waves. The sonication device was fixed to the external face of the pipe with jubilee clips. The whole pipe system had to be under water (or at least most of the piping had to be under water) to facilitate sonication. In the second run, pipes A, B and D were subjected to ultrasound waves. In this case the pipe system was submerged in a water bath. The sonication device was fixed into a clamp, this in turn clamped onto the pipe work. A pre-test check on the damping effect of the clamp showed damping to be significant. Similarly the 4 mm wall thickness of the pipe wall may be anticipated to provide damping.

Pipe A had 316L and 904L welds and argon was used to purge oxygen during welding whilst pipe B had the two welds but no argon was used to purge oxygen. Pipe D was pickled and passivated but no argon was used during welding. The ultrasound probe used worked well in water and after the run the system was subjected to ultrasound waves as shown in Figures 3.11 and 3.12.



Figure 3.11: Arrangement during use of ultrasound waves for run 1 on (a) pipe C and (b) pipe D before swabbing. NB: sonication device as fastened to pipes using jubilee clamps

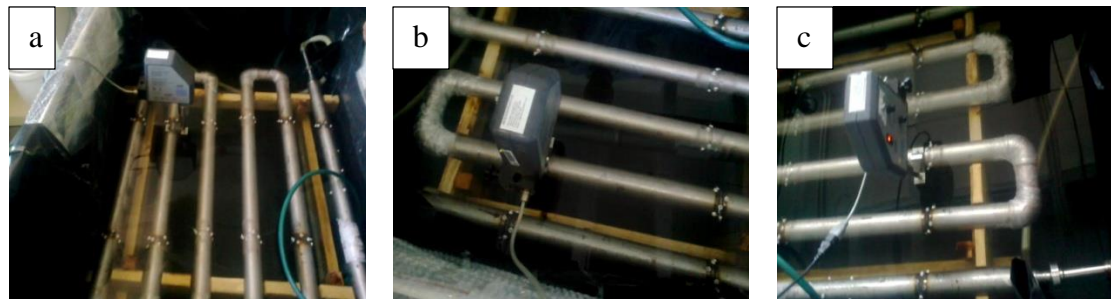


Figure 3.12: Arrangement during use of ultrasound waves for run 2 on (a) pipe A, (b) pipe B and (c) pipe D before swabbing. NB: sonication device was fastened to pipes using a 1.001kg clamp

For run 1 in pipe C, ultrasound waves were applied in the direction of flow for 10 minutes but in pipe D, they were applied against the direction of flow for 5 minutes.

For run 2 in pipe A, ultrasound waves were applied in the direction of flow for 5 minutes but in pipes B and D, they were applied against the direction of flow for 5 minutes. There was water inside the pipe systems and ultrasound waves were transmitted from the probe to the pipe wall as it was clamped to the pipe wall using jubilee clips for run 1 and a plate clamped to the pipe and ultrasonic probe inserted inside in run 2 (see Figure 3.12). The ultrasound waves were then transferred to the inside walls of the pipes and then to the water inside the pipes to have any effect. In run 1, the probe was clamped just above C5-HAZ and D8-HAZ while for run 2, the probe was clamped on A1-316, B1-316 and D8-HAZ according to Figure 3.9.

The results for each pipe were recorded and compared against other pipes to check on the effectiveness of ultrasound waves and the effect of pipe treatments done on biofilm formation and cleaning. A summary table of the conditions was given in Table 3.5.

Table 3.5: Summary of all conditions of the pilot rig for dynamic experiments

Pipe	Argon	Subjected to US*	Type of weld			Pickled and passivated
	purged		316L	904L	HAZ	
A	yes	yes	yes	yes	no	no
B	no	yes	yes	yes	no	no
C	no	no	yes	no	yes	yes
D	no	yes	no	yes	yes	yes
E	yes	no	yes	yes	no	no
F	no	no	yes	yes	no	no

*US – Ultrasound waves

Water was circulated at different flowrates; at 0.13 m/s and 0.30 m/s for circulation and CIP respectively during run 1. For run 2, the flowrates were 0.34 m/s and 0.30 m/s for circulation and CIP respectively. Run 1 was meant to imitate what happens inside brewing vessels while run 2 was meant to imitate what happened inside brewing pipes.

Temperature changes during operation

Using centrifugal pumps resulted in temperature increases due to increase in momentum because it was a closed system. As such, the ambient and experimental temperatures were monitored for both runs and the difference between operating and ambient temperatures was calculated to determine

if the change was still the same. Run 1 was performed in winter giving low operating temperatures but run 2 was performed under summer conditions giving higher temperatures.

Temperature control was not performed as in industry it is not practical to control temperature in all pipe systems but only in vessels. However, biofilms were confirmed to have formed and attached on pipe walls.

References

- Boe-Hansen, R., Martiny, A.C., Arvin, E. and Albrechtsen, H.-J. (2003) Monitoring biofilm formation and activity in drinking water distribution networks under oligotrophic conditions, *Water Science and Technology*, **47(5)**, 91–97.
- Boulangé-Petermann, L., Rault, R., and Bellon-Fontaine, M-N. (1997) Adhesion of streptococcus thermophilus to stainless steel with different surface topography and roughness, *Biofouling: The Journal of Bioadhesion and Biofilm Research*, **11(3)**, 201–216.
- Carbone, M. J. (2001) Obtaining internal surface samples from an in-service pipe, United States Patent, Patent number: US 6,318,192 B1, date of Patent: November 20, 2001, Filed; October 20, 1998.
- Deines, P., Sekar, R., Husband, P. S., Boxall, J. B., Osborn, A. M. and Biggs, C. A. (2010) A new coupon design for simultaneous analysis of in situ microbial biofilm formation and

community structure in drinking water distribution systems, *Applied Microbiology and Biotechnology*, **87(2)**, 749–756.

Flint, S. H. (1998) Formation and control of biofilms of thermo-resistant *Streptococci* on stainless steel, Food Technology Department, Massey University, New Zealand, pp. 1–237.

Horcas, I., Fernandez, R., Gomez-Rodriguez, J. M., Colchero, J., Gomez-Herrero, J. and Baro, A. M. (2007) WSxM: A software for scanning probe microscopy and a tool for nanotechnology, *Review of Scientific Instruments*, **78**, 013705 (2007).

Ince, N.H. and Belen, R. (2001) Aqueous phase disinfection with power ultrasound: Process kinetics and effect of solid catalysts, *Environmental Science and Technology*, **35(9)**, 1885–1888.

Ivanova, E. P., Truong, V. K., Webb, H. K., Baulin, V. A., Wang, J. Y., Mohammadi, N., Wang, F., Fluke, C. and Crawford, R. J. (2011) Differential attraction and repulsion of *Staphylococcus aureus* and *Pseudomonas aeruginosa* on molecularly smooth titanium films, *Scientific Reports*, **1(165)**, 1–8.

Juhna, T., Birzniece, D. and Rubulis, J. (2007) Effect of phosphorus on survival of *Escherichia coli* in drinking water biofilms, *Applied and Environmental Microbiology*, **73(11)**, 3755–3758.

- Lee, Y. (2013) An evaluation of microbial and chemical contamination sources related to the deterioration of tap water quality in the household water supply system, *International Journal of Environmental Research and Public Health*, **10(9)**, 4143–4160.
- Pachepsky, Y., Morrow, J., Guber, A., Shelton, D., Rowland, R. and Davies, G. (2011) Effect of biofilm in irrigation pipes on microbial quality of irrigation water, *Letters in Applied Microbiology*, **54(3)**, 217–224.
- Park, S-K. and Kim, Y-K. (2008) Effect of chloramine concentration on biofilm maintenance on pipe surfaces exposed to nutrient-limited drinking water, *Water SA*, **34(3)**, 373–380.
- Simões, M. J. V. (2005) Use of biocides and surfactants to control *Pseudomonas fluorescens* biofilms: Role of the hydrodynamic conditions, PhD thesis, Department of Chemical and Biological Engineering, University of Minho, Portugal, pp. 1–223.
- Sithole, L. N. S. (2007) Antimicrobial properties of anodised and silver plated aluminium alloys, Fourth year research report, WITS University, 39–42.
- Szczotko, M. and Krogulski, A. (2010) Assessment of microbial growth on the surface of materials in contact with water intended for human consumption using ATP method, *Polish Journal of Microbiology*, **59(4)**, 289–294.
- Vinnichenko, M., Chevolleau, Th., Pham, M.T., Poperenko, L. and Maitz, M.F. (2002) Spectroellipsometric, AFM and XPS probing of stainless steel surfaces subjected to biological influences, *Applied Surface Science*, **201(1)**, 41–50.

- Woodling, S. E. and Moraru, C. I. (2005) Influence of surface topography on the effectiveness of pulsed light treatment for the inactivation of *Listeria innocua* on stainless-steel surfaces, *Journal of Food Science*, **70(7)**, M345–M351.
- Wu, X., Joyce, E. M. and Mason, T. J. (2012) Evaluation of the mechanisms of the effect of ultrasound on *Microcystis aeruginosa* at different ultrasonic frequencies, *Water Research*, **46(9)**, 2851–2858.
- Yu, J., Kim, D. and Lee, T. (2010) Microbial diversity in biofilms on water distribution pipes of different materials, *Water Science and Technology*, **61(1)**, 163–171.

CHAPTER FOUR

**"I FIND THAT THE HARDER I WORK, THE MORE LUCK I SEEM TO
HAVE."**

- THOMAS JEFFERSON (1743-1826)

4. RESULTS AND DISCUSSION

4.1 Static experiments

4.1.1 Controlling biofilms using ultrasound waves

This section is based on work presented at local conferences and an international conference:

- (i) Mamvura, T.A., Iyuke, S.E. and Paterson, A. E. (2012) Ultrasound waves used to control soil films, *SAIChE conference*, Durban, South Africa, September 2012.
- (ii) Mamvura, T.A., Iyuke, S.E. and Paterson, A. E. (2012) Ultrasound waves used to control soil films, *Postgraduate Symposium*, Johannesburg, South Africa, October 2012.
- (iii) Mamvura, T.A., Iyuke, S.E. and Paterson, A. E. (2013) Ultrasound waves used to control soil films in brewing industry, Third International Conference on Biotechnology Engineering (ICBioE2013) held on 2–4 July 2013 at Berjaya Time Square Hotel, Kuala Lumpur, Malaysia, see Appendix IV.

Effect of amplitude on biofilm removal

Ultrasound intensity/amplitude in water was investigated to discover its effect on removal of *E. coli* biofilms on:

- i. front surface of coupons (facing ultrasound waves)
- ii. different welds on coupons (facing ultrasound waves)
- iii. back surface of coupons (not facing the ultrasound waves)
- iv. back surfaces of different welds on coupons (not facing ultrasound waves)

Disinfection efficiency was used as a measure of comparison and the results were summarised in Figures 4.1 (for front surfaces) and 4.2 (for back surfaces). Amplitude was given as a percentage of the maximum amplitude of waves generated by sonicator.

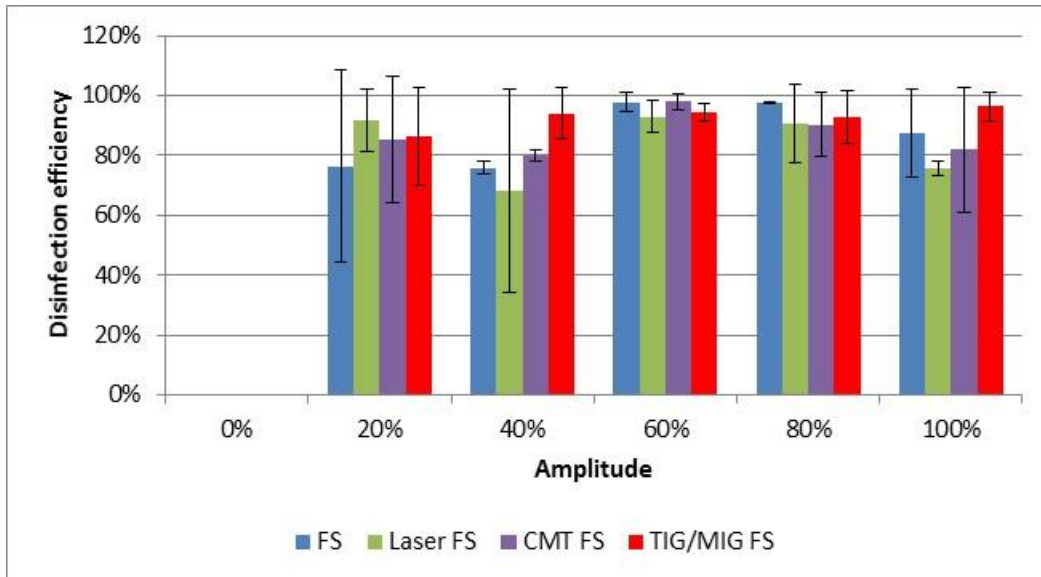


Figure 4.1: Effect of ultrasound intensity on the removal of biofilms for surfaces facing ultrasound waves. FS – front surface, Laser – Laser welding, CMT – Cold Metal Transfer, and TIG/MIG – Tungsten or Metal Inert Gas processes. Five experiments were conducted and each experiment was repeated twice

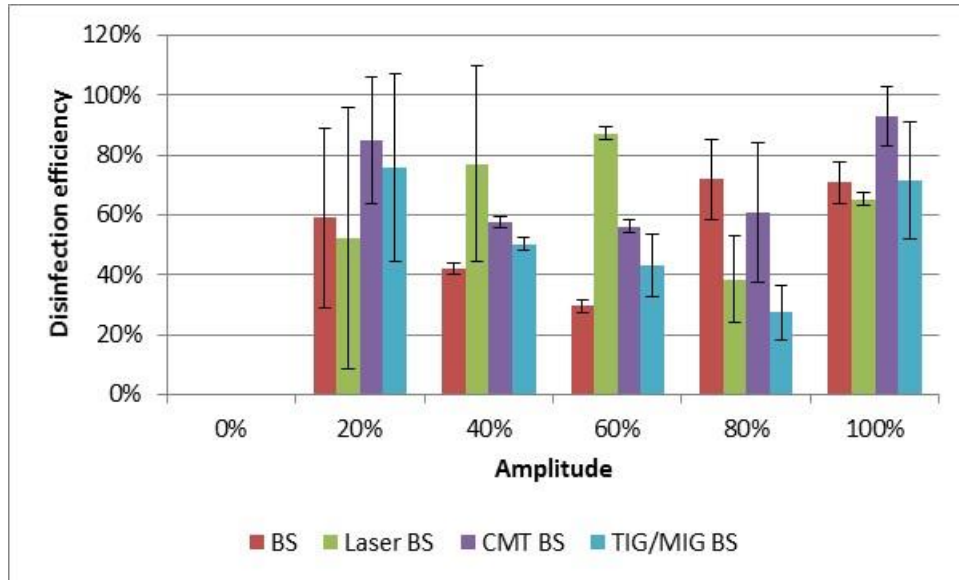


Figure 4.2: Effect of ultrasound intensity on the removal of biofilms for surfaces not facing ultrasound waves. BS – back surface. Five experiments were conducted and each experiment was repeated twice

Maximum disinfection efficiency was 100% but due to statistical analysis, the standard deviation for some results surpassed 100% efficiency and this should not be taken to mean that disinfection efficiency was more than 100%. This was observed on most results during the analysis. Results showed robust application for all ranges of amplitude giving efficiencies >70% for surfaces facing ultrasound waves (except for Laser weld with 68% at 40% amplitude) and efficiencies between 25 and 90% for surfaces not facing ultrasound waves. This implied that there was generally lack of sensitivity due to change in amplitude as results were in the acceptable range, above 70%, for

surfaces facing ultrasound waves with greatest efficiency observed at an amplitude of 60% (disinfection efficiency $\geq 92\%$) for all surfaces.

The back surface and all the welds at the back showed inconsistency with increase in amplitude but generally there was removal of biofilms which was a positive especially for vessels which overflow leading to biofilm formation on the outside. These observations made it possible to apply ultrasound waves on the outside of industrial pipes and have an effect on the inside surfaces as they could be transmitted through SS surfaces.

Effect of time of exposure on biofilm removal

The total time of exposure of ultrasound waves on the biofilm was investigated to determine its effect and the results were summarised in Figures 4.3 (for front surfaces) and 4.4 (for back surfaces).

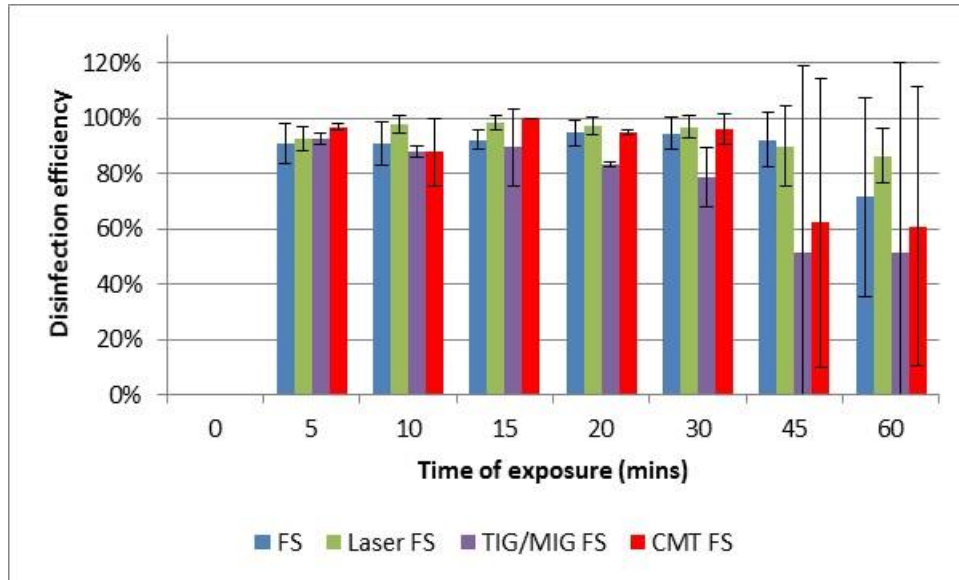


Figure 4.3: Effect of time of exposure on the removal of biofilms for surfaces facing ultrasound waves. Seven experiments were conducted and each experiment was repeated twice

The results showed robust application (disinfection efficiency did not vary significantly for the whole time change up to 30 minutes) up to 30 minutes exposure time (disinfection efficiencies >70%) for surfaces facing ultrasound waves and efficiencies between 25 and 100% for surfaces not facing ultrasound waves. After 30 minutes the disinfection efficiencies started to drop down, particularly for TIG/MIG and CMT welds. The reason may have been due to prolonged exposure time which leads to some of *E. coli* cells bursting and the contents of the cells re-attaching to SS surfaces again thereby reducing the disinfection efficiency observed. Alternatively, there was encouraged re-growth of bacterial cells with prolonged exposure time leading to reduced efficiencies observed. The back surface and all the welds at the back showed inconsistency with

increase in time of exposure even though there was removal of biofilms which was a positive result.

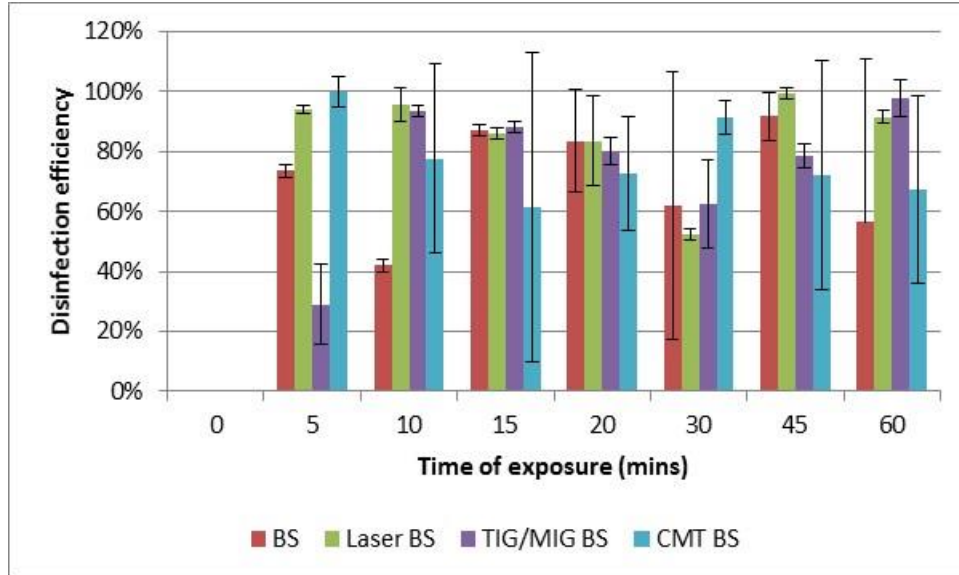


Figure 4.4: Effect of time of exposure on the removal of biofilms for surfaces not facing ultrasound waves. Seven experiments were conducted and each experiment was repeated twice

A plot of N/N_0 against time should be a straight line from the origin for first order kinetics as shown in literature (Álvarez *et al.*, 2003; Kubo *et al.*, 2005). However, the data obtained could not fit a straight line (line not shown to improve clarity of graphs) when plotted as the regression coefficient R^2 were very low (<0.20) leading to the conclusion that rate of disinfection did not follow first order kinetics (see Figures 4.5 and 4.6 for surface in contact and not facing ultrasound waves respectively).

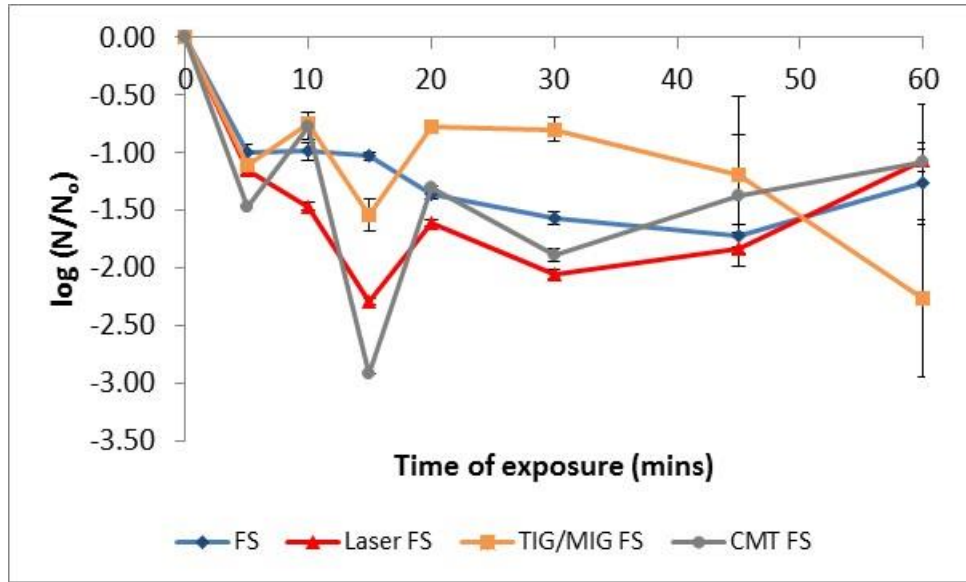


Figure 4.5: A plot of $\log(N/N_0)$ against time for surfaces that were facing ultrasound waves

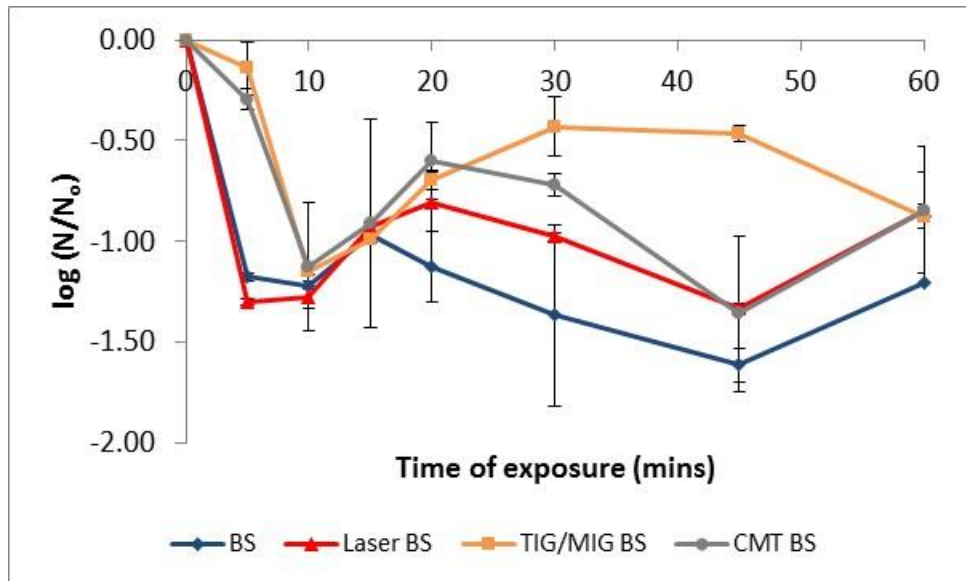


Figure 4.6: A plot of $\log(N/N_0)$ against time for surfaces that were not facing ultrasound waves

Effect of distance between the probe and coupons

The effect of the distance from probe producing ultrasound waves to the coupon surface on removal of biofilms was investigated and the results are presented in Figures 4.7 (for front surfaces) and 4.8 (for back surfaces).

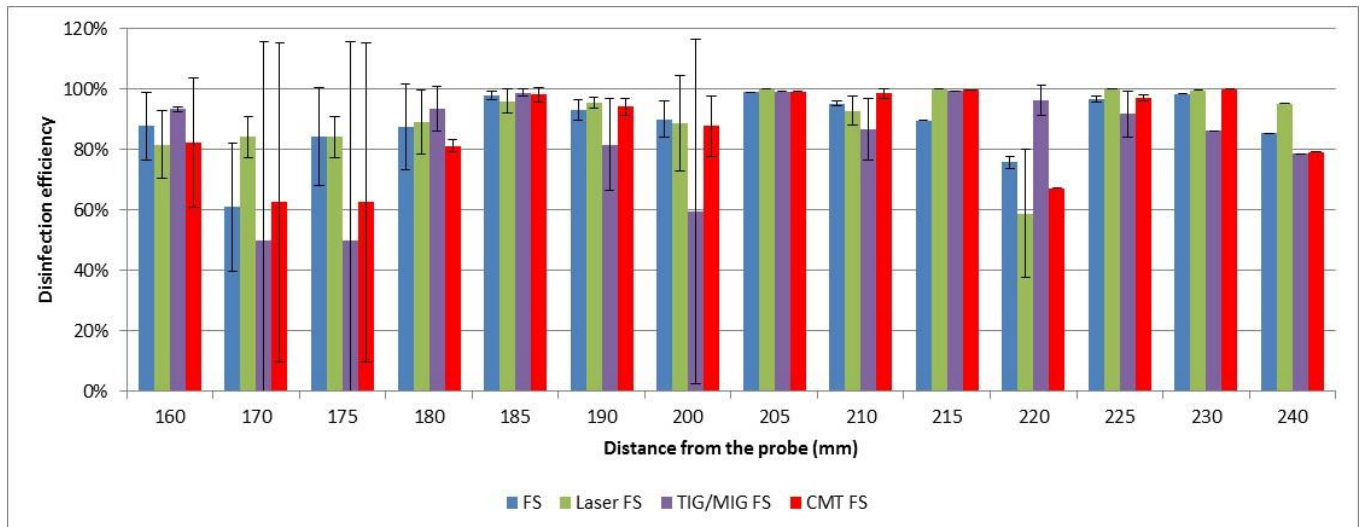


Figure 4.7: Effect of distance of probe from coupon surface on the removal of biofilms for surfaces facing ultrasound waves. Fourteen experiments were conducted and each experiment was repeated twice

From Figure 4.7 it was observed that the disinfection efficiency of biofilms for surfaces facing ultrasound waves varied with change in distance from the probe, but the effect was not greatly hindered as efficiencies $\geq 60\%$ were obtained along the whole distance up to 240 mm except at 170 and 175 mm.

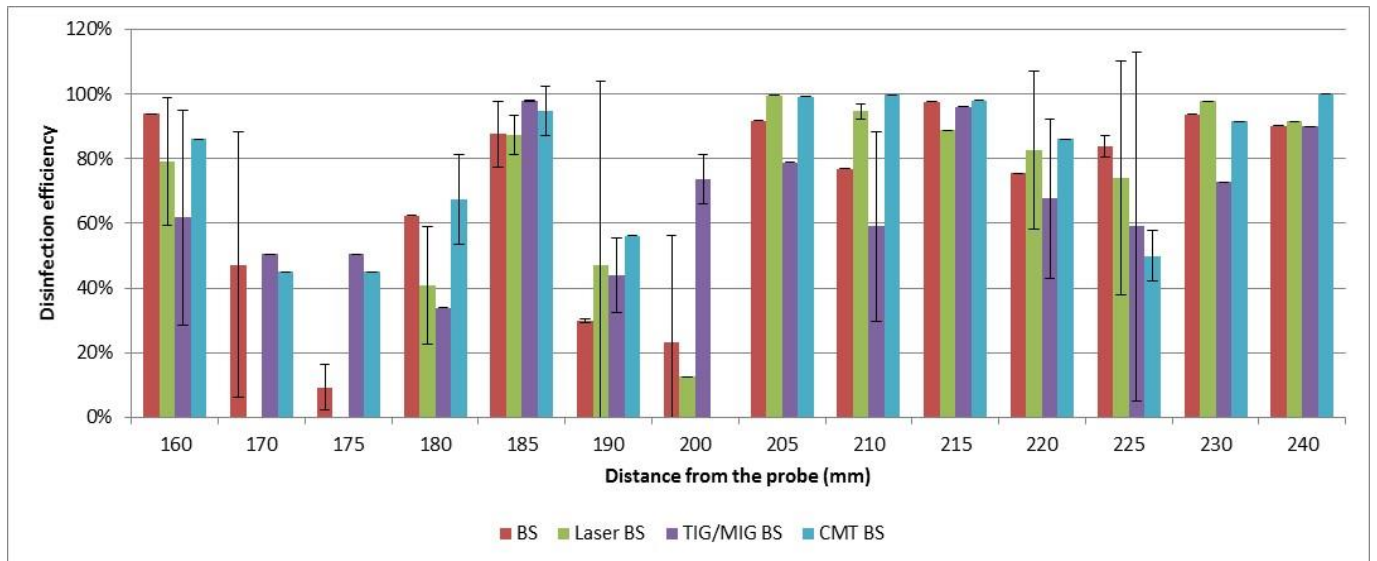


Figure 4.8: Effect of distance of probe from coupon surface on the removal of biofilms for surfaces not facing ultrasound waves. Fourteen experiments were conducted and each experiment was repeated twice

The back surface and all the welds at the back showed inconsistency with increase in distance from the probe but there was removal of biofilms which was a positive result to be considered. However, there was a lot of deviation from the results for the whole range maybe due to reflection of waves at the surface.

These observations meant that ultrasound probes could be arranged in series or in parallel to each other along a pipe length or process vessel to enhance the effect of ultrasound waves against

biofilms in the brewing industries staggered at optimum distances between them. Surfaces not facing ultrasound waves did not show the same trend except at greater lengths of 225 to 240 mm, however, elimination of biofilms was successful in some instances showing the advantages that can be gained when using ultrasound waves on the inside of pipes or process vessels by eliminating biofilms on the back surface. Mott *et al.* (1998) found process efficiencies >80% at 70 and 500 mm while removing *Proteus mirabilis* biofilms from water-filled glass tubes at 20 kHz. These results were in line with observations from the current study.

In general high-power ultrasound did not result in 100% elimination of *E. coli* biofilms (except at various conditions) attached to SS. Failure of ultrasound waves to eliminate all biofilm bacterial cells on most occasions meant that the process had to be used in combination with other systems. The fact that it eliminated most of the bacterial cells from SS surfaces meant the process could be used as a primary method followed by a secondary method to eliminate the remaining bacteria or used simultaneously with e.g. ozone, chlorine in a CIP process, with the oxidant used in reduced quantities; i.e. the process could result in reduced costs.

Discussions

Removal of biofilms using ultrasound waves has been investigated before particularly in the dental industry for toothbrush applications (Dror *et al.*, 2009; Parini and Pitt, 2005; Verkaik *et al.*, 2010). Nishikawa *et al.* (2010) concluded that ultrasound waves at lower frequencies resulted in 80% or more removal of biofilms alone and addition of a biocide further enhanced the effect to 100%.

Oulahal *et al.* (2004) did not see any effect of time of exposure of waves at 40 kHz on *E. coli* up to 60 seconds with removal of biofilms being 30%. Combined treatment with ultrasound waves in chelating solutions (EDTA or EGTA) for 10 seconds was found to be efficient in removal of milk biofilms with *E. coli*; resulting in 61% and 69% removal respectively (Oulahal *et al.*, 2004). Wu *et al.* (2012) investigated *M. aeruginosa* at three different frequencies (20, 580 and 1146 kHz) over 30 minutes and concluded that lower frequencies resulted in higher reduction of biofilms. The same conclusions were also reached by Mason *et al.* (2011).

Joyce *et al.* (2010) investigated ultrasound waves on algae up to 30 minutes at five different frequencies (20, 40, 580, 864 and 1146 kHz) and found optimum time of 5 minutes at 20 kHz, 20 minutes at 40 kHz, and above 30 minutes at 580, 864 and 1146 kHz showing increase in time with increase in frequency. Rajasekhar *et al.* (2012) concluded that increasing exposure time up to 20 minutes resulted in greater reduction in cell numbers and greater inhibition of the growth of remaining *M. aeruginosa* cells which was in accordance with general observations in sonochemistry. However, treatment for exposure time greater than 10 minutes at lower power intensity led to immediate increase of microcystin levels in the treated water. Prolonged exposure (> 10 minutes) to ultrasound waves at higher power intensities led to a reduction of the microcystin concentration, which was attributed to ultrasonic degradation.

The results obtained confirmed that ultrasound waves were able to control biofilms and partly confirmed that ultrasound waves were able to go through walls of SS pipes (3 mm thick coupon plates). However, the inconsistent results obtained for back surfaces showed that most of the energy was either absorbed or reflected during the operation and it presented difficulties in next set of experiments (dynamic experiments) and in industrial application. This was because in industry it was not practical to disassemble pipes and vessels so as to use ultrasound waves but the process needed adoption so that it could be used on outside of pipe walls.

4.1.2 Surface profile changes during use of ultrasound waves

This section was based on work presented at an international conference, a local symposium and a paper under review:

- (i) Mamvura, T.A., Iyuke, S.E. and Paterson, A. E. (2013) Stainless steel surface topography changes during sonication with ultrasound waves used to control soil films, Third International Conference on Biotechnology Engineering (ICBioE2013) held on 2-4 July 2013 at Berjaya Time Square Hotel, Kuala Lumpur, Malaysia, see Appendix IV.
- (ii) Mamvura, T.A., Iyuke, S.E. and Paterson, A. E. (2013) Stainless steel surface topography changes during sonication with ultrasound waves used to control soil films, *Postgraduate Symposium*, Johannesburg, South Africa, August 2013.
- (iii) Mamvura, T.A., Iyuke, S.E. and Paterson, A. E. (2013) Investigation on the effect of ultrasound waves on stainless steel surfaces during removal of soil films, *Advances in Environmental Biology*, under review.

Surface profile of stainless steel

Surfaces used in the food and beverage industry normally have average roughness (R_a) < 800 nm although, values up to 3200 nm would be acceptable as long as the cleaning fluid flowrate during CIP is sufficient enough to remove biofilms from the surfaces (Frantsen and Mathiesen, 2009; Holah, 2000; Jullien *et al.*, 2003). However, Detry *et al.*, (2010) concluded that rough SS surfaces are characterised by $R_a > 500$ nm. The surface morphology of the SS surfaces used in the beverage industry is mainly attributed to mechanical and chemical polishing processes (Vinnichenko *et al.*, 2002). Mechanical polishing results from using rotating rotor blades while chemical polishing results from pickling and passivating.

Changes in surface topography

The results for surface topography and surface morphology for normal surface and welded surfaces are presented in the following section.

Surface profile of different surfaces used

Surface profile for the four surfaces used in the study (normal surface, laser, CMT and MIG weld surfaces) were analysed before being used in the experiments and results are shown in Figures 4.9, 4.10, 4.11 and 4.12.

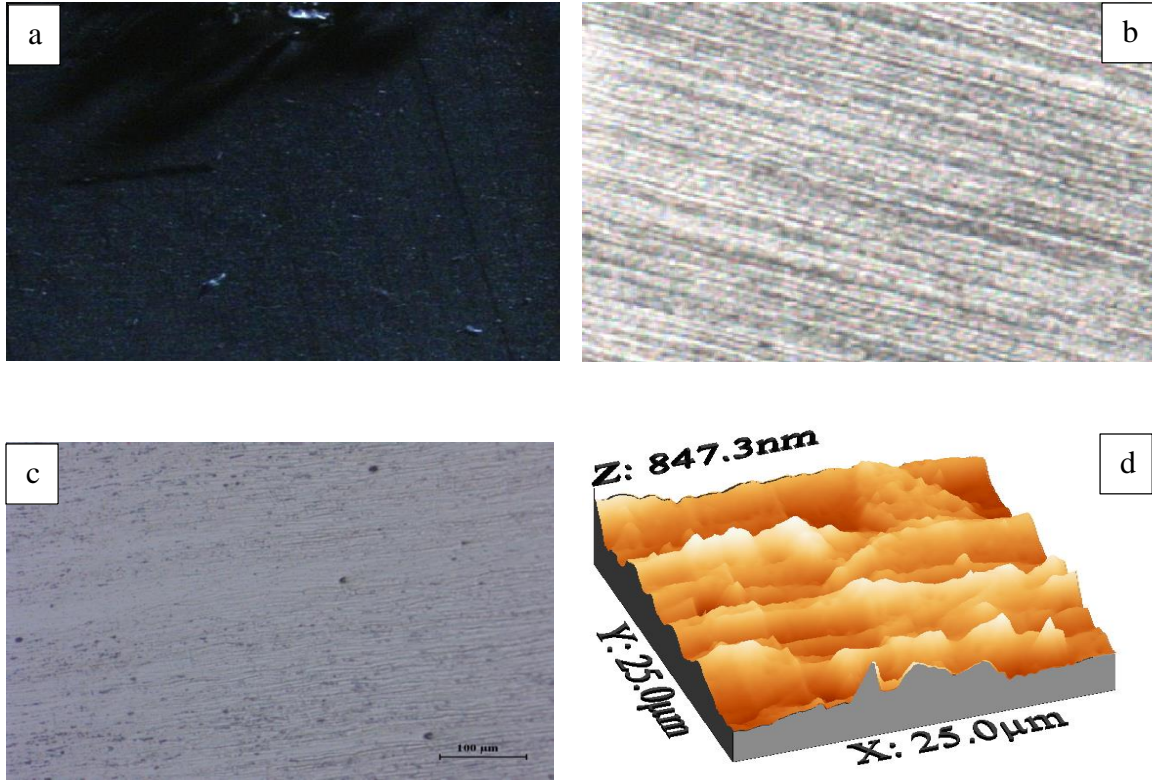


Figure 4.9: Surface analysis for normal surface. (a) 5x (b) polished and etched 50x (c) polished and etched 200x (d) AFM for $25 \times 25 \mu\text{m}^2$ surface area

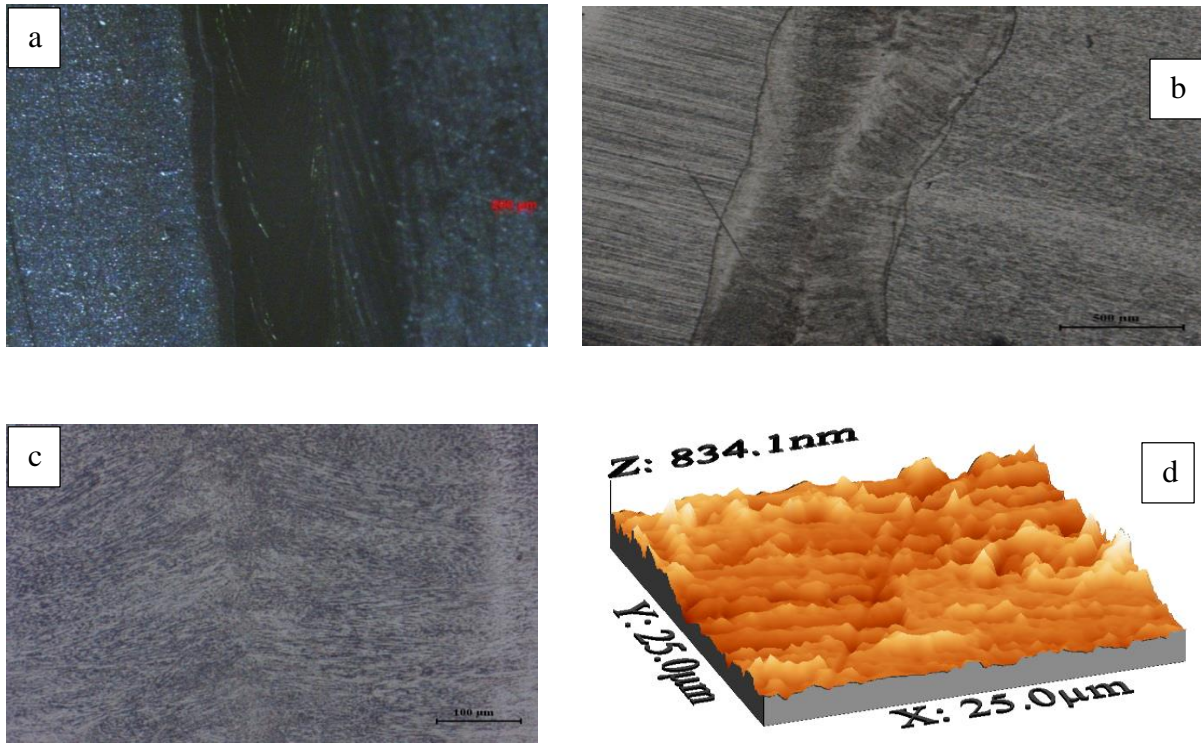


Figure 4.10: Surface analysis for laser weld surface. (a) 5x (b) polished and etched 50x (c) polished and etched 200x (d) AFM for 25x25 μm^2 surface area

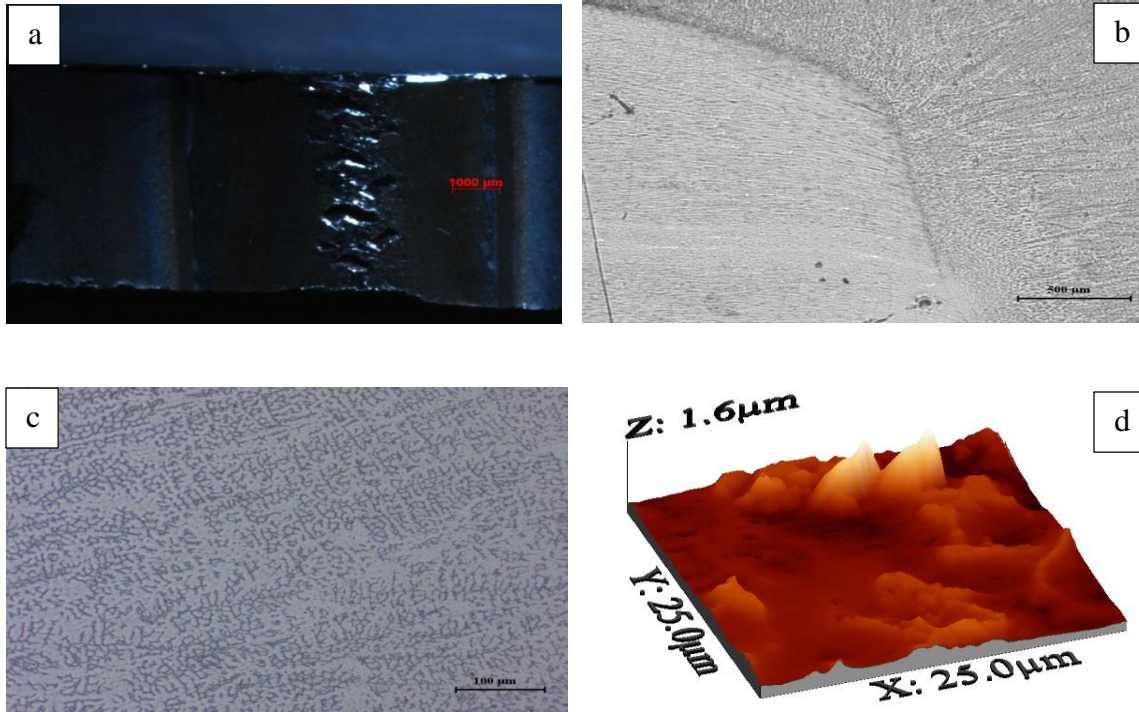


Figure 4.11: Surface analysis for CMT weld surface. (a) 5x (b) polished and etched 50x (c) polished and etched 200x (d) AFM for $25 \times 25 \mu\text{m}^2$ surface area

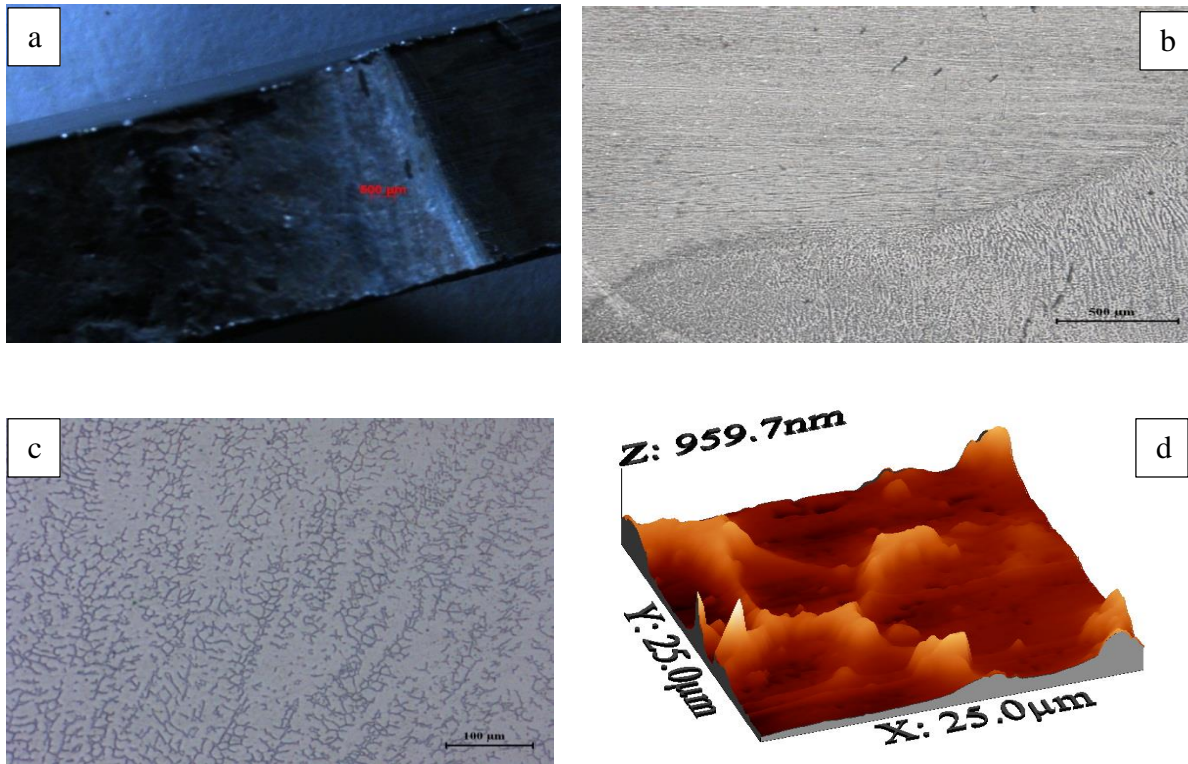


Figure 4.12: Surface analysis for MIG weld surface. (a) 5x (b) polished and etched 50x (c) polished and etched 200x (d) AFM for $25 \times 25 \mu\text{m}^2$ surface area

The figures showed that as SS surfaces were welded, the profile become rough as seen by an increase in peaks. CMT and MIG weld surfaces showed that the surfaces contained mainly peaks and few pits/valleys and such surfaces encouraged biofilm formation. A test was done to determine the bacterial loading and this was compared against R_{max} for the surfaces and the results are presented in Table 4.1.

Table 4.1: E. coli bacterial loading concentration against surface type and maximum height

Surface type	R _{max} (μm)	Average bacterial loading (x10 ⁷) cfu/ml
Normal surface	0.85	79.16±12.64
Laser weld surface	0.83	77.03±14.08
CMT weld surface	1.60	84.80±14.91
MIG weld surface	0.96	143.54±13.14

From the table it was deduced that bacterial loading increased from laser weld to normal surface to CMT weld and finally MIG weld. The results were similar to changes in R_{max} for the surfaces which followed the order of laser weld, normal surface, MIG weld and finally CMT weld. These results gave further evidence as to why welding was prone to MIC as it resulted in rough surfaces which attracted bacteria resulting in biofilms.

Sreekumari *et al.* (2005) obtained the same observations that welds showed very high bacterial attachment as compared to HAZ or normal surface whilst analysing two different bacteria both isolated from groundwater corrosive environment in Japan, viz. *Pseudomonas* sp. and *Bacillus* sp., a gram negative and positive strain, respectively on SS 304L in a laboratory. The reasons for the preferential colonisation of bacteria near the welds were thought to be the substratum roughness, difference in material composition (parent material had a homogeneous wrought structure; HAZ and welded surfaces had heterogeneous structures) and surface properties like surface energy.

Surface topography analysis

Experiments were conducted using 24 kHz ultrasound waves on coupons subjected to 9 adhesion-cleaning cycles. Surface topography was done and the results are presented in Table 4.2 with mean and standard deviations obtained from six sampling positions.

Table 4.2: Surface topography data (mean±SD) for the different surfaces used in the study. Analysis was done four and six times, before and after being subjected to cleaning cycles respectively (n = 4 before and n = 6 after being subjected to ultrasound waves)

Parameter		Normal surface	Laser weld	CMT weld	MIG weld
R _a (nm)	Before	325±4	325±4	325±4	325±4
	After	192±1	117±2	194±4	148±11
	Change	41%	64%	40%	54%
R _q (nm)	Before	395±4	395±4	395±4	395±4
	After	237±3	155±1	252±3	190±15
	Change	40%	61%	36%	52%
R _{max} x10 ³ (nm)	Before	2.28±0.02	2.28±0.02	2.28±0.02	2.28±0.02
	After	1.68±0.17	2.00±0.33	1.28±0.02	1.59±0.02
	Change	26%	12%	44%	30%

All surfaces were compared against normal surface parameters as it was the starting surface finish before welding and subjecting to ultrasound waves. This enabled helped to clarify the changes that occur when welding was performed and the effect of ultrasound waves from the original surface finish.

Surface roughness (R_a) of approximately $0.3 \mu\text{m}$ showed that the surface finish was 2B (Lelièvre *et al.*, 2002) and this was the case for normal surfaces before being subjected to ultrasound waves after adhesion-cleaning cycles. Increase in R_a before treatment followed the trend laser weld \Rightarrow normal surface \Rightarrow CMT \Rightarrow MIG and increase in R_a after treatment followed the trend laser weld \Rightarrow MIG \Rightarrow normal surface \Rightarrow CMT. There was significant change in surface topography after treatment with ultrasound waves for all surfaces as seen from % change calculated. Other authors came to the same conclusion that ultrasound waves resulted in smoother surfaces which gave better surface cleanability. Other industries make use of ultrasonic electropolishing which yield fairly uniform, patterned (cratered) surfaces which are attractive for food and beverage applications (Detry *et al.*, 2010; Eliaz and Nissan, 2007; Ivanova *et al.*, 2011; Zand *et al.*, 2012). Increase in R_{max} before treatment followed the trend laser weld \Rightarrow normal surface \Rightarrow CMT \Rightarrow MIG and increase in R_{max} after treatment followed the trend laser weld \Rightarrow normal surface \Rightarrow MIG \Rightarrow CMT showing a significant change in R_{max} after treatment with ultrasound waves for all surfaces. The trend was almost similar and it further gave evidence that welding gave rough surfaces which are prone to biofilm formation and difficulties in cleaning the surfaces.

According to Detry *et al.* (2010), surface topography of coupons before and after being subjected to ultrasound waves showed that they were comparatively smooth i.e. all R_a values were less than 500 nm. High R_a , R_q and R_{max} values before treatment showed that the surface profile could be considered rough as compared to after treatment with ultrasound waves, showing an advantage of ultrasound waves of making the surfaces smooth during treatment. R_q and R_{max} values followed the same trend as R_a for all coupon surfaces.

Surface morphology analysis

Surface morphology was done for experiments on coupons subjected to 9 adhesion-cleaning cycles and the results are presented in Table 4.3.

R_{skw} was commonly used to describe the symmetry of the surface and the table showed that for normal surface, $R_{skw} < 0$ indicating the presence of pits/valleys and this negatively skewed surface was good for lubrication purposes. Welded surfaces had $R_{skw} > 0$ which indicated the presence of peaks. The data was in agreement and it showed that after welding, the surfaces had peaks that gave rough surfaces i.e. welding processes resulted in surfaces mainly composed of peaks as compared to normal surfaces which were composed of pits/valleys.

Table 4.3: Surface morphology data (mean±SD) for the different surfaces used in the study. Analysis was done four and six times, before and after being subjected to cleaning cycles respectively (n = 4 before and n = 6 after being subjected to ultrasound waves)

Surface	R _{skw}		R _{kur}		
	Before	After	Before	After	Change
NOS	-0.937±0.001	-0.807±0.037	3.11±0.02	3.28±0.01	(5%)
LSW	-0.937±0.001	0.216±0.056	3.11±0.02	7.47±0.38	(140%)
CMT	-0.937±0.001	0.225±0.020	3.11±0.02	2.23±0.02	28
MIG	-0.937±0.001	0.622±0.020	3.11±0.02	3.58±0.02	(15%)

NOS–normal surface; LSW–laser weld surface; CMT–CMT weld surface; MIG–MIG weld surface. Brackets showed negative change for R_{kur} before and after being subjected to ultrasound waves

Small changes in R_{skw} for normal surface showed that there was little effect after use of ultrasound waves i.e. erosion was experienced to a minimum. For the welded surfaces, peaks were more pronounced in MIG weld followed by CMT weld followed by laser weld and this was in agreement with bacterial loading trend as well.

R_{kur} was used to measure the peakedness of the surface and CMT weld surface had $R_{kur} < 3$ which showed lack of high peaks i.e. peaks were greatly eroded during exposure to ultrasound waves and a decrease in R_{kur} meant that the surface was flattening during exposure before ultimately forming pits/valleys just like normal surfaces. This is an advantage as it leads to a smoother surface which is good for lubrication and discourage biofilm formation. Normal surface had $R_{kur} \approx 3$ which showed a more even and “smooth” surface and a small change in R_{kur} before and after treatment with ultrasound waves meant that no erosion was experienced i.e. the surface was resistant to ultrasound waves as seen from Table 4.3. Laser and MIG weld surfaces had $R_{kur} > 3$ which meant that there was presence of high peaks and increase in R_{kur} observed which meant that surfaces had more pits than normal surface i.e. weld surfaces were rough as compared to normal surface and this favoured biofilm formation. From the data it was also shown that the erosion process was slower on laser and MIG weld surfaces as compared to CMT weld surfaces.

Surface profile before and after exposure to ultrasound waves

Analysis before and after treatment was done but only results for normal surface was presented (see Figure 4.13). The images revealed that normal surface had an increase in pits/valleys after treatment and the grain sizes were smaller. Surfaces with pits/valleys are good for lubrication purposes and the normal surface falls under that category. However, as revealed before, after welding surfaces resulted in peaks which gave poor lubrication conditions.

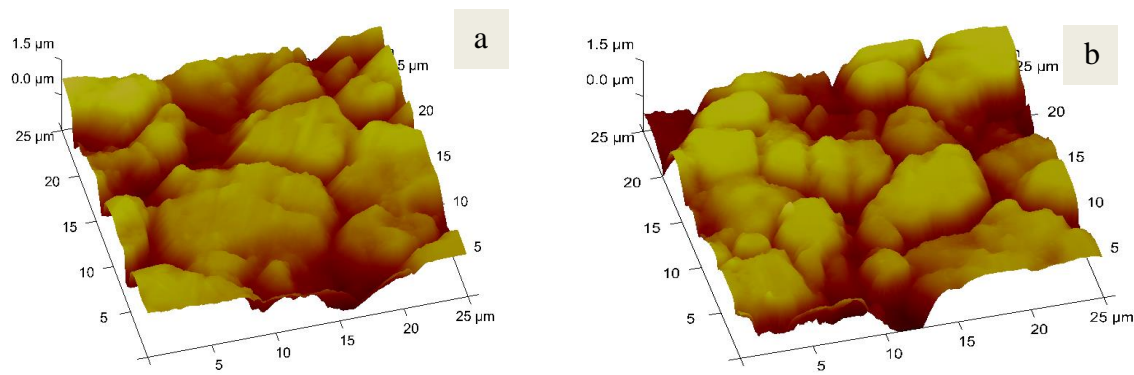


Figure 4.13: Change in surface profile for normal surface in the presence of ultrasound waves. (a) before treatment and (b) after treatment.

Discussions

The observations seen during the study were attributed to implosion of gas bubbles that occurred during cavitation when using ultrasound waves whilst cleaning biofilms, leading to abrasion of coupon surfaces as observed by Ivanova *et al.* (2011) for titanium surfaces and Haosheng and Shihan (2009) for polished steel surfaces. However, erosion is normally not uniform as bubble implosions are never uniform across the surfaces and this led to the creation of rough surfaces that encouraged biofilm formation.

From these observations, three types of surfaces could be defined with respect to surface topography and morphology: (i) polished surfaces where bacteria could be entrapped in grooves as on normal surfaces of coupons used, (ii) pickled surfaces where microorganisms could be entrapped in the grain boundaries as on weld surfaces on coupons or after surface erosion of

coupons due to ultrasound waves and (iii) smooth surfaces like glass (Boulangé-Petermann *et al.*, 1997). During the study it was observed that biofilms were able to form successfully on SS coupons particularly on welds due to grooves or grain boundaries; however, there was greater attachment on the welds due to the thermal stresses than on normal surfaces due to frequency stresses caused by the ultrasound waves.

4.1.3 Energy changes during treatment with ultrasound waves

High-power ultrasound has the ability to cause acoustic cavitation and it can be used to inactivate microbes (Ince and Belen, 2001; Laborde *et al.*, 1998). Heat is generated in the medium by absorbing ultrasonic energy from the waves (acoustic energy) resulting in mechanical, physical and chemical effects observed (Miller, 1987).

Relationship between maximum acoustic pressure and maximum displacement of typical waves

Acoustic pressure (P_a) or displacement (x) produced by sound waves are time (t) and frequency (f) dependent. At any time, t , the displacement, x , of an individual liquid molecule from its mean position has been shown from physics to be:

$$x = x_o \sin(2\pi ft) \quad \text{Equation 4.1}$$

where x_o is maximum displacement of the particle

Differentiation of Equation 4.1 leads to an expression for particle velocity

$$v = \frac{dx}{dt} = v_o \cos(2\pi ft) \quad \text{Equation 4.2}$$

where $v_o (=2\pi fx_o)$ is maximum velocity of particles

Differentiation of equation 4.2 gives an expression for particle acceleration

$$a = \frac{dv}{dt} = \frac{d^2x}{dt^2} = -a_o \sin(2\pi ft) \quad \text{Equation 4.3}$$

where $a_o (= -4\pi^2 f^2 x_o)$ is maximum acceleration of the particle

Besides the variation in molecules' position when the sound wave travels through the liquid, there is variation in pressure. As with displacement, pressure is calculated as follows:

$$P_a = P_A \sin(2\pi ft) \quad \text{Equation 4.4}$$

where P_A is maximum pressure amplitude

The pressure is higher than normal where the molecules are in compression and lower than normal where the molecules are in rarefaction implying displacement and pressure are out of phase (see Figure 4.14) for a wave of 24 kHz frequency.

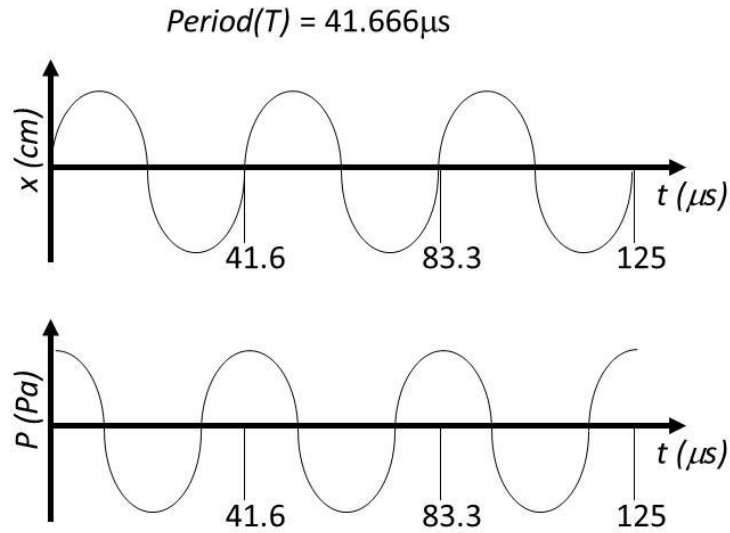


Figure 4.14: Plots showing displacement (x) and pressure (P) against time (t) for a typical wave

Ultrasonic processors in the system are designed to deliver constant amplitude and when adjusted, they cause a change in ultrasound intensity i.e. when the resistance to the movement of the probe increases, additional power will be delivered by the power supply to ensure that the excursion at the probe tip remains constant (Kobus and Kusińska, 2008).

Combining equations 6.8 (from Appendix III) and $v_o = 2\pi f x_o$ allowed determination of x_o from maximum pressure amplitude (P_A) as:

$$x_o = \frac{P_A}{2\pi f \rho c} \quad \text{Equation 4.5}$$

where ρ is the density of the liquid and c and f are the velocity and frequency of the wave which remain almost constant in water at 1500 m s^{-1} and 24 kHz respectively

Energy changes during treatment with ultrasound waves

An ultrasonic processor transforms electrical energy into other kinds of energies during its operation (see Figure 3.3). Electrical energy from the power supply is converted into mechanical energy in the form of oscillations of the piezoelectric crystal when the processor is switched on (Löning *et al.*, 2002).

The mechanical energy is then converted into acoustical energy in the form of ultrasonic waves which progress through a liquid medium resulting in liquid molecules oscillating about their mean position until the average distance between them exceed the critical molecular distance necessary to hold the liquid in contact leading to its breakdown and in the process forming cavitation bubbles i.e. energy transition from acoustical to cavitational; and finally to heat estimated by monitoring rate of temperature change (Catallo and Junk, 1995; Kobus and Kusińska, 2008; Löning *et al.*, 2002).

Certain assumptions need to be considered when analysing the energy changes during treatment with ultrasound waves:

- (i) The effects of cavitation are approximately the same for every position in the reactor (Son *et al.*, 2009)
- (ii) Conduction provides the only means of heat transfer (Hoffmann *et al.*, 1996)
- (iii) A uniform temperature is attained within the bubble immediately after collapse (Hoffmann *et al.*, 1996)

The relationship between I and P_A has been shown from Appendix III, equation C.9 as:

$$I = \frac{(P_A)^2}{2\rho c} \quad \text{Equation 4.6}$$

where I is power intensity measured in power per cross-sectional area (W/cm^2)

The equation enables the determination of power intensity from measurements of P_A at a particular amplitude setting. Acoustic impedance ($= \rho c$) is characteristic of a liquid and it is always constant regardless of any change in the frequency.

Adjusting the amplitude setting of the ultrasonicator results in change of all six types of energies, as such knowledge of its actual influence was essential particularly on the conversion efficiency.

Three kinds of energy measurements which could be determined easily: electrical energy, acoustical (calorimetric or ultrasonic) energy and cavitation energy could be used to quantify energy conversion efficiency by measuring either primary or secondary effects caused by propagation of waves in the liquid medium (Kobus and Kusińska, 2008). The power was expressed in watts per unit area of the emitting surface (W/cm^2) known as power intensity, or watts per unit volume of irradiated liquid (W/cm^3) known as power density (Kardos and Luche, 2001; Sathiskumar and Madras, 2012).

Electrical energy

Electrical energy (input power) could be determined by three different methods: (i) using a multimeter with a data logger where the signal would be recorded at periodic time and averaged for the signal generator (ii) using a hydrophone to measure the maximum pressure amplitude achieved when the hydrophone is close to the emitting ultrasound probe and using equation 4.6 to calculate power intensity, and (iii) measuring rise in temperature, T , of a known volume of distilled water with time, t , in the absence of cooling with a simplified heat transfer analysis giving the rate of energy input (electrical power), P_{ele} , being transferred to the system (Son *et al.*, 2012), see Appendix III for three different heat balances that could be done to determine the electrical power input.

Electrical power input was measured over the whole amplitude range. The results are presented in Figure 4.15 for measurements of V and I (Measurements) and for power density from use of Nexus hydrophone (Calculations).

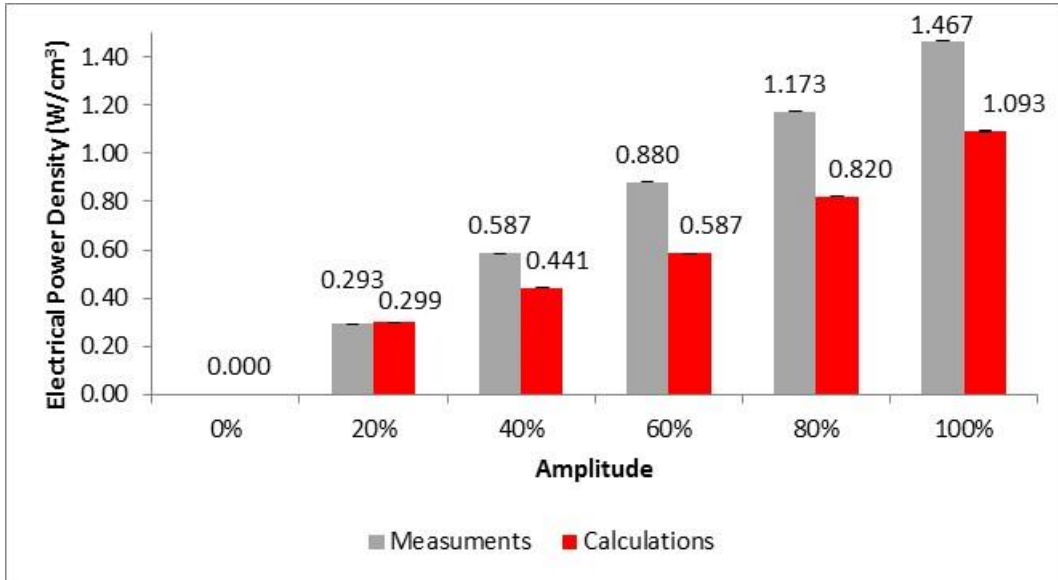


Figure 4.15: Electrical power density with change in amplitude due to treatment of distilled water with ultrasound waves. Experiments were repeated twice to get standard deviations ($n = 2$)

There was a gradual increase in power density input when amplitude was increased from the two methods. The increase in power with amplitude was supported by literature as it was modelled to be a quadratic relationship as in equation 4.6. This relationship was expected as the input power determined the amplitude of the ultrasound waves observed. Kobus and Kusińska (2008) found that specific power densities increased in a non-linear way with increasing ultrasonic amplitude

with the best fitting of regression line obtained for a second order polynomial when using 20 kHz waves from a horn of maximum amplitude of 35 μm on water and ethanol during their study. Mañas *et al.* (2000) obtained a linear relationship between amplitude and electrical power input when using distilled water at 40 °C and ultrasound waves with a frequency of 20 kHz. Löning *et al.* (2002) performed experiments at 20 kHz in water and observed that the specific power quantities were described with a second order polynomial fit, which corresponded with the theoretical relationship between power input and amplitude.

Measured power density gave a linear relationship against amplitude while hydrophone data gave a second order relationship but from the literature it seemed mostly that a second order relationship should be obtained. Error analysis was conducted and the results are presented in Table 4.4 with values calculated from VI data.

Table 4.4: Error analysis between electrical power density from Figure 4.15

Amplitude	0%	20%	40%	60%	80%	100%
Error	0%	-2.07%	24.81%	33.31%	30.09%	25.50%

The data showed that the error variation was large from 40% amplitude and therefore data from one method had to be used as the maximum acceptable error was $\leq 5\%$. The maximum pressure

amplitude obtained from the hydrophone was used to determine the maximum displacement by equation 4.6 and the results for the change in the amplitude were shown in Table 4.5.

Table 4.5: Maximum displacement, maximum velocity and maximum acceleration experienced by water molecules during treatment with ultrasound waves

Amplitude	Maximum displacement amplitude (μm)		Maximum velocity (m/s)		Maximum acceleration (m s^{-2}) $\times 10^6$	
	*M	♦C	*M	♦C	*M	♦C
0%	0	0	0	0	0	0
20%	62.62	63.26	9.44	9.54	-1.42	-1.44
40%	88.56	76.79	13.35	11.58	-2.01	-1.75
60%	108.46	88.57	16.36	13.36	-2.47	-2.01
80%	125.24	104.71	18.89	15.79	-2.85	-2.38
100%	140.02	120.85	21.11	18.22	-3.18	-2.75

*M – data obtained from calculations using VI parameters measure using a data logger

♦C – data obtained from calculations using Nexus hydrophone data i.e. these were from calculations using Equations 4.1, 4.2 and 4.3

The results showed that the maximum displacement at 100% amplitude was 120.85 μm (from Nexus hydrophone data), an error of 3.32% which was within the acceptable range of $\leq 5\%$ against rated displacement amplitude of 125 μm while it was 104.02 μm (from measured data), an error of 12.01% which was outside the acceptable range of $\leq 5\%$ against the rated displacement amplitude. This helped to confirm that the calculated power density values were close to the actual measurements when using the Nexus hydrophone and the data was used for future calculations.

Maximum displacement amplitude, velocity of molecules and acceleration of the molecules all increased as the amplitude setting was increased. This was due to an increase in the input power which drove the molecules even faster; however, acceleration was out of phase with displacement (see Equations 4.1, 4.2 and 4.3).

Acoustical energy

Acoustical energy could be calculated by measuring the temperature increase of water under ultrasound irradiation and using Equation 4.7 (Kardos and Luche, 2001; Sathiskumar and Madras, 2012).

$$P_{aco} = mC_p \frac{dT}{dt} \quad \text{Equation 4.7}$$

Integrating and rearranging the equation gave:

$$T - T_o = \frac{P_{aco}}{\rho_{water}C_p} t \quad \text{Equation 4.8}$$

where P_{aco} is acoustical power, dT/dt is rate of temperature change, C_p is specific-heat capacity of water (4.2 J/g K) at constant pressure, ρ is density of distilled water subjected to ultrasound waves, T_o is the initial temperature of distilled water and T is temperature at a particular time, t

A graph of T against t has an intercept of T_o and a gradient of $\frac{P_{aco}}{mC_p}$ which enabled determination of acoustical energy density. The heat generated by ultrasound irradiation was mainly due to sound attenuation/absorption in the medium. Heat lost to the surroundings could be assumed to be negligible in small-scale reactors for small time periods of about 5 minutes (Son *et al.*, 2012). Acoustical power was determined by monitoring rate of temperature change and the results are presented in Figure 4.16.

The trend showed that the rate of temperature increased linearly with amplitude i.e. as the amplitude was increased, the power input to the distilled water increased leading to higher temperature rates which ultimately resulted in an increase in acoustical energy. Beckett and Hua (2001) performed experiments using ultrapure water at 205, 358, 618 and 1071 kHz, and obtained maximum rates of temperature changes of 0.148; 0.155; 0.158 and 0.165 °C/min respectively which showed an increase in rate of temperature with an increase in frequency.

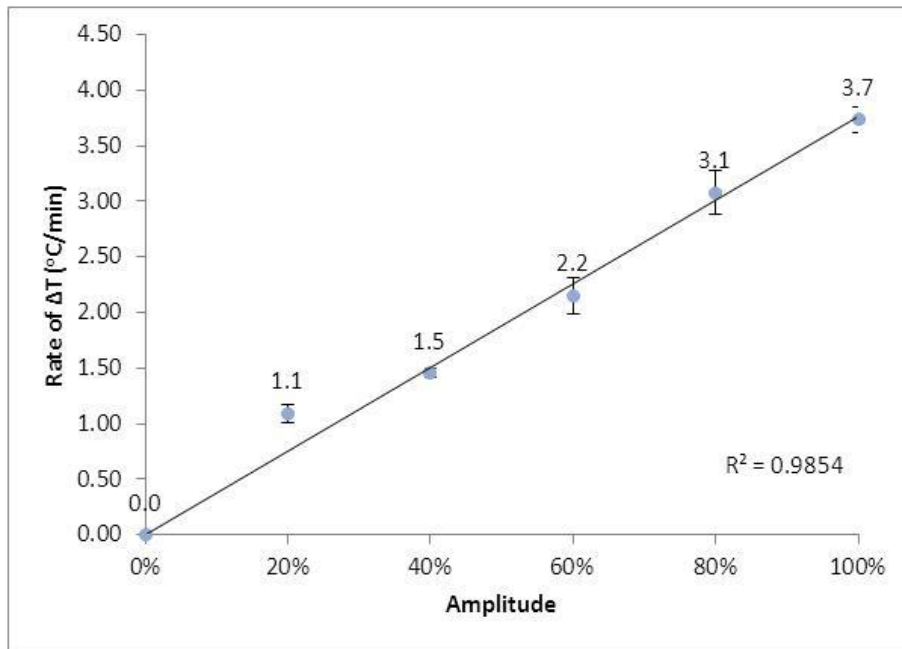


Figure 4.16: Rate of temperature change rise with change in amplitude due to treatment of distilled water with ultrasound waves. Experiments were repeated three time to get standard deviations (n = 3)

Acoustical power density data calculated from rate of temperature change was presented in Figure 4.17.

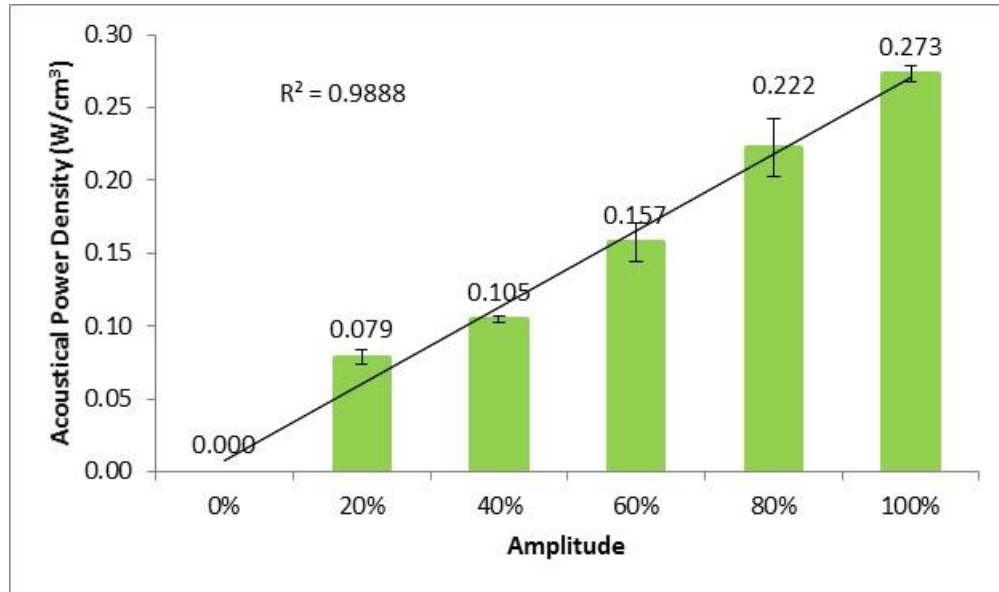


Figure 4.17: Acoustical energy change with amplitude due to treatment of distilled water with ultrasound waves. Experiments were repeated twice to get standard deviations ($n = 2$)

There was a linear relationship between acoustical power density and amplitude as confirmed by the correlation coefficient ($R^2 = 0.9867$) showing that as the amplitude was increased due to an increase in the input electrical energy, the acoustical energy generated in the distilled water increased proportionally. Raso *et al.* (1999) performed experiment using distilled water at 20 kHz and obtained a linear relationship (strong positive correlation i.e. $R^2 \geq 0.97$) between amplitude and acoustical power in line with current study. Mañas *et al.* (2000) obtained a linear relationship between amplitude and acoustical power when using distilled water at 40 °C and 20 kHz ($R^2 \approx 1$).

The power density transferred to the distilled water as acoustical energy was lower as compared to the electrical energy input i.e., from 1.10 W/cm^3 to 0.28 W/cm^3 at 100% amplitude, an energy conversion efficiency of 25% which showed a loss in energy during the conversion process mainly due to attenuation of sound waves in the distilled water during propagation. Son *et al.* (2011) performed experiments at 36 and 108 kHz in liquid water: the measured maximum electrical power density were 0.098 and 0.116 W/cm^3 while the measured maximum acoustic power density were 0.042 and 0.048 W/cm^3 at maximum amplitude respectively. This showed energy conversion efficiencies of 42.9% and 41.4% at 36 and 108 kHz respectively. Löning *et al.* (2002) performed experiments at 20 kHz in water and observed the efficiency of conversion from electrical to acoustical power was in the region of 70 – 80%.

Theoretically, the attenuation should increase with an increase in amplitude leading to the observed trend of higher acoustical energy at higher amplitudes. The decrease in conversion efficiency from electrical to acoustical power was due to energy imparted to the stationary water molecules for them to vibrate periodically about their mean position to form the acoustic pressure wave and cavitation observed. The other reason could have been loss of energy as heat from the container walls.

Cavitation energy

Cavitation energy could be determined by two different methods and the results obtained compared. The two methods were as follows:

1. Cavitation energy could be obtained by measuring the calorimetric energy in both cavitating and non-cavitating liquid and using Equation 4.9:

$$E_{cavitation} = E_{cavitating} - E_{non-cavitating} \quad \text{Equation 4.9}$$

where $E_{cavitation}$ is cavitation power density, $E_{cavitating}$ is calorimetric power density of cavitating liquid, and $E_{non-cavitating}$ is calorimetric power density of non-cavitating liquid

2. Cavitation energy could also be determined by using a hydrophone at the specific distance away from the probe to measure the maximum pressure amplitude achieved from the emitting ultrasound probe which was experienced by coupons at that distance and using equation 4.6 to calculate cavitation power intensity.

A cavitating liquid was prepared by fully aerating distilled water or using the normal gas content at ambient temperatures while non-cavitating liquid was prepared by boiling distilled water to completely deaerate it, storing in a sealed bottle, and keeping it at room temperature overnight for cooling. The deaerated water was then poured very gently into a reactor to prevent re-aeration; however, it is always difficult to completely degas liquid water (Bapat and Pandit, 2008; Son *et al.*, 2012).

Cavitation energy was determined by monitoring rate of temperature change for cavitating and non-cavitating water with amplitude (Temp rise) and compared to the data obtained using the Nexus hydrophone (Hydrophone), see Figure 4.18.

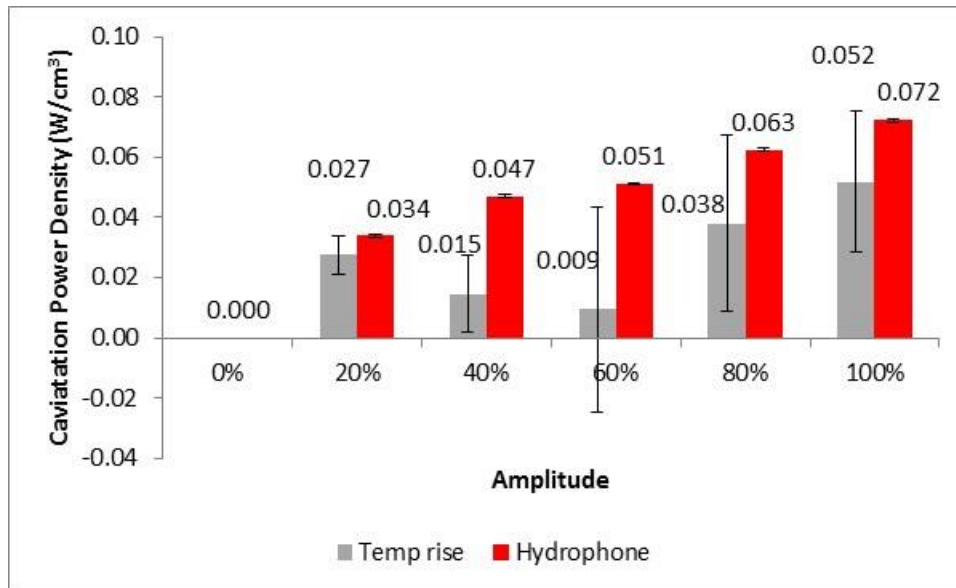


Figure 4.18: Cavitation energy change with amplitude due to treatment of distilled water with ultrasound waves. Experiments were repeated twice to get standard deviations ($n = 2$)

There was a linear relationship between cavitation energy and amplitude for the two different methods but the correlation coefficients were low 0.6173 and 0.8104 for cavitation power density calculated using calorimetric method and Nexus hydrophone respectively. The decrease in linearity as the energy was converted from electrical to cavitation energy observed could be attributed to an increase in attenuation with an increase in amplitude leading to loss of energy as the conversion approached the least energy state (heat). The increase in the standard error observed for data obtained from calorimetric method as amplitude increased could have been due to an

increase in acoustic streaming (vibration of bubbles in the system reducing the number of bubbles explosions at a particular time as compared to explosions at lower amplitudes) and more random explosions occurring at higher amplitudes leading to inconsistencies in measured cavitating and non- cavitating energies with change in amplitude.

There was higher deviation from data obtained using calorimetric method while the Nexus hydrophone had low deviation between the data and the values could be relied upon. Cavitation power density data from the hydrophone were measured at a distance of 250 mm between the hydrophone and the ultrasound probe, which was the same distance that was used during bacterial disinfection experiments i.e. the distance between the coupons and the ultrasound probe was the same as the hydrophone and the probe. Error analysis was conducted and the results are presented in Table 4.6 with data calculated from Nexus hydrophone taken as correct values.

Table 4.6: Error analysis between cavitation power density values

Amplitude	0%	20%	40%	60%	80%	100%
Error	0%	18.8%	69.0%	81.5%	39.1%	28.2%

The data showed that the error variation was large for the whole range of amplitude settings and therefore data from Nexus hydrophone was used for future calculations (as the maximum acceptable error was supposed to be $\leq 5\%$).

Cavitation energy could only be detected after attenuation had occurred leading to stretching of bond lengths of water molecules resulting in bubble formation and explosion; and the less the explosions, the lower the cavitation energy measured. Cavitation is an uncontrolled process as such the measured cavitation energy differed with a change in amplitude. Acoustic streaming which is vibration of gas bubbles, might have been experienced leading to lower cavitation energies determined mainly at 40 and 60% amplitude.

Energy conversion efficiency

The efficiency of conversion of electrical energy to acoustical and cavitation energies was computed from the data obtained and it was presented in Figure 4.19. The values obtained using the Nexus hydrophone for electrical power density and cavitation power density were used together with calorimetric data for acoustical power density.

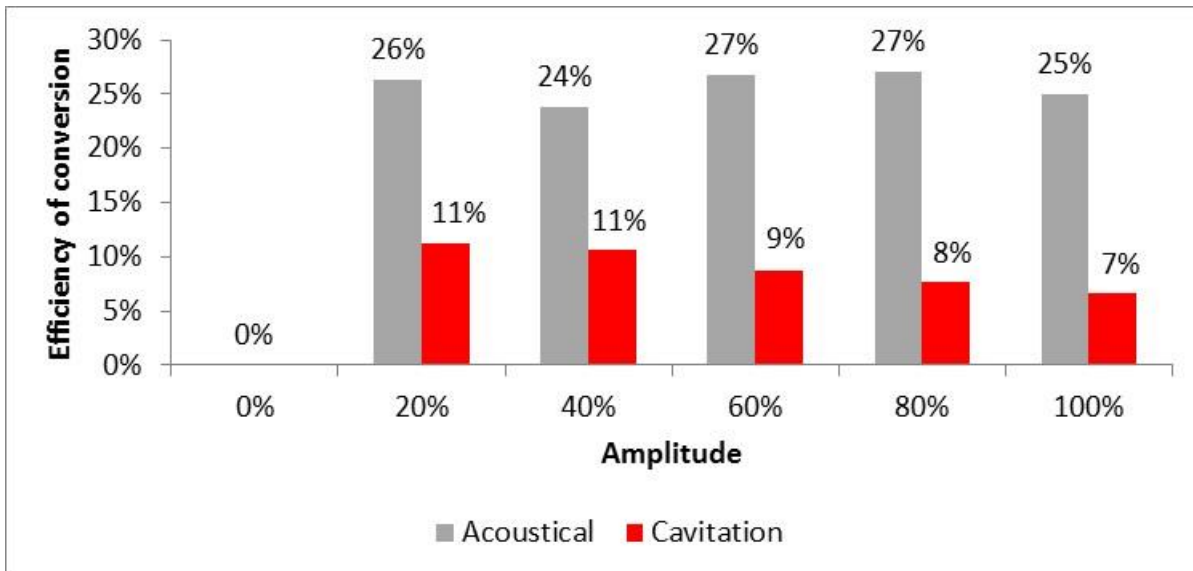


Figure 4.19: Efficiency of change in electrical energy to acoustical and cavitation energies with change in amplitude during treatment of distilled water with ultrasound waves

The energy conversion efficiency to acoustical and cavitation energies decreased as amplitude was increased and this could have been due to an increase in acoustic streaming leading to less bubble explosions and a higher sound attenuation/absorption in the medium due to an increase in input power density. The dip observed at 40% amplitude may have been due to the onset of acoustic streaming. Other authors performed studies which were comparable to the current study, Jyoti and Pandit (2001) had energy conversion from electrical to cavitation of 3% using 22 kHz waves to disinfect water while Kobus and Kusińska (2008) had efficiencies < 1% at 20 kHz. Ratoarinoro *et al.* (1995) obtained energy conversion from electrical to acoustical of 26% at maximum amplitude

(comparable with 25% in the current study at 100% amplitude) using ultrasound waves at 20 kHz in toluene at constant height of 28 mm.

Change in power density with distance from the probe - sound attenuation

During the propagation of a plane wave through a medium the intensity of the wave decreased as the distance from the radiating source increased. The intensity at some distance, d , from the source was given by:

$$I = I_0 e^{-2\alpha d} \quad \text{Equation 4.10a}$$

where α is the absorption (attenuation) coefficient

The equation could be rearranged to determine the attenuation coefficient:

$$\alpha = -\frac{\ln\left(\frac{I}{I_0}\right)}{2d} \quad \text{Equation 4.10b}$$

This attenuation could arise as a result of reflection, refraction, diffraction or scattering of the wave or it may be the result of converting some of the mechanical (kinetic) energy of the wave into heat or sound, the latter being the most important in liquids. As the molecules of the liquid vibrated under the action of the sound wave, they experienced viscous interactions which degraded the acoustical energy into heat and the absorption of this degrading acoustical energy gave rise to the small observed bulk heating effect during the applications of high-power ultrasound (Mason and Lorimer, 2002).

The power density was monitored with a change in distance between the ultrasound probe and the Nexus hydrophone and the results are presented in Figure 4.20 for a change in amplitude from 20% to 100% of maximum amplitude.

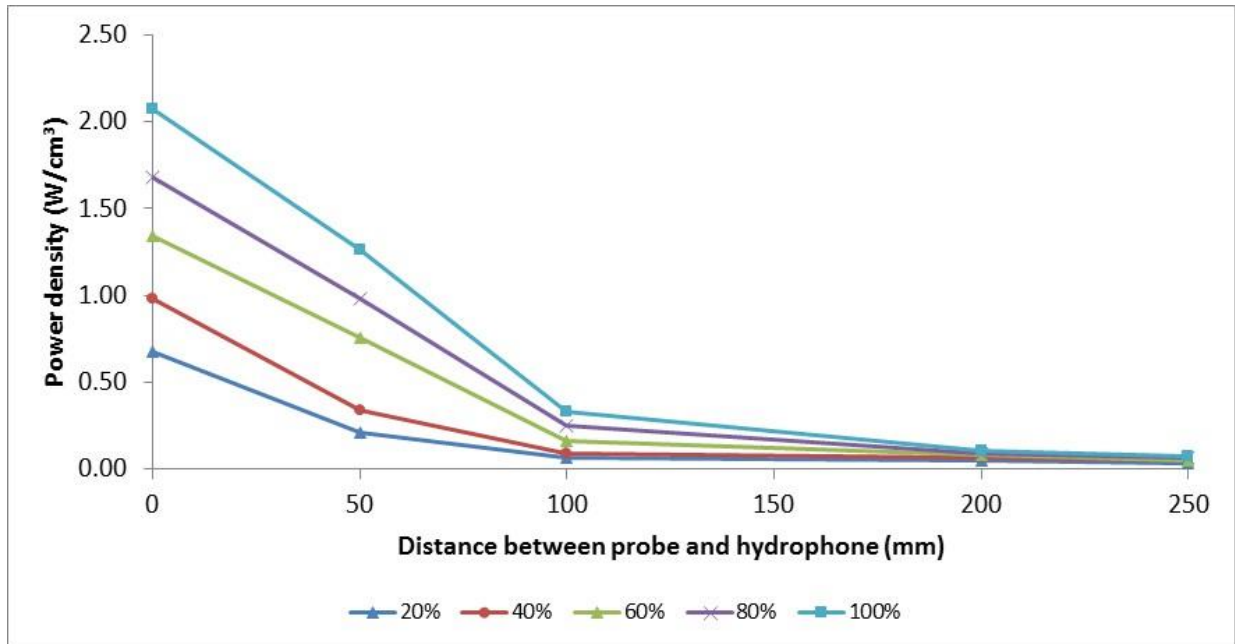


Figure 4.20: Effect of change in power density with distance from the probe

The investigations were limited to a distance of 250 mm away as any further increase could not reveal any more information as the power density was close to zero. However, this was contrary to the efficiency of bacterial disinfection which was not affected by distance from the probe as observed in section 4.1.1. The results showed a decrease in power density with distance away from

the probe and this was due to an increase in sound attenuation with increase in distance as shown by equation 4.10a.

Son *et al.* (2011) observed the same trend for distances up to 450 mm at frequencies of 36 and 108 kHz for both electrical and acoustical power densities. Son *et al.* (2009) obtained the same trend at 170 kHz frequency but the power density decreased linearly with distance from probe at other frequencies of 35, 72 and 110 kHz. Toma *et al.* (2011) observed a decrease in temperature rate with an increase in distance from probe up to 500 mm (increase in liquid height was used during the authors' study) during a study at 20 and 490 kHz in different liquids. The decrease in temperature rate could be translated as a decrease in acoustical energy which was the same trend observed during the current study. Son *et al.* (2007) observed inconsistent results as energy intensities did not decrease as the distance from the transducer module to the probe increased up to 900 mm for 35, 72, 110 and 170 kHz waves using tap water.

The attenuation coefficient was determined with change in amplitude and distance from the probe and the results were shown Figure 4.21.

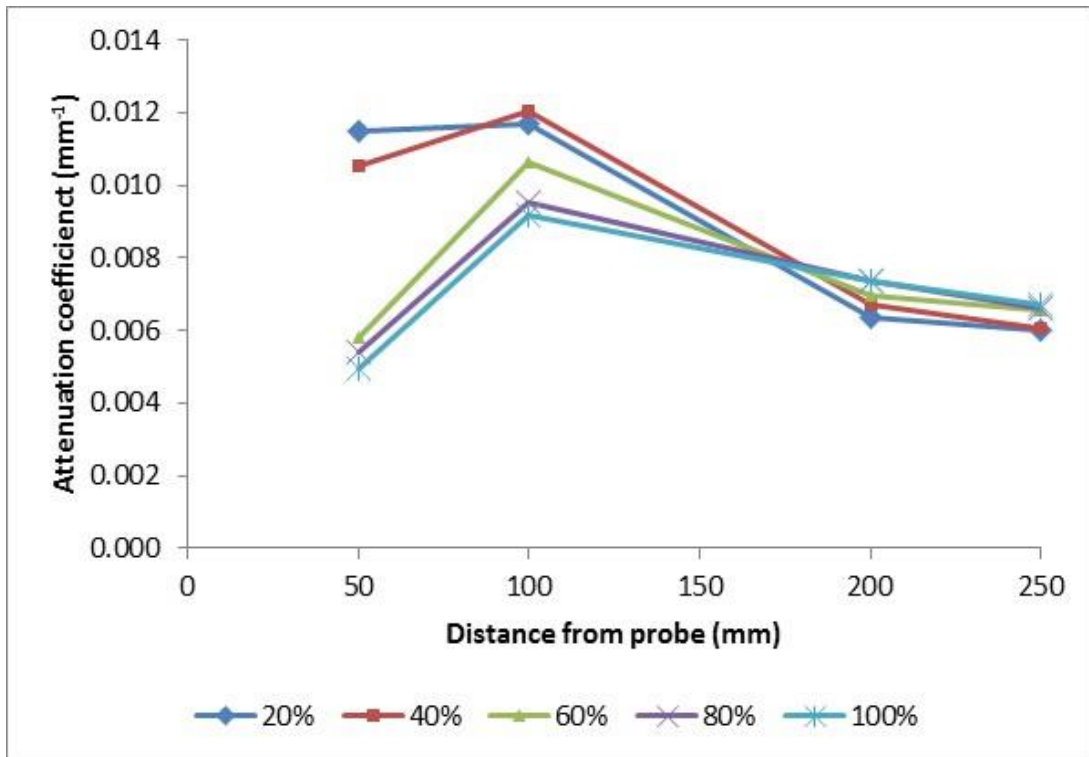


Figure 4.21: Effect of change in amplitude and distance from the probe on the attenuation coefficient

The data showed that the attenuation decreased with an increase in distance from the probe at a fixed amplitude value and it decreased with an increase in amplitude at a fixed distance from the probe. As the distance from the probe increased the relationship between attenuation and amplitude was observed to interchange with more attenuation experienced at higher amplitude settings. Attenuation at 40% amplitude was more than at 20% as from a distance of 100 mm and this could help to explain the drop in the energy conversion from electrical to acoustical energy. There was

more resistance at 40% amplitude than at other amplitude settings and that is why the conversion dropped to its lowest value for acoustical energy at this amplitude.

4.1.4 Button experiments

316L and 904L weld filler rods were melted under argon to form one 316L button and one 904L button and two 904L square coupons to check bacterial loading and treatment with ultrasound waves at 750 mm from ultrasonic probe. Two 316L square coupons cut from 316L SS metal coupons used in previous study were included as control. All coupons and buttons were subjected to minor grinding to obtain same surface profile. The surface grinding was done using 240 grit, followed by 600 grit and finally 1200 grit on a Knuth rotor (Struers, Denmark). The coupons were then immersed in *E. coli* solution and the results are presented in Table 4.7.

Table 4.7: Bacterial loading before treatment with ultrasound waves on SS buttons and coupons

Material	316L-Button	904L-Button	316L-Coupons	904L-Coupons
Bacterial loading ($\times 10^7$ cfu/ml)	2.42 \pm 0.47	3.35 \pm 0.27	3.13 \pm 0.09	3.52 \pm 0.02

Results from the table showed that 904L button and coupons (average) had higher bacterial loading of *E. coli* as compared to 316L button and coupons. This showed that the Cu imbedded in the 904L weld fillers did not have any effect on bacterial loading for the duration of this study. The trend observed may have been due to surface roughness of the buttons and coupons. Coupon surfaces

for 904L and 316L exhibited a wrought structure which resulted in higher surface roughness values leading to increased biofilm intensity unlike buttons which had a homogeneous structure after melting under argon. The 904L button had a rough surface probably due to the increased metal concentration (Cr and Ni and presence of Cu) and it was difficult to melt and form into buttons. The square coupons were rough as compared to the buttons and grinding had an effect but there was always room for improvement.

Disinfection efficiency was done using ultrasound waves at 100% amplitude, continuous operation and at a distance of 750 mm between the probe and coupons or buttons. The results were shown in Figure 4.22.

The data showed very low disinfection efficiency for coupon surfaces as compared to buttons. The data when compared to normal coupon and welded surfaces investigated earlier at distances of 250 mm showed that the efficiencies were low as compared to efficiencies greater than 70% for distances of 250 mm. The conclusion from the results was that ultrasound waves had little effect at greater distances.

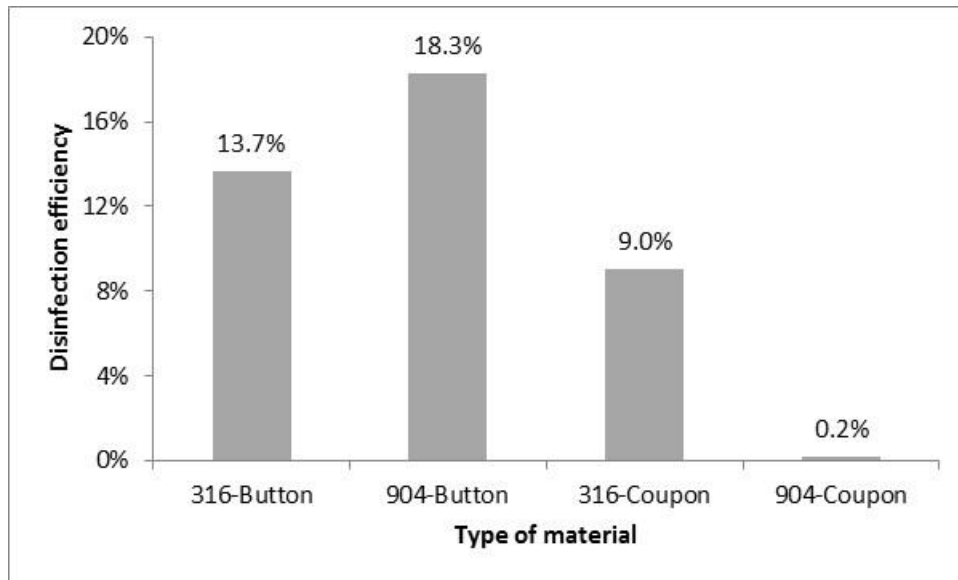


Figure 4.22: Effect of ultrasound intensity on the removal of biofilms for button and coupon surfaces facing ultrasound waves at a distance of 750 mm

Standard deviations calculated were very high and this meant that the results could not be relied on. This could be due to the fact that the swabbing surfaces were very small and this affected the procedure of initial swabbing, treatment with ultrasound waves and final swabbing; with swabbing being conducted twice on each surface.

This study had comparisons to a study done earlier at University of the Witwatersrand, South Africa by Sithole (2007) using aluminium with silver metal deposited. The effect of Ag as a biocide is the same as Cu but for our study, filler rods with embedded Cu were available off the shelf i.e. Ag and Cu both act as bactericides using a similar method; whereby cell death was due to bonding

between the metal and the nucleus, preventing any cell processes from taking place and thereby leading to cell death. The results obtained by Sithole (2007) are presented in Figure 4.23.

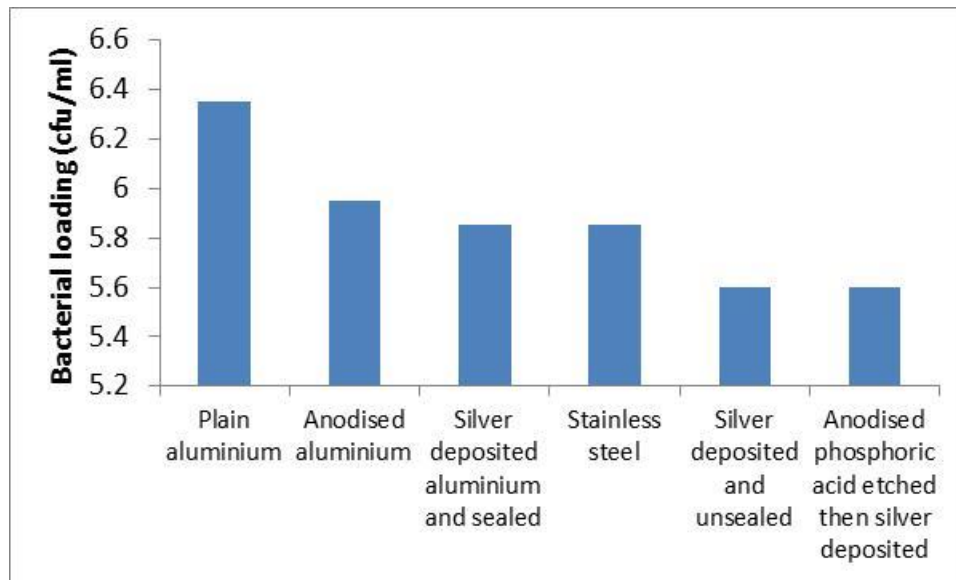


Figure 4.23: Results of bacterial loading on aluminium surfaces with different treatments (Sithole, 2007)

Figure 4.23 showed reduced attachment due to silver deposited on aluminium surface but the silver had to be unsealed i.e. it should be free to dissolve into the bacterial solution from the aluminium surface and attack the bacterial cells. The bactericide worked by re-dissolving into solution, being transported to the microorganism cell wall, metal uptake through the cell membrane and bonding to the nucleus thereby stopping cell processes leading to cell death. The Cu in 904L filler welds

was in intergranular spaces to a homogeneous material and as such, it could not dissolve out of the metal structure and into bacterial solution to have an effect. Literature has shown that it is difficult to embed or dissolve other metals into SS structure due to their low solubility and these results also showed that after welding using filler rods with copper as a bactericide did not provide a possible solution to the problem. However, the 904L welds were used under dynamic experiments to check their effect after circulating the solution for about five weeks.

4.2 Dynamic experiments

The purpose was to address the following questions:

- Is there an increased concentration of biofilm in welding areas?
- Which weld filler between 316L and 904L results in higher biofilm formation?
- Does the flow direction influence results (geometric impacts)?
- What is the influence of the HAZ?
- What benefits are achieved by using argon?
- What benefits are achieved by pickling and passivation?
- How effective is the CIP process?
- How does the CIP process degrade over the length of the pipe as the concentration declines?

4.2.1. Welding filler characterisation

904L and 316L filler rods were characterised at SAIW and the results were shown in Table 4.8 together with the current standard composition (see Appendix V for full table and specifications for mill pipes from Euro Steel, South Africa).

Table 4.8: Comparison of 316L and 904L welding rods composition

Element	Standard	Average 316L		Standard	Average 904L		316L
	316L	XRF	Spectro*	904L	XRF	Spectro*	SS pipes
C	<0.03		0.021	<0.02		0.029	0.016
Si	<0.03	0.410	0.202	<1.0	0.445	0.250	0.318
P	<0.045	0.004	0.035	<0.045	0.002	0.047	0.026
S	<0.03	0.149	0.011	<0.035	0.001	<0.01	0.006
Cr	16-18	18.259	18.110	19–23	18.977	19.877	16.760
Mo	2.0-3.0	2.482	2.420	4–5	4.346	4.618	2.090
Ni	10-14	11.803	11.190	23 – 28	24.732	22.433	11.090
Mn	<2.0	1.804	1.738	<2.0	1.421	1.443	1.639
Cu		0.137	0.122	1–2	1.548	1.507	
Ti		0.003	0.008		0.225	0.010	
V		0.044	0.093		0.041	0.091	
W		0.037	0.247		0.014	0.242	
Fe		64.632	65.610		48.206	49.313	
Co		0.237	0.058		0.043	0.098	
Nb		0.000	0.028		0.000	0.021	
TOTAL		100.001	99.893		100.000	99.979	

*Spectro – Spectrometer

The parent metal pipes which were welded using these 316L and 904L filler rods were also characterised at the mill (production site for the pipe) and the results are presented in Table 4.8.

The important points to note were the increased Cr, Ni and Cu content in the 904L as compared to the 316L filler and the 316L SS pipe resulting in increased corrosion resistance. This meant that after welding one would anticipate better corrosion resistance from 904L welding than from 316L welding on the same pipe. Ni content was twice as much in 904L than in 316L filler rods and mill pipes giving better corrosion resistance. The increased Cu present in 904L acted as a surface biocide and it was embedded in the orbital TIG welds used on the test rig. The silver used as a biocide in the aluminium work previously cited (Sithole, 2007) worked in the same way. From the point of view of the current experiment, silver is both expensive and not readily available in the form of commercially available filler rods. 904L rods were used to check the impact of a biocide on welds and the results would be comparable to the use of silver.

Carbon could only be detected by spectrometer and it was below the maximum permitted amount of 0.03% for both welding rods and mill pipes. The % C coupled with the time period of welding meant that sensitisation was unlikely to be experienced during or after welding as there was less

carbon and insufficient time at the required temperatures to combine with chromium to form chromium carbide.

The results shown in Table 4.8 pointed to reduced biofilm intensity and increased corrosion resistance after welding with 904L filler rods as compared to 316L welds.

4.2.2. Flow and velocity measurements

The results for calibration for the two pumps used are presented in Figure 4.24. Pump 1 was a variable speed pump but pump was fixed. All flowrates in Figure 4.24 from 20 to 50Hz were for pump 1 only and pump 2 was labelled as such. The details for the pumps were as follows: pump 1 (Lowara variable speed pump, 0.61 kW; Lowara, Italy) and pump 2 (Marlin pump, 0.75 kW; Femco, South Africa).

Water circulation was performed at 0.13 m/s and 0.34 m/s for runs 1 and 2 respectively while CIP was performed at 0.31 m/s for both runs. This meant that run 2 was performed at more than twice (2.6 times) the flowrate for run 1. However, the velocities used were below the recommended range of 1.5 – 4 m/s that ensured removal of gross biofilms during CIP process (Chisti and Moo-Young, 1994; Czechowski and Banner, 1992; Lelièvre *et al.*, 2002; Lorenzen, 2005; Praeckel, 2009; van Asselt and te Giffel, 2005). Cluett *et al.*, (2003) recommended flow velocities ≥ 3 m/s for 50 mm pipes to achieve effective CIP range.

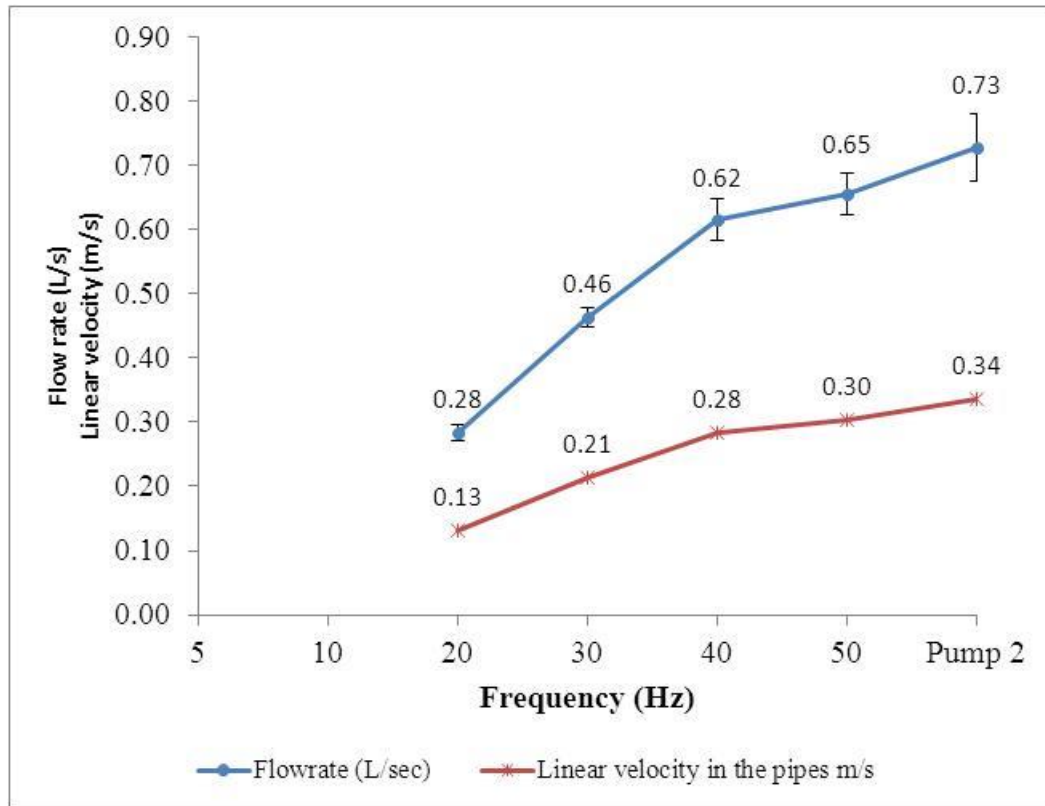


Figure 4.24: Pump calibration chart showing flowrate and linear speed for runs 1 and 2. Experiments were repeated three times to get standard deviations ($n = 3$)

On the other hand, this meant that biofilm formation was favoured by the low flowrates which can be experienced in brewing vessels and large pipe diameters. For CIP, the velocities were inadequate than those required in the brewing industries as mentioned from authors above.

The low linear speeds and flowrates were due to the variable pump available onsite and this may have resulted in ineffectiveness of the CIP process. However, the low flowrate was favourable for formation of biofilms on pipe walls and brewing vessel surfaces. Pump 2 was used for run 2 to mimic conditions experienced in brewing pipes while run 1 was performed at 0.13 m/s using pump 1 to mimic conditions experienced in brewing vessels.

4.2.3. CIP systems in combination with ultrasound waves

Comparing surface roughness of 316SS pipe with 316L coupons used in previous study

Surface topography analysis

Surface topography for the inside and outside of the new pipes as supplied was done and the results are presented in Table 4.9.

Table 4.9: Surface topography data (mean±SD) for SS 316 pipe surfaces used in the study. Experiments were repeated four times for both inside and outside of pipes to get standard deviations (n = 4)

Parameter	R _a (nm)	R _q (nm)	R _{max} (nm)
Pipe inside	307±3	385±2	3100±130
Pipe outside	891±7	1151±11	6417±9
Normal coupon surface from previous study	325±4	395±4	2280±20

R_a value for the inside of pipe was similar to that for the normal surface of coupons before treatment with ultrasound waves (307 nm against 325 nm respectively) showing that surface roughness was similar and would give rise to almost the same bacterial loading under the same conditions. Surface finish applied on inside of the pipe was a 2B finish (Lelièvre *et al.*, 2002) and it was regarded as a smooth since $R_a < 500$ nm, while for outside of the pipe it was rough, $R_a > 500$ nm (Detry *et al.*, 2010).

R_q values followed the same trend and were similar with those for coupon normal surface i.e. 385 nm against 395 nm for pipe inside and normal surface of coupon before treatment with ultrasound waves respectively. This reinforced the fact that the surface was similar to that of the coupon and results under static experiments were applicable to this stage of the study.

R_{max} for 316L pipes was higher (3.10 against 2.28 μm) than for normal surfaces of 316L coupons used in the previous study and this implied that there was potential for an increase in biofilm intensity on 316L pipes than on 316L coupon surfaces.

Surface morphology analysis

Surface morphology for the pipe inside and outside was done and the results are presented in Table 4.10.

Table 4.10: Surface morphology data (mean±SD) for SS 316 pipe surfaces used in the study. Experiments were repeated four times for both inside and outside of pipes to get standard deviations (n = 4)

Parameter	R_{skw}	R_{kur}
Pipe inside	-0.083±0.050	3.35±0.17
Pipe outside	0.975±0.026	4.37±0.04
Normal coupon surface from previous study	-0.937±0.001	3.11±0.02

The data showed that $R_{skw} < 0$ for pipe inside. This indicated the presence of pits/valleys and $R_{skw} > 0$ for pipe outside showing presence of peaks. The pipe inside was similar to normal coupon surfaces which had pits/valleys while the pipe outside was similar to coupon surfaces after welding which had peaks. R_{skw} value for the pipe inside was bigger than for the normal surface before treatment with ultrasound waves (-0.083 against -0.937 respectively).

However, the fact that the value was close to zero showed that the surface was almost symmetrical i.e. there was almost a balance between valleys/pits and peaks. The outside of the pipe showed presence of mostly peaks suggesting that it was not properly polished as it was regarded as a non-functional surface (section 2.5.5.).

R_{kur} values ≈ 3 showing that the inner surface was almost even for pipe inside and it was comparable to normal coupon surface before treatment with ultrasound waves (3.35 against 3.11 respectively) while outside of pipe surface, $R_{kur} > 3$ showing that there was presence of high peaks as confirmed by R_{skw} data. The pipe inside was almost an ideal surface as $R_{skw} \approx 0$ and $R_{kur} \approx 3$ i.e. the same conclusion that was reached for normal coupon surface before exposure to ultrasound waves.

This inside surface did not encourage formation of biofilms. It was appropriate for use as a control during dynamic experiments. This was done on pipe F in between the two welds as discussed previously (section 3.2.3) with sampling ports available.

The data obtained meant that the results from the static study were applicable to the dynamic study as surface topography and morphology values were compatible for the inside surface of the pipes only.

Analyzing condition of welds on the inside and outside

The welding was manual TIG and undertaken by one competent person over the same period at the SAIW. Welds were applied from the outside with no internal backing. The weld root and weld cap on the inside and outside of the pipes respectfully was photographed. The results were shown in Figures 4.25 and 4.26.

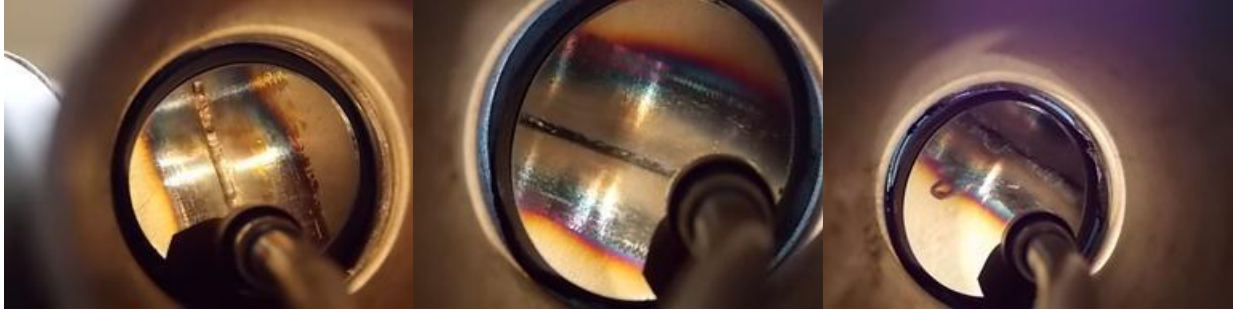


Figure 4.25: Examples of welds produced using 904L weld filler rods

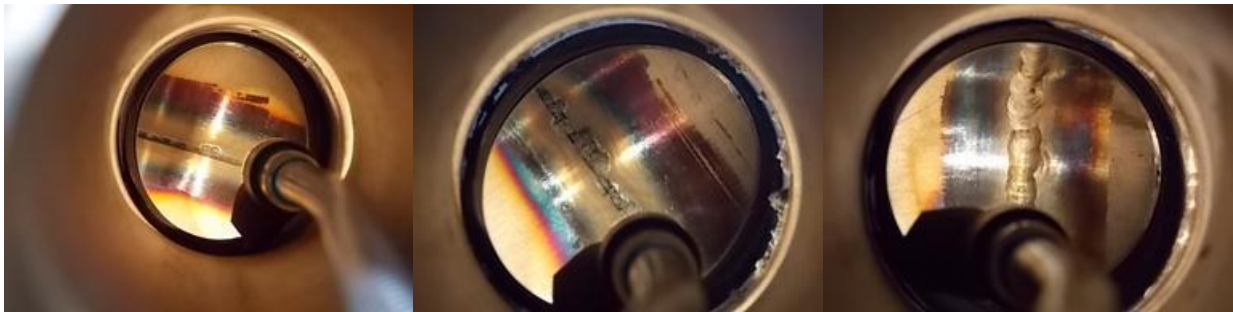


Figure 4.26: Examples of welds produced using 316L weld filler rods

Random, typical internal views illustrated the complexity of root control. Over and under-penetration was evident providing possible growth areas for biofilms. Whilst most of the welds were acceptable on the outside (see Figure 4.27) the inside showed major problems when compared to the ideal orbital welding.



Figure 4.27: Photographs of weld caps of 50 mm ID, 3.91 mm wall thickness, 316L pipe apparatus conducted at SAIW using TIG welding and using 316L and 904L filler rods

Initial experimental studies using Clean-Trace™ NG Bioluminometer

Initial analysis was done to determine the effectiveness of the methodology chosen. The swabbing technique (swabbing from sample points provided by grub screws) allowed swabbing mostly on the swab head. This was unlike on typical and desirable whole surface swabbing when swabbing was done inside the pipe. However the same method was used for all swabbing at inspection port positions. The results obtained from the rig without any liquid or CIP done are presented in Table 4.11. Swabbing was done and assessed using a Clean-Trace™ NG bioluminometer.

Table 4.11: Blank swabs done at different points on dry pipe surfaces

Pipe	Swabbing point	Biofilm intensity	Comments
E	Swab on weld	20 RLU	Sampling done from grub screw onto swab head
F	Swab inside pipe	3097 RLU	Sampling done inside pipe on all swab surfaces
F	Swab on weld	41 RLU	Sampling done from grub screw onto swab head
F	Swab on HAZ	51 RLU	Sampling done from grub screw onto swab head
F	Swab on smooth surface	126 RLU	Sampling done from grub screw onto swab head on the smooth surfaces of pipe F

Certain points were noted from this initial study:

1. ATP picked up live and dead microorganism cells so wiping or treating with alcohol made no difference as alcohol could not remove contaminating microorganisms which may deposit due to ATP swabs during the swabbing process
2. Low RLU readings may mean that there was not much build-up of biofilm intensity on the swab head. Swabbing using the swab head over a restricted area instead of on the side over a wider area seems likely to affect readings downwards
3. It was easier to swab on smooth surface or on HAZ area than on weld roots. This would affect the values for biofilm intensity to be determined during the study

Correlation of RLU values to bacterial counts has been tried but there was no definite correlation as RLU indicates presence of bacteria (dead or alive) and product residues (organics) while

bacterial counts just assessed live bacteria. In industry, bioluminometers are used to detect presence of product residues which need to be removed as they support biofilm formation by conditioning the surface to be favourable for attachment of microorganisms.

Temperature change during dynamic experiments

Temperature changes during the two runs were monitored in the study and the results are presented in Figures 4.28 and 4.29 for runs 1 and 2 respectively.

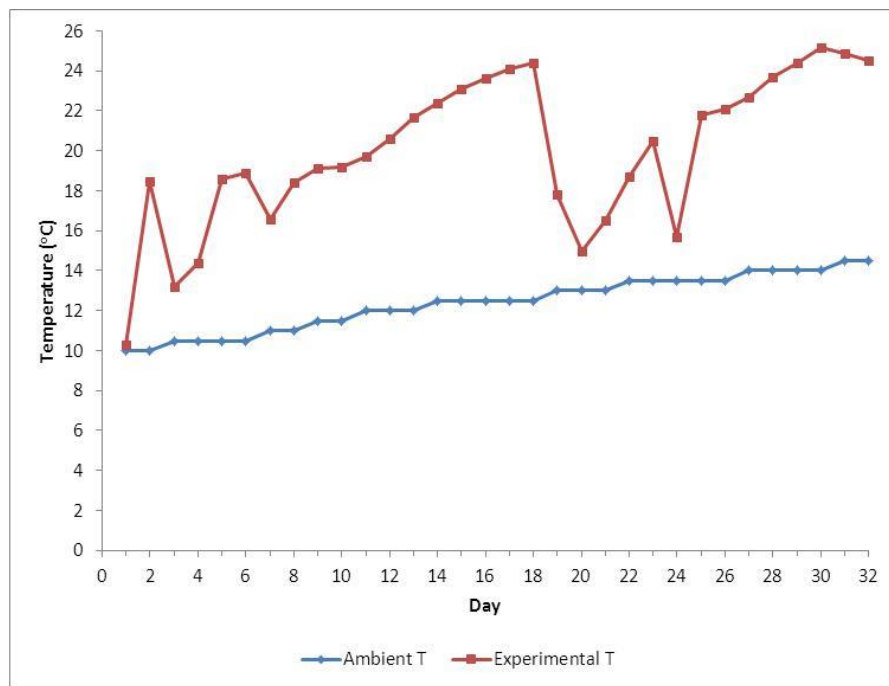


Figure 4.28: Graph showing ambient temperature (ambient T) and experimental temperature (Experimental T) with change in time for run 1

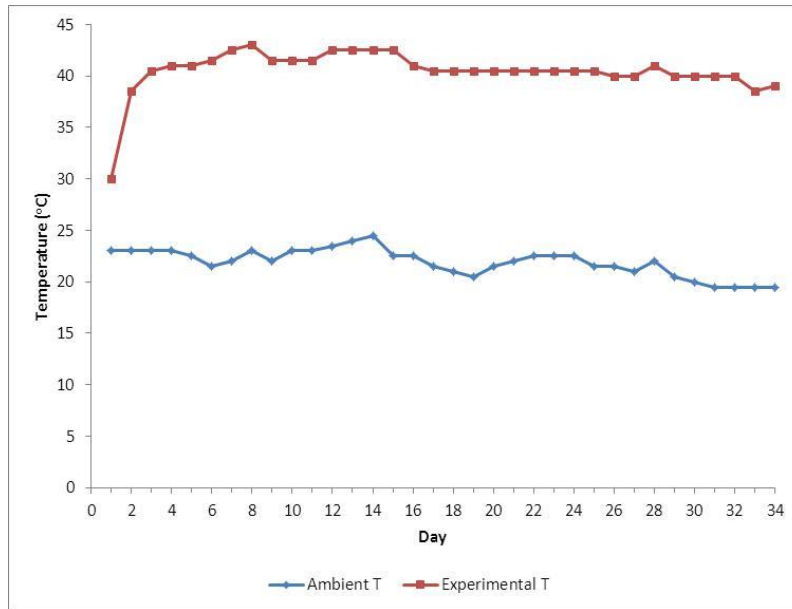


Figure 4.29: Graph showing ambient temperature (ambient T) and experimental temperature (Experimental T) with change in time for run 2

From the figures it was observed that run 1 was undertaken under low temperatures in winter (average ambient temperature was 12.4 °C and average operating temperature was 20.0 °C). Run 2 was undertaken under high temperatures in early summer (average ambient temperature was 21.9 °C and average operating temperature was 40.5 °C). The average temperature difference was calculated as 7.6 and 18.6 °C for runs 1 and 2 respectively. The calculation showed that temperature rise for run 2 was almost twice that for run 1. However, comparison could be made as the duration of the experiments was similar. The elevated operating temperatures for run 2 were due to both higher ambient conditions and a higher operating flowrate.

Dynamic experimental studies (Runs 1 and 2)

The following important points were followed during swabbing of the rig:

- Swabbing was done clockwise in the direction of flow e.g. if sample point 1 was at the top (0°), sample point 2 was 120° clockwise in the direction of flow and 3 was 240° clockwise
- Sample points 1-3 related to swabbing before the weld, 4-6 on the weld and 7-9 after the weld in the direction of flow from all pipes (A to pipe F)
- Note that swabbing done from the top (0°), actually swept the bottom of the pipe surface. Swab sweeping was confined to about 90° arc between sampling points

Water being circulated was sampled and analysed and the results are presented in Table 4.12 for run 1.

The results showed a gradual increase in biofilm intensity in the circulating water with time and this was taken as confirmation that biofilms were attaching on pipe walls. Sampling was also done after 5 weeks for run 1 at the entry point of the rig and at the exit; and the results are presented in Table 4.13. The data from Table 4.13 showed a gradual increase in biofilm intensity from the entry to the exit of the rig as confirmed by results for circulating water. The data further confirmed an increase in biofilm intensity from the entry to the exit of the rig and this may have been due to increased deposition of organic matter and microorganisms at the exit of the rig. This may have been due to the reducer at the end which could help in trapping organic molecules and

microorganisms inside the rig and mostly concentrated in pipe F. It was taken to indicate a gradual build-up of biofilm over the length of the pipe and used to normalise readings.

Table 4.12: Results for water sampling using Aqua-Trace for run 1

Sampling point	Biofilm intensity (RLU)	Comments
Initial water sample	29	Sampling done on municipal water at the start and kept in the fridge at 4°C and analysis done using water swabs
Sample after 3 weeks	522	Sampling done on the day from a sampling port and using water swabs
Sample after 5 weeks	1963 10182 (run 2)	Sampling done before stopping water circulation from a sampling port and using water swabs
Inside fermenter after 3 weeks	5714	Sampling done from inside the fermenter using surface swabs
Inside fermenter after 5 weeks	14 804	Sampling done from inside the fermenter using surface swabs

Table 4.13: Sampling done at the entry and exit of the rig for runs 1 and 2

Sampling point	Biofilm intensity		Comments
	Run 1	Run 2	
Entry of the rig	80 986	1079	This showed increased biofilm intensity
Exit of the rig	237 738	3175	Higher intensity

Note: both runs experienced a 3 fold increase across the rig

Tables 4.12 and 4.13 showed an increase in biofilm intensity with time confirming that municipal water supported biofilm growth. If municipal water was not treated properly at the beginning of the brewing process product contamination and/or MIC seemed likely.

Simões (2005 page 52) investigated biofilm formation on cylindrical SS pipes on the outside and determined intensity as CFU/cm², where area was calculated by πDL , D = outside diameter (inside diameter in the current study) and L = cylindrical length (length before and after the weld in this study i.e. 20 mm). The calculated surface area for the current study was as follows:

$$Surface\ area = \pi D_{inside} L = \pi * 5.251cm * 2cm = 33.0cm^2$$

Biofilm intensities during the study were measured and recorded in Appendix VI. The data was normalised by dividing by surface area and expressed as RLU/cm² in line with other authors as mentioned above. For example after CIP and after water circulation for run1, pipe A, sampling

point 1 had the following intensities: 44 and 53 290 RLU respectively. The normalisation process was as follows:

$$\text{Intensity after CIP} = \frac{44RLU}{33.0cm^2} = 1.3RLU/cm^2$$

$$\text{Intensity after water circulation} = \frac{53290RLU}{33.0cm^2} = 1615RLU/cm^2$$

This was done to all data in Appendix VI to give data in Appendix VII and data presented in this section during analysis. Treatments done to the six pipes (summarised in Table 3.5) in the test rig were analysed to see their effect on biofilm formation, CIP process and on use of ultrasound waves (Appendix VII for individual pipes). Analysis was done on biofilm intensity per area before test runs (after CIP) and after 5 weeks circulating municipal water in the pipes (after biofilm formation). Analysis looked at several factors, namely:

- (i) Effect of fluid flowrate on formation of biofilms and CIP process. This was achieved by comparing results for CIP process and biofilm formation from runs 1 and 2. The analysis addressed the questions “Does the flow direction influence results (geometric impacts)? and was there any observed differences between the first and second pipe experiments?”
- (ii) Effect of chemical and water flowrate around the pipe on CIP process and biofilm formation respectively. This was achieved by comparing results from control pipe F, station 12 around the pipe i.e. 360° around the pipe. This analysis addressed the two questions “How effective was CIP?” and “Was there any difference between the results of side walls as compared to the results of top and bottom of the pipe? The top of the pipe

was analysed because the pipe may not flow full while the bottom of the pipe may result in depositing of solids due to high density”

- (iii) Effect of pipe position on CIP process and biofilm formation. This was achieved by comparing results from pipes A to F looking at the same welds and pipe treatments. This analysis addressed the question “How does the CIP process degrade over the length of the pipe as the concentration decreases?”
- (iv) Effect of using 316L or 904L weld fillers on CIP process and biofilm control. This was achieved by comparing results for all pipes for same weld type. 904L welds had copper that acted as a biocide. This analysis addressed the question “Does using 316L as a filler show worse effects than 904L?”
- (v) Effect of argon purging on CIP process and biofilm formation. This was achieved by comparing results from pipes E and F. Pipes A and B could be compared but they were subjected to ultrasound waves and as such, they would not give a true representation of CIP and biofilm formation processes. This analysis addressed the question “What benefit is achieved by using argon?”
- (vi) Effect of different welds when pickled and passivated on CIP process and biofilm intensity by comparing results from pipes C and D for 316L and 904L welds as well as HAZ welds on pipes C and D. This analysis addressed the questions “What benefits are achieved by pickling and passivation? and What is the influence of the heat affected zone? and What was the effect of the HAZ?”

- (vii) Effect of ultrasound waves on CIP process and biofilm control. This was achieved by comparing results from pipes C and D – HAZ welds for run 1 and pipes A, B and D for run 2. This analysis addressed the question “How effective are ultrasound waves in controlling biofilms?”

Table 3.4 which showed the industrial tolerances required was normalised and summarised in Table 4.14 for easy comparison as it was the standard industrial control.

Table 4.14: Normalised data from Clean-Trace™ NG bioluminometer

Intensity range	Normalise intensity	Explanation	Corrective action
0 – 150 RLU	0 – 4.5 RLU/cm ²	Surface relatively clean	No CIP required
150 – 300 RLU	4.5 – 9.1 RLU/cm ²	Caution area	Continuous monitoring
>300 RLU	> 9.1 RLU/cm ²	Unacceptable	CIP required

- (i) Effect of fluid flowrate on CIP process and biofilm formation

The results for the two runs are presented in Appendix VII and in Tables 4.15 and 4.16. CIP was done initially followed by swabbing and this was to see the effect of CIP process and any initial biofilm residues. CIP was followed by five weeks of water circulation to build biofilm and hence in the results for swabbing after CIP and after biofilm formation are presented.

Table 4.15: Summary of biofilm intensity for all pipes after CIP process and biofilm formation for run 1

Pipe	After CIP process (RLU/cm ²)			After biofilm formation (RLU/cm ²)		
	316L weld	904L weld	HAZ weld	316L weld	904L weld	HAZ weld
A	1.1	1.4		779	909	
B	1.2	1.6		732	854	
C	1.3		1.0	1102		890
D		1.6	1.0		1033	703
E	1.6	2.1		978	1882	
F	2.2	1.7		1769	1618	

The results showed that run 1 had higher biofilm intensity than run 2 and this was due to the high water flowrate operated for run 2 (0.34 m/s) as compared to flowrate for run 1 (0.13 m/s) leading to reduced biofilm intensities i.e. biofilms did not have enough time to attach and grow leading to lower intensities observed. This meant that if pipes were left stagnant during processing this led to higher biofilms formed and removing the biofilms with CIP process was difficult as observed in the study. Biofilm intensity was observed to increase from start of the rig to the end. This may have been due to degradation of CIP chemicals along pipe lengths and with duration of time.

Table 4.16: Summary of biofilm intensity for all pipes after CIP process and biofilm formation for run 2

Pipe	After CIP process (RLU/cm ²)			After biofilm formation (RLU/cm ²)		
	316L weld	904L weld	HAZ weld	316L weld	904L weld	HAZ weld
A	3.1	4.7		92	164	
B	3.7	3.4		89	138	
C	7.3		5.8	168		160
D		4.2	3.7		206	176
E	5.3	3.2		214	228	
F	6.6	7.5		260	237	

It was further observed that low biofilm intensities were easy to clean (run 2) than high intensities (run 1) but the process was not 100% efficient, justifying the need to use ultrasound waves in combination with CIP process.

Comparing against the standard showed that after CIP for run 1, the surfaces were clean according to industrial standards as all the intensities were less than 4.5 RLU/cm². For run 2, the surfaces were not clean as most of the intensities were greater than 4.5 RLU/cm², except for a few exceptions. 4.5 RLU/cm² was the minimum amount required before corrective action needs to be undertaken. This gave further evidence that after first run, biofilms grew easily and they became

difficult to eliminate as they increase with time and more runs. After water circulation, biofilm intensities were very high (all intensities were greater than 9.1 RLU/cm²; run 1 had greater intensities than run 2) and CIP was recommended.

The data for intensities at the entry and exit of the rig (Table 4.13) showed that there was a general increase in biofilm intensities along the pipe lengths. This was attributed to deposition of biofilms along the length and the effect of the pipe reducer on pipe F which helped to trap biofilms about to escape back to the fermenter. High biofilm intensities have been observed in industries where there are pipe bends, reducers, valves, welded areas and any components that restrict flow as they trap organic and inorganic components leading to biofilm formation.

(ii) Effect of chemical and water flowrate around pipe circumference on CIP and biofilm intensity

The position was measured in degrees in the direction of flow and in clockwise direction for the control points. Swabs taken at 0° meant swabbing from the top of the pipe i.e. intensity at the bottom of the pipe while swabs at 200° meant swabbing from the bottom of the pipe i.e. intensity at the top of the pipe. Results are shown in Figures 4.30 and 4.31 for CIP and biofilm intensity.

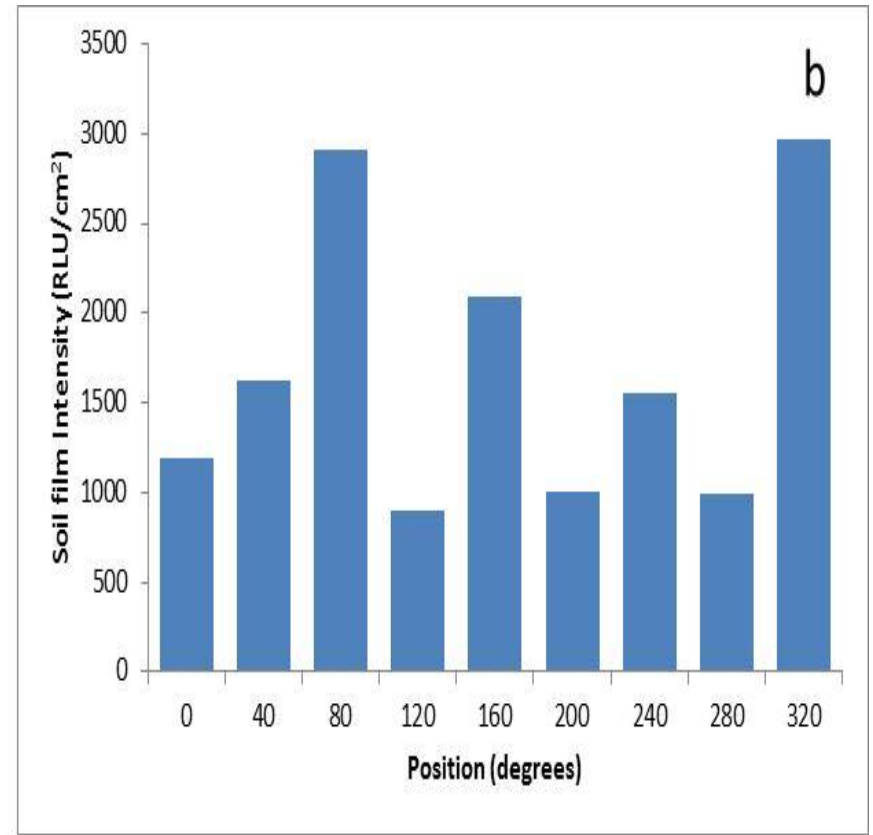
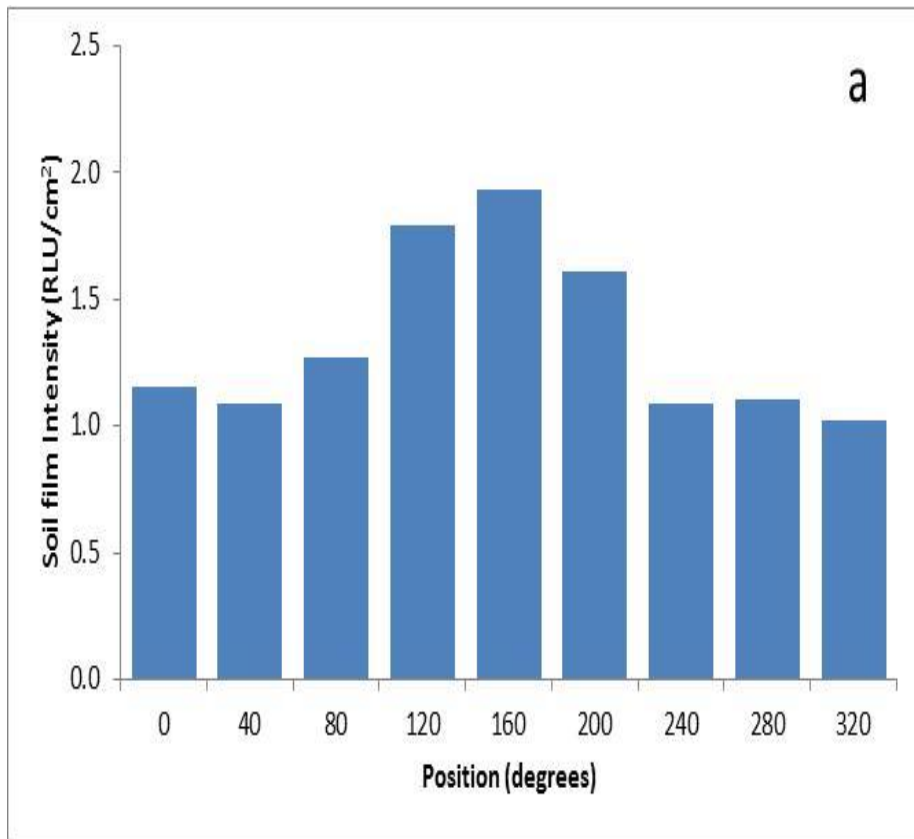


Figure 4.30: Effect of water flow for run 1 after (a) CIP process and (b) biofilm formation. Note the 140 times scale difference on the y-axes for graphs (a) and (b)

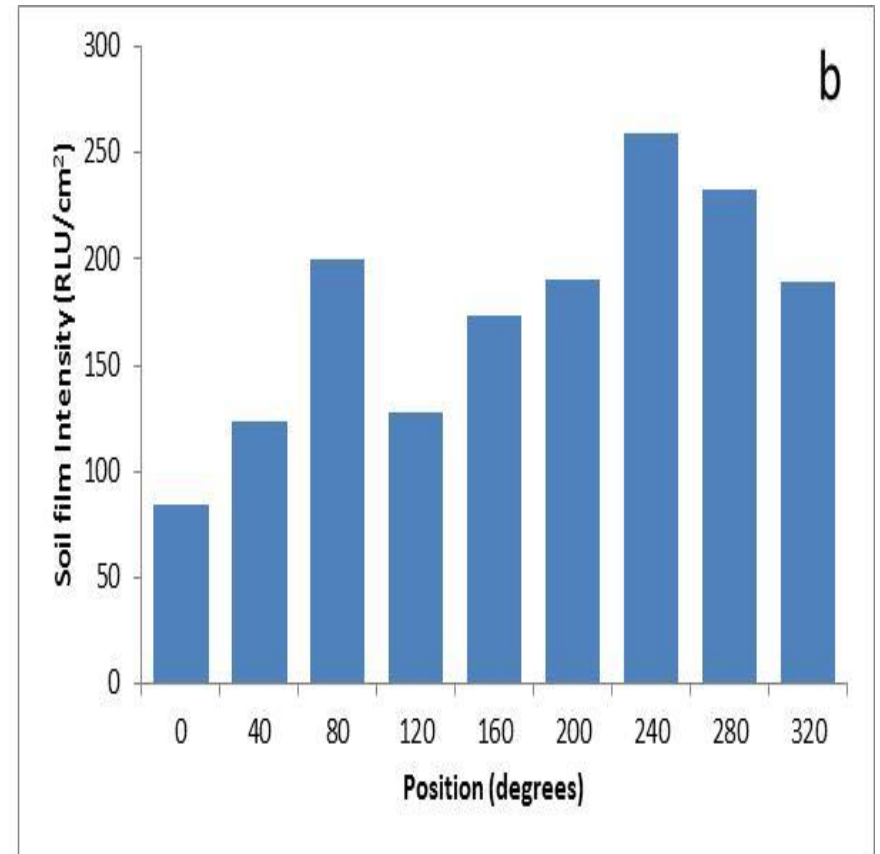
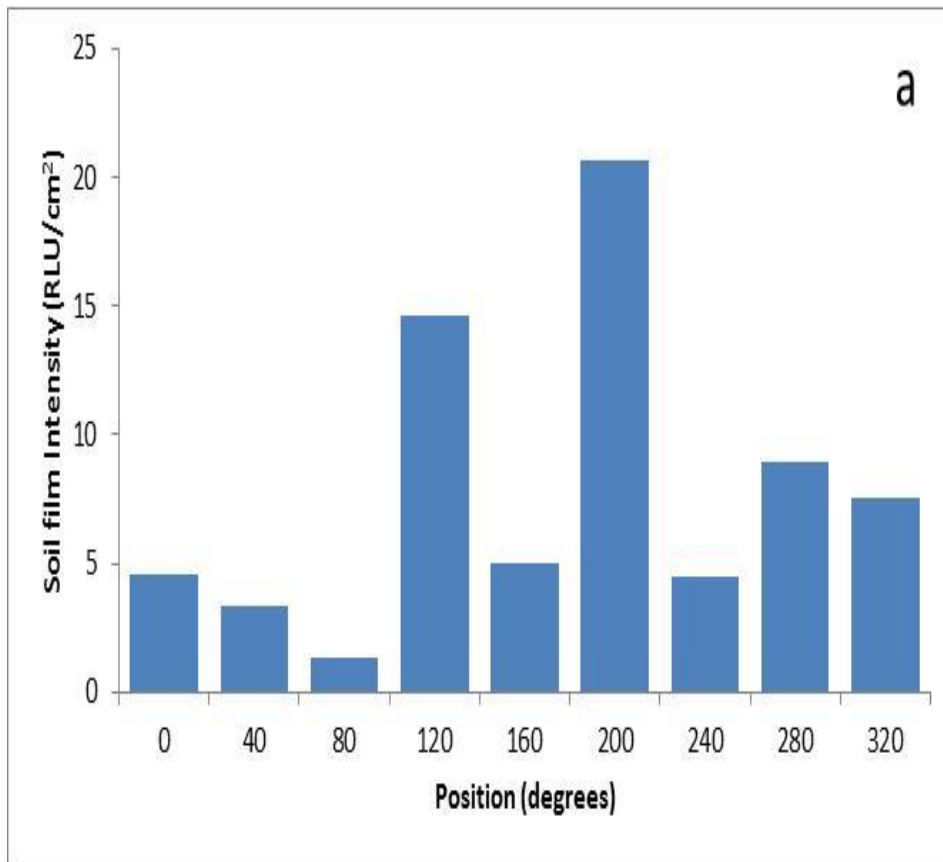


Figure 4.31: Effect of water flow for run 2 after (a) CIP process and (b) biofilm formation. Note the 12 times scale difference on the y-axes for graphs (a) and (b)

Results showing high intensity at 200° and low intensity at 0° showed ineffectiveness of CIP at the top of the pipe i.e. chemicals did not reach the top pipe surface while results showing high intensity at 0° and low intensity at 200° after water circulation showed that water flow had an effect on biofilm intensity.

Figures 4.30(a) and 4.31(a) showed that CIP was not effective at the top of the pipe because of high intensity at 200° and positions near 200°. Figure 4.30 (b) showed that during water circulation, biofilm intensity mainly formed at the bottom of the pipe and at the sides i.e. intensity was high at and around 0° positions. CIP process was done after water circulation and swabbing around the top of the pipe showed that the intensity was still high i.e. CIP was not 100% effective once biofilms were observed on pipe surfaces.

Run 2 was undertaken partly to check the effect of successive runs on CIP process and biofilm intensity. The results showed that CIP was ineffective at the top of the pipe (Figure 4.31a). This is the trend observed in the food and beverage industry (Czechowski and Banner, 1992) and showed that with successive runs of products, CIP became less and less effective against biofilms. This justifies the need to find another process to aid the current technology. Figure 4.31(b) showed that biofilms were formed around the whole pipe surfaces. CIP was done after the experiments and swabbing at random confirmed high biofilm intensities for higher loading (run 1) and low biofilm intensity for lower loading (run 2).

(iii) Effect of pipe position on CIP process and biofilm intensity

The treatment done to pipes A and E, and B and F were similar and the only change was effect of pipe position with respect to water flow. The results are presented in Tables 4.17 and 4.18 to check if water flow had any effect on CIP process and biofilm formation.

The three points noted before weld, on weld and after weld could best be understood by revisiting Figure 3.10 and Tables 3.2 and 3.3. Figure 3.10 showed that there were three equally spaced sampling points before the weld, three sampling points on the weld and three sampling points after weld. The three assessment lines were staggered by 40° making a total of nine sampling points for each sampling position e.g. A1-316.

Tables 4.17 and 4.18 showed that after CIP process, water flowrate had an effect on welds but there was no significant effect of water flowrate before and after the welds except a few points on pipe E. This was confirmed by subtracting biofilm intensities for pipe A316/904 from pipe E316/904 and pipe B316/904 from pipe F316/904 to nullify the effect of argon. The results were all positive and negligible before and after welds but significant on welds. This seems likely to be attributed to weld root concerns as shown in Figure 4.26. However, during biofilm formation the effect of water flow began to be significant as seen from high biofilm intensities on welds for pipe E against pipe A, particularly on the 904L welds. The same trend was also observed when pipes B and F were compared as they had the same treatment.

Table 4.17: Effect of water flow along pipes for runs 1 and 2 after CIP and biofilm formation for 316L weld (measurements in RLU/cm²)

A and E for 316L weld							
		Before weld		On weld		After weld	
		After CIP	After BF formation	After CIP	After BF formation	After CIP	After BF formation
Run 1	A	1.3	1615	0.9	472	0.9	774
	A	1.4	307	0.4	1125	1.4	625
	A	1.1	835	1.1	802	1.2	458
	E	1.2	1124	2.4	1453	1.5	502
	E	1.2	1766	1.2	1083	1.4	933
	E	1.5	451	2.9	800	1.3	687
Run 2	A	1.9	132	2.0	83	2.4	166
	A	3.6	58	2.5	60	2.9	82
	A	5.6	54	4.4	107	2.7	86
	E	1.9	139	4.2	112	3.0	163
	E	5.8	187	3.4	545	8.6	209
	E	3.3	272	13.3	147	4.2	149

BF – biofilm formation

Table 4.18: Effect of water flow along pipes for runs 1 and 2 after CIP and biofilm formation for 904L weld (measurements in RLU/cm²)

A and E for 904L weld							
		Before weld		On weld		After weld	
		After CIP	After BF formation	After CIP	After BF formation	After CIP	After BF formation
Run 1	A	1.6	648	1.5	1007	1.3	1000
	A	1.5	921	1.5	1439	0.9	731
	A	1.5	959	1.7	217	1.0	1257
	E	1.7	2923	1.5	3211	2.3	468
	E	1.5	3770	6.9	1256	1.7	1902
	E	0.9	1020	0.6	1383	2.0	1006
Run 2	A	5.2	159	4.4	148	4.6	165
	A	5.2	233	5.2	112	4.8	133
	A	3.2	55	3.2	371	6.8	97
	E	8.3	248	2.0	408	4.2	159
	E	3.5	204	3.2	243	2.0	257
	E	2.0	249	1.9	218	1.8	61

BF – biofilm formation

Appendix VII includes tables for individual pipes against the control and they showed that biofilm intensities increased from pipe A to F. The tables also showed that 904L welds had higher biofilm intensities than 316L welds (see summarised results in Tables 4.15 and 4.16) except when pickling and passivation was undertaken after welding. HAZ welds (stations on pipes C and D) had the least biofilm intensities showing that after pickling and passivation on welded surfaces, surface roughness decreased leading to lower biofilm formation. Biofilm intensity increased two-fold from pipe A to pipe F for both welds after CIP process and biofilm formation but a big change was observed from pipe E to pipe F. This may have been due to the reducer at pipe F, trapping all organics and microorganisms inside the pipe and thereby increasing the biofilm intensity in that pipe.

(iv) Effect of using different filler rods (316L or 904L) on CIP process and biofilm intensity

Different weld filler rods were analysed to see their effect on CIP process and biofilm intensity. The changes observed during the runs on pipe welds were compared i.e. the effect of weld filler 316L from pipe A to F was determined separately from the effect of 904L weld filler. Pipes A and E; B and F; and C and D had the same treatment and the effect of the type of treatment was analysed. All pipes had 316L and 904L welds to determine the effect of copper as a biocide except for pipes C and D which had alternating welds. Results are presented in Tables 4.19, 4.20, 4.21 and 4.22.

Table 4.19: Effect of using 316L weld filler rods on CIP and biofilm formation for run 1
(measurements in RLU/cm²)

	Before weld		On weld		After weld	
	After CIP	After BF formation	After CIP	After CIP	After BF formation	After CIP
A	1.3	1615	0.9	472	0.9	774
A	1.4	307	0.4	1125	1.4	625
A	1.1	835	1.1	802	1.2	458
B	0.5	883	0.6	415	1.4	1404
B	1.0	729	0.6	1230	2.6	419
B	1.4	298	1.5	604	1.5	601
C	2.9	727	1.2	477	2.1	1221
C	1.3	1408	0.7	1370	0.8	466
C	0.5	1123	1.2	2041	1.2	1088
E	1.2	1124	2.4	1453	1.5	502
E	1.2	1766	1.2	1083	1.4	933
E	1.5	451	2.9	800	1.3	687
F	2.8	1785	1.7	3673	2.6	1133
F	1.1	2094	1.7	1410	2.1	2384
F	0.6	413	6.2	1382	0.9	1646

BF – biofilm formation

Table 4.20: Effect of using 904L weld filler rods on CIP and biofilm formation for run 1
(measurements in RLU/cm²)

	Before weld		On weld		After weld	
	After CIP	After BF formation	After CIP	After CIP	After BF formation	After CIP
A	1.6	648	1.5	1007	1.3	1000
A	1.5	921	1.5	1439	0.9	731
A	1.5	959	1.7	217	1.0	1257
B	2.1	677	1.7	534	1.3	1809
B	0.8	724	1.0	1813	0.7	300
B	2.1	363	2.0	545	2.7	921
D	1.2	590	2.8	2525	3.3	1203
D	0.6	788	2.5	890	0.9	879
D	0.8	493	1.7	1500	0.9	426
E	1.7	2923	1.5	3211	2.3	468
E	1.5	3770	6.9	1256	1.7	1902
E	0.9	1020	0.6	1383	2.0	1006
F	1.3	1824	1.3	1483	1.6	3257
F	1.3	832	1.6	1058	3.2	2486
F	1.2	852	0.9	1328	2.6	1441

BF – biofilm formation

Table 4.21: Effect of using 316L weld filler rods on CIP and biofilm formation for run 2
(measurements in RLU/cm²)

	Before weld		On weld		After weld	
	After CIP	After BF formation	After CIP	After CIP	After BF formation	After CIP
A	1.9	132	2.0	83	2.4	166
A	3.6	58	2.5	60	2.9	82
A	5.6	54	4.4	107	2.7	86
B	1.8	75	5.1	131	3.2	56
B	1.0	103	13.3	89	1.9	24
B	1.1	142	1.5	86	4.4	97
C	5.8	58	3.2	183	5.4	174
C	2.9	126	11.5	240	9.7	139
C	1.3	184	25.1	250	0.9	158
E	1.9	139	4.2	112	3.0	163
E	5.8	187	3.4	545	8.6	209
E	3.3	272	13.3	147	4.2	149
F	1.5	469	6.3	641	3.8	161
F	13.1	229	11.8	223	5.4	288
F	4.3	74	7.1	134	5.8	120

BF – biofilm formation

Table 4.22: Effect of using 904L weld filler rods on CIP and biofilm formation for run 2
(measurements in RLU/cm²)

	Before weld		On weld		After weld	
	After CIP	After BF formation	After CIP	After CIP	After BF formation	After CIP
A	5.2	159	4.4	148	4.6	165
A	5.2	233	5.2	112	4.8	133
A	3.2	55	3.2	371	6.8	97
B	5.0	138	5.0	136	1.2	89
B	1.6	116	6.4	262	2.8	159
B	1.2	69	4.8	100	2.6	173
D	4.4	173	4.3	613	3.9	165
D	3.8	102	6.4	128	2.1	225
D	5.0	123	6.5	200	1.1	126
E	8.3	248	2.0	408	4.2	159
E	3.5	204	3.2	243	2.0	257
E	2.0	249	1.9	218	1.8	61
F	11.8	100	6.6	549	4.5	356
F	15.2	116	4.3	187	2.1	326
F	6.5	85	16.0	243	0.8	173

BF – biofilm formation

In general, 904L welds had higher biofilm intensities than 316L welds after CIP process and biofilm formation (Tables 4.15 and 4.16; and Tables 4.19 to 4.22). The average biofilm intensity after CIP was 1.5 and 1.7 RLU/cm² for 316L and 904L welds respectively for run 1 and 5.2 and 4.6 RLU/cm² for run 2 showing that Cu had no measurable effect on intensity during CIP process. After biofilm formation (5 weeks), the average biofilm intensity was 1072 and 1259 RLU/cm² for 316L and 904L welds respectively for run 1 and 165 and 195 RLU/cm² for 316L and 904L welds respectively run 2 showing that copper had no effect on biofilm formation process. The higher biofilm intensity observed from 904L welds after water circulation for both runs may have been due to the type of welds produced which were not as good as 316L welds (see Figures 4.25 and 4.26).

The welds from 904L rods had poor root penetration suggesting the need for different weld parameters to those established for 316L. The chemical content was different from the pipes giving different grain boundaries on the welds and this led to higher biofilm intensities.

(v) Effect of argon purging during welding on CIP process and biofilm intensity

The purpose of argon purging was to exclude oxygen and the formation of iron oxide. This was assessed by comparing pipes E and F and the results are presented in Tables 4.23 and 4.24. Generally, there was higher biofilm intensity on welds undertaken in the absence of argon purging (pipes B and F).

Table 4.23: Effect of argon purging during welding for runs 1 and 2 after CIP and biofilm formation for 316L weld (measurements in RLU/cm²)

E and F for 316L weld							
		Before weld		On weld		After weld	
		After CIP	After BF formation	After CIP	After BF formation	After CIP	After BF formation
Run 1	E	1.2	1124	2.4	1453	1.5	502
	E	1.2	1766	1.2	1083	1.4	933
	E	1.5	451	2.9	800	1.3	687
	F	2.8	1785	1.7	3673	2.6	1133
	F	1.1	2094	1.7	1410	2.1	2384
	F	0.6	413	6.2	1382	0.9	1646
Run 2	E	1.9	139	4.2	112	3.0	163
	E	5.8	187	3.4	545	8.6	209
	E	3.3	272	13.3	147	4.2	149
	F	1.5	469	6.3	641	3.8	161
	F	13.1	229	11.8	223	5.4	288
	F	4.3	74	7.1	134	5.8	120

BF – biofilm formation

Table 4.24: Effect of argon purging during welding for runs 1 and 2 after CIP and biofilm formation for 904L weld (measurements in RLU/cm²)

E and F for 904L weld							
		Before weld		On weld		After weld	
		After CIP	After BF formation	After CIP	After BF formation	After CIP	After BF formation
Run 1	E	1.7	2923	1.5	3211	2.3	468
	E	1.5	3770	6.9	1256	1.7	1902
	E	0.9	1020	0.6	1383	2.0	1006
	F	1.3	1824	1.3	1483	1.6	3257
	F	1.3	832	1.6	1058	3.2	2486
	F	1.2	852	0.9	1328	2.6	1441
Run 2	E	8.3	248	2.0	408	4.2	159
	E	3.5	204	3.2	243	2.0	257
	E	2.0	249	1.9	218	1.8	61
	F	11.8	100	6.6	549	4.5	356
	F	15.2	116	4.3	187	2.1	326
	F	6.5	85	16.0	243	0.8	173

BF – biofilm formation

This was attributed to rough welds produced in the absence of argon purging as compared to welds produced whilst purging (pipes A and E). The roughness was attributed to formation of iron oxide during welding, leading to rough surface finishes which encouraged biofilm formation and made cleaning under CIP less effective. Figure 4.25 showed that 904L filler rods produced welds with poor penetration and concavity which encouraged biofilm formation.

However, if the welds were pickled and passivated, biofilm intensities were expected to be lower. In the study, pipes C and D were pickled and passivated after welding in the absence of argon purging. (see Tables 4.25 and 4.26). The results from Tables 4.25 and 4.26 showed that pickling and passivation led to a general reduction of biofilm intensities after both CIP process and biofilm formation. Controlled pickling and passivation led to chemical polishing giving smooth surfaces that did not encourage biofilm formation (see section 1.5.1).

Pickling and passivation is used to counteract the effects of welding in industry. The process cannot always be adequately performed after welding due to the number of welds on one plant and also the location of the welds. This applies particularly during maintenance. Any welding done on pipes which cannot be pickled and passivated will result in problems with biofilm formation and/or MIC.

Table 4.25: Effect of pickling and passivation after welding in the absence of argon for runs 1 and 2 after CIP and biofilm formation for 316L welds (measurements in RLU/cm²)

		F and C for 316L weld					
		Before weld		On weld		After weld	
		After CIP	After BF formation	After CIP	After BF formation	After CIP	After BF formation
Run 1	F	2.8	1785	1.7	3673	2.6	1133
	F	1.1	2094	1.7	1410	2.1	2384
	F	0.6	413	6.2	1382	0.9	1646
	C	2.9	727	1.2	477	2.1	1221
	C	1.3	1408	0.7	1370	0.8	466
	C	0.5	1123	1.2	2041	1.2	1088
Run 2	F	1.5	469	6.3	641	3.8	161
	F	13.1	229	11.8	223	5.4	288
	F	4.3	74	7.1	134	5.8	120
	C	5.8	58	3.2	183	5.4	174
	C	2.9	126	11.5	240	9.7	139
	C	1.3	184	25.1	250	0.9	158

BF – biofilm formation

Table 4.26: Effect of pickling and passivation after welding in the absence of argon for runs 1 and 2 after CIP and biofilm formation for 904L welds (measurements in RLU/cm²)

F and D for 904L weld							
		Before weld		On weld		After weld	
		After CIP	After BF formation	After CIP	After BF formation	After CIP	After BF formation
Run 1	F	1.3	1824	1.3	1483	1.6	3257
	F	1.3	832	1.6	1058	3.2	2486
	F	1.2	852	0.9	1328	2.6	1441
	D	1.2	590	2.8	2525	3.3	1203
	D	0.6	788	2.5	890	0.9	879
	D	0.8	493	1.7	1500	0.9	426
Run 2	F	11.8	100	6.6	549	4.5	356
	F	15.2	116	4.3	187	2.1	326
	F	6.5	85	16.0	243	0.8	173
	D	4.4	1773	4.3	613	3.9	165
	D	3.8	102	6.4	128	2.1	225
	D	5.0	123	6.5	200	1.1	126

BF – biofilm formation

(vi) Effect of pickling and passivating welds not purged on CIP and biofilm intensity

The analysis was done on pipes C and D as they had identical treatments. The results are presented in Tables 4.27 and 4.28 for 316L, 904L and HAZ welds. Generally 316L weld (pipe C) had higher biofilm intensity than 904L weld (pipe D) showing the positive effect of pickling and passivating. The effect of Cu as a biocide was evident maybe due to the fact that the Cu may have been exposed at the grain boundaries after chemical polishing resulting from pickling and passivating. Generally HAZ weld from pipe C showed higher intensity than from pipe D. There was no reason attributed as the pipes were subjected to the same conditions during pickling and passivation.

(vii) Effect of subjecting ultrasound waves on CIP and biofilm intensity

Ultrasound waves were applied by clamping the sonication device onto the outside of “hot spot” positions of pipes and running experiments under water. Ultrasound waves in combination with CIP process led to better biofilm control but the combination did not eliminate all biofilms (Table 4.29).

Ultrasound waves were applied on HAZ welds for pipes C and D. The results showed better control on pipe D than pipe C in run 1. This may have been due to the time of exposure of 5 and 10 minutes for pipes D and C respectively. For run 2, ultrasound waves were applied on 316L welds for pipes A and B, and HAZ weld for pipe D for 5 minutes. The results showed that there was better control on 316L welds for pipes A and B i.e. there was the least biofilm intensity than for any other pipe weld. However, HAZ weld on pipe D showed higher intensities.

Table 4.27: Effect of pickling and passivating after welding for runs 1 and 2 after CIP and biofilm formation for 316L weld (measurements in RLU/cm²)

C and D for 316L and 904L welds							
		Before weld		On weld		After weld	
		After CIP	After BF formation	After CIP	After BF formation	After CIP	After BF formation
Run 1	C	2.9	727	1.2	477	2.1	1221
	C	1.3	1408	0.7	1370	0.8	466
	C	0.5	1123	1.2	2041	1.2	1088
	D	1.2	590	2.8	2525	3.3	1203
	D	0.6	788	2.5	890	0.9	879
	D	0.8	493	1.7	1500	0.9	426
Run 2	C	5.8	58	3.2	183	5.4	174
	C	2.9	126	11.5	240	9.7	139
	C	1.3	184	25.1	250	0.9	158
	D	4.4	1773	4.3	613	3.9	165
	D	3.8	102	6.4	128	2.1	225
	D	5.0	123	6.5	200	1.1	126

BF – biofilm formation

Table 4.28: Effect of pickling and passivating after welding for runs 1 and 2 after CIP and biofilm formation for HAZ welds (measurements in RLU/cm²)

C and D for HAZ welds							
		Before weld		On weld		After weld	
		After CIP	After BF formation	After CIP	After BF formation	After CIP	After BF formation
Run 1	C-HAZ	2.6	1199	1.2	1407	0.5	471
	C-HAZ	0.5	911	0.4	1228	0.6	633
	C-HAZ	1.7	619	0.8	956	0.8	590
	D-HAZ	1.3	590	0.7	2525	0.6	1203
	D-HAZ	1.0	788	0.4	890	1.3	879
	D-HAZ	0.8	493	1.0	1500	1.5	426
Run 2	C-HAZ	8.5	81	9.1	270	5.8	201
	C-HAZ	1.7	33	9.5	156	5.5	166
	C-HAZ	4.2	144	4.4	231	3.2	159
	D-HAZ	1.5	121	4.5	208	2.9	355
	D-HAZ	6.4	164	3.6	142	1.0	177
	D-HAZ	3.7	101	7.7	166	1.7	148

BF – biofilm formation

Table 4.29: Results showing combined effect of ultrasound waves and CIP process on biofilm intensity for runs 1 and 2

Pipe	Run 1 (RLU/cm ²)			Run 2 (RLU/cm ²)		
	Type of weld under investigation					
	316L	904L	HAZ	316L	904L	HAZ
A	779	909		92 (sonicated)	164	
B	732	854		89 (sonicated)	138	
C	1102		890 (sonicated)	168		160
D		1033	703 (sonicated)		206	176 (sonicated)
E	978	1882		214	228	
F	1769	1618		260	237	

All welds written sonicated were subjected to ultrasound waves under water when the probe was clamped at that weld type

Ultrasound waves in combination with CIP process did not result in 100% elimination of biofilms. This may have been due to the damping effect of the mass of steel used in the clamp (m = 1001 g), the interface between the clamp and the pipe, the pipe wall thickness (4mm) or the limited power of the laboratory ultrasound device used. This led to inefficiencies in transferring ultrasound waves through the 316L SS pipes. After CIP, intensities were still above 9.1 RLU/cm² concluding that the combination of the two processes did not result in acceptable industrial standards or the best standard of 100% disinfection efficiency. However, the experiments showed that ultrasound

waves were effective against biofilms but more investigations need to be conducted to optimise the transfer of ultrasound waves from the probe to the surfaces of 316 SS pipes. The device which was used in the experiments worked well in water. Ultrasound devices which can operate in air are available off the shelf for further investigations. However, contact with an ultrasound specialist company in the UK, Hilsonic, suggests developing an ultrasonic transducer that can be clamped around a pipe that will transmit the energy into the pipe to cavitate the fluid inside and perform a cleaning function is available as a prototype. For a pipe of internal diameter of 50 mm and 1.6 mm wall thickness, a 400 W unit with a clamping arrangement to be designed was suggested by a specialist company in the UK, Hilsonic. This is twice the power of the laboratory equipment used and the 1.6 mm wall thickness stiffness is some 14.6 times $[(3.91/1.60)^3]$ less than the 4 mm pipe thickness tested.

4.3 Summary of research results

4.3.1 Biofilms in the beverage industry

Planktonic cells become sessile cells (clump together) when nutrients become limited. The microorganisms attempt to locate organic material attached to the process equipment to which they can adhere to and live on. When this is achieved, a partly reversible and irreversible attachment process starts and the formation of biofilm takes place. The microorganisms in biofilms are resistant towards various counter measures and it is therefore important to prevent biofilm formation by using the correct surface design methods, detergents and disinfectants, and any other technologies. In addition, the choice of material of construction and joining methods chosen has

an important influence on the inclination of biofilm formation. Biofilms are often found in cracks, corners, gaskets, joints, crevices and welds in the pipe material or in dead ends in the pipe system.

Consideration of the conditions in the pipe shows that local turbulence effects can cause specific areas of growth of biofilms, particularly around welds and in dead areas. Normally with welds one may expect some micro-cracking where microorganisms can settle and form biofilms. In some areas, the characteristics of the pipe material are not constant due to welding. In process vessels and pipes build-up of biofilms is as a result of geometry e.g. around tight corners where the inner side is slower flowing than the outer because of the kinetic energy of flow. To conclude, biofilms have been shown to form mostly under laminar conditions and in crevices or dead spaces.

4.3.2 Water analysis with emphasis on biofilm formation

Water management in breweries remains a critical and practical problem due to water scarcity and decreased quality. This has led to breweries using municipal water for all their functions including beer brewing. Beverage drinks comprises water between 92 and 100% and because it accounts for the majority of the beverage, it has the capacity to affect the final product both in taste, health or appearance. However, as demonstrated water could support biofilms and this increases with time and reduced flow speeds i.e. stagnant water in pipes.

4.3.3 Controlling biofilms using ultrasound waves

Ultrasonic technologies could be used in the future of the food and beverage industry as their use potentially resulted in reduced biocide consumption, no modification to nutrients present or

formation of carcinogenic products but greatly enhanced biofilm removal. Efficiencies of disinfection were in the region of 70 to 100% but the goal was to achieve 100% removal leading to the combined use of ultrasound waves and reduced biocide quantities. Studies on the effect of ultrasound waves on the biocide need to be conducted to determine the best combination so as to have a combined effect of the two systems. The temperature rise observed during the experiments does narrow the search to biocides that are stable at elevated temperatures but this effect is more pronounced on materials and fluids that have low specific heat capacity which leads to higher temperature changes.

4.3.4 Surface profile changes during use of ultrasound waves

Perfect surfaces should have the following characteristics: (i) low bacterial loading, (ii) low R_a , (iii) low R_{max} , (iv) $R_{skw} = 0$, and (v) $R_{kur} = 3$

The different coupon surfaces investigated were ranked from the best to worst from results:

- | | |
|---------------------|---|
| ○ Bacterial loading | Laser weld⇒Normal surface⇒CMT weld⇒MIG weld |
| ○ R_{max} | Laser weld⇒Normal surface⇒MIG weld⇒CMT weld |
| ○ R_a and R_q | Laser weld⇒MIG weld⇒Normal surface⇒CMT weld |
| ○ R_{skw} | Normal surface⇒Laser weld⇒MIG weld⇒CMT weld |
| ○ R_{kur} | Normal surface⇒CMT weld⇒MIG weld⇒Laser weld |

The following points were observed:

- Welding resulted in rough surfaces which increased biofilm attachment as observed from R_a , R_{max} and bacterial loading data
- Heat stresses (high temperatures for CMT, Laser and MIG welds) resulted in weaker surfaces which were prone to stress erosion from ultrasound waves resulting in increased bacterial loading from R_{skw} and R_{kur} data
- Change in R_{skw} and R_{kur} on welded surfaces showed the negative effect of ultrasound waves on the surface but it was effective in biofilm control as it enabled penetration of the EPS matrix as seen from the previous chapter
- Laser weld gave the best results and it was concluded as the best welding technique but its drawback is on costs as it was expensive as compared to CMT and MIG/TIG

Ultrasound waves were found to erode SS material almost evenly along the coupon surface, thus maintaining the shape of the peaks and valleys; however, the erosion that occurred during treatment could be controlled and reduced by operating at lower temperatures by operating the ultrasonic probe in pulse mode in the transport media. These observations could be linked to other authors as well (Eliaz and Nissan, 2007). The effect was similar to chemical polishing which decreases peaks and evens out the surface.

Detry *et al.* (2010) showed that the relation between the size of the surface defect and the size of microbial cell was important, i.e. microbial cells are retained more by surface defects of similar size. Grooves larger than the bacteria would behave more like a flat surface while small scratches

where bacteria could not enter would only reduce the contact area of the cell (Detry *et al.*, 2010). *E. coli* cells with lengths of 2–3.4 μm and diameters of 0.5–0.9 μm on average (Trueba and Woldring, 1980) could settle in grooves or grain boundaries of surfaces used; however, they were discouraged more on laser welds followed normal surfaces and after significant surface erosion had occurred on all surfaces after prolonged treatment. Regardless of the scale at which roughness was analysed, these measurements were merely statistical values describing a surface, and enabled experimental results to be explained only in part. The development of other surface parameters to characterise adhesion should be encouraged.

Surface methods could only measure surface residual stresses in one direction. These stresses could be observed only around the weld beam or coupon surface but it did not give any information on the internal material strength (Uzun and Bilge, 2010). This was seen as a disadvantage as the material could fail due to high frequency vibration fatigue failure resulting from treatment with ultrasound waves.

4.3.5 Energy changes during treatment with ultrasound waves

Of the methods used, the Nexus hydrophone showed consistent results for electrical and cavitation power densities while the acoustical energy could only be determined by the calorimetric method. The decrease in the energy with distance from the probe was expected as shown in the literature and it was shown that there was a small variation as the amplitude increased.

Ultrasonic technology could have a strong presence in the future of the food and beverage industry in controlling biofilms as:

- It is considered to be a green technology because all processes that occur in the presence of ultrasound waves during control of biofilms could be reversed, a positive attribute as compared to conventional methods that are used (e.g. CIP chemicals) that have the capability of polluting the environment due to irreversible reactions that occur to form harmful carcinogens and the difficulty to dispose-off the waste generated from the processes
- The moderate temperature rise observed in the bulk solution (less than 10°C over 1 hour) was experienced during use of ultrasound waves and it does not adversely affect the nutritional value of the beverages in the production process and also this process is undertaken when production has been stopped

However, ultrasound waves have no residual effect which acts after the treatment process as compared to other chemicals such as chlorine gas and the results showed that it does not give 100% bacterial disinfection i.e. there was need to combine the technology with another method to achieve a target of 100%.

4.3.6 CIP systems in combination with ultrasound waves

It was shown that welding done to pipe surfaces resulted in rough surfaces. This had a negative effect on cleaning efficiency and favoured increased biofilm intensity. However, surface modification e.g. pickling and passivation, done to pipes after welding had a corrective action reducing biofilm intensity if done properly.

Integration of ultrasound waves into existing brewing technologies is possible. The only drawback was its inefficiency or decreased efficiency when operating in air at interfaces. This does not take away the duty of formulating a proper design and fabrication approach as was demonstrated in this study as reported (there was an increase in biofilm intensity from pipe A to F, mainly due to many dead spots that were deliberately included in the test rig).

In conclusion, it was demonstrated that biofilms could be caused and supported by municipal water alone. Once they form they are difficult to deal with using CIP processes. However, the use of ultrasound waves in combination with CIP was effective at shorter distances between the probe and hot spots, for shorter residence times, and for thin pipe thickness when applied outside. More research is needed to be done to further optimise the process for production process plants and to integrate it into existing CIP technology.

Focus should be dedicated to using ultrasound devices capable of reproducing the micro-bubbles and cavitation, replicating sonication, but that work externally in air to aid CIP process by clamping them to “hot spots.”

References

- Álvarez, I., Mañas, P., Sala, F. J. and Condón, S. (2003) Inactivation of *Salmonella enterica* Serovar Enteritidis by ultrasonic waves under pressure at different water activities, *Applied and Environmental Microbiology*, **69**(1), 668–672.
- Antoniadis, A., Poullos, I., Nikolakaki, E. and Mantzavinos, D. (2007) Sonochemical disinfection of municipal wastewater, *Journal of Hazardous Materials*, **146**(3), 492–495.
- Bapat, P. S. and Pandit, A. B. (2008) Thermodynamic and kinetic considerations of nucleation and stabilization of acoustic cavitation bubbles in water, *Ultrasonics Sonochemistry*, **15**(1), 65–77.
- Beckett, M. A. and Hua, I. (2001) Impact of ultrasonic frequency on aqueous sonoluminescence and sonochemistry, *The Journal of Physical Chemistry A*, **105**(15), 3796–3802.
- Boulangé-Petermann, L., Rault, R., and Bellon-Fontaine, M-N. (1997) Adhesion of streptococcus thermophilus to stainless steel with different surface topography and roughness, *Biofouling: The Journal of Bioadhesion and Biofilm Research*, **11**(3), 201–216.
- Butz, P. and Tauscher, B. (2002) Emerging technologies: chemical aspects, *Food Research International*, **35**(2-3), 279–284.
- Catallo, W. J. and Junk, T. (1995) Sonochemical dechlorination of hazardous wastes in aqueous systems, *Waste Management*, **15**(4), 303–309.
- Chisti, Y. and Moo-Young, M. (1994) Clean-in-place systems for industrial bioreactors: design, validation and operation, *Journal of Industrial Microbiology*, **13**(4), 201–207.

- Cluett, J., Rowlands, D., Khanyile, D. and Hulse, G. (2003) Principles of hygiene in the beverage industry, The Institute of Brewing and Distilling (IBD)–Africa Section, Supreme Printers, Hout Bay, South Africa, ISBN: 0-620-31335-8, First Edition, pp. 41.
- Czechowski, M. H. and Banner, M. (1992) Control of biofilms in breweries through cleaning and sanitizing, *MBAA Technical Quarterly*, **29(3)**, 86–88.
- Detry, J. G., Sindic, M. and Deroanne, C. (2010) Hygiene and cleanability: A focus on surfaces, *Critical Reviews in Food Science and Nutrition*, **50(7)**, 583–604.
- Dror, N., Mandel, M., Hazan, Z. and Lavie, G. (2009) Advances in microbial biofilm prevention on indwelling medical devices with emphasis on usage of acoustic energy, *Sensors*, **9(4)**, 2538–2554.
- Eliaz, N. and Nissan, O. (2007) Innovative processes for electropolishing of medical devices made of stainless steels, *Journal of Biomedical Materials Research Part A*, **83A(2)**, 546–557.
- Francolini, I. and Donelli, G., (2010) Prevention and control of biofilm based medical-device-related infections, *FEMS Immunology and Medical Microbiology*, **59(3)**, 227–238.
- Frantsen, J. E. and Mathiesen, T. (2009) Specifying stainless steel surfaces for the brewery, dairy and pharmaceutical sectors, NACE Corrosion, Paper 09573, Atlanta, USA, 19 pages.
- Goode, K. R., Asteriadou, K., Fryer, P. J., Picksley, M. and Robbins, P. T. (2010) Characterising the cleaning mechanisms of yeast and the implications for Cleaning In Place (CIP), *Food and Bioproducts Processing*, **88(4)**, 365–374.
- Haosheng, C. and Shihan, L. (2009) Inelastic damages by stress wave on steel surface at the incubation stage of vibration cavitation erosion, *Wear*, **266(1–2)**, 69–75.

- Hoffmann, M. R., Hua, I. and Höchemer, R. (1996) Application of ultrasonic irradiation for the degradation of chemical contaminants in water, *Ultrasonics Sonochemistry*, **3(3)**, S163–S172.
- Holah, J. T. (2000) Food processing equipment design and cleanability, Monograph, Flair-Flow Europe technical manual (F-FE 377A/00), (Teagasc Organisation), Dublin, 47p.
- Hua, I. and Thompson, J. E. (2000) Inactivation of *Escherichia coli* by sonication at discrete ultrasonic frequencies, *Water Research*, **34(15)**, 3888–3893.
- Ince, N.H. and Belen, R. (2001) Aqueous phase disinfection with power ultrasound: Process kinetics and effect of solid catalysts, *Environmental Science and Technology*, **35(9)**, 1885–1888.
- Ivanova, E. P., Truong, V. K., Webb, H. K., Baulin, V. A., Wang, J. Y., Mohammadi, N., Wang, F., Fluke, C. and Crawford, R. J. (2011) Differential attraction and repulsion of *Staphylococcus aureus* and *Pseudomonas aeruginosa* on molecularly smooth titanium films, *Scientific Reports*, **1(165)**, 1–8.
- Joyce, E. M, and Mason, T. J. (2008) Sonication used as a biocide, A review: Ultrasound a greener alternative to chemical biocides? *Chemistry Today*, **26(6)**, 22–26.
- Joyce, E. M., Wu, X. and Mason, T. J. (2010) Effect of ultrasonic frequency and power on algae suspensions, *Journal of Environmental Science and Health Part A*, **45(7)**, 863–866.
- Joyce, E. M, and Mason, T. J. (2008) Sonication used as a biocide, A review: Ultrasound a greener alternative to chemical biocides? *Chemistry Today*, **26(6)**, 22–26.

- Jyoti, K. K. and Pandit, A. B. (2001) Water disinfection by acoustic and hydrodynamic cavitation, *Biochemical Engineering Journal*, **7(3)**, 201–212.
- Jullien, C., Bénézech, T., Carpentier, B., Lebret, V. and Faille, C. (2003) Identification of surface characteristics relevant to the hygienic status of stainless steel for the food industry, *Journal of Food Engineering*, **56(1)**, 77–87.
- Kardos, N. and Luche, J-L. (2001) Sonochemistry of carbohydrate compounds, *Carbohydrate Research*, **332(2)**, 115–131.
- Kobus, Z. and Kusińska, E. (2008) Influence of physical properties of liquid on acoustic power of ultrasonic processor, *TEKA Kom. Mot. Energ. Roln. – OL PAN*, **8a**, 71–78.
- Kubo, M., Onodera, R., Shibasaki-Kitakawa, N., Tsumoto, K. and Yonemoto, T. (2005) Kinetics of ultrasonic disinfection of *Escherichia coli* in the presence of titanium dioxide particles, *Biotechnology progress*, **21(3)**, 897–901.
- Laborde, J-L., Bouyer, C., Caltagirone, J.-P. and Gérard, A. (1998) Acoustic bubble cavitation at low frequencies, *Ultrasonics*, **36(1-5)**, 589–594.
- Lelièvre, C., Antonini, G., Faille, C. and Bénézech, T. (2002) Modelling of cleaning kinetics of pipes soiled by *Bacillus* spores assuming a process combining removal and deposition, *Food and Bioproducts Processing*, **80(4)**, 305–311.
- Löning, J-M., Horst, C. and Hoffmann, U. (2002) Investigations on the energy conversion in sonochemical processes, *Ultrasonics Sonochemistry*, **9(3)**, 169–179.

- Lorenzen, K. (2005) Improving cleaning-in-place (CIP). In: Handbook of hygiene control in the food industry, H. L. M. Lelieveld, M. A. Mostert and J. Holah (Eds), Woodhead Publishing Limited, Cambridge, England, pp 425–444.
- Mamvura, T.A., Iyuke, S.E., Cluett, J. D. and Paterson, A. E. (2011) Soil films in the beverage industry: A review, *Journal of the Institute of Brewing*, **117(4)**, 608–616.
- Mañas, P., Pagán, R. and Raso, J. (2000) Predicting lethal effect of ultrasonic waves under pressure treatments on *Listeria monocytogenes* ATCC 15313 by power measurements, *Journal of Food Science*, **65(4)**, 663–667.
- Mancier, V. and Leclercq, D. (2007) New flowmetric measurement methods of power dissipated by an ultrasonic generator in an aqueous medium, *Ultrasonics Sonochemistry*, **14(2)**, 99–106.
- Mason, T. J., Cobley, A. J., Graves, J. E. and Morgan, D. (2011) New evidence for the inverse dependence of mechanical and chemical effects on the frequency of ultrasound, *Ultrasonics Sonochemistry*, **18(1)**, 226–230.
- Mason, T.J. and Lorimer, J.P. (2002) General Principles. In: Applied Sonochemistry – Uses of power ultrasound in chemistry and processing, T.J. Mason and J.P. Lorimer (Eds), Wiley-VCH Verlag GmbH, Weinheim, Germany, pg. 25–72.
- Miller, D. L. (1987) A review of the ultrasonic bioeffects of microsonation, gas-body activation, and related cavitation-like phenomena, *Ultrasound in Medicine and Biology*, **13(8)**, 443–470.

- Mott, I. E. C., Stickler, D. J., Coakley, W.T. and Bott, T. R. (1998) The removal of bacterial biofilm from water-filled tubes using axially propagated ultrasound, *Journal of Applied Microbiology*, **84(4)**, 509–514.
- Mummery, L. (1992) Surface texture analysis. In: *The Handbook*, Hommelwerke GmbH, Schnurr Druck, Germany, pp. 1–7.
- Nishikawa, T., Yoshida, A., Khanal, A., Habu, M., Yoshioka, I., Toyoshima, K., Takehara, T., Nishihara, T., Tachibana, K. and Tominaga, K. (2010) A study of the efficacy of ultrasonic waves in removing biofilms, *Gerodontology*, **27(3)**, 199–206.
- Oulahal, N., Martial-Gros, A., Bonneau, M. and Blum, L. J. (2004) Combined effect of chelating agents and ultrasound on biofilm removal from stainless steel surfaces: Application to “*Escherichia coli* milk” and “*Staphylococcus aureus* milk” biofilms, *Biofilms*, **1(1)**, 65–73.
- Parini, M. R. and Pitt, W. G. (2005) Removal of oral biofilms by bubbles: The effect of bubble impingement angle and sonic waves, *Journal of the American Dental Association*, **136(12)**, 1688–1693.
- Praeckel, U. (2009) Cleaning and disinfecting. In: *Handbook of Brewing; Processes, technology, markets*, H. M. Eßlinger, Ed, Wiley-VCH Verlag GmbH and Co, Weinheim, Germany, pp. 595–620.
- Rajasekhar, P., Fan, L., Nguyen, T. and Roddick, F.A. (2012) Impact of sonication at 20 kHz on *Microcystis aeruginosa*, *Anabaena circinalis* and *Chlorella* sp., *Water Research*, **46(5)**, 1473–1481.

- Raso, J., Mañas, P., Pagán, R. and Sala, F. J. (1999) Influence of different factors on the output power transferred into medium by ultrasound, *Ultrasonics Sonochemistry*, **5(4)**, 157–162.
- Ratoarinoro., Contamine, F., Wilhelm, A.M., Berlan, J. and Delmas, H. (1995) Power measurement in sonochemistry, *Ultrasonics Sonochemistry*, **2(1)**, 43–47.
- Sathiskumar, P.S. and Madras, G. (2012) Ultrasonic degradation of butadiene, styrene and their copolymers, *Ultrasonics Sonochemistry*, **19(3)**, 503–508.
- Simões, M. J. V. (2005) Use of biocides and surfactants to control *Pseudomonas fluorescens* biofilms: Role of the hydrodynamic conditions, PhD thesis, Department of Chemical and Biological Engineering, University of Minho, Portugal, pp. 1–223.
- Sithole, L. N. S. (2007) Antimicrobial properties of anodised and silver plated aluminium alloys, Fourth year research report, WITS University, 39–42.
- Son, Y., Lim, M. and Khim, J. (2007) Analysis of the ultrasonic energy in pilot-scale sonoreactors, *Proceedings of Symposium on Ultrasonic Electronics*, **28**, 111–112, (14-16 November, 2007).
- Son, Y., Lim, M. and Khim, J. (2009) Investigation of acoustic cavitation energy in a large-scale sonoreactor, *Ultrasonics Sonochemistry*, **16(4)**, 552–556.
- Son, Y., Lim, M., Ashokkumar, M. and Khim, J. (2011) Geometric optimization of sonoreactors for the enhancement of sonochemical activity, *The Journal of Physical Chemistry C*, **115(10)**, 4096–4103.

- Son, Y., Lim, M., Khim, J., Kim, L-H. and Ashokkumar, M. (2012) Comparison of calorimetric energy and cavitation energy for the removal of bisphenol-A: The effects of frequency and liquid height, *Chemical Engineering Journal*, **183**, 39–45.
- Sreekumari, K., Sato, Y. and Kikuchi, Y. (2005) Antibacterial metals – A viable solution for bacterial attachment and microbiologically influenced corrosion, *Materials Transactions*, **46(7)**, 1636–1645.
- Tang, J.W., Wu, Q.Y., Hao, H.W., Chen, Y. and Wu, M. (2004) Effect of 1.7 MHz ultrasound on a gas-vacuolate cyanobacterium and a gas-vacuole negative cyanobacterium, *Colloids and Surfaces B: Biointerfaces*, **36(2)**, 115–121.
- Toma, M., Fukutomi, S., Asakura, Y. and Koda, S. (2011) A calorimetric study of energy conversion efficiency of a sonochemical reactor at 500 kHz for organic solvents, *Ultrasonics Sonochemistry*, **18(1)**, 197–208.
- Trueba, F. J. and Woldringh, C. L. (1980) Changes in cell diameter during the division cycle of *Escherichia coli*, *Journal of Bacteriology*, **142(3)**, 869–878.
- Uzun, F. and Bilge, A. N. (2010) Investigation of total welding residual stress by using ultrasonic wave velocity variations, *Gazi University Journal of Science*, **24(1)**, 43–49.
- van Asselt, A. J. and te Giffel, M. Z. (2005) Pathogen resistance to sanitizers. In: Handbook of hygiene control in the food industry, H. L. M. Lelieveld, M. A. Mostert and J. Holah (Eds), Woodhead Publishing Limited, Cambridge, England, pp. 69–88.

- Verkaik, M. J., Busscher, H. J., Rustema-Abbing, M., Slomp, A. M., Abbas, F. and van der Mei, H. C. (2010) Oral biofilm models for mechanical plaque removal, *Clinical Oral Investigations*, **14(4)**, 403–409.
- Vinnichenko, M., Chevolleau, Th., Pham, M.T., Poperenko, L. and Maitz, M.F. (2002) Spectroellipsometric, AFM and XPS probing of stainless steel surfaces subjected to biological influences, *Applied Surface Science*, **201(1)**, 41–50.
- Woodling, S. E. and Moraru, C. I. (2005) Influence of surface topography on the effectiveness of pulsed light treatment for the inactivation of *Listeria innocua* on stainless-steel surfaces, *Journal of Food Science*, **70(7)**, M345–M351.
- Wu, X., Joyce, E. M. and Mason, T. J. (2012) Evaluation of the mechanisms of the effect of ultrasound on *Microcystis aeruginosa* at different ultrasonic frequencies, *Water Research*, **46(9)**, 2851–2858.
- Zand, R. Z., Verbeken, K. and Adriaens, A. (2012) Electrochemical assessment of the self-healing properties of cerium doped sol-gel coatings on 304L stainless steel substrates, *International Journal of Electrochemical Science*, **7(10)**, 9592–9608.

CHAPTER FIVE

"THERE ARE NO FACTS, ONLY INTERPRETATIONS."

- FRIEDRICH NIETZSCHE (1844-1900)

5. CONCLUSIONS AND RECOMMENDATIONS

5.1. Conclusions

The focus of the research study was centred on controlling and/or eliminating biofilms attached to food-grade SS surfaces using current CIP systems assisted by ultrasound waves at low frequency (high-power ultrasound) for application in food and beverage industry, pharmaceutical, health and other sectors. Ultrasound waves at 24 kHz were used and the results showed that they were effective against biofilms when used alone or in combination with CIP systems. Disinfection efficiencies $\geq 70\%$ were achieved and it was concluded the waves do indeed assist in controlling biofilms. However, the transfer process, from the probe to the inside of the pipe surfaces where biofilms were attached in dynamic experiments, still needs further investigation to ensure its practical application in food and beverage industries and this resulted in the process not eliminating biofilms (i.e. efficiencies of 100% were not consistently achieved). The conclusions (main ideas) that came from the study were summarised as follows:

- ✓ Biofilms took less time to form on food-grade surfaces and they were difficult to remove using current CIP procedures but as shown ultrasound waves could play a part in controlling them (using reduced CIP chemical quantities) and the costs associated with their integration are very low
- ✓ Biofilms were mainly composed of organic, inorganic and biological (microorganisms) components. Organic and inorganic components of biofilms could be controlled with existing technologies in the brewing industry. However, microorganisms were difficult to control as

they multiplied exponentially encouraging more biofilm formation if 100% disinfection was not reached.

- ✓ Water is the main ingredient in beverages and as such, its composition greatly affected the final product quality. It was demonstrated that water could support biofilm growth and its treatment is of utmost importance. However, with water scarcity being experienced, water purification methods need to be improved to combat biofilm formation
- ✓ From the study, it was shown that ultrasound waves could pass through metal surfaces and clean the inside surface but the efficiency of the process ranged between 10 and 100% with regards to disinfection process. The efficiencies were low and inconsistent because the thicknesses were high (3.91 mm for SS pipes and 3 mm for SS coupon plates), the clamping device used was heavy (1001 g) and also the device had to be under water for effective cooling during operation
- ✓ During operation, energy conversion rate was determined to be very low from electrical to cavitation and with scale-up it is envisaged it will be even lower but this was outweighed by the benefits of using ultrasound waves mentioned
- ✓ Welding SS surfaces and pipework increased surface roughness and the capacity to support biofilm formation; however, it was demonstrated that during use of ultrasound waves the surfaces became smoother with time leading to reduced biofilm intensities
- ✓ There was increased concentration of biofilm on and around weld areas include HAZs and it was difficult to control biofilms around such areas due to increased roughness. This was because welding introduces rough surfaces, geometrical difficulties (over-penetration and

under-penetration), and gave wrought structures (formation of iron oxide or separation on grain boundaries)

- ✓ From the study it was concluded that using 316L fillers resulted in better biofilm control than using 904L fillers (even though 904L welds had copper as a biocide) except when the welds were pickled and passivated. In this case 904L fillers resulted in lower intensities than 316L fillers
- ✓ It was also observed that welding in the presence of argon gave better welds that resulted in reduced biofilm formation
- ✓ Pickling and passivation done on pipes after welding without argon gave increased biofilm control and reduced bacterial loads and this is applied in areas where it is difficult to weld under argon gas
- ✓ During dynamic study, it was concluded that the flow, flow direction and pipe position influenced biofilm formation, its control and the CIP process
- ✓ The CIP process to date was observed to be ineffective against biofilms and it became less effective with continuous use of pipes and process vessels. It was observed that the CIP process became less effective along pipe lengths and process vessels i.e. the further, the pipe or vessel from the CIP source, the less effective was the process
- ✓ Commercial tolerances on thin-walled pipework does significantly affect orbital welding outcomes resulting in rough surfaces which favour biofilm formation
- ✓ On a positive note:

- Surface topography and morphology data could be used to predict bacterial loading as rough surfaces are more prone to loading than smooth surfaces
- The effects of biofilm development on corrosion prevalence and bacterial load are now better understood and these affect both bacterial load and the need for pure water during CIP
- Material specifications particularly regarding sulfur limits affecting penetration have changed and this is affecting weld procedures positively

5.2.Future work and recommendations

The study undertaken also led to new unanswered questions which could be investigated in future.

Some of the unanswered questions are:

- ✓ Ultrasound waves were tested outside pipes but a study whilst the probe is inserted in the pipe should be considered
- ✓ Further investigation on optimising clamping the probe to outside of pipes to transfer ultrasound waves should be conducted. This is a practical application in industry as it allows sterile cleaning of pipes and vessels which cannot be opened during operation or CIP.
- ✓ The defects on the pipes that affect the welding process leading to poor welds have not been considered and in future an investigation should be done and incorporated with the obtained results
- ✓ In line with that point is to look at the probability of success of getting a perfect weld taking into consideration all pipe defects, filler defects, welding process defects and other factors

- ✓ Use of more than one ultrasound probe staggered along a pipe or process vessel should be considered together with results obtained in the study
- ✓ Studies on the effect of ultrasound waves on biocides need to be conducted to obtain the best combination of the two technologies using sonicators that work in air
- ✓ The microorganisms in biofilms are resistant towards various counter measures and it is therefore important to prevent biofilm formation by using the correct surface design methods, detergents and disinfectants, and any other technologies. In addition, cleaning should be performed frequently
- ✓ Treatment to eliminate bacterial species capable of forming biofilms should be undertaken. The treatment method to be used should offer residual effect and not have any effect on the final product.

APPENDICES

**"WHEN YOU DO THE COMMON THINGS IN LIFE IN AN UNCOMMON
WAY, YOU WILL COMMAND THE ATTENTION OF THE WORLD."**

- GEORGE WASHINGTON CARVER (1864-1943)

APPENDICES

A. Appendix I: Surface topography and surface morphology parameters

The five parameters used are defined as:

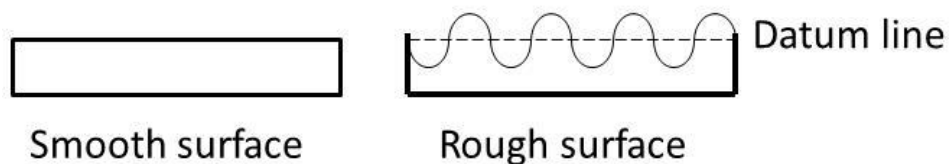
A.1. Average roughness (R_a)

It is the average distance from the profile to the mean line over the length of assessment, measured in μinch or μm and it is determined by the following formula:

$$R_a = \frac{1}{l_m} \int_0^{l_m} |y(x)| dx$$

where l_m is the number of sampling points and $y(x)$ is the residual surface.

R_a does not differentiate between peaks and valleys (Mummery, 1992). The mean line is a form of reference datum and all the descriptors used to characterise the surface topographies are measured with respect to this line. The mean line is the plane that represents the geometrical plane of the surface where the volumes above and below the plane are equal. The larger the value of R_a , the greater the roughness profile of the surface roughness (Scardino *et al.*, 2008). The following image gives a qualitative vision of this parameter:



A.2. Root-mean-square (RMS) profile height (R_q)

This is the square root of the average of the square of the deviation of the profile from the mean line and it is determined by the following formula:

$$R_q = \sqrt{\frac{1}{l_m} \int_0^{l_m} y^2(x) dx}$$

R_a and R_q are frequently used to express surface roughness but cannot differentiate between the peaks and valleys of a surface and therefore are considered somewhat deceptive (Mummery, 1992; Woodling and Moraru, 2005).

A.3. Maximum peak-to-valley height (R_{max})

It is the maximum peak-to-valley height within one cut-off (Mummery, 1992).

A.4. Surface skewness (R_{skw})

It is a measure of the direction of the asymmetry of the distribution of heights in the sample or a measure of the average of the first derivative of the surface i.e. the departure of the surface from symmetry. This statistical parameter is given by the following expression:

$$R_{skw} = \frac{\sum_{i=1}^N (Z_i - Z_{ave})^3}{N \sigma^3}$$

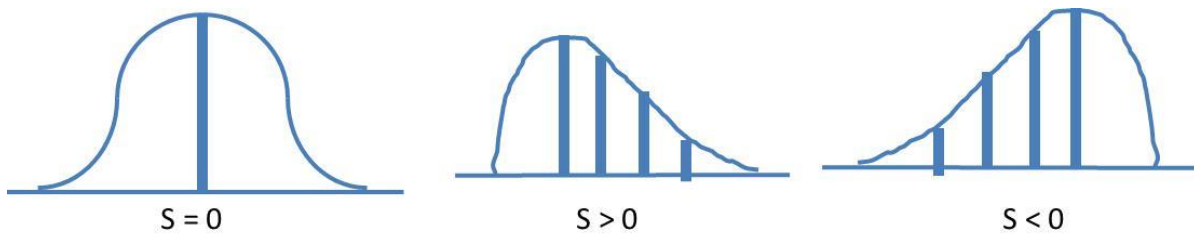
where

$$\sigma = \sqrt{\frac{\sum_{i=1}^N (Z_i - Z_{ave})^2}{N}}$$

The numerical value of R_{skw} gives information about the direction of the asymmetry of the distribution of heights:

- If $R_{skw} > 0$: positive asymmetry i.e. indicates that the surface is made up of mainly peaks and asperities
- If $R_{skw} = 0$: symmetric distribution
- If $R_{skw} < 0$: negative asymmetry i.e. indicates that the surface is made up of mainly pits or valleys

Therefore a negatively skewed surface is good for lubrication purposes. The following image gives a qualitative vision of this parameter:



A.5. Surface kurtosis (R_{kur})

It is a measure of the peakedness of the distribution of heights in the sample by comparing it to the normal distribution. This statistical parameter is given by the following expression:

$$R_{kur} = \frac{\sum_{i=1}^N (Z_i - Z_{ave})^4}{N\sigma^4}$$

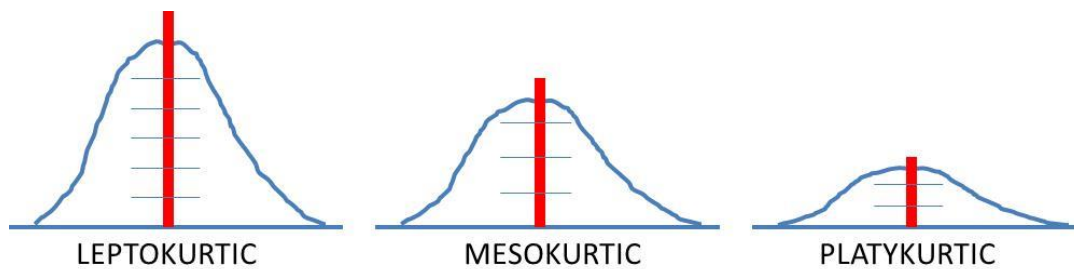
where

$$\sigma = \sqrt{\frac{\sum_{i=1}^N (Z_i - Z_{ave})^2}{N}}$$

The numerical value of R_{kur} gives us information about the distribution of heights:

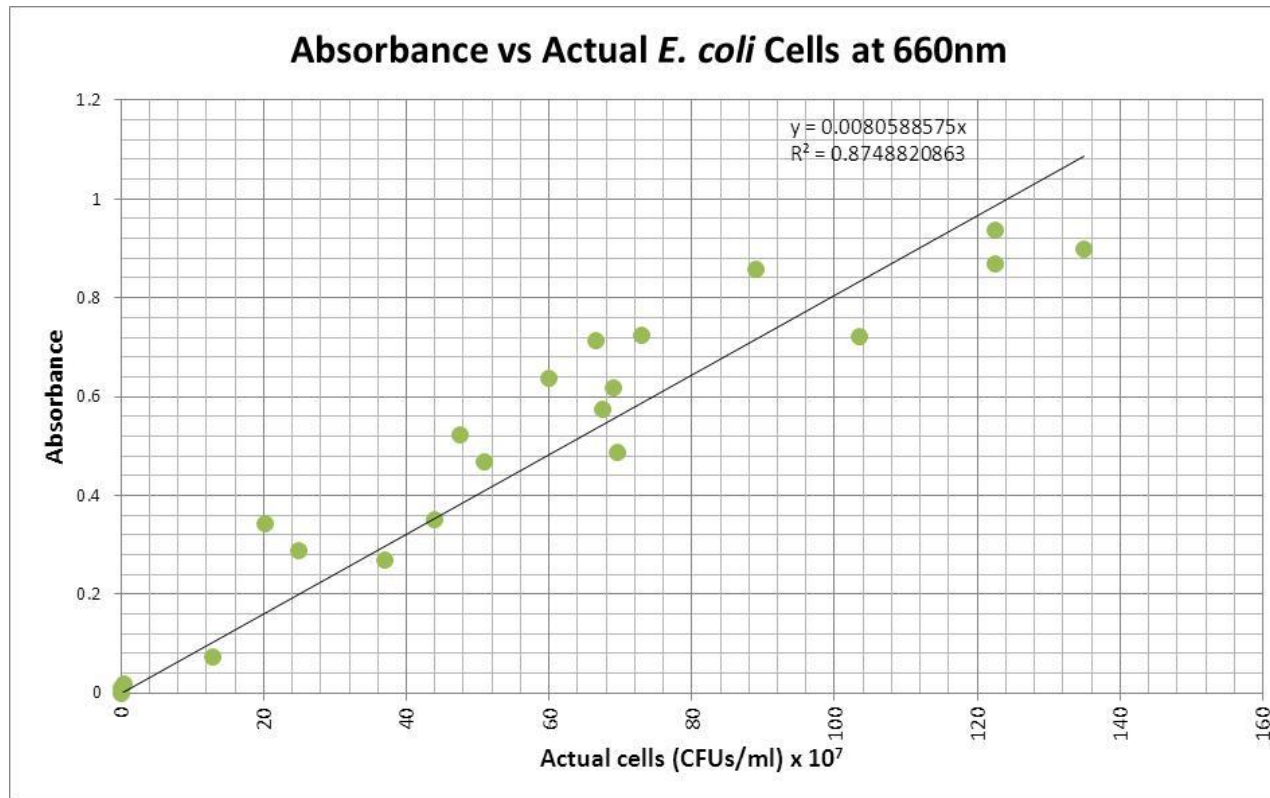
- If $R_{kur} > 3$: leptokurtic distribution (high peaks or deep valleys)
- If $R_{kur} = 3$: mesokurtic distribution (normally distributed surface)
- If $R_{kur} < 3$: platykurtic distribution (lack of high peaks or deep valleys)

If the surface heights are normally distributed (i.e. bell curve) then R_{skw} is 0 and R_{kur} is 3. The following image gives a qualitative vision of this parameter:



B. Appendix II: Calibration chart for SQ-4802 Double Beam Scanning UV/Visible Spectrophotometer at 660 nm

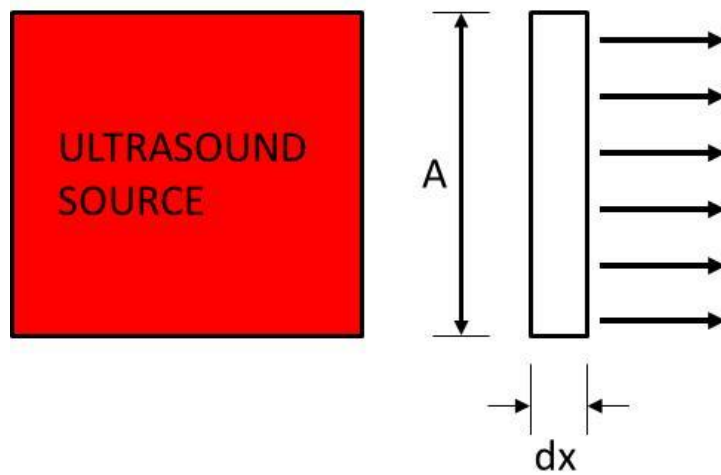
Calibration was done at 660 nm using *E. coli* cells and the chart is given below:



C. Appendix III: Calculations for electrical power input

C.1. Calculating electrical power input using hydrophone

Particles of the medium that are set in vibratory motion with ultrasound waves will possess kinetic energy from the waves, and hence the energy (the intensity) associated with the ultrasound waves can be deduced. Consider the movement of a layer of the medium of area A and thickness dx (i.e. volume Adx) under the action of ultrasound waves (Figure 6.1).



Relationship between sound source and wave

The kinetic energy ($mv^2/2$) of the layer is given by:

$$KE = \frac{1}{2}(\rho Adx)v^2$$

Equation C.1

The energy for the whole wave E_t may be obtained by summing all such elements (i.e. integrating equation C.1) to give:

$$E_t = \frac{1}{2}(\rho Ax)v^2 \quad \text{Equation C.2}$$

And the energy per unit volume (Ax) or energy density (E) is:

$$E = \frac{1}{2}\rho v^2 \quad \text{Equation C.3}$$

For sound energy passing through cross-sectional area (A) with a velocity, c , then the volume swept out in time, t , is Act , and the energy flowing in time, t , is given by $E Act$. Since intensity (I) is defined as the amount of energy flowing per area of ultrasound probe (A) per time (t):

$$I = E c \quad \text{Equation C.4}$$

Substituting for E from equation C.3 into C.4 gives

$$I = \frac{1}{2}\rho cv^2 \quad \text{Equation C.5}$$

For a plane progressive wave, the particle velocity, v , can be shown to be related to acoustic pressure, P_a , by:

$$\frac{P_a}{v} = \rho c \quad \text{Equation C.6}$$

where ρ is the density of the liquid and c is the velocity of sound in the liquid. Dimensional analysis confirms the formula to be correct.

Substituting for v from equation C.6 into equation C.5 gives

$$I = \frac{(P_a)^2}{2\rho c} \quad \text{Equation C.7}$$

For maximum particle velocity, v_o , the amplitude of the oscillating acoustic pressure, P_A , is given by:

$$\frac{P_A}{v_o} = \rho c \quad \text{Equation C.8}$$

And thus the maximum intensity of the sound wave may be expressed as:

$$I = \frac{P_A^2}{2\rho c} \quad \text{Equation C.9}$$

i.e. the sound intensity is proportional to the square of the acoustic amplitude.

To measure the sound intensity at a particular point in a liquid, either determine the maximum velocity (v_o) or maximum pressure amplitude (P_A); however, this is extremely difficult to calculate in practice and therefore a calorimetric determination of the total ultrasonic energy delivered to the liquid is considered to be sufficient.

C.2. Heat balances to determine electrical energy consumed by a horn-type sonicator

C.2.1. Method 1

The first heat balance is as follows:

$$E_{ele} = mC_p \frac{dT}{dt} + UA_w(T_o - T_{amb}) \quad \text{Equation C.10}$$

where T_o and T_{amb} are the initial temperature of the liquid and ambient temperature, respectively, A_w is the wetted area, m is the mass of water, C_p is the specific heat (4.2J/g K for water), and U is the bulk heat loss coefficient (Hoffmann *et al.*, 1996)

The solution to this equation gives the temperature variation with time in a non-thermostatic reactor which is used to determine the input energy

$$T = \left(T_o - T_{amb} \frac{E_{ele}}{UA_w} \right) e^{\left(-UA_w t / mC_p \right)} + T_{amb} + QUA_w \quad \text{Equation C.11}$$

C.2.2. Method 2

In this method all causes of heat exchange between the liquid and its surroundings are taken into account (Mancier and Leclercq, 2007). The energy balance can be written as:

$$P_{ele} = P_{liq} + P_{lost} + P_{app} \quad \text{Equation C.12}$$

where P_{ele} is the power provided by the ultrasonicator as power input, P_{liq} is the power absorbed by the liquid, P_{lost} are thermal losses between the liquid and the ambient temperature via the walls of the vessel and partially immersed equipment, P_{app} are thermal losses due to the stored energy in the walls of the container or reactor and in the immersed equipment

If the liquid temperature is homogeneous, then

$$P_{liq} = m_{liq} C_{p,liq} \frac{dT}{dt} \quad \text{and} \quad P_{app} = m_{app} C_{p,app} \frac{dT}{dt} \quad \text{Equation C.13}$$

where m_{liq} , $C_{p,liq}$ is the thermal capacitance of the liquid; m_{app} , $C_{p,app}$ is the thermal capacitance of the immersed part of equipment; T is its temperature and t , the time

Substituting equations C.13 into equation C.12 and rearranging gives:

$$dT = \frac{P_{ele} - P_{lost}}{m_{liq} C_{p,liq} + m_{app} C_{p,app}} dt \quad \text{Equation C.14}$$

If the experiment is undertaken over short periods of time, P_{lost} can be neglected because the heat flow does not have enough time to migrate towards the outside (Mancier and Leclercq, 2007).

Integrating equation C.14 gives:

$$T = \frac{P_{ele}}{m_{liq} C_{p,liq} + m_{app} C_{p,app}} t + T_o \quad \text{Equation C.15}$$

A graph of T against t is a straight line starting at the initial temperature of the distilled water (T_o)

with a slope of $\frac{P_{ele}}{m_{liq} C_{p,liq} + m_{app} C_{p,app}}$.

The input power P_{ele} can be calculated by two experiments are done: a reference one using the electrical heater to produce by Joule effect with a accurately known heat power ($P_{ele} = P_{Joule}$) and

a second one whose power is unknown ($P_{ele} = P_x$). The ratio of the slopes of the $T = f(t)$ straight lines of the two experiments gives:

$$P_x = \frac{a_x P_{joule}}{a_{joule}} \quad \text{Equation C.16}$$

where a_x is the value of the slope obtained for the experiment at unknown power, a_{joule} is the value of the slope obtained for the reference experiment at known power

To obtain the most precise measurements of P_x , a_{joule} is taken close to a_x so that the neglected terms are of the same order of magnitude and are minimised (Mancier and Leclercq, 2007).

C.2.3. Method 3

In this method, experiments are carried out to evaluate the actual ultrasound intensity absorbed by the liquid using calorimetry by assuming that the liquid is pure and there are no heat losses from the system (Sathiskumar and Madras, 2012). The ultrasonic energy dissipated in the liquid can be determined by the following equation:

$$P_{ele} = m C_p \frac{dT}{dt} \quad \text{Equation C.17}$$

which on integrating gives:

$$T - T_o = \frac{P_{ele}}{m C_p} t \quad \text{Equation C.18}$$

where P_{ele} is the input power (W), m is the mass of the water (g), C_p is the specific heat of water ($J g^{-1} K^{-1}$), dT/dt is the rate of temperature rise ($K s^{-1}$), T_o is the initial temperature and T is the temperature as a function of time.

The experiment is conducted with a small beaker for both water and another liquid (ethanol or acetone) with the same amount of liquid and the experiments will be conducted for 20 minutes with any increase in temperature of the liquid monitored as a function of time. This is then plotted and linearly regressed based on equation 7.18 to obtain the power supplied (Sathiskumar and Madras, 2012). Because the value of C_p is different for ethanol or acetone and water, the rise in temperature of the liquid will be different but the value of the power obtained will be the same in both the cases.

D. Appendix IV: Certificates for international conference held in Malaysia





الجامعة الإسلامية العالمية ماليزيا
INTERNATIONAL ISLAMIC UNIVERSITY MALAYSIA
يُونِيسْتِي اِسْلَامْ اِنْتَارَا اِيْحْسَابَا مِلْدَسِيَا



Certificate of Appreciation



Awarded to

TIRIVAVIRI AUGUSTINE MAMVURA

for presenting a paper titled

**Stainless Steel Surface Profile Changes during
use of Ultrasound Waves to Control Soil Films**

in the 3rd International Conference on Biotechnology Engineering
(ICBioE 2013), in Conjunction with IIUM Engineering Congress 2013
held at

Berjaya Times Square Hotel, Kuala Lumpur, Malaysia
2nd - 4th July, 2013



Assoc. Prof. Dr. Faridah Yusof
Chairman, ICBioE 2013

E. Appendix V: Filler composition

Sample ID	316L		904L		904L A		904L B		Average		St Dev	
Method	XRF	Spectr	XRF	Spectr	XRF	Spectr	XRF	Spectr	XRF	Spectr	XRF	Spectr
C		0.021		0.010		0.041		0.036		0.029		0.017
Si	0.410	0.202	0.561	0.232	0.341	0.255	0.434	0.263	0.445	0.250	0.110	0.016
P	0.004	0.035	0.007	0.034	0.000	0.054	0.000	0.052	0.002	0.047	0.004	0.011
S	0.149	0.011	0.002	<0.01	0.000	<0.01	0.000	<0.01	0.001	<0.01	0.001	0.000
Cr	18.259	18.110	20.320	20.730	18.479	19.550	18.132	19.350	18.977	19.877	1.176	0.746
Mo	2.482	2.420	4.234	4.717	4.409	4.704	4.394	4.433	4.346	4.618	0.097	0.160
Ni	11.803	11.190	24.905	23.120	24.850	21.990	24.440	22.190	24.732	22.433	0.254	0.603
Mn	1.804	1.738	1.488	1.507	1.353	1.408	1.422	1.415	1.421	1.443	0.068	0.055
Cu	0.137	0.122	1.508	1.502	1.579	1.536	1.556	1.484	1.548	1.507	0.036	0.026
Ti	0.003	0.008	0.012	0.010	0.002	0.010	0.661	0.010	0.225	0.010	0.378	0.000
V	0.044	0.093	0.027	0.078	0.032	0.097	0.065	0.099	0.041	0.091	0.021	0.012
W	0.037	0.247	0.041	0.256	0.000	0.220	0.000	0.249	0.014	0.242	0.024	0.019
Fe	64.632	65.610	46.765	47.720	48.956	49.970	48.897	50.250	48.206	49.313	1.248	1.387
Co	0.237	0.058	0.129	0.042	0.000	0.123	0.000	0.128	0.043	0.098	0.074	0.048
Nb	0.000	0.028	0.000	0.015	0.000	0.023	0.000	0.025	0.000	0.021	0.000	0.005
Total	100.001	99.893	99.999	99.973	100.001	99.981	100.001	99.984	100.000	99.979		

Euro Steel Mill pipe specifications and characterisation

Sample ID	Specifications'		Results	
Method	Min	Max	Ladle	Product
C	0.000	0.035	0.019	0.016
Si	0.000	1.000	0.340	0.318
P	0.000	0.045	0.026	0.026
S	0.000	0.030	0.001	0.006
Cr	16.000	18.000	16.700	16.760
Mo	2.000	3.000	2.000	2.090
Ni	11.000	14.000	11.080	11.090
Mn	0.000	2.000	1.590	1.639
Cu				
Ti				
V				
W				
Fe				
Co				
Nb				
Total	29.000	38.110	31.756	31.945

F. Appendix VI: Dynamic experiments data collected and recorded for experiments 1 and 2 after CIP and five weeks of water circulation

For run 1, after CIP on 13.08.2013

Sample	RLU	Sample	RLU	Sample	RLU	Sample	RLU	Sample	RLU	Sample	RLU
A1-1	44	B3-1	43	C5-1	85	D7-1	108	E9-1	41	F11-1	52
A1-2	46	B3-2	23	C5-2	18	D7-2	30	E9-2	41	F11-2	104
A1-3	36	B3-3	89	C5-3	55	D7-3	29	E9-3	50	F11-3	86
A1-4	31	B3-4	57	C5-4	40	D7-4	93	E9-4	78	F11-4	42
A1-5	14	B3-5	33	C5-5	13	D7-5	81	E9-5	41	F11-5	54
A1-6	36	B3-6	67	C5-6	28	D7-6	55	E9-6	95	F11-6	30
A1-7	31	B3-7	70	C5-7	18	D7-7	40	E9-7	48	F11-7	43
A1-8	46	B3-8	26	C5-8	21	D7-8	21	E9-8	47	F11-8	42
A1-9	38	B3-9	69	C5-9	25	D7-9	26	E9-9	44	F11-9	38

A2-10	53	B4-10	46	C6-10	95	D8-10	20	E10-10	56	F13-22	85
A2-11	49	B4-11	86	C6-11	42	D8-11	43	E10-11	48	F13-23	68
A2-12	49	B4-12	50	C6-12	15	D8-12	49	E10-12	29	F13-24	31
A2-13	49	B4-13	20	C6-13	40	D8-13	22	E10-13	48	F13-25	56
A2-14	51	B4-14	19	C6-14	24	D8-14	12	E10-14	228	F13-26	56
A2-15	55	B4-15	49	C6-15	41	D8-15	34	E10-15	19	F13-27	204
A2-16	43	B4-16	16	C6-16	69	D8-16	44	E10-16	76	F13-28	92
A2-17	30	B4-17	34	C6-17	26	D8-17	33	E10-17	56	F13-29	35
A2-18	34	B4-18	45	C6-18	39	D8-18	27	E10-18	65	F13-30	21
F12-10	40	F12-13	59	F12-16	49	F12-19	28				
F12-11	28	F12-14	36	F12-17	24	F12-20	111				
F12-12	40	F12-15	38	F12-18	24	F12-21	53				

For run 1, after five weeks circulating water to build biofilms on 18.09.2013

Sample	RLU	Sample	RLU	Sample	RLU	Sample	RLU	Sample	RLU	Sample	RLU
A1-1	53290	B3-1	59676	C5-1	39565	D7-1	39675	E9-1	37090	F11-1	107444
A1-2	10122	B3-2	9888	C5-2	30062	D7-2	28992	E9-2	58251	F11-2	82007
A1-3	27558	B3-3	30396	C5-3	20421	D7-3	14041	E9-3	14889	F11-3	47537
A1-4	15587	B3-4	17605	C5-4	46436	D7-4	83323	E9-4	47943	F11-4	48943
A1-5	37124	B3-5	59802	C5-5	40499	D7-5	29350	E9-5	35731	F11-5	34912
A1-6	26467	B3-6	17978	C5-6	31555	D7-6	49506	E9-6	26403	F11-6	43816
A1-7	25536	B3-7	22342	C5-7	15535	D7-7	19477	E9-7	16559	F11-7	60185
A1-8	20622	B3-8	23879	C5-8	20877	D7-8	25988	E9-8	30781	F11-8	27438
A1-9	15100	B3-9	11967	C5-9	19472	D7-9	16260	E9-9	22656	F11-9	28109
A2-10	21390	B4-10	46318	C6-10	24000	D8-10	27038	E10-10	96439	F13-22	37371

A2-11	30391	B4-11	13819	C6-11	46464	D8-11	49302	E10-11	124371	F13-23	78651
A2-12	31630	B4-12	19842	C6-12	37054	D8-12	7244	E10-12	33665	F13-24	54315
A2-13	33217	B4-13	13688	C6-13	15734	D8-13	29773	E10-13	105955	F13-25	121185
A2-14	47483	B4-14	40581	C6-14	45206	D8-14	18471	E10-14	41448	F13-26	46511
A2-15	7146	B4-15	19939	C6-15	67323	D8-15	15005	E10-15	45627	F13-27	45610
A2-16	32990	B4-16	29142	C6-16	40284	D8-16	8358	E10-16	15430	F13-28	58887
A2-17	24111	B4-17	24064	C6-17	15388	D8-17	23300	E10-17	62739	F13-29	69079
A2-18	41485	B4-18	9834	C6-18	35881	D8-18	30224	E10-18	33194	F13-30	13625
F12-10	89414	F12-13	29630	F12-16	101093	F12-19	85384				
F12-11	20357	F12-14	51390	F12-17	35753	F12-20	28319				
F12-12	37479	F12-15	39140	F12-18	118317	F12-21	57369				

Pipe start	80986
Pipe end	237738
Fermenter	14804

For run 2, after CIP on 07.11.2013

Sample	RLU	Sample	RLU	Sample	RLU	Sample	RLU	Sample	RLU	Sample	RLU
A1-1	64	B3-1	40	C5-1	281	D7-1	128	E9-1	62	F11-1	149
A1-2	118	B3-2	93	C5-2	57	D7-2	68	E9-2	190	F11-2	68
A1-3	185	B3-3	85	C5-3	138	D7-3	35	E9-3	110	F11-3	26
A1-4	65	B3-4	164	C5-4	299	D7-4	142	E9-4	139	F11-4	217
A1-5	82	B3-5	212	C5-5	315	D7-5	211	E9-5	111	F11-5	141
A1-6	145	B3-6	158	C5-6	145	D7-6	216	E9-6	440	F11-6	527
A1-7	79	B3-7	166	C5-7	192	D7-7	145	E9-7	100	F11-7	389
A1-8	97	B3-8	53	C5-8	180	D7-8	125	E9-8	284	F11-8	503
A1-9	90	B3-9	39	C5-9	105	D7-9	165	E9-9	140	F11-9	213
A2-10	172	B4-10	107	C6-10	191	D8-10	95	E10-10	273	F13-22	124

A2-11	171	B4-11	63	C6-11	97	D8-11	33	E10-11	114	F13-23	177
A2-12	105	B4-12	145	C6-12	43	D8-12	56	E10-12	65	F13-24	190
A2-13	146	B4-13	168	C6-13	104	D8-13	149	E10-13	67	F13-25	209
A2-14	172	B4-14	440	C6-14	380	D8-14	118	E10-14	104	F13-26	389
A2-15	105	B4-15	50	C6-15	827	D8-15	255	E10-15	63	F13-27	234
A2-16	151	B4-16	61	C6-16	178	D8-16	51	E10-16	139	F13-28	50
A2-17	158	B4-17	34	C6-17	319	D8-17	210	E10-17	66	F13-29	432
A2-18	223	B4-18	35	C6-18	29	D8-18	123	E10-18	58	F13-30	143
F12-10	894	F12-13	254	F12-16	122	F12-19	483				
F12-11	151	F12-14	443	F12-17	222	F12-20	148				
F12-12	48	F12-15	32	F12-18	151	F12-21	150				

For run 2, after five weeks circulating water to build biofilms on 12.12.2013

Sample	RLU	Sample	RLU	Sample	RLU	Sample	RLU	Sample	RLU	Sample	RLU
A1-1	4358	B3-1	2921	C5-1	2662	D7-1	5444	E9-1	4574	F11-1	11756
A1-2	1918	B3-2	5260	C5-2	1103	D7-2	7407	E9-2	6173	F11-2	10761
A1-3	1787	B3-3	5693	C5-3	4746	D7-3	4149	E9-3	8965	F11-3	5707
A1-4	2750	B3-4	4487	C5-4	8896	D7-4	20232	E9-4	3681	F11-4	18118
A1-5	1992	B3-5	8638	C5-5	5147	D7-5	4226	E9-5	17995	F11-5	6169
A1-6	3536	B3-6	3307	C5-6	7625	D7-6	6613	E9-6	4862	F11-6	8030
A1-7	5461	B3-7	4541	C5-7	6648	D7-7	5724	E9-7	5378	F11-7	3290
A1-8	2718	B3-8	3829	C5-8	5468	D7-8	3377	E9-8	6880	F11-8	3831
A1-9	2829	B3-9	2262	C5-9	5241	D7-9	4061	E9-9	4906	F11-9	2790
A2-10	5251	B4-10	1847	C6-10	1916	D8-10	11717	E10-10	8197	F13-22	5297

A2-11	7676	B4-11	799	C6-11	4143	D8-11	5832	E10-11	6742	F13-23	9492
A2-12	1815	B4-12	3199	C6-12	6083	D8-12	4893	E10-12	8211	F13-24	3949
A2-13	4881	B4-13	4334	C6-13	6042	D8-13	6862	E10-13	13477	F13-25	21133
A2-14	3707	B4-14	2941	C6-14	7934	D8-14	4695	E10-14	8001	F13-26	7370
A2-15	12230	B4-15	2825	C6-15	8254	D8-15	5485	E10-15	7192	F13-27	4426
A2-16	5435	B4-16	2462	C6-16	5747	D8-16	3997	E10-16	5247	F13-28	15482
A2-17	4395	B4-17	3394	C6-17	4598	D8-17	5409	E10-17	8488	F13-29	7549
A2-18	3209	B4-18	4695	C6-18	5220	D8-18	3343	E10-18	2001	F13-30	2448
F12-10	4232	F12-13	5333	F12-16	6534	F12-19	6133				
F12-11	8548	F12-14	8900	F12-17	5251	F12-20	6768				
F12-12	2767	F12-15	2844	F12-18	6501	F12-21	6624				

Pipe start	1079
Pipe end	3175
Fermenter	-

G. Appendix VII: Dynamic experimental data for individual pipes after CIP and biofilm formation processes

Data for pipe A for run 1 showing CIP process and biofilm formation against control

Sampling position	After CIP			After biofilm formation		
	Control	A-316	A-904	Control	A-316	A-904
Before weld	1.1	1.3	1.6	1620	1615	648
Before weld	1.9	1.4	1.5	2093	307	921
Before weld	1.1	1.1	1.5	991	835	959
On weld	1.2	0.9	1.5	1186	472	1007
On weld	1.8	0.4	1.5	898	1125	1439
On weld	1.1	1.1	1.7	1558	802	217
After weld	1.0	0.9	1.3	2970	774	1000
After weld	1.3	1.4	0.9	2905	625	731
After weld	1.6	1.2	1.0	1009	458	1257
Average	1.3	1.1	1.4	1692	779	909

Data for pipe A for run 2 showing CIP process and biofilm formation against control

Sampling position	After CIP			After biofilm formation		
	Control	A-316	A-904	Control	A-316	A-904
Before weld	4.5	1.9	5.2	84	132	159
Before weld	14.6	3.6	5.2	128	58	233
Before weld	4.5	5.6	3.2	259	54	55
On weld	7.5	2.0	4.4	190	83	148
On weld	1.3	2.5	5.2	200	60	112
On weld	20.6	4.4	3.2	190	107	371
After weld	9.0	2.4	4.6	233	166	165
After weld	3.4	2.9	4.8	123	82	133
After weld	5.0	2.7	6.8	174	86	97
Average	7.8	3.1	4.7	176	92	164

Data for pipe B for run 1 showing CIP process and biofilm formation against control

Sampling position	After CIP			After biofilm formation		
	Control	B-316	B-904	Control	B-316	B-904
Before weld	1.2	0.5	2.1	1186	883	677
Before weld	1.1	1.0	0.8	1558	729	724
Before weld	1.8	1.4	2.1	898	298	363
On weld	1.1	0.6	1.7	1620	415	534
On weld	1.1	0.6	1.0	991	1230	1813
On weld	1.9	1.5	2.0	2093	604	545
After weld	1.3	1.4	1.3	2905	1404	1809
After weld	1.0	2.6	0.7	2970	419	300
After weld	1.6	1.5	2.7	1009	601	921
Average	1.3	1.2	1.6	1692	732	854

Data for pipe B for run 2 showing CIP process and biofilm formation against control

Sampling position	After CIP			After biofilm formation		
	Control	B-316	B-904	Control	B-316	B-904
Before weld	7.5	1.8	5.0	190	75	138
Before weld	20.6	1.0	1.6	190	103	116
Before weld	1.3	1.1	1.2	200	142	69
On weld	4.5	5.1	5.0	84	131	136
On weld	4.5	13.3	6.4	259	89	262
On weld	14.6	1.5	4.8	128	86	100
After weld	3.4	3.2	1.2	123	56	89
After weld	9.0	1.9	2.8	233	24	159
After weld	5.0	4.4	2.6	174	97	173
Average	7.8	3.7	3.4	176	89	138

Data for pipe C for run 1 showing CIP process and biofilm formation against control

Sampling position	After CIP			After biofilm formation		
	Control	C-316	C-HAZ	Control	C-316	C-HAZ
Before weld	1.2	2.9	2.6	1186	727	1199
Before weld	1.8	1.3	0.5	898	1408	911
Before weld	1.1	0.5	1.7	1558	1123	619
On weld	1.0	1.2	1.2	2970	477	1407
On weld	1.3	0.7	0.4	2905	1370	1228
On weld	1.6	1.2	0.8	1009	2041	956
After weld	1.1	2.1	0.5	991	1221	471
After weld	1.1	0.8	0.6	1620	466	633
After weld	1.9	1.2	0.8	2093	1088	590
Average	1.3	1.3	1.0	1692	1102	890

Data for pipe C for run 2 showing CIP process and biofilm formation against control

Sampling position	After CIP			After biofilm formation		
	Control	C-316	C-HAZ	Control	C-316	C-HAZ
Before weld	1.3	5.8	8.5	200	58	81
Before weld	20.6	2.9	1.7	190	126	33
Before weld	7.5	1.3	4.2	190	184	144
On weld	3.4	3.2	9.1	123	183	270
On weld	5.0	11.5	9.5	174	240	156
On weld	9.0	25.1	4.4	233	250	231
After weld	4.5	5.4	5.8	84	174	201
After weld	14.6	9.7	5.5	128	139	166
After weld	4.5	0.9	3.2	259	158	159
Average	7.8	7.3	5.8	176	168	160

Data for pipe D for run 1 showing CIP process and biofilm formation against control

Sampling position	After CIP			After biofilm formation		
	Control	D-904	D-HAZ	Control	D-904	D-HAZ
Before weld	1.0	1.2	1.3	2970	590	253
Before weld	1.6	0.6	1.0	1009	788	706
Before weld	1.3	0.8	0.8	2905	493	916
On weld	1.2	2.8	0.7	1186	2525	902
On weld	1.1	2.5	0.4	1558	890	560
On weld	1.8	1.7	1.0	898	1500	455
After weld	1.1	3.3	0.6	1620	1203	820
After weld	1.1	0.9	1.3	991	879	1494
After weld	1.9	0.9	1.5	2093	426	220
Average	1.3	1.6	1.0	1692	1033	703

Data for pipe D for run 2 showing CIP process and biofilm formation against control

Sampling position	After CIP			After biofilm formation		
	Control	D-904	D-HAZ	Control	D-904	D-HAZ
Before weld	4.5	4.4	1.5	84	173	121
Before weld	4.5	3.8	6.4	259	102	164
Before weld	14.6	5.0	3.7	128	123	101
On weld	3.4	4.3	4.5	123	613	208
On weld	9.0	6.4	3.6	233	128	142
On weld	5.0	6.5	7.7	174	200	166
After weld	1.3	3.9	2.9	200	165	355
After weld	7.5	2.1	1.0	190	225	177
After weld	20.6	1.1	1.7	190	126	148
Average	7.8	4.2	3.7	176	206	176

Data for pipe E for run 1 showing CIP process and biofilm formation against control

Sampling position	After CIP			After biofilm formation		
	Control	E-316	E-904	Control	E-316	E-904
Before weld	1.2	1.2	1.7	1186	1124	2923
Before weld	1.8	1.2	1.5	898	1766	3770
Before weld	1.1	1.5	0.9	1558	451	1020
On weld	1.0	2.4	1.5	2970	1453	3211
On weld	1.3	1.2	6.9	2905	1083	1256
On weld	1.6	2.9	0.6	1009	800	1383
After weld	1.1	1.5	2.3	991	502	468
After weld	1.1	1.4	1.7	1620	933	1902
After weld	1.9	1.3	2.0	2093	687	1006
Average	1.3	1.6	2.1	1692	978	1882

Data for pipe E for run 2 showing CIP process and biofilm formation against control

Sampling position	After CIP			After biofilm formation		
	Control	E-316	E-904	Control	E-316	E-904
Before weld	1.3	1.9	8.3	200	139	248
Before weld	20.6	5.8	3.5	190	187	204
Before weld	7.5	3.3	2.0	190	272	249
On weld	3.4	4.2	2.0	123	112	408
On weld	5.0	3.4	3.2	174	545	243
On weld	9.0	13.3	1.9	233	147	218
After weld	4.5	3.0	4.2	84	163	159
After weld	14.6	8.6	2.0	128	209	257
After weld	4.5	4.2	1.8	259	149	61
Average	7.8	5.3	3.2	176	214	228

Data for pipe F for run 1 showing CIP process and biofilm formation against control

Sampling position	After CIP			After biofilm formation		
	Control	F-316	F-904	Control	F-316	F-904
Before weld	1.0	2.8	1.3	2970	1785	1824
Before weld	1.6	1.1	1.3	1009	2094	832
Before weld	1.3	0.6	1.2	2905	413	852
On weld	1.2	1.7	1.3	1186	3673	1483
On weld	1.1	1.7	1.6	1558	1410	1058
On weld	1.8	6.2	0.9	898	1382	1328
After weld	1.1	2.6	1.6	1620	1133	3257
After weld	1.1	2.1	3.2	991	2384	2486
After weld	1.9	0.9	2.6	2093	1646	1441
Average	1.3	2.2	1.7	1692	1769	1618

Data for pipe F for run 2 showing CIP process and biofilm formation against control

Sampling position	After CIP			After biofilm formation		
	Control	F-316	F-904	Control	F-316	F-904
Before weld	4.5	1.5	11.8	84	469	100
Before weld	4.5	13.1	15.2	259	229	116
Before weld	14.6	4.3	6.5	128	74	85
On weld	3.4	6.3	6.6	123	641	549
On weld	9.0	11.8	4.3	233	223	187
On weld	5.0	7.1	16.0	174	134	243
After weld	1.3	3.8	4.5	200	161	356
After weld	7.5	5.4	2.1	190	288	326
After weld	20.6	5.8	0.8	190	120	173
Average	7.8	6.6	7.5	176	260	237

H. Appendix VIII: Publications and Conferences

1. Mamvura, T.A., Iyuke, S.E., Cluett, J. D. and Paterson, A. E. (2011) Soil films in the beverage industry: A review, *Journal of the Institute of Brewing*, **117(4)**, 608–616.
2. Mamvura, T.A., Iyuke, S.E. and Paterson, A. E. (2012) Ultrasound waves used to control soil films, *SAIChE conference*, Durban, South Africa, September 2012.
3. Mamvura, T.A., Iyuke, S.E. and Paterson, A. E. (2012) Ultrasound waves used to control soil films, *Postgraduate Symposium*, Johannesburg, South Africa, October 2012.
4. Mamvura, T.A., Iyuke, S.E. and Paterson, A. E. (2013) Stainless steel surface topography changes during sonication with ultrasound waves used to control soil films, Third International Conference on Biotechnology Engineering (ICBioE2013) held on 2-4 July 2013 at Berjaya Time Square Hotel, Kuala Lumpur, Malaysia.
5. Mamvura, T.A., Iyuke, S.E. and Paterson, A. E. (2013) Ultrasound waves used to control soil films in brewing industry, Third International Conference on Biotechnology Engineering (ICBioE2013) held on 2-4 July 2013 at Berjaya Time Square Hotel, Kuala Lumpur, Malaysia.
6. Mamvura, T.A., Iyuke, S.E. and Paterson, A. E. (2013) Stainless steel surface topography changes during sonication with ultrasound waves used to control soil films, *Postgraduate Symposium*, Johannesburg, South Africa, August 2013.
7. Mamvura, T.A., Iyuke, S.E. and Paterson, A. E. (2013) Investigation on the effect of ultrasound waves on stainless steel surfaces during removal of soil films, *Advances in Environmental Biology*, under review.